ISSN 1881-7831 Online ISSN 1881-784X

DD&T

Drug Discoveries & Therapeutics

Volume 19, Number 1
February 2025

IRCA BSSA

IACMHR

www.ddtjournal.com

DD&T
Drug Discoveries & Therapeutics

ISSN: 1881-7831
Online ISSN: 1881-784X
CODEN: DDTRBX
Issues/Year: 6
Language: English
Publisher: IACMHR Co., Ltd.

Drug Discoveries & Therapeutics is one of a series of peer-reviewed journals of the International Research and Cooperation Association for Bio & Socio-Sciences Advancement (IRCA-BSSA) Group. It is published bimonthly by the International Advancement Center for Medicine & Health Research Co., Ltd. (IACMHR Co., Ltd.) and supported by the IRCA-BSSA.

Drug Discoveries & Therapeutics publishes contributions in all fields of pharmaceutical and therapeutic research such as medicinal chemistry, pharmacology, pharmaceutical analysis, pharmaceutics, pharmaceutical administration, and experimental and clinical studies of effects, mechanisms, or uses of various treatments. Studies in drug-related fields such as biology, biochemistry, physiology, microbiology, and immunology are also within the scope of this journal.

Drug Discoveries & Therapeutics publishes Original Articles, Brief Reports, Reviews, Policy Forum articles, Case Reports, Communications, Editorials, News, and Letters on all aspects of the field of pharmaceutical research. All contributions should seek to promote international collaboration in pharmaceutical science.

Editorial Board

Editorial and Head Office:

Pearl City Koishikawa 603,
2-4-5 Kasuga, Bunkyo-ku,
Tokyo 112-0003, Japan
E-mail: office@ddtjournal.com

Drug Discoveries & Therapeutics

Editorial and Head Office

Pearl City Koishikawa 603, 2-4-5 Kasuga, Bunkyo-ku,
Tokyo 112-0003, Japan

E-mail: office@ddtjournal.com
URL: www.ddtjournal.com

CONTENTS

Volume 19, Number 1, 2025

Original Article

Brief Report

Correspondence

Original Article

DOI: 10.5582/ddt.2025.01008

Fosfomycin-associated adverse events: A disproportionality analysis of the FDA Adverse Event Reporting System

Luxuan Yang[1], Wenyong Zhang[1], Xiujuan Shen[1], Meiqin Liu[1], Meiying Wu[2,*], Dan Xiao[1,*]

[1] Department of Infection Disease, The Fifth People's Hospital of Suzhou, Suzhou, Jiangsu, China;
[2] Department of Pulmonary Medicine, The Fifth People's Hospital of Suzhou, Suzhou, Jiangsu, China.

SUMMARY: Fosfomycin, with its unique mechanism of action, has emerged as a promising option for clinicians to combat antimicrobial resistance and the limited availability of effective drugs, which has led to an increase in associated adverse events (AEs). This study aims to explore the AEs caused by fosfomycin through data mining of the US FDA Adverse Event Reporting System (FAERS) to inform clinical safety. As revealed by FAERS, the 796 fosfomycin-associated AEs occurred more commonly in females (61.90%), with Italy reporting the highest incidence (32.40%), and have a significant rise with peak years in 2018 and 2019. The analysis revealed that gastrointestinal disorders, injury, poisoning and procedural complications, and skin and subcutaneous tissue disorders were among the most commonly reported system organ classes (SOCs), accounting for 16.29%, 13.50%, and 11.26% of cases, respectively. The median time to onset (TTO) for fosfomycin associated AEs was 2 days, indicating an early failure type distribution. Off-label use, diarrhoea, and nausea were among the top 50 most frequent AEs, with reporting odds ratios (RORs) of 3.39, 3.87, and 1.79, respectively. These findings emphasize the need for careful monitoring of fosfomycin use, particularly among female patients and in high-reporting regions. The unique profile of fosfomycin associated AEs identified in this analysis calls for a reevaluation of existing safety profiles, as it may differ from previous studies and product labeling. Our findings offer important insights for medical and public health fields, and are essential for enhancing pharmacovigilance and refining clinical management.

Keywords: Fosfomycin, FDA Adverse Event Reporting System, characteristic, managements

1. Introduction

As the problem of antibiotic resistance is increasing alarmingly, physicians have turned to older antibiotics, such as fosfomycin. It is a phosphoenolpyruvate analogue produced by *Streptomyces* spp., discovered in 1969 and approved for treating urinary tract infections. It inhibits bacterial cell wall *via* MurA binding, enters bacteria through cAMP-dependent pathways, reduces adherence to urinary and respiratory epithelial cells, penetrates biofilms, and enhances neutrophil killing through immunomodulation (*1,2*). In addition, fosfomycin exhibits broad-spectrum activity against various Gram-positive and Gram-negative bacteria, including multi-drug-resistant strains, and is well-distributed in multiple tissues, with potential for synergistic action with other antibiotics (*3*). Owing to its unique mechanism of action and outstanding therapeutic efficacy, its clinical application has extended to respiratory, skin and soft tissue infections, and combination therapy in recent years (*1*), raising more issues that require in-depth consideration.

Fosfomycin was generally regarded as safe, with few adverse effects, including gastrointestinal symptoms, skin rashes, electrolyte disturbances, transient changes in blood markers, and abnormalities in liver function (*1,4*). However, some unexpected adverse effects have been identified recently, such as agranulocytosis (*5*) and pseudomembranous colitis (*6*), prompting the need for a systematic integration and evaluation of the fosfomycin-associated adverse events (AEs). The FDA Adverse Event Reporting System (FAERS) database is an essential tool for post-marketing surveillance and early drug safety issue detection, offering regularly updated real-world adverse event reports from various sources (*4,6*). Therefore, we conduct a comprehensively analyzed system-specific side effects of fosfomycin using this database. Our findings can help physicians and health policymakers monitor adverse drug reactions and provide recommendations for the safe clinical use of fosfomycin.

2. Methods

2.1. Ethics statement

This study utilized data from the FAERS, a publicly available and anonymized database. As no individual patient data or identifiers were involved, this analysis was exempt from formal ethics committee review by the Ethical Review Committee of The Fifth People's Hospital of Suzhou. The study conformed to the ethical principles outlined in the Declaration of Helsinki (as revised in 2013, https://wma.net/what-we-do/medical-ethics/declaration-of-helsinki).

2.2. Data source

We performed a retrospective pharmacovigilance study from Quarter 1 (Q1) in 2004 to Q3 in 2024, utilizing the extracted data with 'fosfomycin' as the main suspect (PS), in order to examine fosfomycin-associated AEs that were recorded in the FAERS database. The FAERS data were downloaded from the FDA official website (available at *https://fis.fda.gov/extensions/FPD-QDE-FAERS/FPD-QDE-FAERS.html*). The database included seven data files, namely patient demographic information (DEMO), drug/biologic information (DRUG), adverse events (REAC), patient outcomes (OUTC), report sources (RPSR), start/end dates of drug therapy (THER) and indications for drug (INDI) (*7*). A relation was established in the FAERS database architecture to connect each data file by some special identification numbers. We managed FAERS data by Python Version 3.9 for further analysis. Statistical analysis was carried out using Microsoft Office Excel 2021. Informed consent was waived in this observational study since it used data from an international public database that had been anonymized.

2.3. Data extraction

Duplication is unavoidable because the reports are spontaneous, hence the deduplication procedure should be carried out before analysis. We carried out the deduplication in accordance with FDA guidelines. When the CASEID and PRIMARYID were the same, we manually reviewed the reports to eliminate the lower PRIMARYID. Moreover, the CASEID which listed in the deleted cases file was further eliminated. We then identified fosfomycin-associated cases in both the 'drugname' and 'prod_ai' columns using 'fosfomycin' in the 'DRUG' files. To improve accuracy, the 'role_cod' as PS was chosen in the DRUG files. All AEs in FAERS are coded by the preferred term (PT) from standardized Medical Dictionary for Regulatory Activities 26.0 (MedDRA 26.0), including five levels, system organ class (SOC), high-level group term (HLGT), high-level term (HLT), PT and lowest-level term (LLT). Accordingly, MedDRA was used to classify AEs in each report to the corresponding SOC levels in Python. All fosfomycin-associated cases extracted from the FAERS database were performed pharmacovigilance analysis according to MedDRA at both SOC and PT levels. We then retrieved and described the detailed information, including patient characteristics such as gender, age and weight, indications, reporting areas, outcomes and reporters, *etc.* The specific process of data extraction, processing and analysis is illustrated in Figure 1.

2.4. Data mining

Since we are unsure of the precise denominators, it is not possible to statistically calculate the incidence of

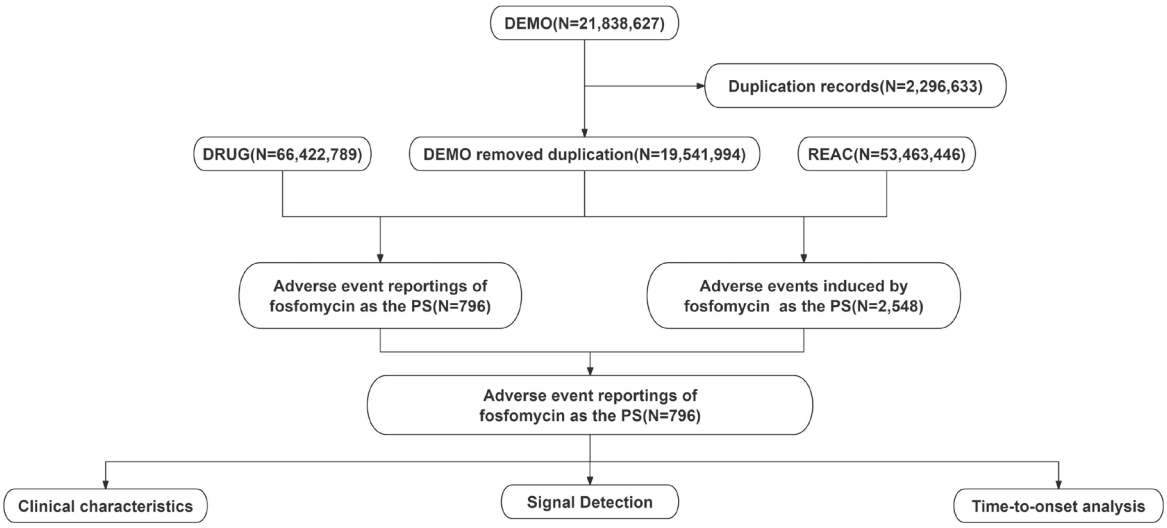

Figure 1. The flow diagram of selecting fosfomycin-related AEs from FAERS. 21,838,627 DEMO, 66,422,789 DRUG, and 53,463,446 REAC records were screened. database adverse event reporting of fosfomycin as the PS (N = 796) was subjected to clinical characteristics, signal detection, and time to onset analysis.

AEs using the FAERS information. Disproportionality analysis, an efficient technique in pharmacovigilance research, can be utilized to recognize indications of disproportionate reporting for adverse events associated with fosfomycin, nevertheless (*8*). The reporting odds ratio (ROR), proportional reporting ratio (PRR), bayesian confidence propagation neural network (BCPNN), and multiitem gamma Poisson shrinker (MGPS) were among the Bayesian and frequentist techniques used to investigate the relationship between fosfomycin and its adverse events. The calculation of the four algorithms is based on the 2 × 2 table of proportional imbalance method (Table 1). AEs were identified as signals when the four algorithms met the criteria simultaneously. The equations and criteria for the four algorithms are shown in Table 2. The higher the indicator value, the stronger the AE signal, suggesting a stronger association between the target drug fosfomycin and its AEs (*9*). PTs and SOCs were used for encoding, categorizing and localizing the signals to analyze the specific SOC involved in AE signals. PTs with reported counts ≥ 3 were selected in our study.

3. Results

3.1. Descriptive analysis

In our study, 21,838,627 AE reports were retained, among which 796 reports were associated with fosfomycin after the exclusion of duplicates. The basic characteristics of patients with fosfomycin-associated AEs were summarized in Table 3. The proportion of women in the reports was significantly higher than men (61.9% *vs.* 11.3%). The patients between 18 and 65 years accounted for the largest proportion (23.1%), while 58.3% of the AEs had missing age data. The top five countries reporting these adverse events were Italy (32.4%), the United States (20.7%), France (9.2%), Spain (4.8%), and Germany (4.4%). The annual reporting trend indicated a notable increase in reports over time, with peak reporting years in 2018 (23.0%) and 2019 (25.8%). More than half of the cases were submitted by Medicine-related workers (68.4%), while 30.3% were submitted by consumers. The reported cases shows a significant rise with peak years in 2018 and 2019, followed by a mild decline.

Table 1. Two-by-two contingency table for disproportionality analyses

	Target Aes	Other AEs	Total
Fosfomycin	A	B	a +b
Other drugs	C	D	c+d
Total	a+c	b+d	a+b+c+d

3.2. Disproportionality analysis

Fosfomycin associated AEs occurrence were distributed across 27 organ systems, the number of case reports for which are shown in Figure 2. The top five SOCs were gastrointestinal disorders (*n* = 415, 16.29%), injury, poisoning and procedural complications (*n* = 344, 13.50%), general disorders and administration site conditions (*n* = 319, 12.52%), skin and subcutaneous tissue disorders (*n* = 287, 11.26%) and nervous system disorders (*n* = 202, 7.93%). Hepatobiliary disorders (ROR = 2.81), pregnancy, puerperium and perinatal conditions (ROR = 2.64), ear and labyrinth disorders (ROR = 2.54), skin and subcutaneous tissue disorders (ROR = 2.22), gastrointestinal disorders (ROR = 2.06) and immune system disorders (ROR = 2.06) were the SOCs with the highest ROR values, indicating a stronger signal for fosfomycin associated AEs (Table 4).

The number of reporting PTs were shown in Table 5, including 35 significant PTs. The results showed that the top 10 PT signals in the reports were off label use, diarrhoea, nausea, product use issue, vomiting, pruritus, urticaria, overdose, dyspnoea and dizziness. Notably, some new and unexpected significant AEs were also found in this study, such as PTs of lip oedema and dysentery.

The analysis of fosfomycin associated AEs in Table 6

Table 2. Four major algorithms used for signal detection

Algorithms	Equation	Criteria
ROR	ROR=ad/b/c 95%CI=$e^{\ln(ROR)\pm1.96(1/a+1/b+1/c+1/d)^{0.5}}$	lower limit of 95% CI>1, N≥3
PRR	PRR=a(c+d)/c/(a+b) χ^2=[(ad-bc)^2](a+b+c+d)/[(a+b)(c+d)(a+c)(b+d)]	PRR≥2, χ^2≥4, N≥3
BCPNN	IC=$\log_2$a(a+b+c+d)(a+c)(a+b) 95%CI= E(IC) ± 2V(IC)^0.5	IC025>0
MGPS	EBGM=a(a+b+c+d)/(a+c)/(a+b) 95%CI=$e^{\ln(EBGM)\pm1.96(1/a+1/b+1/c+1/d)^{0.5}}$	EBGM05>2

Abbreviation: a, number of reports containing both the target drug and target adverse drug reaction; b, number of reports containing other adverse drug reaction of the target drug; c, number of reports containing the target adverse drug reaction of other drugs; d, number of reports containing other drugs and other adverse drug reactions. 95%CI, 95% confidence interval; N, the number of reports; χ2, chi-squared; IC, information component; IC025, the lower limit of 95% CI of the IC; E(IC), the IC expectations; V(IC), the variance of IC; EBGM, empirical Bayesian geometric mean; EBGM05, the lower limit of 95% CI of EBGM.

Table 3. Clinical characteristics of fosfomycin- associated AEs from the FAERS database (Q1 2004 - Q3 2024)

Characteristics	Case numbers	Case proportion (%)
Number of reports	796	
Gender		
Male	90	11.3%
Female	493	61.9%
Miss	213	26.8%
Age(years)		
<18	11	1.4%
18-65	184	23.1%
>65	137	17.2%
Miss	464	58.3%
Top 5 Reported Countries		
Italy	258	32.4%
United States	165	20.7%
France	73	9.2%
Spain	38	4.8%
Germany	35	4.4%
Reporter		
Consumer	241	30.3%
Health professional	45	5.7%
Physician	195	24.5%
Other health-professional	205	25.8%
Pharmacist	99	12.4%
Miss	11	1.4%
Reporting year		
2004	5	1.3%
2005	5	1.3%
2006	2	0.5%
2007	2	0.5%
2008	4	1.0%
2009	7	1.8%
2010	15	3.8%
2011	13	3.3%
2012	29	7.3%
2013	27	6.8%
2014	22	5.6%
2015	39	9.8%
2016	45	11.4%
2017	42	10.6%
2018	91	23.0%
2019	102	25.8%
2020	70	17.7%
2021	77	19.4%
2022	63	15.9%
2023	73	18.4%
2024	63	15.9%

Abbreviation: interquartile range, IQR.

demonstrates that the median time to onset (TTO) was 2 days (IQR: 1.00–6.00 days), with 75% of cases occurring within the first 6 days of treatment. Additionally, the Weibull distribution analysis revealed a shape parameter (β) of 0.59 (95% CI: 0.55–0.64), suggesting a decreasing hazard rate over time.

4. Discussion

Fosfomycin, a long-standing broad-spectrum antibiotic, re-emerges as pivotal in combating multidrug-resistant infections, and its critical role in modern antimicrobial stewardship is underscored by its prominence in managing complex infections (*1-3*). Despite decades of clinical use, the expanding indications and diverse patient populations for fosfomycin have led to a shifting adverse events. Ongoing safety monitoring across various populations is crucial, particularly for the detection and management of potential adverse reactions. The FAERS database serves as a critical platform for collecting and analyzing drug-related adverse AEs, providing essential data for pharmacovigilance and drug safety evaluation (*6*). Our study employs quantitative signal detection methods to analyze fosfomycin associated AEs within the FAERS database, providing evidence based insights to optimize its clinical use.

A systematic review of fosfomycin associated AEs was conducted through structured data mining from the FAERS, covering reports from Q1 2004 to Q3 2024, with 796 cases meeting inclusion criteria. This study noted a slightly higher incidence of AEs in females, a difference not previously reported. The observed gender disparity likely arises from intersecting biological and epidemiological factors. As fosfomycin is FDA (Food and Drug Administration)-approved for urinary tract infections, a condition with 50-fold higher incidence in women, this population inherently experiences greater drug exposure (*10,11*). Sex-specific pharmacokinetic profiles, characterized by prolonged drug elimination and elevated plasma concentrations in women, may exacerbate toxicity risks (*12,13*). Notably, fosfomycin's FDA-approved use in pregnancy introduces a vulnerable subgroup, as that serious adverse reactions are more frequently reported in pregnant women than in non-pregnant women of the same age (*14*). Additionally, female patients are more inclined to report adverse reactions (*15*). These intersecting factors collectively constitute the foundation of the observed gender differences. The analysis of age-related differences was limited to preliminary assessments due to extensive missing data. Lower AEs were observed in children, possibly related to lower drug usage and indeed higher safety in children (*16,17*).

Italy exhibited the highest proportion of fosfomycin related AEs (32.4%), which likely due to Italy's dual role as fosfomycin producer/consumer (*17,18*), combined with potential pharmacogenomic influences. CYP450 enzymes, critical mediators of drug metabolism, demonstrate ethnogeographic variability, with Italian populations displaying distinct CYP2D6 ultra-rapid metabolizer (UM) phenotypic frequencies compared to other European and global cohorts (*13*). Although no direct evidence links CYP2D6-UM status to fosfomycin toxicity, it is hypothesized that accelerated conversion to reactive metabolites or CYP-mediated alterations in renal/hepatic clearance might theoretically elevate AE risks. These genetic predispositions likely interact with regional prescribing patterns (*e.g.*, higher UTI treatment frequency in women) and surveillance biases to amplify observed disparities. Future studies must integrate population-specific CYP genotyping and AE severity

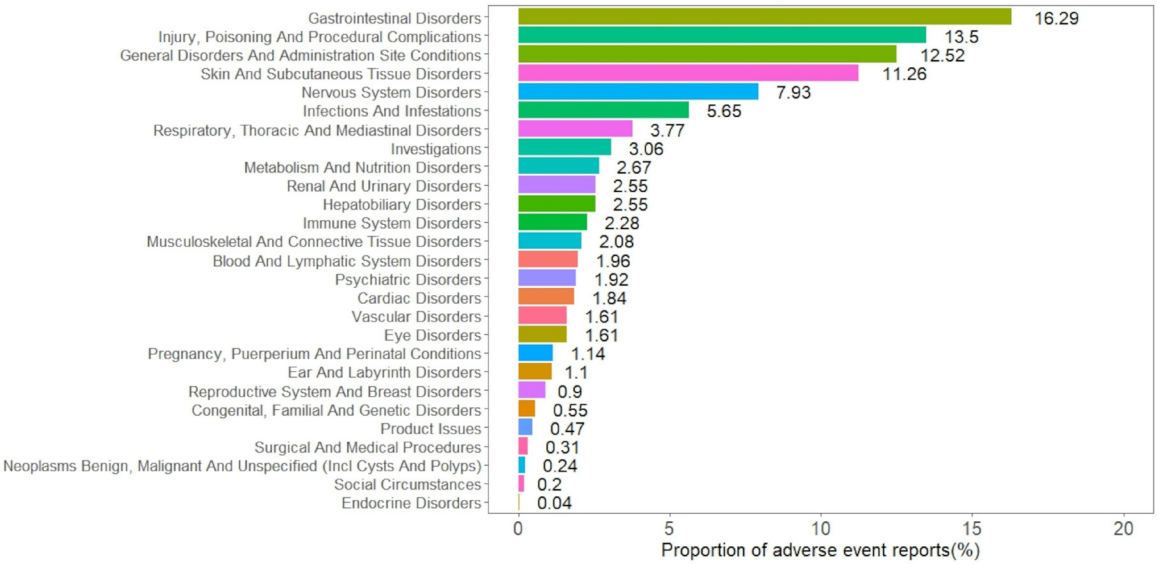

Figure 2. The reported cases of ADEs at each SOC level. The proportion of adverse event reports for each system organ class was shown. Gastrointestinal Disorders had the highest proportion (16.29%), followed by injury, poisoning and procedural complications (13.5%), general disorders and administration site conditions (12.52%), skin and subcutaneous issue disorders (7.93%), and nervous system disorders (6.65%).

Table 4. Signal strength of fosfomycin- associated AEs across system organ classes in the FAERS database

SOC	Numbers	ROR (95%CI)	PRR (χ^2)	EBGM (EBGM05)	IC (IC025)
Gastrointestinal disorders*	415	2.06 (1.86-2.29)	1.89 (190.24)	1.89 (1.73)	0.92 (0.77)
Infections and infestations	144	1.07 (0.9-1.26)	1.06 (0.59)	1.06 (0.92)	0.09 (-0.16)
Injury, poisoning and procedural complications*	344	1.5 (1.34-1.68)	1.43 (49.69)	1.43 (1.3)	0.52 (0.35)
Ear and labyrinth disorders*	28	2.54 (1.75-3.69)	2.53 (25.93)	2.53 (1.85)	1.34 (0.8)
General disorders and administration site conditions	319	0.67 (0.6-0.76)	0.71 (44.62)	0.71 (0.65)	-0.49 (-0.66)
Metabolism and nutrition disorders	68	1.24 (0.97-1.58)	1.23 (3.03)	1.23 (1.01)	0.3 (-0.05)
Investigations	78	0.47 (0.38-0.59)	0.49 (44.26)	0.49 (0.41)	-1.03 (-1.36)
Skin and subcutaneous tissue disorders*	287	2.22 (1.96-2.51)	2.08 (169.97)	2.08 (1.88)	1.06 (0.88)
Renal and urinary disorders*	65	1.38 (1.08-1.77)	1.37 (6.71)	1.37 (1.12)	0.46 (0.1)
Blood and lymphatic system disorders	50	1.15 (0.87-1.51)	1.14 (0.9)	1.14 (0.9)	0.19 (-0.22)
Respiratory, thoracic and mediastinal disorders	96	0.77 (0.63-0.95)	0.78 (6.08)	0.78 (0.66)	-0.35 (-0.65)
Musculoskeletal and connective tissue disorders	53	0.38 (0.29-0.5)	0.39 (53.21)	0.39 (0.31)	-1.36 (-1.75)
Vascular disorders	41	0.73 (0.54-1)	0.74 (3.87)	0.74 (0.57)	-0.44 (-0.89)
Immune system disorders*	58	2.06 (1.59-2.67)	2.03 (30.83)	2.03 (1.64)	1.02 (0.64)
Hepatobiliary disorders*	65	2.81 (2.2-3.6)	2.77 (74.1)	2.77 (2.25)	1.47 (1.11)
Eye disorders	41	0.79 (0.58-1.08)	0.8 (2.19)	0.8 (0.61)	-0.33 (-0.78)
Psychiatric disorders	49	0.32 (0.24-0.43)	0.33 (68.92)	0.33 (0.26)	-1.58 (-1.99)
Cardiac disorders	47	0.68 (0.51-0.91)	0.69 (6.77)	0.69 (0.54)	-0.54 (-0.96)
Nervous system disorders	202	0.92 (0.8-1.06)	0.93 (1.29)	0.93 (0.82)	-0.11 (-0.32)
Congenital, familial and genetic disorders*	14	1.79 (1.06-3.03)	1.79 (4.86)	1.79 (1.15)	0.84 (0.09)
Surgical and medical procedures	8	0.23 (0.11-0.46)	0.23 (20.85)	0.23 (0.13)	-2.12 (-3.08)
Pregnancy, puerperium and perinatal conditions*	29	2.64 (1.83-3.81)	2.62 (29.23)	2.62 (1.93)	1.39 (0.86)
Reproductive system and breast disorders	23	1.09 (0.72-1.64)	1.09 (0.17)	1.09 (0.77)	0.12 (-0.47)
Social circumstances	5	0.45 (0.19-1.08)	0.45 (3.4)	0.45 (0.22)	-1.16 (-2.34)
Endocrine disorders	1	0.15 (0.02-1.09)	0.15 (4.69)	0.15 (0.03)	-2.71 (-4.75)
Product issues	12	0.29 (0.17-0.52)	0.3 (20.17)	0.3 (0.19)	-1.75 (-2.55)
Neoplasms benign, malignant and unspecified (incl cysts and polyps)	6	0.09 (0.04-0.19)	0.09 (58.29)	0.09 (0.05)	-3.51 (-4.6)

Abbreviation: Asterisks (*) indicate statistically significant signals in algorithm; ROR, reporting odds ratio; PRR, proportional reporting ratio; EBGM, empirical Bayesian geometric mean; EBGM05, the lower limit of the 95% CI of EBGM; IC, information component; IC025, the lower limit of the 95% CI of the IC; CI, confidence interval; AEs, adverse events.

assessments to differentiate genetic contributions from confounding sociomedical variables.

The surge in adverse event reports during 2018-2019 likely reflects dual contributing factors. First, international guidelines (*e.g.*, German, Italian, and antimicrobial resistance consensus) issued in 2016–2017 explicitly recommended fosfomycin as first-line therapy for multidrug-resistant UTIs, particularly against ESBL-

Table 5. Top 50 most frequent adverse events for Fosfomycin at the preferred term level from FAERS

PT	Numbers	ROR (95%CI)	PRR (χ^2)	EBGM (EBGM05)	IC (IC025)
Off label use*	112	3.39 (2.8-4.09)	3.28 (180.2)	3.28 (2.8)	1.71 (1.44)
Diarrhoea*	101	3.87 (3.17-4.72)	3.75 (206.14)	3.75 (3.18)	1.91 (1.62)
Nausea*	59	1.79 (1.38-2.32)	1.77 (20.05)	1.77 (1.43)	0.82 (0.45)
Drug ineffective	57	1.02 (0.79-1.33)	1.02 (0.03)	1.02 (0.82)	0.03 (-0.35)
Product use issue*	50	6.66 (5.03-8.81)	6.55 (235.77)	6.55 (5.18)	2.71 (2.3)
Vomiting*	48	2.47 (1.86-3.29)	2.44 (41.2)	2.44 (1.92)	1.29 (0.87)
Pruritus*	43	2.92 (2.16-3.95)	2.89 (53.37)	2.89 (2.24)	1.53 (1.09)
Urticaria*	43	6.39 (4.73-8.64)	6.3 (192.12)	6.3 (4.89)	2.65 (2.22)
Overdose*	40	4.24 (3.1-5.79)	4.19 (97.3)	4.18 (3.22)	2.07 (1.61)
Dyspnoea*	38	1.59 (1.15-2.19)	1.58 (8.16)	1.58 (1.21)	0.66 (0.19)
Headache	34	1.28 (0.91-1.79)	1.27 (2)	1.27 (0.96)	0.35 (-0.14)
Dizzines*s	31	1.47 (1.03-2.09)	1.46 (4.57)	1.46 (1.09)	0.55 (0.04)
Malaise*	29	1.53 (1.06-2.21)	1.52 (5.26)	1.52 (1.12)	0.61 (0.08)
Asthenia*	28	1.76 (1.21-2.55)	1.75 (9)	1.75 (1.28)	0.8 (0.27)
Hypersensitivity*	28	3.59 (2.47-5.21)	3.56 (51.77)	3.56 (2.61)	1.83 (1.29)
Rash*	28	1.57 (1.08-2.28)	1.56 (5.75)	1.56 (1.15)	0.65 (0.11)
Fatigue	27	0.82 (0.56-1.2)	0.82 (1.04)	0.82 (0.6)	-0.28 (-0.83)
Erythema*	27	3.12 (2.13-4.56)	3.1 (38.46)	3.1 (2.25)	1.63 (1.08)
Pyrexia*	23	1.55 (1.03-2.34)	1.55 (4.5)	1.55 (1.1)	0.63 (0.04)
Urinary tract infection*	23	3.23 (2.14-4.88)	3.21 (35.16)	3.21 (2.28)	1.68 (1.09)
Abdominal pain*	21	2.15 (1.4-3.3)	2.14 (12.75)	2.14 (1.49)	1.1 (0.48)
Abdominal pain upper*	20	2.33 (1.5-3.62)	2.32 (15.11)	2.32 (1.61)	1.22 (0.58)
Product use in unapproved indication*	19	2.06 (1.31-3.23)	2.05 (10.23)	2.05 (1.4)	1.03 (0.39)
Pathogen resistance*	17	44.47 (27.58-71.68)	44.18 (715.96)	44.08 (29.57)	5.46 (4.78)
Decreased appetite	15	1.56 (0.94-2.59)	1.55 (2.98)	1.55 (1.02)	0.64 (-0.09)
Syncope*	15	3.49 (2.1-5.8)	3.48 (26.51)	3.48 (2.27)	1.8 (1.07)
Pain	14	0.52 (0.31-0.88)	0.53 (6.06)	0.53 (0.34)	-0.93 (-1.68)
Tachycardia*	13	3.46 (2.01-5.96)	3.45 (22.6)	3.45 (2.18)	1.78 (1.01)
Drug hypersensitivity	13	1.54 (0.89-2.66)	1.54 (2.45)	1.54 (0.97)	0.62 (-0.15)
Hypokalaemia*	12	6.22 (3.53-10.97)	6.2 (52.33)	6.2 (3.85)	2.63 (1.83)
Neutropenia*	12	2.1 (1.19-3.71)	2.1 (6.91)	2.1 (1.31)	1.07 (0.27)
Loss of consciousness*	12	2.19 (1.24-3.86)	2.18 (7.72)	2.18 (1.36)	1.13 (0.32)
Hypotension	11	1.29 (0.71-2.33)	1.29 (0.7)	1.29 (0.78)	0.36 (-0.47)
Condition aggravated	11	0.9 (0.5-1.63)	0.9 (0.12)	0.9 (0.55)	-0.15 (-0.99)
Exposure during pregnancy*	11	4.35 (2.41-7.87)	4.34 (28.26)	4.34 (2.64)	2.12 (1.28)
Prescribed overdose*	10	12.37 (6.65-23.02)	12.32 (104.02)	12.32 (7.32)	3.62 (2.75)
Paraesthesia	10	1.46 (0.79-2.72)	1.46 (1.46)	1.46 (0.87)	0.55 (-0.32)
Tremor	10	1.39 (0.75-2.59)	1.39 (1.11)	1.39 (0.83)	0.48 (-0.39)
Product prescribing error*	10	10.82 (5.82-20.14)	10.78 (88.76)	10.78 (6.41)	3.43 (2.56)
Lip oedema*	10	54.86 (29.46-102.16)	54.64 (525.29)	54.5 (32.39)	5.77 (4.9)
Dysentery*	9	113.39 (58.83-218.57)	113 (993.71)	112.39 (64.9)	6.81 (5.9)
Back pain	9	0.9 (0.47-1.73)	0.9 (0.1)	0.9 (0.52)	-0.15 (-1.06)
Rash erythematous*	9	4.97 (2.58-9.56)	4.95 (28.42)	4.95 (2.86)	2.31 (1.39)
Vertigo*	9	3.44 (1.79-6.61)	3.43 (15.48)	3.43 (1.98)	1.78 (0.86)
Oedema peripheral	8	1.49 (0.74-2.98)	1.49 (1.28)	1.49 (0.83)	0.57 (-0.39)
Abdominal distension	8	1.84 (0.92-3.69)	1.84 (3.09)	1.84 (1.03)	0.88 (-0.08)
Hepatocellular injury*	8	12.64 (6.31-25.31)	12.6 (85.43)	12.6 (7.05)	3.65 (2.69)
Rash maculo-papular*	8	8.71 (4.35-17.43)	8.68 (54.38)	8.68 (4.86)	3.12 (2.15)
Palpitations	8	1.61 (0.8-3.22)	1.61 (1.85)	1.61 (0.9)	0.69 (-0.28)
Dehydration	8	1.4 (0.7-2.79)	1.39 (0.9)	1.39 (0.78)	0.48 (-0.48)

Abbreviation: Asterisks (*) indicate statistically significant signals in algorithm; ROR, reporting odds ratio; PRR, proportional reporting ratio; EBGM, empirical Bayesian geometric mean; EBGM05, the lower limit of the 95% CI of EBGM; IC, information component; IC025, the lower limit of the 95% CI of the IC; CI, confidence interval; PT, preferred term.

Table 6. Time to onset of fosfomycin-associated adverse events and Weibull distribution analysis

Drug	TTO (days)		Weibull distribution		
	Case reports	Median (d)(IQR)	Scale parameter: α (95%CI)	Shape parameter: β (95%CI)	Type
Fosfomycin	225	2.00 (1.00,6.00)	6.43(4.92,7.93)	0.59 (0.55,0.64)	Early failure

Abbreviation: TTO, time to onset; CI, confidence interval; IQR, interquartile range.

producing Enterobacteriaceae and fluoroquinolone-resistant strains (*19-22*), driving increased clinical utilization. Second, enhancements in the FAERS database improved adverse event detection: the 2018 DrugCentral update standardized adverse event terminology and drug coding (*23*), while optimized data mining algorithms (*24*) and expanded consumer reporting mechanisms (*15*) elevated reporting sensitivity and accessibility. This peak likely represents combined effects of heightened drug exposure and improved surveillance efficacy. Further quantification through temporal prescription data and report source analysis would clarify their relative contributions.

Comparing with a decade-old FAERS-based study on fosfomycin associated AEs (*4*) and recent research (*5-6,10,25*), our study revealed that persistent gastrointestinal disorders and skin and subcutaneous tissue disorders, reduced blood and lymphatic system disorders, and the increase of nervous system disorders. This situation may arises from the increasing use of fosfomycin and its ability to penetrate the blood-brain barrier during meningitis (*26-28*), its role in combination therapies with interacting drugs (*29-31*), and its prolonged infusion and administration in patients with renal impairment (*31-32*) – all factors increasing nervous system disorders. Facing this new context of antibiotic use, clinicians should be encouraged to pay closer attention to neurological AEs to enhance patients' experience of care.

Among the SOCs with ROR > 2, we identified two new SOCs with high ROR, namely, pregnancy, puerperium and perinatal conditions and ear and labyrinth disorders. Although fosfomycin is generally considered safe and effective during pregnancy and lactation (*10*), its low protein binding contributes to its good diffusion into fluids and tissues, including placenta and latex (*1-2*), so it has to be considered that fosfomycin may have adverse effects throughout pregnancy. It's worth to explore the ear and labyrinth disorders, as it has been demonstrated that fosfomycin can reduce ototoxicity in combination therapy many years ago (*33,34*). While both SOCs demonstrated statistically significant associations with fosfomycin, the limited case reports in the FAERS database and absence of clinical documentation suggest their overall incidence rates may remain relatively low. Further research and ongoing monitoring are warranted to better elucidate the clinical implications of these findings.

The most frequently reported PT is off-label use, as fosfomycin, while approved for urinary tract infections, it is clinically employed for a variety of infections in multiple anatomical sites (*10,27-32*). Meanwhile, product use issue and overdose, also appeared in the top 10 PTs, which may suggest that fosfomycin's expanded therapeutic scope may increase medication-related risks, necessitating heightened vigilance in clinical practice. Among the other TOP 10 PTs, we identified two special PTs: dyspnoea and dizziness. There is currently no clear evidence based relationship between fosfomycin and dyspnoea. Considering that fosfomycin is now also used for pulmonary infections (*29-32*), it cannot be ruled out that the dyspnoea is due to the patient's underlying disease, which requires close attention in clinical practice. The dizziness is consistent with the increase of nervous system disorders mentioned in the SOC analyses, further suggesting the need for vigilance concerning the neurological AEs associated with the use of fosfomycin.

There are two off-label PTs worth further exploration: lip edema and dysentery. Lip oedema may be classified as one of the skin and subcutaneous tissue disorders; however, it is proposed as a separate PT, and no studies examining the correlation between lip oedema and fosfomycin, which warrants further attention. Fosfomycin is generally used to treat dysentery; however, it can also lead to antibiotic-associated pseudomembranous colitis (*6*). This raises the possibility that fosfomycin may disrupt the normal gut flora, resulting in dysentery-like symptoms, which needs further investigation.

The median TTO was 2 days, and the hazard rate decreased over time, indicating that the fosfomycin associated AEs were early onset. Although some unexpected AEs were found in this study, close monitoring during the early stages of treatment can significantly reduce the risk.

Our study, while providing valuable insights into fosfomycin safety, has several limitations: (1) Potential biases inherent to FAERS' passive surveillance system, including reporting inaccuracies and delays; (2) Inability to determine AE incidence rates due to unavailable total patient exposure data; (3) Demonstration of statistical associations rather than established biological causality. Future research should employ prospective designs integrating epidemiological and clinical trial data to better characterize the drug's safety profile.

5. Conclusion

This study methodically assessed fosfomycin associated AEs through a comprehensive analysis of the FAERS database from Q1 2004 to Q3 2024. Our investigation not only validated known safety information but also uncovered potential risks, including off-label reports of several novel and unexpected AEs such as dyspnoea, dizziness, lip oedema, and dysentery. Our research provides valuable insights for medical practice and public health decision making, and further studies are needed to confirm these findings.

Funding: This work was supported by Suzhou Clinical Centre for Respiratory Infectious Diseases (Szlcyxzx202108) and Suzhou Youth Science and Technology Project (KJXW2023050).

Conflict of Interest: The authors have no conflicts of interest to disclose.

References

1. Falagas ME, Vouloumanou EK, Samonis G, Vardakas KZ. Fosfomycin. Clin Microbiol Rev. 2016; 29:321-347.
2. Kahan FM, Kahan JS, Cassidy PJ, Kropp H. The mechanism of action of fosfomycin (phosphonomycin). Ann N Y Acad Sci. 1974; 235:364-386.
3. Michalopoulos AS, Livaditis IG, Gougoutas V. The revival of fosfomycin. Int J Infect Dis. 2011; 15:e732-e739.
4. Iarikov D, Wassel R, Farley J, Nambiar S. Adverse Events Associated with Fosfomycin Use: Review of the Literature and Analyses of the FDA Adverse Event Reporting System Database. Infect Dis Ther. 2015; 4:433-458.
5. Matusik E, Demanet J, Alves I, Tone A, Ettahar N, Lemtiri J, Potey C, Gautier S, Lambiotte F, Gaboriau L. Fosfomycin-induced agranulocytosis: a case report and review of the literature. BMC Infect Dis. 2023; 23:685.
6. Chen J, Yu W, Zhang W, Sun C, Zhang W. Antibiotics-associated pseudomembranous colitis: a disproportionality analysis of the US food and drug administration adverse event reporting system (FAERS) database. Expert Opin Drug Saf. 2024; 23:1359-1365.
7. Shu Y, Ding Y, Liu Y, Wu P, He X, Zhang Q. Post-marketing safety concerns with secukinumab: A disproportionality analysis of the FDA adverse event reporting system. Front Pharmacol. 2022; 13:862508.
8. Evans SJ, Waller PC, Davis S. Use of proportional reporting ratios (PRRs) for signal generation from spontaneous adverse drug reac tion reports. Pharmacoepidemiol Drug Saf. 2001; 10:483-486.
9. Slattery J, Alvarez Y, Hidalgo A. Choosing thresholds for statistical signal detection with the proportional reporting ratio. Drug Saf. 2013; 36:687-692.
10. Konwar M, Gogtay NJ, Ravi R, Thatte UM, Bose D. Evaluation of efficacy and safety of fosfomycin *versus* nitrofurantoin for the treatment of uncomplicated lower urinary tract infection (UTI) in women - A systematic review and meta-analysis. J Chemother. 2022; 34:139-148.
11. Kwok M, McGeorge S, Mayer-Coverdale J, Graves B, Paterson DL, Harris PNA, Esler R, Dowling C, Britton S, Roberts MJ. Guideline of guidelines: management of recurrent urinary tract infections in women. BJU Int. 2022; 130 Suppl 3(Suppl 3):11-22.
12. Zucker I, Prendergast BJ. Sex differences in pharmacokinetics predict adverse drug reactions in women. Biol Sex Differ. 2020; 11:32.
13. Cacabelos R, Naidoo V, Corzo L, Cacabelos N, Carril JC. Genophenotypic Factors and Pharmacogenomics in Adverse Drug Reactions. Int J Mol Sci. 2021; 22:13302.
14. Balon M, Tessier S, Damase-Michel C, Cottin J, Lambert A, Thompson MA, Benevent J, Lacroix I. Adverse drug reactions in pregnant women: Do they differ from those in non-pregnant women of childbearing age? Therapie. 2023; 78:165-173.
15. Toki T, Ono S. Spontaneous Reporting on Adverse Events by Consumers in the United States: An Analysis of the Food and Drug Administration Adverse Event Reporting System Database. Drugs Real World Outcomes. 2018; 5:117-128.
16. Purcell R, Yeoh D, Bowen A, *et al*. A multicentre, retrospective audit of fosfomycin use for urinary tract infections in Australian children and adolescents. J Antimicrob Chemother. 2023; 78:1616-1621.
17. Roversi M, Musolino A, Di Giuseppe M, Tripiciano C, Cursi L, Lancella L, Krzysztofiak A. Back to the Future: Intravenous Fosfomycin is Safe and Effective for the Treatment of Complicated Infections in Children. Pediatr Infect Dis J. 2024; 43:426-429.
18. Anastasia A, Bonura S, Rubino R, Giammanco GM, Miccichè I, Di Pace MR, Colomba C, Cascio A. The Use of Intravenous Fosfomycin in Clinical Practice: A 5-Year Retrospective Study in a Tertiary Hospital in Italy. Antibiotics (Basel). 2023; 12:971.
19. Kranz J, Schmidt S, Lebert C, Schneidewind L, Mandraka F, Kunze M, Helbig S, Vahlensieck W, Naber K, Schmiemann G, Wagenlehner FM. The 2017 Update of the German Clinical Guideline on Epidemiology, Diagnostics, Therapy, Prevention, and Management of Uncomplicated Urinary Tract Infections in Adult Patients. Part II: Therapy and Prevention. Urol Int. 2018; 100:271-278.
20. Pitout JD, Chan WW, Church DL. Tackling antimicrobial resistance in lower urinary tract infections: treatment options. Expert Rev Anti Infect Ther. 2016; 14:621-632.
21. Kranz J, Schmidt S, Lebert C, Schneidewind L, Schmiemann G, Wagenlehner F. Uncomplicated Bacterial Community-Acquired Urinary Tract Infection in Adults. Dtsch Arztebl Int. 2017; 114:866-873.
22. Concia E, Bragantini D, Mazzaferri F. Clinical evaluation of guidelines and therapeutic approaches in multi drug-resistant urinary tract infections. J Chemother. 2017; 29(sup1):19-28.
23. Ursu O, Holmes J, Bologa CG, Yang JJ, Mathias SL, Stathias V, Nguyen DT, Schürer S, Oprea T. DrugCentral 2018: an update. Nucleic Acids Res. 2019; 47:963-970.
24. Bone A, Houck K. The benefits of data mining. Elife. 2017; 6:e30280.
25. Sojo-Dorado J, López-Hernández I, Rosso-Fernandez C, *et al*. Effectiveness of Fosfomycin for the Treatment of Multidrug-Resistant *Escherichia coli* Bacteremic Urinary Tract Infections: A Randomized Clinical Trial. JAMA Netw Open. 2022; 5:e2137277.
26. Grabein B, Graninger W, Rodríguez Baño J, Dinh A, Liesenfeld DB. Intravenous fosfomycin-back to the future. Systematic review and meta-analysis of the clinical literature. Clin Microbiol Infect. 2017; 23:363-372.
27. Tsegka KG, Voulgaris GL, Kyriakidou M, Falagas ME. Intravenous fosfomycin for the treatment of patients with central nervous system infections: evaluation of the published evidence. Expert Rev Anti Infect Ther. 2020; 18:657-668.
28. Lenzi A, Saccani B, Di Gregorio M, *et al.* Fosfomycin-Containing Regimens for the Treatment of Central Nervous System Infections in a Neonatal Intensive Care Unit: A Case Series Study. Antibiotics (Basel). 2024; 13:667.
29. Butler DA, Patel N, O'Donnell JN, Lodise TP. Combination therapy with IV fosfomycin for adult patients with serious Gram-negative infections: a review of the literature. J Antimicrob Chemother. 2024; 79:2421-2459.
30. Corona A, De Santis V, Agarossi A, Prete A, Cattaneo D, Tomasini G, Bonetti G, Patroni A, Latronico N. Antibiotic Therapy Strategies for Treating Gram-Negative Severe

Infections in the Critically Ill: A Narrative Review. Antibiotics (Basel). 2023; 12:1262.
31. Antonello RM, Di Bella S, Maraolo AE, Luzzati R. Fosfomycin in continuous or prolonged infusion for systemic bacterial infections: a systematic review of its dosing regimen proposal from *in vitro*, *in vivo* and clinical studies. Eur J Clin Microbiol Infect Dis. 2021; 40:1117-1126.
32. Hüppe T, Götz KM, Meiser A, de Faria Fernandes A, Maurer F, Groesdonk HV, Volk T, Lehr T, Kreuer S. Population pharmacokinetic modeling of multiple-dose intravenous fosfomycin in critically ill patients during continuous venovenous hemodialysis. Sci Rep. 2023; 13:18132.
33. Ohtani I, Ohtsuki K, Aikawa T, Sato Y, Anzai T, Ouchi J, Saito T. Protective effect of fosfomycin against aminoglycoside ototoxicity. ORL J Otorhinolaryngol Relat Spec. 1985; 47:42-48.
34. Leach JL, Wright CG, Edwards LB, Meyerhoff WL. Effect of topical fosfomycin on polymyxin B ototoxicity. Arch Otolaryngol Head Neck Surg. 1990; 116:49-53.

Received February 9, 2025; Revised February 22, 2025; Accepted February 23, 2025.

**Address correspondence to:*
Meiying Wu, Department of Pulmonary Medicine, The Fifth People ' s Hospital of Suzhou, Jiangshu, China.
E-mail: wu_my@126.com

Dan Xiao, Department of Infection Disease, The Fifth People ' s Hospital of Suzhou, Suzhou, Jiangshu, China.
E-mail: 596775823@qq.com

Released online in J-STAGE as advance publication February 26, 2025.

Original Article

DOI: 10.5582/ddt.2024.01090

Characteristics and patterns of adverse event reports in the Japanese Adverse Drug Event Report database over two decades (2004–2023): Exploring findings on sexes and age groups

Hiroyuki Tanaka[1,*], Masaki Takigawa[2], Naohito Ide[3], Toshihiro Ishii[1]

[1] Department of Practical Pharmacy, Faculty of Pharmaceutical Sciences, Toho University, Chiba, Japan;
[2] Department of Clinical Pharmaceutics, Faculty of Pharmaceutical Sciences, Toho University, Chiba, Japan;
[3] Department of Practical Pharmacy, Nihon Pharmaceutical University, Saitama, Japan.

SUMMARY: Recently, increased attention has been paid to the consideration of individual characteristics, including sex and age, in the context of medication use and adverse events. However, the characteristics and patterns of adverse events reported in the Japanese Adverse Drug Event Report (JADER) database stratified by sex and age have not yet been clarified. This study aimed to clarify the characteristics and patterns of adverse event reports in the JADER database over a 20-year period (April 2004–March 2024). Data were stratified into 20 groups based on sex and age (aged 0–9 years, 10–19 years, 20–29 years, 30–39 years, 40–49 years, 50–59 years, 60–69 years, 70–79 years, 80–89 years, and ≥90 years). The female/male ratio of adverse event reports in JADER was 0.95. The largest group comprised males in their 70s. Adjusting for the proportion of adverse event reports in each group according to the demographic composition in 2015 highlighted that the reporting rates of adverse events were higher in people aged ≥70 years and that females aged 20–49 years reported more adverse events than males. Medical history, causative drugs, and adverse events reported to JADER were characterized by combinations of sex and age. Our results provide additional insights into the interpretation of previous studies using JADER. In addition, the results of this study will help understand the characteristics of adverse event reports contained in JADER and conduct appropriate subgroup and sensitivity analyses.

Keywords: Japanese Adverse Drug Event Report database, medication safety, pharmacovigilance, reporting patterns, sex–age stratification

1. Introduction

Post-marketing surveillance is essential because not all adverse effects of drugs can be identified in pre-marketing clinical trials. Spontaneous reporting systems for adverse events play an important role in pharmacovigilance by providing information from real-world clinical settings throughout a drug's life. There are a variety of spontaneous adverse event reporting databases in the world, including the World Health Organization's global database of reports on adverse events for medicines and vaccines (VigiBase®) and the Food and Drug Administration (FDA) Adverse Event Reporting System (FAERS). In Japan, the Pharmaceuticals and Medical Devices Agency (PMDA) maintains the Japanese Adverse Drug Event Report (JADER) database, which has accumulated adverse events reported to the PMDA since April 1, 2004.

Various studies have been conducted using databases that report spontaneous adverse events. Most of these are hypothesis-generating studies that utilize signal detection techniques to assess the association between drug use and occurrence of adverse events (*1*). Recently, the use of spontaneous adverse event reporting databases has increased. JADER has also been used in studies to analyze adverse event reporting patterns in specific patient populations, such as children (*2*), the elderly (*3*), pregnant women (*4*), and people living with HIV (*5*), as well as to evaluate the quality of adverse event reporting in Japan (*6*).

Although there are various limitations in interpreting studies using spontaneous adverse event reporting databases, results from studies using FAERS and VigiBase® have been used as evidence that the rate at which females experience adverse drug events is twice that of males (*7,8*). Although pharmacokinetics and pharmacodynamics are typically used to explain these sex differences, many factors can influence the

distribution of adverse event reports by sex, including the well-known disparities in the rates at which males and females use prescription drugs (*9,10*). Conversely, it has been suggested that upon adjusting for sex differences in drug use, the sex differences in adverse event reporting in FAERS may be smaller than previously thought (*11*). Furthermore, studies using VigiBase® have shown that the extent of the sex differences in adverse event reporting is small in the Asian region, including Japan (*8*). Although age, like sex, is a factor that influences disease, medications, vaccination, and the occurrence of adverse events, and may also affect the distribution of adverse event reports, the pattern of adverse event reporting by age in Japan remains unclear.

In this study, adverse event reports stored in the JADER database were stratified by sex and age at 10-year intervals, and the characteristics and patterns of adverse event reports in the various groups classified according to these criteria were analyzed.

2. Materials and Methods

2.1. Data source

Data covering April 2004 to March 2024 were extracted from the JADER database and used in this analysis. In JADER, data are provided in four files: "demo," "drug," "reac," and "hist," and the data in each file can be linked by an identification number. Patient age is rounded to every 10 years (*e.g.*, 10s, 20s, and 30s), although there are also reports of patients registered as first–third trimester pregnancies, infants, children, adults, the elderly, or unknown. As sex and age were the primary variables of interest in this study, only reports in which they could be clearly determined were included in this analysis.

2.2. Demographic data

Information on sex, age, and reporting year is included in the demo file. To characterize adverse event reports by sex and age, the data were stratified into 20 groups based on a combination of sex and age (aged 0–9 years, 10–19 years, 20–29 years, 30–39 years, 40–49 years, 50–59 years, 60–69 years, 70–79 years, 80–89 years, and ≥90 years). In Japan, the national population census is conducted every 5 years. It was conducted four times between 2004 and 2023 (2005, 2010, 2015, and 2020). The 2015 data, which were considered to best reflect population trends within the study period, were used in this study. To visualize the age distribution of adverse event reports relative to that of the national population, the number of reports was normalized to the 2015 national population distribution. Population data were obtained from e-Stat (*https://www.e-stat.go.jp/*; accessed on Nov 9, 2024).

2.3. Medical histories

Information related to medical history (history of present illness, medication history, tobacco use, and alcohol use) is included in the hist file. Medical history is not always registered, possibly due to simple reporting errors. In the case of adverse event reports due to vaccination or drugs used during pregnancy and delivery, there may also be no relevant medical history. Medical history was reported based on the preferred term (PT) levels in the Medical Dictionary for Regulatory Activities (MedDRA). The study listed the top ten medical histories in each group, stratified by sex and age. Additionally, the number and percentage of patients with unregistered medical histories were investigated.

2.4. Causative drugs

Information related to drug use is included in the drug file. Drugs are classified into three categories based on their involvement in the occurrence of adverse events: "suspected drug," "drug interaction," and "concomitant drug." In this study, drugs classified as "suspected drug" or "drug interaction" were defined as "causative drug" based on previous research (*12*). We investigated the generic names of the top 10 causative drugs in each group and mapped them to the second level of the (Anatomical Therapeutic Chemical) ATC code (the main therapeutic class) (*https://www.kegg.jp/brite/br08303*, accessed on Nov 9, 2024). Drugs may have more than one ATC code; in such cases, they were counted under all ATC codes. Two coronavirus RNA vaccines, COMIRNATY® (Pfizer-BioNTech) and Spikevax® (Moderna), were used particularly frequently in Japan and were registered in JADER so that they could be recognized by their generic names; thus, they were counted separately. This information is always available, because each report contains at least one causative drug.

2.5. Adverse events

Information related to the adverse events is included in the reac file. Adverse events registered in the JADER database are based on the MedDRA-PT levels. In this study, we mapped all PT-level adverse events reported in each group to the 27 system organ classes (SOCs) at the top of the MedDRA hierarchy and then removed duplicates. PTs may belong to more than one SOC category. In this study, we counted all the SOCs for each case. This information is always available because each report includes at least one PT-level adverse event.

2.6. Statistical analysis

All data were analyzed using Microsoft® Excel® 2018

(Microsoft Corp., Redmond, WA, USA). In the analysis of adverse events at the SOC level, sex differences were considered to exist if the difference in the proportion of reported events between the sexes in each age group was ≥ 3.0%. This is because the occurrence of any particular adverse event may be low. When applying the chi-square test or Fisher's exact test to analyze big data, very small differences can be detected as statistically significant. Conversely, Cramer's V, as used for the effect size of the chi-square test or Fisher's exact test, tends to be low when the data distribution is skewed (*e.g.*, when most of the data points are concentrated in a specific category). Because the purpose of this study was to understand the overview of JADER, statistical significance was not considered important.

2.7. Ethical considerations

This study was conducted in accordance with the ethical principles of the Declaration of Helsinki and the Ethical Guidelines for Medical and Health Research Involving Human Subjects. This study used only publicly available data and did not involve direct access to study subjects. Therefore, the ethics committee of the author's institution waived the review of this study. All data from JADER were fully anonymized by the relevant regulatory authorities prior to access.

3. Results

3.1. Demographic data

There were 908,928 adverse event reports in the JADER database during the study period, of which 801,163 contained complete information on sex (males, 410,544, females, 390,619; female/male ratio, 0.95) and age. Figure 1 shows the time trend of the number of adverse event reports in the JADER database. A detailed breakdown of the number of adverse event reports for the combinations of sex and age groups is presented in Table 1, and a tree map was created based on this information (Figure 2A). The largest group was males in their 70s, followed by males in their 60s, and females in their 70s. The female/male ratio was < 0.9 in those aged < 10 years and those in their 60s and 70s; it was > 1.1 in those in their 20s, 30s, and 40s, and those ≥ 90 years. Figure 2B shows the tree map created after normalizing the proportion of adverse event reports in

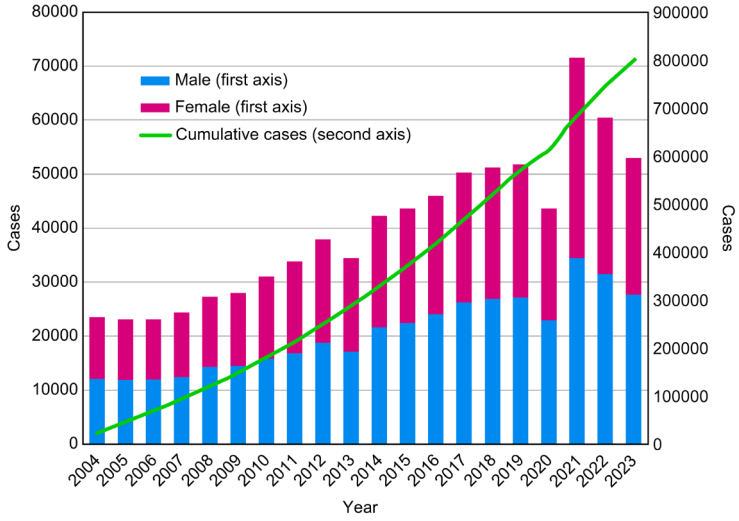

Figure 1. Time trends of the number of adverse event reports in the Japanese Adverse Drug Event Report database.

Table 1. A detailed breakdown of the number of adverse event reports for combinations of sex and age

Age (years)	Male [cases, rate (%)]	Female [cases, rate (%)]	Total [cases, rate (%)]	Female/Male
0–9	15,548 (1.94)	12,122 (1.51)	27,670 (3.45)	0.78
10–19	10,993 (1.37)	11,941 (1.49)	22,934 (2.86)	1.09
20–29	11,187 (1.40)	17,514 (2.19)	28,701 (3.58)	1.57
30–39	17,407 (2.17)	27,339 (3.41)	44,746 (5.59)	1.57
40–49	28,882 (3.61)	35,571 (4.44)	64,453 (8.04)	1.23
50–59	51,183 (6.39)	50,486 (6.30)	101,669 (12.69)	0.99
60–69	97,424 (12.16)	77,160 (9.63)	174,584 (21.79)	0.79
70–79	119,642 (14.93)	91,740 (11.45)	211,382 (26.38)	0.77
80–89	52,869 (6.60)	55,720 (6.95)	108,589 (13.55)	1.05
≥90	5,409 (0.68)	11,026 (1.38)	16,435 (2.05)	2.04
Total	410,544 (51.24)	390,619 (48.76)	801,163 (100)	0.95

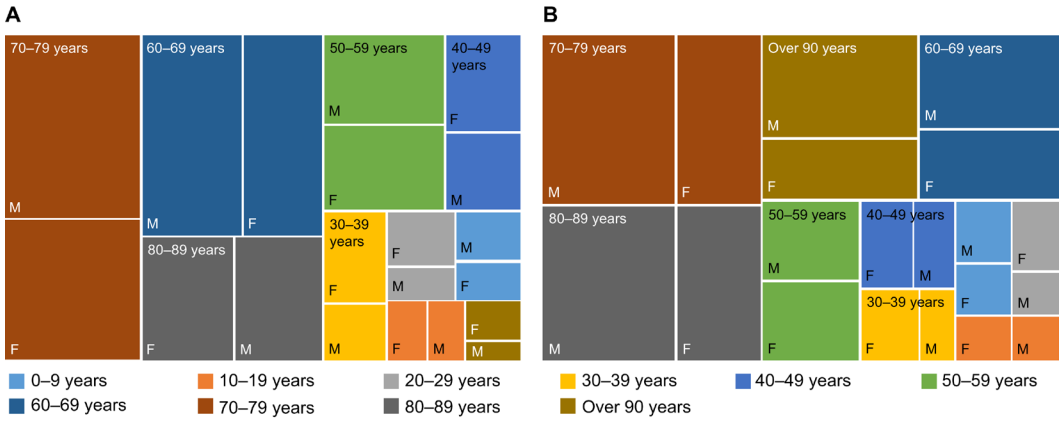

Figure 2. Tree maps based on raw data registered in the Japanese Adverse Drug Event Report database (A) or adjusted to the 2015 Japanese population composition (B). M; male, F; female.

each group to the national population distribution in 2015. Adverse events were reported at a higher rate in the elderly aged ≥ 70 years, and by females more than males in the age group of 20–49 years.

3.2. Medical history

The top ten medical histories for each sex–age group are presented in Table 2. Overall, cancer, infectious diseases, neuropsychiatric disorders, autoimmune diseases, and metabolic syndromes were frequently reported, and their distribution according to sex and age group was similar to that generally known. Hypertension was the most frequently reported medical history in the group aged ≥ 50 years regardless of sex. The rate of unregistered medical histories tended to be higher among the younger age groups than among the older age groups. The concordance rates of the top ten medical histories across different sexes and age groups are shown in Figure 3A. Eight of the top ten medical histories reported for each sex under 10 years of age were common. In other age groups, four to six of the reported top ten medical histories differed between males and females, indicating sex differences in medical history. When examining the concordance rates of medical histories between the age groups for each sex, a high degree of similarity was often observed between adjacent age groups (Figures 3B and 3C). The lowest concordance rate in medical histories between adjacent age groups was observed between males aged 10–19 years and those aged 20–29 years (3/10, 30%), and between females aged < 10 years and those aged 10–19 years (4/10, 40%).

3.3. Causative drugs

The top ten causative drugs in each group, classified by the combination of sex and age, are listed in Table 3. Prednisolone ranked among the top ten causative drugs in most groups, followed by Coronavirus (SARS-CoV-2) RNA vaccine (COMIRNATY®) and tacrolimus hydrate. The distribution of the ATC codes for the top ten causative drugs according to sex and age is shown in Figure 4. The causative drugs reported in females had a wider distribution of ATC codes than those in males (27 *vs.* 23). Drugs belonging to the B01 class (antithrombotic agents) were frequently reported in both males and females aged ≥ 80 years. Drugs belonging to the J07 class (vaccines) were frequently reported in younger age groups. Drugs belonging to the L01 class (antineoplastic agents) were reported more frequently in the 10–19 and 40–79-year age groups, indicating a bimodal distribution. Drugs belonging to the L04 class (immunosuppressants) were reported more frequently in the 10–49-year age group in both males and females.

3.4. Adverse events

Figure 5 shows the reporting rate of SOC-level adverse events in each group divided by sex and age. Among those in their 10s to 40s, there were many SOC-level adverse events, with a difference of 3% or more in reporting rates between males and females. The reporting rate of nervous system disorders among teenage girls was particularly high. The reporting rates of infections and infestations were higher in males than in females aged 10–39 years. Immune system disorders were reported more frequently in females than in males aged between 20–49 years, and more frequently in males than in females in their 70s and 80s. Cardiac disorders were reported more frequently in females than in males in the 10s age group. The reporting rate of vascular disorders was higher in females than in males aged 10–49 years. The reporting rate of respiratory, thoracic, and mediastinal disorders was higher in males than in females over 60 years old. The reporting rates of skin and subcutaneous tissue disorders were higher in females than in males aged 10–59 years. Musculoskeletal and connective tissue disorders were reported more frequently in females than in males in

Table 2. The top ten medical histories for each sex–age group

Medical history	Number of cases	Rate (%)	Medical history	Number of cases	Rate (%)
Male, 0–9 years			**Female, 0–9 years**		
Influenza	526	3.38	Epilepsy	436	3.60
Asthma	516	3.32	Influenza	312	2.57
Epilepsy	472	3.04	Acute lymphocytic leukemia	289	2.38
Kawasaki's disease	419	2.69	Asthma	279	2.30
Acute lymphocytic leukemia	334	2.15	Kawasaki's disease	228	1.88
Patent ductus arteriosus	272	1.75	Patent ductus arteriosus	221	1.82
Nephrotic syndrome	268	1.72	Pyrexia	169	1.39
Factor VIII deficiency	198	1.27	Nephrotic syndrome	164	1.35
Pyrexia	196	1.26	Neuroblastoma	153	1.26
Attention deficit hyperactivity disorder	193	1.24	Premature baby	146	1.20
Unregistered	6,496	41.78	Unregistered	5,221	43.07
Male, 10–19 years			**Female, 10–19 years**		
Influenza	619	5.63	Epilepsy	531	4.45
Epilepsy	588	5.35	Acute lymphocytic leukemia	321	2.69
Acute lymphocytic leukemia	413	3.76	Influenza	274	2.29
Attention deficit hyperactivity disorder	404	3.68	Asthma	254	2.13
Colitis ulcerative	311	2.83	Acute myeloid leukemia	180	1.51
Asthma	288	2.62	Systemic lupus erythematosus	174	1.46
Autism spectrum disorder	270	2.46	Colitis ulcerative	173	1.45
Intellectual disability	215	1.96	Rhinitis allergic	168	1.41
Nephrotic syndrome	215	1.96	Non-tobacco user	148	1.24
Rhinitis allergic	206	1.87	Schizophrenia	143	1.20
Unregistered	3,372	30.67	Unregistered	4,974	41.65
Male, 20–29 years			**Female, 20–29 years**		
Schizophrenia	648	5.79	Schizophrenia	749	4.28
Colitis ulcerative	503	4.50	Depression	575	3.28
Epilepsy	431	3.85	Epilepsy	558	3.19
Depression	298	2.66	Systemic lupus erythematosus	430	2.46
Crohn's disease	270	2.41	Non-tobacco user	315	1.80
HIV infection	204	1.82	Colitis ulcerative	311	1.78
Insomnia	193	1.73	Dysmenorrhea	306	1.75
Intellectual disability	164	1.47	Asthma	286	1.63
Non-tobacco user	153	1.37	Insomnia	260	1.48
Hypertension	152	1.36	Bipolar disorder	234	1.34
Unregistered	3,731	33.35	Unregistered	6,446	36.80
Male, 30–39 years			**Female, 30–39 years**		
Schizophrenia	1,167	6.70	Schizophrenia	1,114	4.07
Hypertension	673	3.87	Systemic lupus erythematosus	816	2.98
HIV infection	586	3.37	Depression	759	2.78
Depression	493	2.83	Rheumatoid arthritis	626	2.29
Epilepsy	488	2.80	Asthma	573	2.10
Colitis ulcerative	440	2.53	Epilepsy	564	2.06
Diabetes mellitus	353	2.03	Hypertension	510	1.87
Hyperuricemia	346	1.99	Insomnia	493	1.80
Crohn's disease	343	1.97	Breast cancer	420	1.54
Insomnia	335	1.92	Non-tobacco user	418	1.53
Unregistered	5,116	29.39	Unregistered	8,982	32.85
Male, 40–49 years			**Female, 40–49 years**		
Hypertension	2,526	8.75	Breast cancer	1,775	5.00
Schizophrenia	1,627	5.63	Hypertension	1,553	4.37
Diabetes mellitus	1,470	5.09	Schizophrenia	1,366	3.84
Hyperuricemia	884	3.06	Rheumatoid arthritis	1,274	2.46
Hyperlipidemia	804	2.78	Depression	876	2.26
Depression	783	2.71	Uterine leiomyoma	854	2.11
Type 2 diabetes mellitus	764	2.65	Asthma	803	2.10
Tobacco user	725	2.51	Diabetes mellitus	749	2.03
Alcohol use	677	2.34	Systemic lupus erythematosus	748	1.92
Insomnia	672	2.33	Metastases to lymph nodes	722	1.87
Unregistered	7,265	25.15	Unregistered	10,188	28.64

Table 2. The top ten medical histories for each sex–age group (continued)

Medical history	Number of cases	Rate (%)	Medical history	Number of cases	Rate (%)
Male, 50–59 years			**Female, 50–59 years**		
Hypertension	6,535	12.77	Hypertension	4,201	8.32
Diabetes mellitus	3,813	7.45	Rheumatoid arthritis	3,109	6.16
Type 2 diabetes mellitus	1,840	3.59	Breast cancer	2,807	5.56
Metastases to lymph nodes	1,782	3.48	Diabetes mellitus	2,020	4.00
Metastases to lung	1,696	3.31	Metastases to lymph nodes	1,501	2.97
Hyperuricemia	1,593	3.11	Metastases to bone	1,459	2.89
Tobacco user	1,584	3.09	Hyperlipidemia	1,385	2.74
Hyperlipidemia	1,569	3.07	Metastases to lung	1,353	2.68
Schizophrenia	1,519	2.97	Metastases to liver	1,279	2.53
Alcohol use	1,382	2.70	Schizophrenia	1,256	2.49
Unregistered	11,870	23.19	Unregistered	12,740	25.23
Male, 60–69 years			**Female, 60–69 years**		
Hypertension	16,271	16.70	Hypertension	10,693	13.86
Diabetes mellitus	9,178	9.42	Rheumatoid arthritis	6,235	8.08
Metastases to lymph nodes	4,377	4.49	Diabetes mellitus	4,729	6.13
Metastases to lung	3,867	3.97	Breast cancer	3,573	4.63
Type 2 diabetes mellitus	3,856	3.96	Hyperlipidemia	3,155	4.09
Atrial fibrillation	3,396	3.49	Osteoporosis	3,143	4.07
Hyperuricemia	3,263	3.35	Metastases to lymph nodes	2,509	3.25
Tobacco user	3,254	3.34	Metastases to lung	2,478	3.21
Hyperlipidemia	3,108	3.19	Metastases to bone	2,205	2.86
Alcohol use	3,076	3.16	Constipation	2,072	2.69
Unregistered	19,854	20.38	Unregistered	16,903	21.91
Male, 70–79 years			**Female, 70–79 years**		
Hypertension	22,472	18.78	Hypertension	17,274	18.83
Diabetes mellitus	11,799	9.86	Rheumatoid arthritis	7,424	8.09
Atrial fibrillation	6,780	5.67	Diabetes mellitus	6,681	7.28
Metastases to lymph nodes	5,214	4.36	Osteoporosis	6,428	7.01
Type 2 diabetes mellitus	4,710	3.94	Hyperlipidemia	4,277	4.66
Metastases to lung	4,377	3.66	Atrial fibrillation	3,444	3.75
Benign prostatic hyperplasia	4,083	3.41	Dyslipidemia	2,910	3.17
Non-small cell lung cancer	4,075	3.41	Constipation	2,906	3.17
Chronic kidney disease	4,075	3.41	Insomnia	2,717	2.96
Hyperuricemia	3,915	3.27	Type 2 diabetes mellitus	2,647	2.89
Unregistered	23,712	19.82	Unregistered	19,904	21.70
Male, 80–89 years			**Female, 80–89 years**		
Hypertension	11,238	21.26	Hypertension	12,797	22.97
Atrial fibrillation	4,892	9.25	Osteoporosis	5,914	10.61
Diabetes mellitus	4,857	9.19	Atrial fibrillation	4,163	7.47
Benign prostatic hyperplasia	2,948	5.58	Diabetes mellitus	3,890	6.98
Chronic kidney disease	2,684	5.08	Rheumatoid arthritis	3,286	5.90
Prostate cancer	2,610	4.94	Hyperlipidemia	2,268	4.07
Type 2 diabetes mellitus	2,153	4.07	Constipation	2,187	3.92
Cerebral infarction	2,068	3.91	Chronic kidney disease	2,184	3.67
Hyperuricemia	1,975	3.74	Dementia	2,045	3.57
Constipation	1,807	3.42	Dyslipidemia	1,987	3.41
Unregistered	11,317	21.41	Unregistered	12,697	22.79
Male, ≥90 years			**Female, ≥90 years**		
Hypertension	1,077	19.91	Hypertension	2,595	23.54
Atrial fibrillation	560	10.35	Osteoporosis	1,091	9.89
Benign prostatic hyperplasia	372	6.88	Atrial fibrillation	992	9.00
Diabetes mellitus	336	6.21	Dementia	758	6.87
Prostate cancer	323	5.97	Diabetes mellitus	671	6.09
Chronic kidney disease	322	5.95	Cardiac failure	646	5.86
Cardiac failure	293	5.42	Cardiac failure chronic	637	5.78
Cardiac failure chronic	289	5.34	Chronic kidney disease	581	5.27
Cerebral infarction	259	4.79	Constipation	553	5.02
Dementia	257	4.75	Dementia Alzheimer's type	531	4.82
Unregistered	1,357	25.09	Unregistered	2,921	26.49

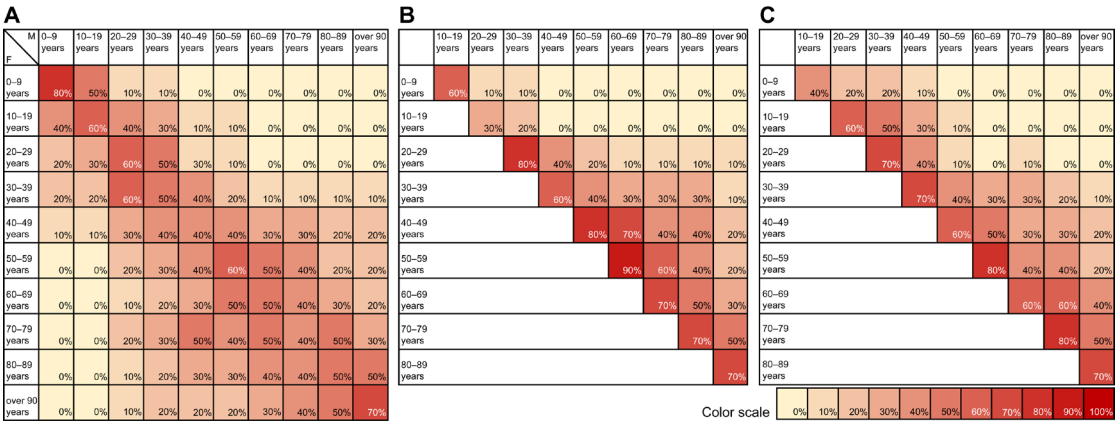

Figure 3. Concordance rate of the top ten medical histories. **A**; females *vs.* males, **B**; male, **C**; female.

the 10s and 80s age groups. Reports of pregnancy, puerperium, and perinatal conditions were mostly concentrated in the under 10, 20s, and 30s age groups, with a higher reporting rate among females than among males in the 20s and 30s age groups. The reporting rate of reproductive system and breast disorders was higher in females than in males aged between 20–49 years. The reporting rates of metabolic and nutritional disorders were higher in females than in males aged ≥ 90 years.

4. Discussion

In this study, we clarified the characteristics and reporting patterns of adverse event reports accumulated in the JADER database over a 20-year period, stratified by sex and age. The results of this study provide important insights that deepen the understanding of research using JADER.

The number of adverse event reports in the JADER database is increasing. Between 2020 and 2022, the number of reports may have varied due to changes in the healthcare system following the COVID-19 pandemic, increased use of the COVID-19 vaccine, and delays in adverse event reporting due to the workload faced by healthcare workers (*13*). In the United States, data have been accumulated in the Vaccine Adverse Event Reporting System (VAERS), which is a monitoring system that identifies immunization safety issues (*14*). However, the post-marketing adverse events of drugs accumulate in the FAERS. Recent studies have shown that the rapid increase in adverse event reports associated with the COVID-19 vaccine affects the results of signal detection based on disproportionality analysis using JADER, VigiBase® and EudraVigilance (*15-18*). Therefore, it is recommended that these databases be analyzed after excluding COVID-19 vaccine reports. In contrast, the FAERS was unaffected by the pandemic because all COVID-19 vaccine reports were included in a separate VAERS database. Currently, a system for collecting spontaneous reports of adverse events specific to vaccination has not been established in Japan; however, the establishment of a vaccine-specific adverse event reporting system should be discussed in the future.

In recent years, increased attention has been paid to the consideration of individual characteristics, including sex and age, in the context of medication use and adverse drug events (*19*). As the spontaneous adverse event reporting database does not contain baseline information on drug use, it is not possible to calculate the incidence of adverse events. Nonetheless, many researchers are recognizing the benefits of using spontaneous adverse event reporting databases and are further exploring methodologies to identify the risk of adverse events by sex and age (*7,20*). We support the promotion of this type of research but believe that a prerequisite is to understand the characteristics of the information contained in spontaneous adverse event report databases. However, the characteristics and patterns of adverse event reporting in the JADER database stratified by sex and age have not yet been clarified. In this study, the female/male ratio of all adverse event reports registered in JADER was 0.95, and no sex differences were observed. This fact appears to be supported by the results of an analysis in the Asian region using VigiBase® (*8*). In contrast, when groups were compared based on combined sex and age, sex differences in adverse event reporting were evident within certain groups. In general, sex and age affect the incidence of side effects. Sex-specific drug prescriptions may confound the assessment of associations between other medications and adverse event reports. For example, drug treatments for breast cancer, dysmenorrhea, prostate cancer, and benign prostatic hyperplasia generally have sex-specific adverse effects. These issues extend to other confounding factors such as age and concomitant medications. Older age and the concomitant use of medications are known risk factors for side effects (*21*). Females tend to live longer than males and take more medications simultaneously (*22,23*), which could induce further aggregate

Table 3. The top ten causative drugs in each group classified by the combination of sex and age

Sex	Age (years)	Causative drugs [ATC code; number of cases]
Male	0–9	Hemophilus b conjugate vaccine (tetanus toxoid conjugate) [J07; 1,447], Pneumococcal 13-valent conjugate vaccine [J07; 1,195], Live attenuated human rotavirus vaccine, oral [J07; 809], Recombinant adsorbed hepatitis B vaccine (yeast-derived) [J07; 691], Adsorbed diphtheria-purified pertussis-tetanus-inactivated polio (sabin strain) combined vaccine [J07; 631], Influenza HA vaccine [J07; 623], Tacrolimus hydrate [L04, D11; 597], Prednisolone [A01, A07, C05, D07, H02, R01, S01, S02, S03; 454], Freeze-dried live attenuated mumps vaccine [J07; 420], Oseltamivir phosphate [J05; 412]
	10–19	Coronavirus (SARS-CoV-2) RNA vaccine (COMIRNATY®) [J07; 714], Tacrolimus hydrate [L04, D11; 532], Prednisolone [A01, A07, C05, D07, H02, R01, S01, S02, S03; 493], Methotrexate [L01, L04; 374], Cyclosporine [L04, S01; 366], Zanamivir hydrate [J05; 311], Etoposide [L01; 287], Carbamazepine [N03; 285], Cyclophosphamide hydrate [L01; 282], Acetaminophen [N02, 279]
	20–29	Coronavirus (SARS-CoV-2) RNA vaccine (COMIRNATY®) [J07; 649], Coronavirus (SARS-CoV-2) RNA vaccine (Spikevax®) [J07; 598], Tacrolimus hydrate [L04, D11; 489], Mesalazine [A07; 374], Prednisolone [A01, A07, C05, D07, H02, R01, S01, S02, S03; 368], Mycophenolate mofetil [L04; 262], Cyclosporine [L04, S01; 261], Infliximab (genetical recombination) [L04; 219], Carbamazepine [N03; 214], Loxoprofen sodium hydrate [M02; 210]
	30–39	Coronavirus (SARS-CoV-2) RNA vaccine (COMIRNATY®) [J07; 684], Tacrolimus hydrate [L04, D11; 661], Prednisolone [A01, A07, C05, D07, H02, R01, S01, S02, S03; 607], Mycophenolate mofetil [L04; 478], Cyclosporine [L04, S01; 432], Loxoprofen sodium hydrate [M02; 392], Clozapine [N05; 388], Coronavirus (SARS-CoV-2) RNA vaccine (Spikevax®) [J07; 350], Infliximab (genetical recombination) [L04; 333], Carbamazepine [N03; 323]
	40–49	Prednisolone [A01, A07, C05, D07, H02, R01, S01, S02, S03; 962], Tacrolimus hydrate [L04, D11; 899], Coronavirus (SARS-CoV-2) RNA vaccine (COMIRNATY®) [J07; 829], Nivolumab (genetical recombination) [L01; 782], Ribavirin [J05; 644], Mycophenolate mofetil [L04; 643], Clozapine [N05; 587], Cyclosporine [L04, S01; 555], Ipilimumab (genetical recombination) [L01; 512], Peginterferon alfa-2b (genetical recombination) [L03; 479]
	50–59	Nivolumab (genetical recombination) [L01; 2,329], Prednisolone [A01, A07, C05, D07, H02, R01, S01, S02, S03; 1,553], Ribavirin [J05; 1,479], Ipilimumab (genetical recombination) [L01; 1,353], Tacrolimus hydrate [L04, D11; 1,311], Cisplatin [L01; 1,215], Oxaliplatin [L01; 1,200], Bevacizumab (genetical recombination) [L01; 1,143], Pembrolizumab (genetical recombination) [L01; 1,069], Peginterferon alfa-2b (genetical recombination) [L03; 1,052]
	60–69	Nivolumab (genetical recombination) [L01; 5,496], Pembrolizumab (genetical recombination) [L01; 3,128], Bevacizumab (genetical recombination) [L01; 3,049], Cisplatin [L01; 2,770], Prednisolone [A01, A07, C05, D07, H02, R01, S01, S02, S03; 2,745], Ipilimumab (genetical recombination) [L01; 2,660], Oxaliplatin [L01; 2,525], Fluorouracil [L01; 2,269], Methotrexate [L01, L04; 2,242], Ribavirin [J05; 2,131]
	70–79	Nivolumab (genetical recombination) [L01; 6,985], Pembrolizumab (genetical recombination) [L01; 4,788], Ipilimumab (genetical recombination) [L01; 3,614], Prednisolone [A01, A07, C05, D07, H02, R01, S01, S02, S03; 3,041], Bevacizumab (genetical recombination) [L01; 2,869], Aspirin [A01, B01, N02; 2,413], Carboplatin [L01; 2,393], Tegafur, gimeracil and oteracil potassium [L01; 2,339], Cisplatin [L01; 2,312], Methotrexate [L01, L04; 2,244]
	80–89	Apixaban [B01; 1,591], Nivolumab (genetical recombination) [L01; 1,507], Aspirin [A01, B01, N02; 1,454], Pembrolizumab (genetical recombination) [L01; 1,260], Prednisolone [A01, A07, C05, D07, H02, R01, S01, S02, S03; 1,202], Coronavirus (SARS-CoV-2) RNA vaccine (COMIRNATY®) [J07; 1,188], Clopidogrel sulfate [B01; 1,110], Rivaroxaban [B01; 1,026], Warfarin potassium [B01; 780], Ipilimumab (genetical recombination) [L01; 760]
	Over 90	Coronavirus (SARS-CoV-2) RNA vaccine (COMIRNATY®) [J07; 277], Apixaban [B01; 243], Aspirin [A01, B01, N02; 135], Rivaroxaban [B01; 133], Edoxaban tosilate hydrate [B01; 114], Enzalutamide [L02; 113], Irradiated red blood cells, leukocytes reduced [B05; 105], Leuprorelin acetate [L02, 98], Roxadustat [B03, 93], Clopidogrel sulfate [B01; 78]

associations. This study revealed that more than half of the adverse event reports included in JADER were from individuals aged 60–89 years. Furthermore, after adjusting the adverse event reports included in JADER to the national population distribution in 2015, it was highlighted that adverse events were reported more frequently in elderly individuals aged ≥ 70 years, and that in individuals aged 10–49 years, the reporting rate of adverse events was higher in females than in males. When comparing JADER with other spontaneous adverse event reporting databases, it is important to provide detailed descriptions of the demographics of each database.

Medical history analysis showed that eight of the top ten medical histories were shared by males and females under 10 years of age, confirming the high concordance rate of medical history. In other age groups, four to six items differed between males and females, confirming sex differences in medical history. Sex is a key factor in many aspects of healthcare, including pregnancy and childbirth, prevalence of chronic diseases, healthcare utilization, and medication use (*19*). Previous studies

Table 3. The top ten causative drugs in each group classified by the combination of sex and age (continued)

Sex	Age (years)	Causative drugs [ATC code; number of cases]
Female	0–9	Hemophilus b conjugate vaccine (tetanus toxoid conjugate) [J07; 1,284], Pneumococcal 13-valent conjugate vaccine [J07; 1,082], Live attenuated human rotavirus vaccine, oral [J07; 731], Recombinant adsorbed hepatitis B vaccine (yeast-derived) [J07; 594], Adsorbed diphtheria-purified pertussis-tetanus-inactivated polio (sabin strain) combined vaccine [J07; 536], Tacrolimus hydrate [L04, D11; 534], Influenza HA vaccine [J07; 367], Rotavirus vaccine, live, oral, pentavalent [J07; 348], Pneumococcal polysaccharide conjugate vaccine [J07; 323], Prednisolone [A01, A07, C05, D07, H02, R01, S01, S02, S03; 315]
	10–19	Recombinant adsorbed bivalent human papillomavirus-like particle vaccine (derived from Trichoplusia ni cells) [J07; 1,567], Coronavirus (SARS-CoV-2) RNA vaccine(COMIRNATY®) [J07; 642], Recombinant adsorbed quadrivalent human papillomavirus virus-like particle vaccine (yeast origin) [J07; 551], Prednisolone [A01, A07, C05, D07, H02, R01, S01, S02, S03; 550], Tacrolimus hydrate [L04, D11; 453], Methotrexate [L01, L04; 338], Acetaminophen [N02, 282], Etoposide [L01, 267], Cyclosporine [L04, S01; 366], Mycophenolate mofetil [L04; 245]
	20–29	Coronavirus (SARS-CoV-2) RNA vaccine (COMIRNATY®) [J07; 1,714], Prednisolone [A01, A07, C05, D07, H02, R01, S01, S02, S03; 629], Tacrolimus hydrate [L04, D11; 543], Lamotrigine [N03; 487], Coronavirus (SARS-CoV-2) RNA vaccine (Spikevax®) [J07; 422], Loxoprofen sodium hydrate [M02; 387], Ritodrine hydrochloride [G02; 341], Drospirenone and ethinylestradiol betadex [G03; 324], Carbamazepine [N03; 310], Cyclosporine [L04, S01; 300]
	30–39	Coronavirus (SARS-CoV-2) RNA vaccine (COMIRNATY®) [J07; 2,027], Prednisolone [A01, A07, C05, D07, H02, R01, S01, S02, S03; 998], Tacrolimus hydrate [L04, D11; 878], Ritodrine hydrochloride [G02; 615], Loxoprofen sodium hydrate [M02; 549], Lamotrigine [N03; 542], Human menopausal gonadotrophin [G03; 518], Methotrexate [L01, L04; 467], Human chorionic gonadotrophin [G03; 463], Mycophenolate mofetil [L04; 422]
	40–49	Coronavirus (SARS-CoV-2) RNA vaccine (COMIRNATY®) [J07; 2,802], Prednisolone [A01, A07, C05, D07, H02, R01, S01, S02, S03; 1,292], Tacrolimus hydrate [L04, D11; 1,023], Methotrexate [L01, L04; 943], Paclitaxel [L01; 745], Bevacizumab (genetical recombination) [L01; 729], Cyclophosphamide hydrate [L01; 638], Pembrolizumab (genetical recombination) [L01; 551], Mycophenolate mofetil [L04; 508], Loxoprofen sodium hydrate [M02; 473]
	50–59	Methotrexate [L01, L04; 2,330], Coronavirus (SARS-CoV-2) RNA vaccine (COMIRNATY®) [J07; 2,298], Prednisolone [A01, A07, C05, D07, H02, R01, S01, S02, S03; 1,959], Bevacizumab (genetical recombination) [L01; 1,362], Pembrolizumab (genetical recombination) [L01; 1,360], Paclitaxel [L01; 1,233], Tacrolimus hydrate [L04, D11; 1,219], Ribavirin [J05; 1,147], Carboplatin [L01; 900], Cyclophosphamide hydrate [L01; 865]
	60–69	Methotrexate [L01, L04; 4,714], Prednisolone [A01, A07, C05, D07, H02, R01, S01, S02, S03; 3,065], Ribavirin [J05; 2,305], Bevacizumab (genetical recombination) [L01; 2,174], Pembrolizumab (genetical recombination) [L01; 2,057], Nivolumab (genetical recombination) [L01; 1,742], Coronavirus (SARS-CoV-2) RNA vaccine (COMIRNATY®) [J07; 1,593], Paclitaxel [L01; 1,576], Peginterferon alfa-2b (genetical recombination) [L03; 1,568], Tacrolimus hydrate [L04, D11; 1,443]
	70–79	Methotrexate [L01, L04; 5,418], Prednisolone [A01, A07, C05, D07, H02, R01, S01, S02, S03; 3,217], Nivolumab (genetical recombination) [L01; 2,247], Pembrolizumab (genetical recombination) [L01; 2,144], Bevacizumab (genetical recombination) [L01; 1,797], Coronavirus (SARS-CoV-2) RNA vaccine (COMIRNATY®) [J07; 1,744], Lenalidomide hydrate [L04; 1,393], Dexamethasone [A01, C05, D07, D10, H02, R01, S01, S02, S03; 1,355], Carboplatin [L01; 1,224], Ipilimumab (genetical recombination) [L01; 1,208]
	80–89	Methotrexate [L01, L04; 1,892], Coronavirus (SARS-CoV-2) RNA vaccine (COMIRNATY®) [J07; 1,577], Apixaban [B01; 1,494], Prednisolone [A01, A07, C05, D07, H02, R01, S01, S02, S03; 1,316], Aspirin [A01, B01, N02; 1,031], Valaciclovir hydrochloride [J05; 986], Rivaroxaban [B01; 932], Alendronate sodium hydrate [M05; 870], Pregabalin [N02; 783], Clopidogrel sulfate [B01; 776]
	Over 90	Coronavirus (SARS-CoV-2) RNA vaccine (COMIRNATY®) [J07; 624], Apixaban [B01; 541], Valaciclovir hydrochloride [J05; 347], Aspirin [A01, B01, N02; 253], Rivaroxaban [B01; 241], Irradiated red blood cells, leukocytes reduced [B05; 204], Edoxaban tosilate hydrate [B01; 199], Furosemide [C03; 181], Glimepiride [A10; 177], Sacubitril valsartan sodium hydrate [C09; 173]

have shown that approximately 27% of the cases enrolled in JADER were patients with cancer treated with antineoplastic agents (*24*). In this study, breast cancer, a cancer specific to women, was ranked in the top ten for those in their 20s to 60s, while prostate cancer, a cancer specific to men, was ranked in the top ten for those in their 80s and older. Furthermore, when comparing the medical histories between age groups, high similarities were often found between adjacent age groups in both males and females. The lowest concordance rates in medical history between adjacent age groups were between the 10s and 20s for males (3/10, 30%) and between < 10 years and 10–19 years for females (4/10, 40%). This information may be useful for performing subgroup analyses.

In the analysis of the causative drugs, reporting

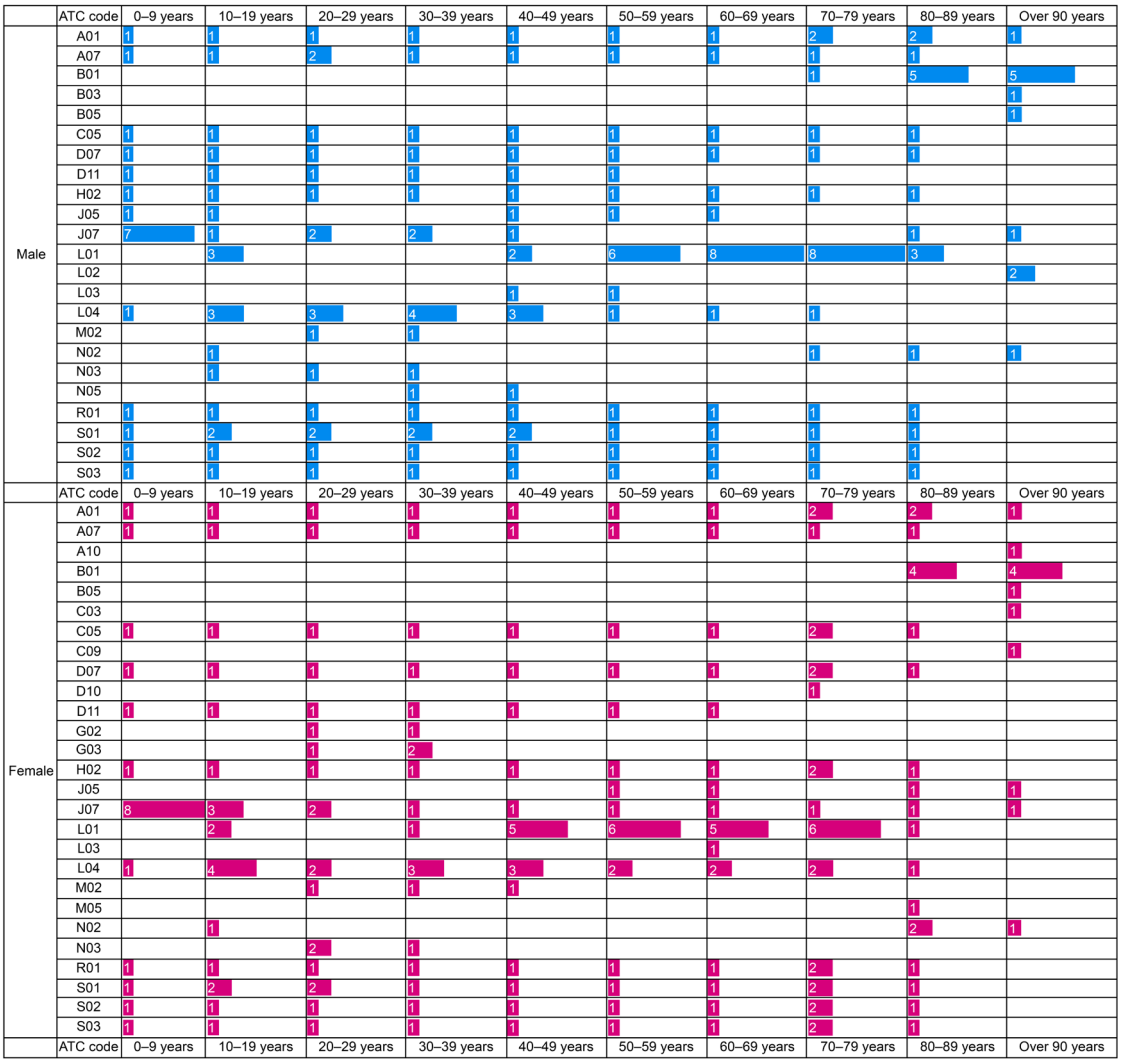

Figure 4. Distribution of ATC codes for the top ten causative drugs by sex and age.

patterns were identified by visualizing the distribution of frequently reported drug names and their ATC codes in groups stratified by sex and age. The causative drugs seem to be clearly influenced by factors such as sex and age, as well as susceptibility to disease and routine vaccinations. In particular, the number of reported vaccines [J07], immunosuppressants [L04], antineoplastic agents [L01], and antithrombotic agents [B01] was characterized by age. Prednisolone was the most commonly reported causative drug in this study, but differences in the administration route and dosage form were not considered. In other words, prednisolone has many ATC codes and indications, which may have influenced the results of this study. Despite vaccinations against COVID-19 only beginning in February 2021, COMIRNATY® ranked in the top ten in 15 of 20 age–sex groups and was the second most commonly reported causative drug overall. Understanding these facts will aid in the correct interpretation of spontaneous adverse event reports and their results. Additionally, analyzing adverse events at the SOC level allowed us to visualize adverse events that were more common or rarer in certain sex or age groups. When conducting subgroup analyses in studies using JADER data for particularly rare events or drugs occurring in specific patient populations, caution is required, as there may not be sufficient reporting. Adverse events seem to be influenced by factors such as sex, age, susceptibility to disease, vaccination, and medication use. The high number of reports on nervous system disorders among teenage girls is largely due to the influence of the human papillomavirus vaccination. Previous research has revealed a sex difference in the number of vaccine-related adverse events reported in JADER between those under 10 years of age and those aged 10–19 years (*25*).

One limitation of this study is that it did not consider actual drug use in Japan. We adjusted for sex and age using the 2015 Japanese population distribution; however, to calculate a more accurate adverse event reporting rate, it may be necessary to adjust for the demographic data of individuals who received medical care. However, this is not easy because JADER includes adverse event reports related to prescription drugs, vaccines, and over-the-counter drugs.

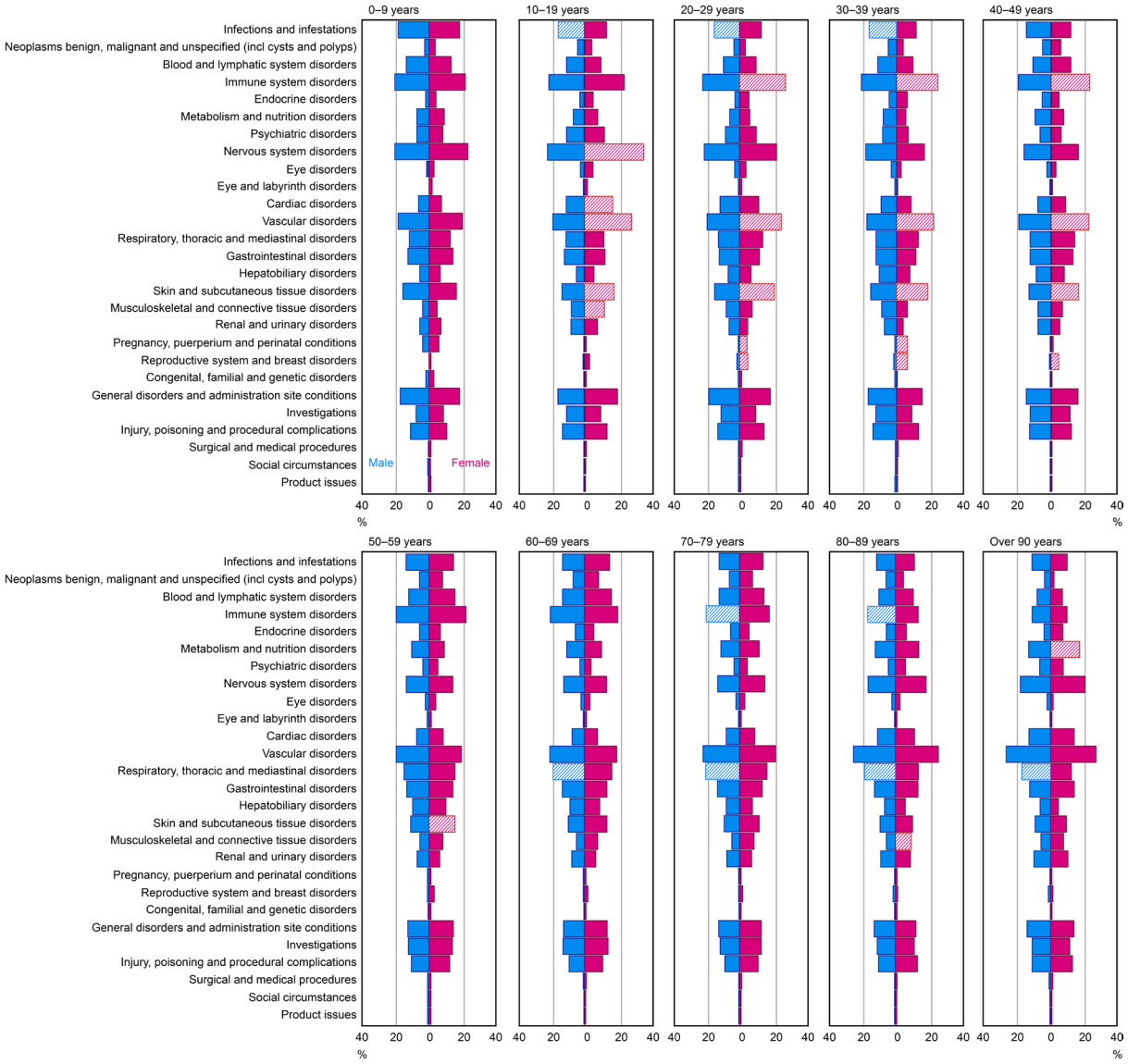

Figure 5. Reporting rate of system organ class-level adverse events in each group classified by the combination of sex and age. For system organ class-level adverse events where there is a difference of ≥ 3% in the reported proportion between males and females, the larger value is shaded.

In this study, we analyzed the characteristics and reporting patterns of adverse events included in the JADER database, focusing on sex and age. These results provide additional insights into the interpretation of previous studies using JADER. In addition, the results of this study will help understand the characteristics of adverse event reports contained in JADER and conduct appropriate subgroup and sensitivity analyses.

Acknowledgements

We would like to acknowledge Editage (*https://www.editage.com/*) for English language editing.

Funding: None.

Conflict of Interest: The authors have no conflicts of interest to disclose.

References

1. Michel C, Scosyrev E, Petrin M, Schmouder R. Can disproportionality analysis of post-marketing case reports be used for comparison of drug safety profiles? Clin Drug Investig. 2017; 37:415-422.
2. Noda A, Sakai T, Obara T, Miyazaki M, Tsuchiya M, Oyanagi G, Murai Y, Mano N. Characteristics of pediatric adverse drug reaction reports in the Japanese Adverse Drug Event Report database. BMC Pharmacol Toxicol. 2020; 21:36.
3. Chisaki Y, Aoji S, Yano Y. Analysis of adverse drug reaction risk in elderly patients using the Japanese Adverse Drug Event Report (JADER) database. Biol Pharm Bull. 2017; 40:824-829.
4. Sakai T, Ohtsu F, Sekiya Y, Mori C, Sakata H, Goto N. Methodology for estimating the risk of adverse drug reactions in pregnant women: analysis of the Japanese Adverse Drug Event Report database. Yakugaku Zasshi. 2016; 136:499-505. (in Japanese)

5. Tanaka H, Satoh M, Takigawa M, Onoda T, Ishii T. Characteristics of adverse event reports among people living with human immunodeficiency virus (HIV) in Japan: Data mining of the Japanese Adverse Drug Event Report database. Drug Discov Ther. 2023; 17:183-190.
6. Tsuchiya M, Obara T, Miyazaki M, Noda A, Takamura C, Mano N. The quality assessment of the Japanese Adverse Drug Event Report database using vigiGrade. Int J Clin Pharm. 2020; 42:728-736.
7. Yu Y, Chen J, Li D, Wang L, Wang W, Liu H. Systematic analysis of adverse event reports for sex differences in adverse drug events. Sci Rep. 2016; 6:24955.
8. Watson S, Caster O, Rochon PA, den Ruijter H. Reported adverse drug reactions in women and men: Aggregated evidence from globally collected individual case reports during half a century. EClinicalMedicine. 2019; 17:100188.
9. Zucker I, Prendergast BJ. Sex differences in pharmacokinetics predict adverse drug reactions in women. Biol Sex Differ. 2020; 11:32.
10. Sportiello L, Capuano A. Sex and gender differences and pharmacovigilance: a knot still to be untied. Front Pharmacol. 2024; 15:1397291.
11. Rushovich T, Gompers A, Lockhart JW, Omidiran I, Worthington S, Richardson SS, Lee KMN. Adverse drug events by sex after adjusting for baseline rates of drug use. JAMA Netw Open. 2023; 6:e2329074.
12. Tanaka H, Yoshiba Y, Watanabe T, Satoh M, Ishii T. Analysis of patients with hypomagnesemia using the Japanese Adverse Drug Event Report database (JADER). J Pharm Pharm Sci. 2018; 21:46-53.
13. Hauben M, Hung E. Effects of the COVID-19 pandemic on spontaneous reporting: Global and national time-series analyses. Clin Ther. 2021; 43:360-368.e5.
14. Shimabukuro TT, Nguyen M, Martin D, DeStefano F. Safety monitoring in the Vaccine Adverse Event Reporting System (VAERS). Vaccine. 2015; 33:4398-4405.
15. Montes-Grajales D, Garcia-Serna R, Mestres J. Impact of the COVID-19 pandemic on the spontaneous reporting and signal detection of adverse drug events. Sci Rep. 2023; 13:18817.
16. Yamaoka K, Fujiwara M, Uchida M, Uesawa Y, Shimizu T. The influence of the rapid increase in the number of adverse event reports for COVID-19 vaccine on the disproportionality analysis using JADER. In Vivo. 2023; 37:345-356.
17. Matsuo H, Tanaka H, Endo K, Ishii T. Influence of rapidly increased numbers of reports on adverse events of the COVID-19 vaccine in the Japanese pharmacovigilance database on disproportionality analysis of antineoplastic drug-associated adverse cardiovascular events. Expert Opin Drug Saf. 2024; 1-5. doi: 10.1080/14740338.2024.2448830.
18. Micallef B, Dogné JM, Sultana J, Straus SMJM, Nisticò R, Serracino-Inglott A, Borg JJ. An exploratory study of the impact of COVID-19 vaccine spontaneous reporting on masking signal detection in EudraVigilance. Drug Saf. 2023; 46:1089-1103.
19. Alwhaibi M, Balkhi B. Gender differences in potentially inappropriate medication use among older adults. Pharmaceuticals (Basel). 2023; 16:869.
20. Zhao Z, Liu R, Wang L, Li L, Song C, Zhang P. A computational framework for identifying age risks in drug-adverse event pairs. AMIA Jt Summits Transl Sci Proc. 2022; 2022:524-533.
21. Zazzara MB, Palmer K, Vetrano DL, Carfì A, Onder G. Adverse drug reactions in older adults: a narrative review of the literature. Eur Geriatr Med. 2021; 12:463-473.
22. Maxwell CJ, Mondor L, Pefoyo Koné AJ, Hogan DB, Wodchis WP. Sex differences in multimorbidity and polypharmacy trends: A repeated cross-sectional study of older adults in Ontario, Canada. PLoS One. 2021; 16:e0250567.
23. Orlando V, Mucherino S, Guarino I, Guerriero F, Trama U, Menditto E. Gender Differences in Medication Use: A drug utilization study based on real world data. Int J Environ Res Public Health. 2020; 17:3926.
24. Matsuo H, Endo K, Tanaka H, Onoda T, Ishii T. Fact-finding survey and exploration of preventive drugs for antineoplastic drug-induced oral mucositis using the Japanese Adverse Drug Event Report database. Sci Pharm. 2024; 92:34.
25. Noda A, Sakai T, Tsuchiya M, Oyanagi G, Obara T, Mano N. Characteristics of adverse events following immunization reporting in children: The Japanese Adverse Drug Event Report database. Vaccines (Basel). 2020; 8:357.

Received November 30, 2024; Revised January 30, 2025; Accepted February 19, 2025.

**Address correspondence to:*
Hiroyuki Tanaka, Department of Practical Pharmacy, Faculty of Pharmaceutical Sciences, Toho University, 2-2-1 Miyama, Funabashi, Chiba 274-8510, Japan.
E-mail: hiroyuki.tanaka@phar.toho-u.ac.jp

Released online in J-STAGE as advance publication February 26, 2025.

Original Article

DOI: 10.5582/ddt.2024.01071

A pharmacovigilance study based on the FAERS database focusing on anticoagulant and hormonal drugs that induce vaginal hemorrhage

Ruohan Li, Panwei Hu, Lin Qian*

Department of Obstetrics and Gynecology, Shuguang Hospital Affiliated to Shanghai University of Traditional Chinese Medicine, Shanghai, China.

SUMMARY: Numerous medications have been associated with an increased risk of vaginal hemorrhage in women. In this study, we analyzed data from the FDA Adverse Event Reporting System (FAERS), focusing on reports of drug-induced vaginal bleeding in women. Risk signals were assessed using disproportionality analyses, specifically the reporting odds ratio (ROR) and the proportional reporting ratio (PRR), to identify significant associations between drugs and adverse events. We found that anticoagulants, hormonal drugs, psychotropic drugs, hypoglycemic agents, antineoplastic agents, anti-inflammatory drugs, immunological agents, and some drugs for osteoporosis were significantly associated with the risk of vaginal hemorrhage. Hormonal drugs, anticoagulants, and particularly antifungal agents were attributed to a notably high proportion of vaginal hemorrhage cases, necessitating further investigation into the underlying mechanisms. Therefore, precise clinical management of medications and optimization of treatment regimens are necessary to reduce the risk of vaginal hemorrhage and improve safety.

Keywords: Pharmacovigilance, drug-Induced vaginal hemorrhage, FDA Adverse Event Reporting System, drug safety

1. Introduction

Vaginal hemorrhage is a prevalent gynecological condition with various potential causes. Idiopathic vaginal hemorrhage in women of reproductive age is often associated with hormonal fluctuations (*1*), pregnancy-related conditions (*2*), endothelial changes (*3*), and structural abnormalities or genetic disorder (*4*) in the reproductive system.

Recent advancements in medical research and diagnostic technology have substantially improved the understanding of vaginal hemorrhage. Diagnostic imaging techniques such as hysteroscopy, ultrasonography (*5*), and magnetic resonance imaging (MRI) (*6*) help identify the cause of vaginal hemorrhage with increased accuracy. Additionally, a holistic patient evaluation, encompassing medical history, physical examinations, and laboratory investigations, is important for validating the cause of hemorrhage and designing targeted treatment strategies.

The clinical management of vaginal hemorrhage varies based on the etiology and the condition of patients. Treatment options may range from pharmacological interventions, which are particularly effective for hormonal imbalances, to surgical procedures necessary for addressing structural abnormalities, such as uterine fibroids or polyps (*7*). Furthermore, lifestyle modifications are a fundamental component of the clinical management of vaginal hemorrhage. The shift towards personalized medicine highlights the importance of customized treatment plans that enhance both therapeutic efficacy and patient satisfaction.

Hormonal drugs, especially those used in contraceptive or hormone replacement therapies, can induce vaginal hemorrhage in some women. Schrager *et al*. (*8*) reported that irregular vaginal hemorrhage was common in 70% of women after the use of long-acting progestin contraceptives such as depot medroxyprogesterone acetate injections and levonorgestrel subdermal implants. For many patients, this hemorrhage becomes more predictable and normalizes over time. Furthermore, anticoagulant drugs have been shown to increase the risk of vaginal hemorrhage. Jignesh *et al.* (*9*) reported that two-thirds of women aged 18-50 years on anticoagulant therapy experienced significant vaginal hemorrhage, which adversely affected their quality of life. These insights highlight the imperative for cautious medication use in women, emphasizing the importance of close monitoring of adverse effects to ensure the safest possible treatment regimens.

In this study, we investigated the drugs with a higher incidence risk of inducing vaginal bleeding by analyzing adverse event reports from the Food and Drug

Administration (FDA), providing crucial insights to improve drug safety in clinical practice.

2. Methods

2.1. Data source

The data used in this study were extracted from the FDA Adverse Event Reporting System (FAERS) database. This publicly accessible database compiles drug safety reports from patients, healthcare professionals, and pharmaceutical manufacturers. The dataset spans reports from the first quarter of 2004 to the first quarter of 2024.

2.2. Data selection

Initial data screening involved removing duplicate and incomplete entries from the dataset, resulting in 2,789 unique medications. Because the top 50 drugs filtered by the preferred terms (PTs) had a limited number of positive signals, which were insufficient for robust data analysis, the scope was expanded to the top 200 drugs for screening. To identify any potentially overlooked adverse events, further analysis and validation were conducted based on higher-level terms (HLTs) and higher-level group terms (HLGTs) in addition to the initial screening based on PTs. Eventually, 34 drugs with positive signals were identified and selected for analysis.

2.3. Ethical approval of studies

The FAERS database represents a global, spontaneous reporting system for drug-induced adverse events. The objective of this study was to conduct signal detection and analysis of drug safety using only publicly available, de-identified data. Therefore, ethical approval was not required. This study complies with the provisions of the Declaration of Helsinki.

2.4. Statistics analysis

Target drugs potentially inducing vaginal hemorrhage were identified by calculating positive signals using the reporting odds ratios (RORs) (*10*) and proportional reporting ratios (PRRs) (*11*). These measures are widely recognized in pharmacovigilance for evaluating the association strength between a drug and an adverse event. For the ROR, the criterion for detecting a positive signal was a lower limit of the 95% confidence interval (CI) exceeding 1, with at least three reported adverse events. For the PRR, a positive signal was indicated when the ratio exceeded 2 and the chi-square statistic (χ^2) was ≥ 4, with at least three reported adverse events (*12*). A drug meeting both criteria was considered to have a significant association with vaginal hemorrhage. The results were expressed as case counts (n) and percentages. Data analysis and visualization were performed using the R (version 4.2.3) software.

3. Results

3.1. Identification of all reports of suspected adverse drug events in FAERS

The data derived from the FAERS database spanning from the first quarter of 2004 to the first quarter of 2024 included 17,785,193 entries after deduplication. Of these entries, 38,608 entries were related to drug-induced vaginal hemorrhage, represented by 37,506 individual records. From an initial list of the top 200 drugs, 34 drugs were identified to have positive signals for inducing vaginal hemorrhage (Figure 1).

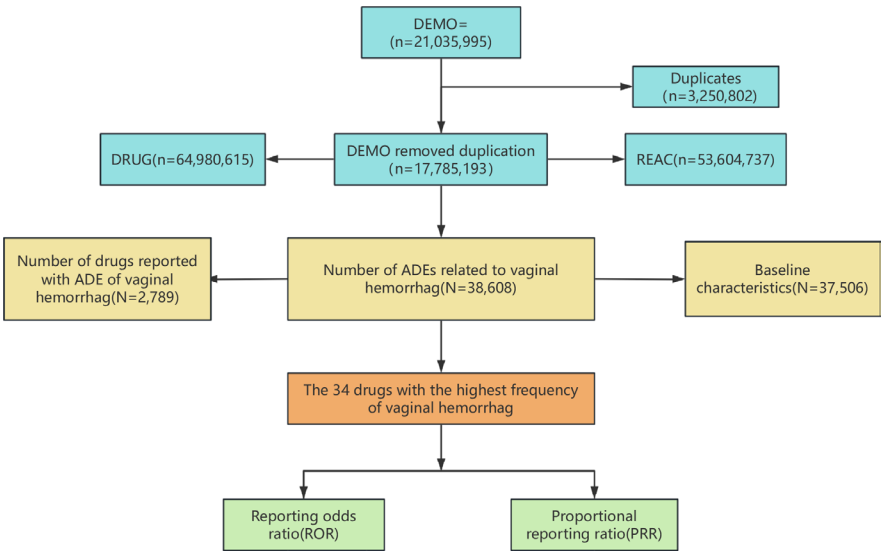

Figure 1. Flowchart demonstrating the protocol for the identification of reports of suspected adverse drug events (ADEs) in the FDA Adverse Event Reporting System (FAERS) database. The data were derived from the FAERS database spanning the first quarter of 2004 to the first quarter of 2024. Of the 200 drugs initially screened, 34 drugs were identified to exhibit positive signals for vaginal hemorrhage.

3.2. Reporters of drug-induced vaginal hemorrhage

Consumer reports comprised the majority of data on drug-induced vaginal hemorrhage, totaling 22,804 cases, followed by reports from physicians and other healthcare professionals, totaling 5,546 and 3,453 (10%) cases, respectively (Figure 2).

3.3. Number of ADEs reported per year

Since the inception of the FAERS database in 2004, the reporting of adverse drug events (ADEs) in the database has shown a year-over-year increase, with fewer reports being published initially owing to the nascent stage of the database and statistical methods. Notably, the number of reports began to increase in 2015, reaching a peak in 2016 with 3,847 cases, and continued to increase until a decline began in 2021 (Figure 3). This decline is most likely attributed to advancements in medical technology that reduced the occurrence of ADEs.

3.4. Positive drugs that induce vaginal hemorrhage

Initial analysis of the top 50 drugs based on the frequency of PTs revealed limited positive signals. Expanding the analysis to the top 200 drugs revealed 34 drugs with significant positive signals (Figure 4). Hormonal medications were prominently represented, with 14 drugs being identified. Levonorgestrel had the highest ROR at 201.97 (95% CI, 196.56-207.53), followed by medroxyprogesterone (ROR, 29.06; 95% CI, 10.79-78.23), mifepristone (ROR, 21.76; 95% CI, 18.65-25.38), estradiol patches (ROR, 14.02; 95% CI, 12.49-15.73), estradiol and norethindrone acetate (ROR, 20.47; 95% CI, 17.28-24.25), and leuprorelin acetate (ROR, 19.46; 95% CI, 18.19-20.8). Among the

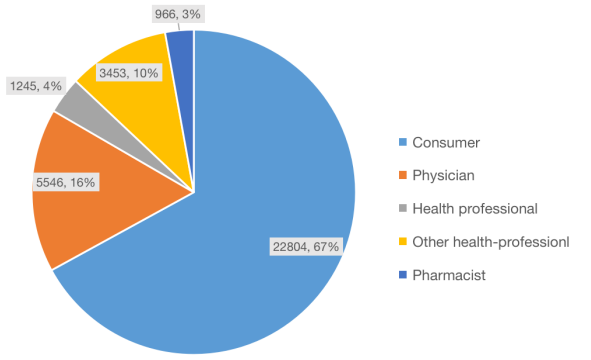

Figure 2. Reporters of ADEs related to vaginal hemorrhage. The majority of ADE reports were submitted by consumers, followed by physicians, pharmacists, and other healthcare professionals.

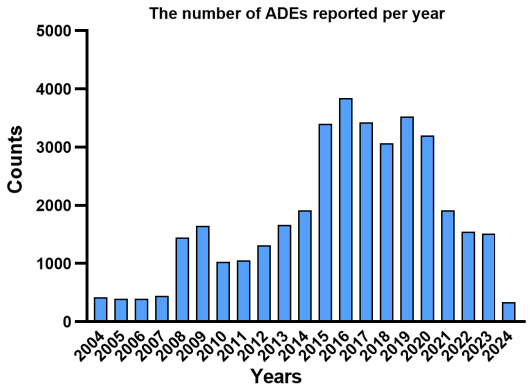

Figure 3. Number of ADEs reported per year. In the FAERS database, the number of ADE reports related to vaginal hemorrhage increased each year since database inception, peaking in 2016 and beginning to decline in 2021.

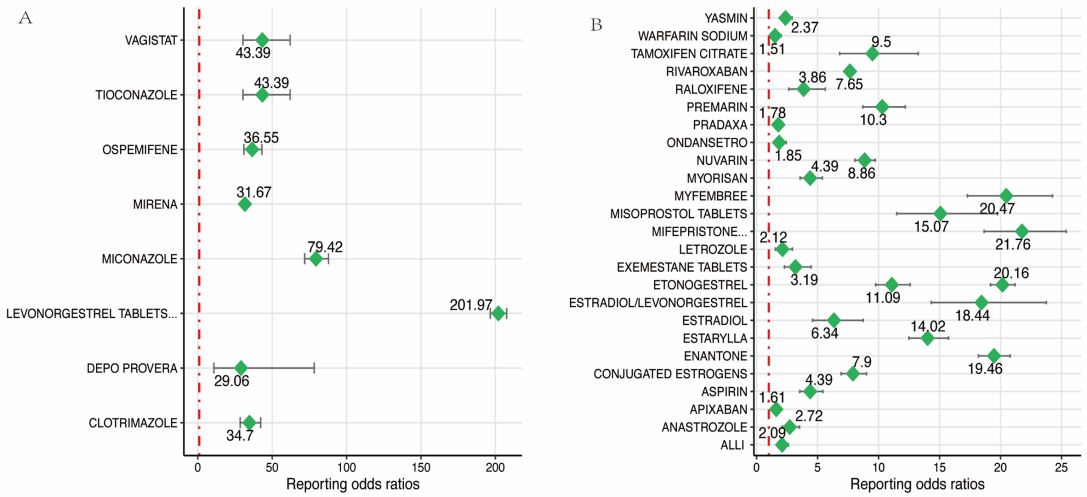

Figure 4. (A) RORs and 95% CIs of drugs with positive signals with ROR greater than 30. (B) RORs and 95% CIs of the remaining drugs with positive signals with ROR less than 30. Analysis of the top 200 drugs according to the PT revealed 34 drugs with positive signals. Among these drugs, hormonal and anticoagulant agents accounted for the largest proportions, followed by antifungal, psychotropic, anti-inflammatory, and hypoglycemic agents. Antifungal drugs had strong positive signals; however, their mechanisms of action in inducing vaginal hemorrhage warrant further investigation.

most common antifungal agents associated with vaginal hemorrhage, miconazole, clotrimazole, and terconazole had RORs of 79.42 (95% CI, 71.82-87.83), 34.71 (95% CI, 28.51-42.25), and 21.76 (95% CI, 18.65-25.38), respectively. Anticoagulants demonstrated positive signals, particularly in patients with cardiovascular and cerebrovascular diseases. These drugs included rivaroxaban (ROR, 7.65; 95% CI, 7.23-8.09), apixaban (a factor Xa inhibitor), aspirin (ROR, 4.39; 95% CI, 3.54-5.43), dabigatran etexilate, and warfarin. The anti-cancer drugs associated with vaginal hemorrhage included anastrozole (ROR, 2.72; 95% CI, 2.1-3.52), letrozole (ROR, 2.12; 95% CI, 1.53-2.94), exemestane tablets (ROR, 3.19; 95% CI, 2.28-4.47), and tamoxifen (ROR, 9.5; 95% CI, 6.81-13.25). In elderly individuals susceptible to osteoporosis, medications such as ospemifene (ROR, 36.55; 95% CI, 30.99-43.12) and raloxifene (ROR, 3.86; 95% CI, 2.64-5.63) were identified as having positive signals. Additionally, drugs with positive signals but lower frequencies included cimetropium bromide, isotretinoin, and ondansetron for peptic ulcers, acne, and emesis, respectively (all drugs with positive signals are detailed in Supplementary Table S1, *https://www.ddtjournal.com/action/getSupplementalData.php?ID=242*).

Excluding the abovementioned 34 drugs from the top 200 drugs, the majority of the drugs were immunomodulatory agents, particularly for multiple sclerosis, such as glatiramer acetate, teriflunomide, mitoxantrone, and natalizumab. In addition, the remaining drugs included a large number of drugs used to treat psoriasis and rheumatoid arthritis, including ustekinumab, tocilizumab, and infliximab. Antidiabetic (*13*) and psychotropic medications, such as antidepressants (*14*), were also included.

3.5. Age distribution of included patients

Drug-induced vaginal hemorrhage was predominantly observed in women aged 18-50 years. The higher estrogen levels may predispose these women to hormone-dependent conditions. The medications administered are often antagonistic to hormones, which increase the incidence of ADEs. Additionally, the incidence of drug-induced vaginal hemorrhage was relatively high in the postmenopausal population up to the age of 70 years (Figure 5). This may be attributed to the increased prevalence of osteoporosis or oncological diseases in the elderly population. These findings indicate that certain drugs used to treat osteoporosis and tumors have a higher risk of inducing vaginal hemorrhage.

3.6. Outcomes of included patients

The majority of individuals with drug-induced vaginal hemorrhage had adopted intervention measures to prevent more severe outcomes. However, the specific prognosis of some patients remained uncertain. Among these patients, 5,231 patients were hospitalized or had an extended hospital stay, accounting for 14% of the total reported cases. Additionally, 549 patients died owing to the adverse events, accounting for 1% of the cases (Figure 6).

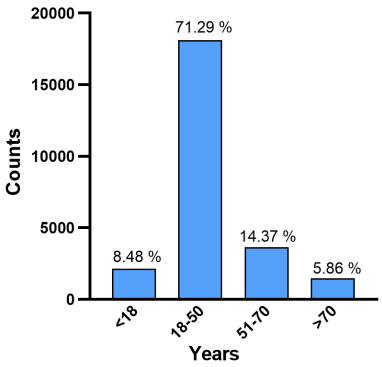

Figure 5. Age distribution of included patients. A majority of drug-induced vaginal hemorrhage cases were reported among women aged 18-50 years, which may be related to the unstable hormone levels in this age group. In addition, a relatively large proportion of pre- and post-menopausal women up to the age of 70 years had drug-induced vaginal hemorrhage, which may be related to the development of oncological diseases and osteoporosis in this age group.

4. Discussion

In this study, a comprehensive and systematic analysis was conducted on the reports of drug-induced vaginal hemorrhage in the FAERS database from 2004 to 2024. The findings provide a reference for reducing the risk of vaginal hemorrhage and promoting more rational medication use.

A total of 34 drugs, including hormonal, anticoagulant, and antifungal agents, were found to be associated with vaginal hemorrhage. Studies have shown that hormonal drugs frequently induce vaginal hemorrhage in women. However, the severity of a hemorrhage often decreases as the dosage of the drug increases. For instance, Festin *et al*. (*15*) found that the severity of initial prolonged vaginal hemorrhage experienced by patients after consuming the first 10 pills of levonorgestrel decreased with continued usage of the drug, with only a small proportion of patients (0.4%) eventually experiencing severe anemia. Similarly, Langer *et al*. (*16*) highlighted that approximately 9% of women discontinued estrogen-progestogen therapy (EPT) using conjugated equine estrogen (CEE) and medroxyprogesterone acetate (MPA) owing to the occurrence of vaginal hemorrhage predominantly within the first 3 months of treatment. In this study, CombiPatch, which is a combination of estrogen and progestogen, was found to be associated with vaginal hemorrhage (ROR, 20.47; 95% CI, 17.28-24.25). Hickey

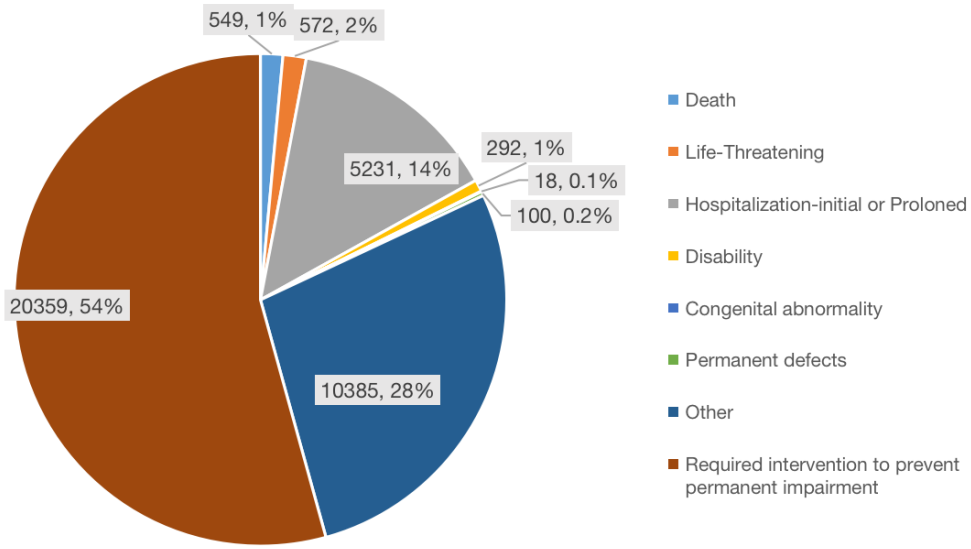

Figure 6. Outcomes of included patients. Most women with drug-induced vaginal hemorrhage had a good prognosis, with only 1% of cases resulting in deaths. The vast majority of these women were hospitalized or had a prolonged hospital stay, whereas a relatively small proportion of the women developed disability, impairment, or other complications.

(*17*) indicated that approximately 40%-60% of patients undergoing hormone therapy experienced irregular vaginal hemorrhage, which may reduce in severity with the use of low-dose estrogen.

Anticoagulant drugs are commonly associated with abnormal hemorrhage, frequently manifesting as vaginal hemorrhage in women. Anderson *et al.* (*18*) analyzed uterine hemorrhage events following oral anticoagulant use. They found a higher incidence of hemorrhage in individuals aged < 50 years than in those aged > 50 years. Huang *et al.* (*19*) showed that individuals on anticoagulant therapy experienced vaginal hemorrhage, requiring blood transfusion on the same day or gynecological surgery within 30 days were significantly more numerous than those not using anticoagulant drugs. Patel *et al.* (*9*) conducted a survey of women on anticoagulants and a control group of women not on anticoagulants. The results showed that two-thirds of women experienced heavy menstrual bleeding after initiating anticoagulant therapy, and the median duration of menstruation increased from 5 to 6 days. Compared with women in the control group, women undergoing anticoagulant therapy had significantly higher PBAC scores (representing the severity of menstrual blood loss) ($P < 0.05$) and lower quality of life scores ($P < 0.05$) (*20*).

Antifungal medications play an important role in gynecological care, particularly in the treatment of vulvovaginal candidiasis. Saghafi *et al.* (*21*) demonstrated that clotrimazole suppositories significantly alleviated itching, burning, and irritation in patients with vaginitis. Similarly, Shi *et al.* (*22*) showed that metronidazole vaginal effervescent tablets effectively reduced the levels of inflammatory markers and increased vaginal pH and cleanliness. However, it is noteworthy that antifungal drugs can strongly interact with anticoagulants, such as warfarin. Kovac *et al.* (*23*) showed that miconazole, in both oral and topical forms, significantly affected the activity of warfarin, increasing the risk of major hemorrhage events. Consequently, when anticoagulants and antifungal medications are used concurrently, the dosage of the anticoagulants should be adjusted to mitigate the risk of hemorrhage. Mechanistically, antifungal drugs can inhibit hepatic microsomal cytochrome P450 (CYP) enzymes, particularly CYP2C9, which is involved in the 7-hydroxylation of oral anticoagulants, thereby influencing the metabolism and therapeutic effects of anticoagulants.

Although the combined use of antifungal and anticoagulant drugs has been shown to increase the risk of hemorrhage, direct evidence supporting the relationship between antifungal drugs and vaginal hemorrhage is insufficient. In this study, we found that certain antifungal drugs had high positive signal values, such as miconazole (ROR, 79.42; 95% CI, 71.82-87.83) and itraconazole (ROR, 43.39; 95% CI, 30.35-62.05), with clotrimazole and sertaconazole showing similar high signal values. However, the precise relationships between these drugs and vaginal hemorrhage and the mechanisms of these drugs in inducing hemorrhage warrant further investigation.

Abnormal uterine hemorrhage is a prevalent gynecological symptom with various potential causes. The common etiological factors include endometrial polyps, adenomyosis, uterine fibroids, atypical hyperplasia of the endometrium, and endometrial cancer. Furthermore, conditions such as blood clotting disorders and polycystic ovary syndrome contribute to ovulatory dysfunction that can result in abnormal

hemorrhage. The impact of medical interventions, such as intrauterine devices, hormonal treatments, and hormone replacement therapies, and the potential side effects of certain medications, which can increase the risk of hemorrhage, should be seriously considered (*24-26*). Increased awareness and careful monitoring of drug-induced vaginal hemorrhage are crucial. Based on the findings of this study, pharmacological agents should be more judiciously used and patients should be vigilantly monitored for hemorrhages. This approach can facilitate the early detection of drug-induced hemorrhage, allowing for the adjustment of treatment plans to incorporate safer drug options, thus improving the safety and well-being of patients. These insights are invaluable for guiding rational medication practices to enhance the safety and effectiveness of medical interventions. With a comprehensive understanding and precise diagnosis of the causes of abnormal uterine hemorrhage and the availability of evidence-based treatment approaches, physicians can develop personalized treatment regimens that can not only improve the quality of life of patients but also strengthen the foundation for clinical decision-making.

In this study, "Vaginal hemorrhage" was used as the PT. According to the MedDRA hierarchical structure, this term is classified under the HLT "VULVOVAGINAL DISORDERS NEC" and the HLGT "VULVOVAGINAL DISORDERS (EXCL INFECTIONS AND INFLAMMATIONS)." Other PTs related to bleeding that are included in these HLT and HLGT categories are "COITAL BLEEDING," "VULVAL HAEMORRHAGE," "HAEMATOCOLPOS," "VAGINAL HAEMATOMA," and "VAGINAL WALL CONGESTION." Signals were detected for each of these PTs. The identified drug categories associated with these PTs were consistent with those associated with "Vaginal hemorrhage." Expanding the data to the top 1000 drugs for general screening showed that all the risk drugs identified by PT can be categorized within the existing drug classes in the current study results, with no new drug categories emerging. Notably, the positive signals for antifungal drug-induced vaginal hemorrhage were strong, warranting further investigation. This consistency further confirms the broadness and reliability of the identified drugs.

A majority of ADE reports in the FAERS database, which is a voluntary reporting system, are submitted by consumers. Therefore, the analytical findings of this study are subject to certain limitations. Despite these limitations, the findings may help improve the scrutinization of drug safety and offer critical guidance for future research into abnormal uterine hemorrhage. In addition, the findings may help develop a more judicious and safe approach to medication usage among researchers and medical practitioners, enabling the identification of latent drug-induced precipitants. This proactive approach may help decrease the risks associated with medication use and increase safety. Furthermore, the findings of this study may help strengthen clinical decision-making with robust empirical backing, improve the understanding of the causes of abnormal uterine hemorrhage, and guide the development of preventive measures for ADEs. Enhancing the safety profiles of pharmacological therapies not only benefits individualized and precise treatment but also advances the overall standard of care in medical practice.

Acknowledgements

We thank FAERS for the availability of the data. We thank Bullet Edits Limited for the linguistic editing and proofreading of the manuscript.

Funding: None.

Conflict of Interest: The authors have no conflicts of interest to disclose.

References

1. Pohl O, Marchand L, Bell D, Gotteland JP. Effects of combined GnRH receptor antagonist linzagolix and hormonal add-back therapy on vaginal bleeding-delayed add-back onset does not improve bleeding pattern. Reprod Sci. 2020; 27:988-995.
2. Hackney DN, Glantz JC. Vaginal bleeding in early pregnancy and preterm birth: systemic review and analysis of heterogeneity. J Matern Fetal Neonatal Med. 2011; 24:778-786.
3. Treacy T, Stokes J, Rochford M, Geisler M, Burke C. Postmenopausal bleeding: Incidence of Endometrial pathology with Endometrial thickness of 3mm-3.9mm. Ir Med J. 2023; 116:728.
4. Van Doan N, Minh Duc N, Kim Ngan V, Van Anh N. McCune-Albright syndrome onset with vaginal bleeding. BMJ Case Rep. 2021; 14:e243401.
5. Algeri P, Spazzini MD, Seca M, Garbo S, Villa A. About uterine enhanced myometrial vascularity: Doppler ultrasound could reduce misdiagnosed life-threatening vaginal bleeding after pregnancy and guide the management. J Ultrasound. 2023; 26:695-701.
6. Zhang Q, Lin C, Wu J, Xu D, Zhu S, Jiang B. Value and influencing factors of preoperative MRI evaluation for previous cesarean scar defect associated abnormal uterine bleeding in patients undergoing laparoscopic surgery. Zhong Nan Da Xue Xue Bao Yi Xue Ban. 2023; 48:1316-1324.
7. Chaudhry S, Berkley C, Warren M. Perimenopausal vaginal bleeding: diagnostic evaluation and therapeutic options. J Womens Health (Larchmt). 2012; 21:302-310.
8. Schrager S, Fox K, Lee R. Abnormal uterine bleeding associated with hormonal contraception. Am Fam Physician. 2024; 109:161-166.
9. Patel JP, Nzelu O, Roberts LN, Johns J, Ross J, Arya R. How do anticoagulants impact menstrual bleeding and quality of life? - The PERIOD study. Res Pract Thromb Haemost. 2023; 7:100072.
10. Sakaeda T, Tamon A, Kadoyama K, Okuno Y. Data

mining of the public version of the FDA Adverse Event Reporting System. Int J Med Sci. 2013; 10:796-803.
11. Böhm R, von Hehn L, Herdegen T, Klein HJ, Bruhn O, Petri H, Höcker J. OpenVigil FDA - Inspection of U.S. American Adverse Drug Events Pharmacovigilance Data and Novel Clinical Applications. PLoS One. 2016; 11:e0157753.
12. Zhou S, Jia B, Kong J, Zhang X, Lei L, Tao Z, Ma L, Xiang Q, Zhou Y, Cui Y. Drug-induced fall risk in older patients: A pharmacovigilance study of FDA adverse event reporting system database. Front Pharmacol. 2022; 13:1044744.
13. Vaccaro CJ, Zaidi SMH, Iskander PA, McFadden E. A Case of Dulaglutide-Induced Vaginal Bleed. Cureus. 2023; 15:e38774.
14. Lupattelli A, Spigset O, Koren G, Nordeng H. Risk of vaginal bleeding and postpartum hemorrhage after use of antidepressants in pregnancy: a study from the Norwegian Mother and Child Cohort Study. J Clin Psychopharmacol. 2014; 34:143-148.
15. Festin MP, Bahamondes L, Nguyen TM, Habib N, Thamkhantho M, Singh K, Gosavi A, Bartfai G, Bito T, Bahamondes M, Kapp N. A prospective, open-label, single arm, multicentre study to evaluate efficacy, safety and acceptability of pericoital oral contraception using levonorgestrel 1.5 mg. Hum Reprod. 2016; 31:530-540.
16. Langer RD, Landgren BM, Rymer J, Helmond FA. Effects of tibolone and continuous combined conjugated equine estrogen/medroxyprogesterone acetate on the endometrium and vaginal bleeding: results of the OPAL study. Am J Obstet Gynecol. 2006; 195:1320-1327.
17. Hickey M, Ambekar M. Abnormal bleeding in postmenopausal hormone users-What do we know today? Maturitas. 2009; 63:45-50.
18. Anderson A, Gassman A, Hou L, Huang TY, Eworuke E, Moeny D, Wong H. Incidence of uterine bleeding following oral anticoagulant use in Food and Drug Administration's Sentinel System. Am J Obstet Gynecol. 2021; 224:403-404.
19. Huang TY, Hou L, Anderson A, Gassman A, Moeny D, Eworuke E. Incidence of severe uterine bleeding outcomes among oral anticoagulant users and nonusers. Am J Obstet Gynecol. 2022; 226:140-143.
20. de Jong CMM, Blondon M, Ay C, *et al.* Incidence and impact of anticoagulation-associated abnormal menstrual bleeding in women after venous thromboembolism. Blood. 2022; 140:1764-1773.
21. Saghafi N, Karjalian M, Ghazanfarpour M, Khorsand I, Rakhshandeh H, Mirteimouri M, Babakhanian M, Khadivzadeh T, Najafzadeh M, Ghorbani A, Pourali L, Bahman S. The effect of a vaginal suppository formulation of dill (*Anethum graveolens*) in comparison to clotrimazole vaginal tablet on the treatment of vulvovaginal candidiasis. J Obstet Gynaecol. 2018; 38:985-988.
22. Shi L, Yang D, Wang X. Clinical Effect of Metronidazole Vaginal Effervescent Tablet Combined with Flavescentis Sophora Suppository in the Treatment of Trichomonas Vaginitis. Contrast Media Mol Imaging. 2022; 2022:1250755.
23. Kovac M, Mitic G, Kovac Z. Miconazole and nystatin used as topical antifungal drugs interact equally strongly with warfarin. J Clin Pharm Ther. 2012; 37:45-48.
24. Kabra R, Fisher M. Abnormal uterine bleeding in adolescents. Curr Probl Pediatr Adolesc Health Care. 2022; 52:101185.
25. Achanna KS, Nanda J. Evaluation and management of abnormal uterine bleeding. Med J Malaysia. 2022; 77:374-383.
26. Hill S, Shetty MK. Abnormal Uterine Bleeding in Reproductive Age Women: Role of Imaging in the Diagnosis and Management. Semin Ultrasound CT MR. 2023; 44:511-518.

Received October 7, 2024; Revised February 11, 2025; Accepted February 18, 2025.

**Address correspondence to:*
Lin Qian, Department of Obstetrics and Gynecology, Shuguang Hospital Affiliated to Shanghai University of Traditional Chinese Medicine, 528 Zhangheng Road, Shanghai, China.
E-mail: ql1217@shutcm.edu.cn

Released online in J-STAGE as advance publication February 23, 2025.

Original Article

DOI: 10.5582/ddt.2024.01088

Efficacy of etanercept biosimilar switching from etanercept reference product, using ultrasound and clinical data in outcomes of real world therapy (ESCORT-NGSK Study)

Remi Sumiyoshi[1,2], Shin-ya Kawashiri[1,3,*], Toshimasa Shimizu[1,2], Tomohiro Koga[1], Rieko Kiya[2], Shigeki Tashiro[2], Yurika Kawazoe[2], Shuntaro Sato[2], Yukitaka Ueki[4], Takahisa Suzuki[5], Masahiko Tsuboi[6], Yoshifumi Tada[7], Toshihiko Hidaka[8], Hirokazu Takaoka[9], Naoki Hosogaya[2], Hiroshi Yamamoto[2], Atsushi Kawakami[1]

[1] Departments of Immunology and Rheumatology, Division of Advanced Preventive Medical Sciences, Nagasaki University Graduate School of Biomedical Sciences, Nagasaki, Japan;
[2] Clinical Research Center, Nagasaki University Hospital, Nagasaki, Japan;
[3] Center for Collaborative Medical Education and Development, Nagasaki University Institute of Biomedical Sciences, Nagasaki, Japan;
[4] Rheumatic Disease Center, Sasebo Chuo Hospital, Sasebo, Japan;
[5] Department of Rheumatology, Japanese Red Cross Nagasaki Genbaku Hospital, Nagasaki, Japan;
[6] Nagasaki Medical Hospital of Rheumatology, Japan;
[7] Department of Rheumatology, Saga University Hospital, Japan;
[8] Institute of Rheumatology, Miyazaki-Zenjinkai Hospital, Miyazaki, Japan;
[9] Section of Internal Medicine and Rheumatology, Kumamoto Shinto General Hospital, Kumamoto, Japan.

SUMMARY: This study aimed to investigate in detail the efficacy of switching from etanercept reference product (RP) to etanercept biosimilar in patients with rheumatoid arthritis (RA) under real-world clinical conditions using clinical indices and musculoskeletal ultrasound (MSUS). This interventional, multicenter, open-label, single-arm clinical trial involved 24- or 52-week follow-up. This study enrolled patients with RA who had been treated with etanercept-RP for ≥ 24 weeks, achieved clinical low disease activity (LDA) or remission, and switched from etanercept-RP to etanercept biosimilar. This study included 20 patients. Of the 17 patients, 16 (94.1%; 95% confidence interval [CI]: 71.3–99.9) remained in LDA/remission on DAS28-ESR at 24 weeks. The dose of 50 mg/week was reduced to 25 mg/week at 24 weeks, and LDA/remission was sustained until 52 weeks in 9 (81.8%, 95% CI: 48.2–97.7] of 11 participants. DAS28-ESR, DAS28-CRP, SDAI, and CDAI scores showed no apparent worsening. The median total PD score remained 0. The switch from etanercept-RP to etanercept biosimilar and subsequent dose reduction demonstrated favorable outcomes, including MSUS evaluation.

Keywords: Rheumatoid arthritis (RA), etanercept, biosimilar, musculoskeletal ultrasound (MSUS), biomarkers

1. Introduction

Rheumatoid arthritis (RA) is an autoimmune disease caused by multiple genetic and environmental factors that triggers autoimmune responses, inducing chronic synovitis in multiple joints, progressive destructive arthritis, and physical dysfunction (*1*). Therefore, the primary treatment goal is to achieve remission through tight control using a treat-to-target strategy (*2*). The advent of biological disease-modifying antirheumatic drugs (bDMARDs) has significantly increased clinical remission rates and expanded the treatment options. However, the high cost of bDMARDs imposes a significant economic burden, making their introduction and continued treatment difficult for some patients. Hence, biosimilars have emerged as a treatment option for RA, anticipated to alleviate patients' economic burden and support healthcare insurance sustainability. In Japan, etanercept biosimilar 1 (brand name Etanercept BS "MA") gained marketing approval in January 2018, matching the indication of etanercept-RP (brand name Enbrel). Etanercept biosimilar 1 is a biologic similar to etanercept-RP, and its equivalence in quality, efficacy, and safety at the time of approval was verified and proven in clinical trials compared to etanercept-RP (*3*). Additionally, the aforementioned studies assessed the efficacy of long-term etanercept biosimilar 1 administration (*3,4*). However, the efficacy of switching

from etanercept-RP to etanercept biosimilar 1 remains unconfirmed under real-world clinical conditions, and no report has evaluated the efficacy of switching from etanercept-RP to etanercept biosimilar in detail using musculoskeletal ultrasound (MSUS) or multiple serum biomarkers.

MSUS, which is non-invasive, objective, inexpensive, and repeatable, surpasses clinical disease activity assessment because it depicts synovial inflammation with high sensitivity (*5,6*). In addition, it is a valuable imaging tool for monitoring the treatment. MSUS reveals subclinical synovitis, a significant finding predictive of joint destruction and relapse even in cases of clinical remission (*7,8*). Therefore, it is important to accurately assess disease activity at the joint level using MSUS and not just clinical disease activity indices that include subjective factors. A multicenter study that prospectively assessed RA activity using MSUS is rare globally. This multicenter study conducted a high-level standardized MSUS assessment and revealed results with clinical value.

A major concern for clinicians is how to continue treatment of patients who achieved low disease activity (LDA)/remission through bDMARDs. The PRESERVE study revealed that reducing the dose of etanercept-RP from 50 mg/week to 25mg/week is beneficial in maintaining LDA/remission in patients who have sustained these levels (*9*). However, the association of reducing the dose of an etanercept biosimilar with maintaining LDA/remission in patients with a good course of treatment using the biosimilar remains unknown.

The present study assessed changes in disease activity after switching from etanercept-RP to etanercept biosimilar 1 and the subsequent dose reduction of etanercept biosimilar 1 more accurately and objectively, using both MSUS and clinical disease activity indicators.

2. Materials and Methods

2.1. Patients

This prospective, open-label, interventional single-arm clinical trial was conducted at the following seven centers: Nagasaki University Hospital, Sasebo Chuo Hospital, Japanese Red Cross Nagasaki Genbaku Hospital, Nagasaki Medical Hospital of Rheumatology, Saga University Hospital, Miyazaki-Zenjinkai Hospital, and Kumamoto Shinto General Hospital.

Inclusion criteria were (1) patients aged ≥ 20 years upon obtaining informed consent, (2) patients with RA fulfilling the American College of Rheumatology (ACR)/ European Alliance of Associations for Rheumatology (EULAR) classification criteria for RA (2010) (*10*), (3) patients treated with etanercept-RP (for subcutaneous injection of 25 mg once weekly, 25 mg twice weekly, 50 mg once weekly, or 50 mg once biweekly) for ≥ 24 weeks and who had been in LDA/remission with no change in etanercept-RP dosage for at least 24 weeks before obtaining consent, and (4) patients who signed a written informed consent after receiving sufficient information.

Exclusion criteria were (1) patients currently receiving oral prednisolone of > 7.5 mg/day upon case enrollment, (2) patients with etanercept biosimilar 1 contraindication, (3) patients who have previously used etanercept biosimilar, (4) patients under treatment with biological agents and JAK inhibitors for RA, except for denosumab, (5) patients whose prednisolone or antirheumatic drug usage and dosage were changed within 4 weeks before case enrollment, (6) patients treated with prohibited drugs or prohibited therapies within 4 weeks before case enrollment, (7) women who are currently pregnant or will not be compliant with a medically approved contraceptive regimen during the study period and lactating women, and (8) patients who were judged unsuitable for this study by the investigator.

This study was approved by (CRB) of Nagasaki University (CRB approval number: CRB7180001). This study was registered in the Japan Registry of Clinical Trials (https://jrct.niph.go.jp) as jRCTs071190046. The study was conducted in accordance with the principles of the Declaration of Helsinki (*11*), the Clinical Trials Act (since February 2019), the Act on the Protection of Personal Information and related regulatory notifications, and this clinical study protocol.

2.2. Intervention

Patients with RA receiving etanercept-RP (subcutaneous injection of 25 mg once weekly, 25 mg twice weekly, 50 mg once weekly, or 50 mg once biweekly) for > 24 weeks and persistent LDA/remission were switched from etanercept-RP to the same dose of etanercept biosimilar 1. Additionally, patients receiving etanercept biosimilar 1 at 50 mg weekly received a reduced dose of 25 mg/ week starting at 24 weeks to investigate the persistence of LDA/remission until 52 weeks. All patients needed to maintain the same csDMARDs and oral corticosteroid doses throughout the study period, as they had been taking before the study. The following treatments were prohibited during the study period: bDMARD or JAK inhibitor, concomitant immunosuppressants (azathioprine, cyclophosphamide, and cyclosporine), oral corticosteroid equivalent to > 7.5 mg/day of prednisolone, and intra-articular corticosteroid injections.

2.3. Outcome measurements

The study visits took place at baseline and after 12, 24, 36, and 52 weeks of treatment. Supplementary Figure S1 (*https://www.ddtjournal.com/action/getSupplementalData.php?ID=244*) shows the assessment schedule. Physicians were blinded to the joint assessments using MSUS.

Each attending physician evaluated clinical disease activity based on the DAS28-C-reactive protein (CRP), DAS28-erythrocyte sedimentation rate (ESR) (*12*), simplified disease activity index (SDAI) (*13*), and clinical disease activity index (CDAI) (*14*). The Health Assessment Questionnaire-Disability Index (HAQ-DI) was used to assess patients' functional status (*15*).

The participants underwent MSUS at baseline and at 12, 24, 36, and 52 weeks. A systematic multiplanar grayscale (GS) and power Doppler (PD) assessment of each patient's joint was conducted using a multifrequency linear transducer (12–24 MHz). PD was utilized based on which Doppler modality was the most sensitive on the individual machines. Doppler settings were adjusted at each hospital according to published recommendations (*16*), and standardized joint and probe positions were employed based on the guidelines published by the Japan College of Rheumatology (JCR). JCR-certified sonographers conducted MSUS assessments at each participating hospital as previously described (*17*). Articular synovitis was assessed with MSUS at dorsal views of 22 joints: bilateral wrist joints, first–fifth metacarpophalangeal (MCP) joints, first interphalangeal joints, and second–fifth proximal interphalangeal joints. Each joint was scored semi-quantitatively for GS and PD on a scale of 0–3. The sum of the GS and PD scores was considered as the total GS and PD scores, respectively. Additionally, we evaluated the Outcome Measures in Rheumatology (OMERACT)-EULAR combined with PDUS scores (*i.e.*, the combined PD score) (*18,19*). The combined PD score incorporates GS and PD scores (*18,19*). A previous investigation confirmed interobserver reliability (*20*). PD remission was defined as a PD score of 0 in 22 joints as previously described (*17,21*).

Radiographic images of the bilateral hands (posteroanterior view) and feet (anteroposterior view) were captured. Trained JCR-certified rheumatologists (T.K. and T.S.) evaluated joint damage progression based on the van der Heijde-modified total Sharp score (vdH-mTSS) method, as previously described (*22*), including 16 areas in each hand for erosions and 15 for joint-space narrowing (*23*).

2.4. Biomarker measurements

The serum concentrations of the following biomarkers were measured. Rheumatoid factor (RF) using a latex agglutination turbidimetric immunoassay (LZ test "Eiken" RF) (Eiken Chemial, Tochigi, Japan). Anti-cyclic citrullinated peptide antibodies (anti-CCP antibodies) were detected using a chemiluminescent immunoassay (STACIA MEBLux test CCP) (Medical & Biological Laboratories Co., Ltd., Tokyo, Japan). Matrix metalloproteinase-3 (MMP-3) using a latex turbidimetric immunoassay (Panaclear MMP-3 "Latex") (Sekisui Medical Company Limited, Tokyo, Japan). Multiplex cytokine/chemokine bead assays with diluted serum supernatants and a MILLIPLEX MAP Human Cytokine/Chemokine Magnetic Bead Panel (Merck Millipore, Billerica, MA, USA)-Bio-Plex Pro Human Cytokine Assays (Bio-Rad, Hercules, CA, USA) analyzed using a Bio-Plex® MAGPIXTM Multiplex Reader (Bio-Rad) following the manufacturer's instructions.

The cytokines/chemokines that were measured with the bead panel include interleukin (IL)-1α, IL-1β, IL-1 receptor antagonist, IL-2, IL-3, IL-4, IL-5, IL-6, IL-7, IL-8, IL-9, IL-10, IL-12 (p40), IL-12 (p70), IL-13, IL-15, IL-17, interferon-gamma (IFN-γ), IFN-α 2, CXCL1 (growth-related oncogene), granulocyte-macrophage colony-stimulating factor (GM-CSF), granulocyte CSF (G-CSF), CX3CL1 (fractalkine), flt-3 ligand, fibroblast growth factor-2, eotaxin, epidermal growth factor, soluble CD40 ligand, vascular endothelial growth factor, tumor necrosis factor (TNF)-β, TNF-α, transforming growth factor-α, CCL4 (macrophage inflammatory protein [MIP]-1β), CCL3 (MIP-1α), CCL22 (macrophage-derived chemokine [MDC]), CCL7 (monocyte chemotactic protein-3), CCL2 (monocyte chemotactic protein-1), and CXCL-10 (IFN-γ-inducible protein [IP]-10). Serum IL-6 and TNF-α levels were measured using specific enzyme-linked immunosorbent assay kits (R&D Systems, Minneapolis, MN, USA).

2.5. Study endpoints

The primary endpoint was the proportion of study participants who sustained LDA/remission at 24 weeks after switching from etanercept-RP to etanercept biosimilar 1 without clinical relapse throughout the observation period. Clinical relapse was defined as (1) two consecutive DAS28-ESR of ≥ 3.2 in specified and unspecified visits, and (2) an increase in the DAS28-ESR value caused by elevated disease activity of RA.

The secondary endpoints of this study were (1) the proportion of study participants who sustained LDA/remission at 12, 36, and 52 weeks without clinical relapse throughout the observation period; (2) changes in the total GS and PD scores and the combined PD score from baseline to 12, 24, 36, and 52 weeks; (3) changes in the DAS28-ESR and DAS28-CRP values from baseline to 12, 24, 36, and 52 weeks; and (4) changes in the SDAI and CDAI values from baseline to 12, 24, 36, and 52 weeks.

2.6. Statistical analysis method

A previous study (*4*) revealed that the proportion of participants who achieved LDA after receiving etanercept-RP, switched to etanercept biosimilar, and maintained LDA for 24 weeks was 82.5%. The present study statistically identified the sample size that would enable the estimation of the 95% confidence interval (CI) for an achievement proportion of 82.5% to be 72.5%–92.5%. The required sample size was calculated

as 55 patients. The target sample size was 62, assuming a withdrawal rate of 10%.

All data are expressed as medians and interquartile ranges (IQR) for continuous variables and numbers with percentages for discrete variables. The 95% CIs for achieving proportions were calculated using the Clopper-Pearson method. In this study, we did not perform hypothesis testing or report point estimates and 95% CIs. The widths of the 95% CIs were not adjusted for multiplicity, and the intervals may not be utilized instead of hypothesis testing. R version 4.2.2 (R Project for Statistical Computing, Vienna, Austria) was used for the statistical analyses.

3. Results

3.1. Patients

This study included only 20 patients at the end of the enrollment period. Of the enrolled patients, 17 were evaluated for DAS28-ESR and clinical relapse at 24 weeks or study discontinuation (full analysis set [FAS]). One patient discontinued the study at 24 weeks after the investigator's decision, leaving 16 patients who completed the study (Supplementary Figure S2, *https://www.ddtjournal.com/action/getSupplementalData.php?ID=244*).

Table 1 shows the baseline patient characteristics. The age of the patients was 64 years (46, 68), and 15 (88%) patients were female. The disease duration was 15 years (7, 21). RF and anti-CCP antibodies were detected in 15 (88%) and 11 (65%) patients, respectively. Other bDMARDs were administered to seven (41%) patients, including three with infliximab, one with adalimumab, two with tocilizumab, and one with abatacept (with possible duplicates among the same individuals). Concomitant medications for RA included MTX in 11 (65%) patients at a dose of 6 mg/week (6, 8). Concomitant prednisolone was administered in 2 (12%) patients at 0.88 mg/day (0.56, 1.19).

Table 1. Baseline characteristics

	n = 17
Age, years	64 (46, 68)
Sex, Female	15 (88)
Height, cm	154 (149, 157)
Weight, kg	52 (47, 56)
Disease duration, years	15 (7, 21)
Rheumatoid factor-positive	15 (88)
Anti-CCP antibody-positive	11 (65)
Duration of etanercept (Enbrel) use, year	2.1 (1.2, 5.1)
Duration of low disease activity/remission, week	67 (56, 100)
Smoking history (ever smoked)	6 (35)
Pack-year*	8 (5, 20)
Complications of osteoporosis	9 (18)
Complications of hypertension	4 (8)
Complications of dyslipidemia	3 (6)
Complications of allergic rhinitis	3 (6)
Previous use of bDMARDs	7 (41)
Infliximab†	3 (18)
Adalimumab†	1 (5.9)
Tocilizumab†	2 (12)
Abatacept†	1 (5.9)
Concomitant medications	
Methotrexate†	11 (65)
Methotrexate dose, mg/week	6 (6.0, 8.0)
Prednisolone†	2 (12)
Prednisolone dose, mg/day	0.88 (0.56, 1.19)

Data are shown as *n* (%) or median (IQR). bDMARDs: biological disease-modifying anti- rheumatic drugs, CCP: cyclic citrullinated peptide, IQR: Interquartile Range. *Missing: n = 13. †Denominator of percentage is 17 patients.

3.2. Efficacy endpoints

The primary endpoint was the proportion of study participants who sustained LDA/remission at 24 weeks after switching from etanercept-RP to etanercept biosimilar 1 without clinical relapse throughout the observation period. The results revealed 16 (94.1%) out of 17 patients (95% CI: 71.3–99.9).

The secondary endpoint was the proportion of patients who met the LDA/remission criteria at 12, 36, and 52 weeks without clinical relapse throughout the observation period. The FAS included 17 patients up to 24 weeks, and only the 50 mg/week dose group was included after 24 weeks; thus, the analysis was conducted on 11 patients after 24 weeks, excluding 1 patient whose treatment was discontinued at 24 weeks. LDA/remission was achieved in all 17 (100%) patients at 12 weeks, of which remission was achieved in 14 (82.4%) patients: 16 (94.1%) and 13 (76.5%) patients at 24 weeks, 9 (81.8%) and 8 (72.7%) patients at 36 weeks, and 10 (90.9%) and 8 (72.7%) patients at 52 weeks. Furthermore, 11 (91.7%) of 12 patients (95% CI: 61.5–99.8) successfully reduced the dose to 25 mg/week from 24 weeks after switching to the study drug in the 50 mg/week dose group. Additionally, 9 (81.8%) of 11 patients (95% CI: 48.2–97.7) reduced their dose from 24 weeks to 25 mg/week and maintained LDA/remission until week 52.

Table 2 presents the changes in the total GS and PD scores, combined PD score, DAS28-ESR, DAS28-CRP, SDAI, and CDAI values from baseline to 12, 24, 36, and 52 weeks. Figure 1 illustrates the median of the actual values for each outcome measure. No changes were observed during any period. The overall PD score remained 0, indicating PD remission in the MSUS assessment. All clinical assessments revealed sustained remission.

3.3. Exploratory endpoints

Changes in the HAQ-DI from baseline to 12, 24, 36, and 52 weeks and vdH-mTSS from baseline to 24 and 52 weeks were assessed (Table 2). The median (IQR) results for the HAQ-DI at baseline and 12, 24, 36, and 52 weeks were 0 (0, 0.5), 0 (0, 0.5), 0 (0, 0.25), 0.25 (0, 1.2), and 0

Table 2. Assessment of efficacy

	Median (IQR)
Total GS score	
changes 0-12 weeks	0 (0, 1)
changes 0-24 weeks	1 (0, 2)
changes 0-36 weeks	0 (-0.5, 1.5)
changes 0-52 weeks	1 (0.5, 2)
Total PD score	
changes 0-12 weeks	0 (0, 0)
changes 0-24 weeks	0 (0, 0)
changes 0-36 weeks	0 (0, 0)
changes 0-52 weeks	0 (0, 0)
Combined PD score	
changes 0-12 weeks	0 (0, 1)
changes 0-24 weeks	1 (0, 2)
changes 0-36 weeks	0 (-0.5, 1.5)
changes 0-52 weeks	1 (0.5, 2)
DAS28-ESR	
changes 0-12 weeks	-0.06 (-0.31, 0.05)
changes 0-24 weeks	0.03 (-0.16, 0.31)
changes 0-36 weeks	0.09 (-0.02, 0.69)
changes 0-52 weeks	0.1 (-0.1, 0.69)
DAS28-CRP	
changes 0-12 weeks	0.06 (-0.03, 0.32)
changes 0-24 weeks	0.04 (-0.05, 0.2)
changes 0-36 weeks	0.11 (-0.04, 0.61)
changes 0-52 weeks	0.14 (-0.09, 0.82)
SDAI	
changes 0-12 weeks	-0.1 (-1, 0)
changes 0-24 weeks	0 (-0.7, 0.3)
changes 0-36 weeks	0.1 (-0.3, 1.3)
changes 0-52 weeks	0 (-1.0, 2.8)
CDAI	
changes 0-12 weeks	-0.3 (-1.2, 0)
changes 0-24 weeks	-0.2 (-0.7, 0.2)
changes 0-36 weeks	-0.2 (-0.7, 1.3)
changes 0-52 weeks	0 (-1.1, 2.5)
HAQ-DI	
changes 0-12 weeks	0 (0, 1.2)
changes 0-24 weeks	0 (0, 0)
changes 0-36 weeks	0 (-0.12, 0)
changes 0-52 weeks	0 (0, 0.12)
vdH-mTSS	
changes 0-24 weeks	0 (0, 0)
changes 0-52 weeks	0 (0, 0.75)

CDAI: clinical disease activity index, CRP: C-reactive protein, DAS28: Disease Activity Score-28, ESR: erythrocyte sedimentation rate, GS: gray scale, HAQ-DI: Health Assessment Questionnaire-Disability Index, IQR: Interquantile range, vdH-mTSS: van der Heijde-modified total Sharp score, PD: power Doppler, SDAI: simplified disease activity index.

(0, 1.2), respectively. The median (IQR) values for vdH-mTSS at baseline and at 24 and 52 weeks were 27 (7, 120), 27 (7, 120), and 27 (7, 94), respectively. All the assessments showed little change. Serum biomarkers were similarly evaluated at baseline and at 24, 36, and 52 weeks, with little change. RF, anti-CCP antibodies, and MMP-3 levels did not change (data not shown). Figure 2 shows the multiple cytokine array. The IL-3 and MIP-1α levels could not be measured. All cytokines/chemokines did not change before and after etanercept biosimilar 1 introduction.

3.4. Safety

The safety analysis set determined 10 adverse events (AEs) (n = 20) from the start of the study to 52 weeks. Among these, one serious AE (SAE) occurred 19 days after initiating the study drug, specifically a left renal abscess. The severity was categorized as grade 3. Consequently, the study drug was discontinued. The patient was hospitalized, underwent surgery, and recovered. The severity of other non-SAEs was categorized as grade 1: mild (no intervention required for adverse events) or grade 2: moderate (minimal/local/noninvasive treatment required). One patient discontinued the study drug because of drug eruption. This study revealed 7 patients with adverse drug reactions, including left renal abscess, acute bronchitis, nasal herpes, pneumonia, injection site reaction, drug eruption, and vomiting, from the start of the study to 52 weeks.

4. Discussion

In this study, patients with RA with disease activity that had subsided were switched from etanercept-RP to etanercept biosimilar 1, maintaining the same dose and administration frequency. The results were positive and consisted of many cases that maintained LDA/remission at 24 weeks. Furthermore, LDA/remission was maintained in approximately 80% of the patients at 52 weeks, even when the dose was reduced to 25 mg/week from week 24. Clinical assessment, MSUS score, joint vdH-mTSS score, and biomarker levels exhibited no changes.

The advent of bDMARDs has undeniably caused significant advances in the treatment of RA; however, bDMARDs are expensive, which limits access to treatment for patients with RA. Drug price is one of the most important factors for drug selection. This is a major problem in managing patients with RA, but biosimilars have demonstrated the potential to solve this problem. In phase III trials (*4,24*), switching from etanercept-RP to etanercept biosimilars was equivalent. The EULAR recommendation (*25*), ACR guidelines (*26*), and the Japan College of Rheumatology clinical practice guidelines (*27*) mention the use of biosimilars. The Japanese government is promoting the use of biosimilars because of their potential to reduce the economic burden on health care budgets. However, some physicians are cautious about the clinical use of biosimilars because of doubts regarding their efficacy and safety. Producing a generic drug with the same molecular structure as that

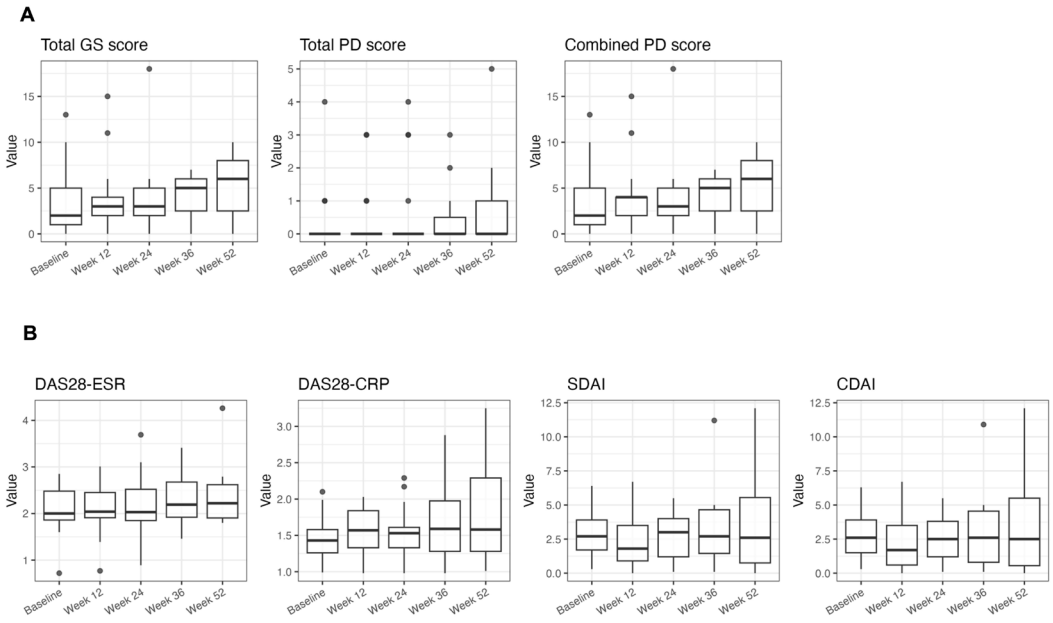

Figure 1. Changes in MSUS scores and clinical disease activity during the study period. (A) MSUS scores and **(B)** clinical disease indicies. Horizontal bar: median, boxes: 25th and 75th percentiles, bars: 5th and 95th percentiles. CDAI: clinical disease activity index, CRP: C-reactive protein, DAS28: Disease Activity Score-28, ESR: erythrocyte sedimentation rate, GS: gray scale, HAQ-DI: Health Assessment Questionnaire-Disability Index, PD: power Doppler, SDAI: simplified disease activity index.

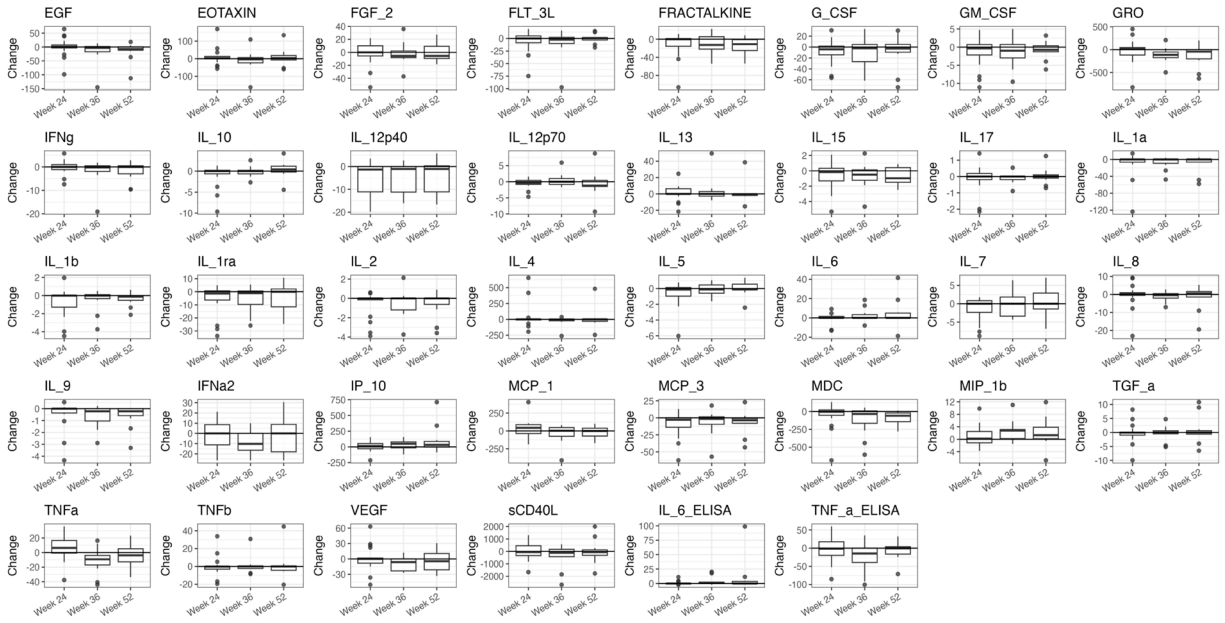

Figure 2. Multiple cytokine array results. Change in each cytokine from baseline at 24, 36, and 52 weeks. None of the changes were significant.

of bDMARD-RP is impossible because bDMARDs are polymeric compounds. Therefore, a robust pharmacovigilance database needs to be established to effectively monitor the post-marketing efficacy and safety of biosimilars. A detailed MSUS-based assessment of the efficacy of switching from etanercept-RP to etanercept biosimilars will provide valuable information, thereby helping clinicians and patients switch with confidence. Additionally, it is necessary to assess the changes in disease activity after the reduction of biosimilars. The PRESERVE study maintained low disease activity in 159 (79.1%) of 201 patients 52 weeks after etanercept was reduced to 25 mg. This study included a 28-week observation period after dose reduction, which was shorter than that of the PRESERVE study, and the results were similar. Additionally, the PRESERVE study (*9*) revealed that the proportion of patients who maintained remission after etanercept dose reduction was higher among those with deep or sustained remission. Tanaka *et al.* (*28*) demonstrated that patients

who achieved disease control following the definitions of sustained ACR/EULAR Boolean remission, CDAI remission, and sustained deep remission by DAS28 were more likely to maintain remission after dose reduction or discontinuation, as evidenced by randomized controlled trial results from studies including PRESERVE and PRIZE (*29*).

Overall, the present study revealed that most patients achieved remission levels in DAS28-ESR, DAS28-CRP, SDAI, and CDAI at baseline that were maintained, and PD remission was sustained, as assessed with MSUS. One patient who did not achieve the primary endpoint had LDA with a baseline DAS28-ESR of 2.66 and did not meet the remission criteria, although both the total GS score and total PD score at baseline were 0 on MSUS. DAS28-ESR exhibited a gradual upward trend and no longer met the LDA criteria, and both total GS and total PD scores on MSUS demonstrated a gradual upward trend after week 24 in this patient. Additionally, the serum levels of IL-6 and CXCL-10 (IP-10) were persistently elevated throughout the course (data not shown).

In this study, clinical assessments such as DAS28-ESR, DAS28-CRP, SADI, and CDAI showed little change after 24 weeks of treatment with etanercept biosimilar1 until week 52, whereas the total GS score and combined PD score of MSUS exhibited an increasing trend. This indicates that MSUS scores may reflect disease activity more accurately than clinical assessment. However, this change was not so bothersome in certain cases. Patients who achieved clinical and PD remission at baseline maintained this status, even after dose reduction of the etanercept biosimilar 1, except for one patient (data not shown). In general, patients who have not achieved clinical and/or PD remission at baseline are more likely to relapse (*30*). The present study yielded similar results.

These results indicate that patients who achieved both clinical and PD remission using etanercept-RP were more likely to remain in remission after switching to the etanercept biosimilar 1 and demonstrated a lower likelihood of relapse after dose reduction.

This study had several limitations. First, the sample size is small. Only 20 patients were registered although 62 cases were expected to be enrolled. This may be because of the absence of an inconsiderable part to the resistance of patients who were stable on etanercept-RP to switching to etanercept biosimilar 1. Concerns about the nocebo effect of switching to etanercept biosimilar 1 existed before the study; however, in the end, no particular problems were observed, as the patients were enrolled after being fully informed. Second, the present study only assessed up to 24 or 52 weeks, and further studies are warranted to enable a long-term evaluation. Third, another aim of this study was to investigate baseline assessment as a predictor of LDA/remission after switching to etanercept biosimilar 1. Owing to the limited number of relapse cases (n = 1), it was challenging to identify clear differences in baseline characteristics, clinical assessments, MSUS findings, and serum biomarkers between LDA/remission and relapse cases. However, the relapse case demonstrated persistently elevated levels of IL-6 and IP-10 throughout the course, which may have been associated with the deterioration of the MSUS scores.

This is the first report to thoroughly evaluate the efficacy of switching from etanercept-RP to etanercept biosimilar 1 with MSUS as well as the efficacy of reducing the dose of etanercept biosimilar 1 with MSUS. Switching from etanercept-RP to etanercept biosimilar 1 is feasible in patients with stable disease activity, and subsequent dose reduction. These results have considerable clinical value.

Acknowledgements

We thank Yoshiro Horai (Sasebo General Med. center), Kazuyoshi Saito (Tobata General Hospital), and Tamami Yoshitama (Yoshitama Clinic for Rheumatic Diseases), all of which are investigators at joint research institutions. We thank our colleagues and staff at the Rheumatology Department of Nagasaki University Hospital for their support.

Funding: This study was funded by AYUMI Pharmaceutical Corporation. (Tokyo, Japan).

Conflict of Interest: Kawakami A received research funding from AYUMI Pharmaceutical Co., Celltrion Healthcare Japan K.K., Gilead Sciences Inc., KIYAN PHARMA Co. Ltd., Janssen Pharmaceutical K.K., ONO Pharmaceutical Co., Asahi Kasei Pharma Corporation, Taisho Pharmaceutical Co. Ltd., Teijin Pharma Co., Chugai Pharmaceutical Co., Kyowa Kirin Co., Boehringer Ingelheim Japan, Abbvie GK, Eli Lilly Japan, Daiichi Sankyo Co., Mitsubishi Tanabe Pharma Co., Bristol-Myers Squibb and Eisai Co. Tada Y received research funding from Chugai Pharmaceutical, and speaker fees from Asahi Kasei Pharma, Astellas Pharma, UCB Japan, Taisyo Pharmaceuticals, Mitsubishi Tanabe Pharma, Eli Lilly Japan, Abbvie, Eisai, Janssen Pharmaceutical, Sanofi, Daiichi-Sankyo, Pfizer Japan, and Bristol Myers Squibb. The other authors have no conflicts of interest to declare.

References

1. Scott DL, Wolfe F, Huizinga TW. Rheumatoid arthritis. Lancet. 2010; 376:1094-1108.
2. Smolen JS, Breedveld FC, Burmester GR, *et al.* Treating rheumatoid arthritis to target: 2014 update of the recommendations of an international task force. Ann Rheum Dis. 2016; 75:3-15.
3. Matsuno H, Tomomitsu M, Hagino A, Shin S, Lee J, Song YW. Phase III, multicentre, double-blind, randomised, parallel-group study to evaluate the similarities between

LBEC0101 and etanercept reference product in terms of efficacy and safety in patients with active rheumatoid arthritis inadequately responding to methotrexate. Ann Rheum Dis. 2018; 77:488-494.
4. Park MC, Matsuno H, Kim J, *et al.* Long-term efficacy, safety and immunogenicity in patients with rheumatoid arthritis continuing on an etanercept biosimilar (LBEC0101) or switching from reference etanercept to LBEC0101: an open-label extension of a phase III multicentre, randomised, double-blind, parallel-group study. Arthritis Res Ther. 2019; 21:122.
5. Colebatch AN, Edwards CJ, Ostergaard M, *et al.* EULAR recommendations for the use of imaging of the joints in the clinical management of rheumatoid arthritis. Ann Rheum Dis. 2013; 72:804-814.
6. Naredo E, Moller I, Cruz A, Carmona L, Garrido J. Power Doppler ultrasonographic monitoring of response to anti-tumor necrosis factor therapy in patients with rheumatoid arthritis. Arthritis Rheum. 2008; 58:2248-2256.
7. Kawashiri SY, Suzuki T, Nakashima Y, Horai Y, Okada A, Iwamoto N, Ichinose K, Tamai M, Arima K, Nakamura H, Origuchi T, Uetani M, Aoyagi K, Eguchi K, Kawakami A. Ultrasonographic examination of rheumatoid arthritis patients who are free of physical synovitis: power Doppler subclinical synovitis is associated with bone erosion. Rheumatology (Oxford). 2014; 53:562-569.
8. Nguyen H, Ruyssen-Witrand A, Gandjbakhch F, Constantin A, Foltz V, Cantagrel A. Prevalence of ultrasound-detected residual synovitis and risk of relapse and structural progression in rheumatoid arthritis patients in clinical remission: a systematic review and meta-analysis. Rheumatology (Oxford). 2014; 53:2110-2118.
9. Smolen JS, Nash P, Durez P, Hall S, Ilivanova E, Irazoque-Palazuelos F, Miranda P, Park MC, Pavelka K, Pedersen R, Szumski A, Hammond C, Koenig AS, Vlahos B. Maintenance, reduction, or withdrawal of etanercept after treatment with etanercept and methotrexate in patients with moderate rheumatoid arthritis (PRESERVE): A randomised controlled trial. Lancet. 2013; 381:918-929.
10. Aletaha D, Neogi T, Silman AJ, *et al.* 2010 Rheumatoid arthritis classification criteria: an American College of Rheumatology/European League Against Rheumatism collaborative initiative. Arthritis Rheum. 2010; 62:2569-2581.
11. World Medical A. World Medical Association Declaration of Helsinki: ethical principles for medical research involving human subjects. JAMA. 2013; 310:2191-2194.
12. Prevoo ML, van 't Hof MA, Kuper HH, van Leeuwen MA, van de Putte LB, van Riel PL. Modified disease activity scores that include twenty-eight-joint counts. Development and validation in a prospective longitudinal study of patients with rheumatoid arthritis. Arthritis Rheum. 1995; 38:44-48.
13. Smolen JS, Breedveld FC, Schiff MH, Kalden JR, Emery P, Eberl G, van Riel PL, Tugwell P. A simplified disease activity index for rheumatoid arthritis for use in clinical practice. Rheumatology (Oxford). 2003; 42:244-257.
14. Aletaha D, Nell VP, Stamm T, Uffmann M, Pflugbeil S, Machold K, Smolen JS. Acute phase reactants add little to composite disease activity indices for rheumatoid arthritis: validation of a clinical activity score. Arthritis Res Ther. 2005; 7:R796-806.
15. Fries JF, Spitz P, Kraines RG, Holman HR. Measurement of patient outcome in arthritis. Arthritis Rheum. 1980; 23:137-145.
16. Torp-Pedersen ST, Terslev L. Settings and artefacts relevant in colour/power Doppler ultrasound in rheumatology. Ann Rheum Dis. 2008; 67:143-149.
17. Nonaka F, Fukui S, Michitsuji T, *et al.* The impact of glucocorticoid use on the outcomes of rheumatoid arthritis in a multicenter ultrasound cohort study. Int J Rheum Dis. 2024; 27:e15118.
18. D'Agostino MA, Boers M, Wakefield RJ, Berner Hammer H, Vittecoq O, Filippou G, Balint P, Moller I, Iagnocco A, Naredo E, Ostergaard M, Gaillez C, Le Bars M. Exploring a new ultrasound score as a clinical predictive tool in patients with rheumatoid arthritis starting abatacept: results from the APPRAISE study. RMD Open. 2016; 2:e000237.
19. Terslev L, Naredo E, Aegerter P, Wakefield RJ, Backhaus M, Balint P, Bruyn GAW, Iagnocco A, Jousse-Joulin S, Schmidt WA, Szkudlarek M, Conaghan PG, Filippucci E, D'Agostino MA. Scoring ultrasound synovitis in rheumatoid arthritis: a EULAR-OMERACT ultrasound taskforce-Part 2: reliability and application to multiple joints of a standardised consensus-based scoring system. RMD Open. 2017; 3:e000427.
20. Nishino A, Kawashiri SY, Koga T, *et al.* Ultrasonographic Efficacy of Biologic and Targeted Synthetic Disease-Modifying Antirheumatic Drug Therapy in Rheumatoid Arthritis From a Multicenter Rheumatoid Arthritis Ultrasound Prospective Cohort in Japan. Arthritis Care Res (Hoboken). 2018; 70:1719-1726.
21. Terslev L, Brahe CH, Ostergaard M, Fana V, Ammitzboll-Danielsen M, Moller T, Krabbe S, Hetland ML, Dohn UM. Using a DAS28-CRP-steered treat-to-target strategy does not eliminate subclinical inflammation as assessed by ultrasonography in rheumatoid arthritis patients in longstanding clinical remission. Arthritis Res Ther. 2021; 23:48.
22. Tanaka Y, Oba K, Koike T, *et al.* Sustained discontinuation of infliximab with a raising-dose strategy after obtaining remission in patients with rheumatoid arthritis: the RRRR study, a randomised controlled trial. Ann Rheum Dis. 2020; 79:94-102.
23. van der Heijde D. How to read radiographs according to the Sharp/van der Heijde method. J Rheumatol. 2000; 27:261-263.
24. Jaworski J, Matucci-Cerinic M, Schulze-Koops H, Buch MH, Kucharz EJ, Allanore Y, Kavanaugh A, Young P, Babic G. Switch from reference etanercept to SDZ ETN, an etanercept biosimilar, does not impact efficacy, safety, and immunogenicity of etanercept in patients with moderate-to-severe rheumatoid arthritis: 48-week results from the phase III, randomized, double-blind EQUIRA study. Arthritis Res Ther. 2019; 21:130.
25. Smolen JS, Landewe RBM, Bergstra SA, *et al.* EULAR recommendations for the management of rheumatoid arthritis with synthetic and biological disease-modifying antirheumatic drugs: 2022 update. Ann Rheum Dis. 2023; 82:3-18.
26. Fraenkel L, Bathon JM, England BR, *et al.* 2021 American College of Rheumatology Guideline for the Treatment of Rheumatoid Arthritis. Arthritis Care Res (Hoboken). 2021; 73:924-939.
27. Nakayama Y, Nagata W, Takeuchi Y, *et al.* Systematic review and meta-analysis for the 2024 update of the Japan College of Rheumatology clinical practice guidelines for the management of rheumatoid arthritis. Mod Rheumatol. 2024; 34:1079-1094.

28. Tanaka Y, Smolen JS, Jones H, Szumski A, Marshall L, Emery P. The effect of deep or sustained remission on maintenance of remission after dose reduction or withdrawal of etanercept in patients with rheumatoid arthritis. Arthritis Res Ther. 2019; 21:164.
29. Emery P, Hammoudeh M, FitzGerald O, Combe B, Martin-Mola E, Buch MH, Krogulec M, Williams T, Gaylord S, Pedersen R, Bukowski J, Vlahos B. Sustained remission with etanercept tapering in early rheumatoid arthritis. N Engl J Med. 2014; 371:1781-1792.
30. Perniola S, Alivernini S, Gremese E, Landolfi G, Carrara G, Iagnocco A, Scire CA. A multiparametric risk table for loss of clinical remission status in patients with rheumatoid arthritis: A starter study post-hoc analysis. Rheumatology (Oxford). 2024; 64:526-532.

Received December 16, 2024; Revised January 29, 2025; Accepted February 17, 2025.

**Address correspondence to:*
Shin-ya Kawashiri, Center for Collaborative Medical Education and Development, Nagasaki University Institute of Biomedical Sciences, Nagasaki, Japan, 1-12-4 Sakamoto, Nagasaki 852-8523, Japan.
E-mail: shin-ya@nagasaki-u.ac.jp

Released online in J-STAGE as advance publication February 26, 2025.

Original Article

DOI: 10.5582/ddt.2025.01000

Emulsification-based liposomal formulation of gallic acid and curcumin as potent topical antioxidants

Takron Chantadee[1,2,3], Siripat Chaichit[1], Kanokwan Kiattisin[1], Worrapan Poomanee[1], Siriporn Okonogi[1,2], Pimpak Phumat[1,2,*]

[1] Department of Pharmaceutical Sciences, Faculty of Pharmacy, Chiang Mai University, Chiang Mai, Thailand;
[2] Center of Excellence in Pharmaceutical Nanotechnology, Chiang Mai University, Chiang Mai, Thailand;
[3] Natural Bioactive and Material for Health Promotion and Drug Delivery System Group (NBM), Faculty of Pharmacy, Silpakorn University, Nakhon Pathom, Thailand.

SUMMARY: Excessive free radicals in the skin cause oxidative stress, damaging cells and leading to aging, melasma, and inflammation. This study developed a liposome system for co-delivering antioxidants to enhance their efficacy in deeper skin layers. Four phenolic compounds were screened for antioxidant activity using DPPH, nitric oxide scavenging, and lipid peroxidation assays. Gallic acid and curcumin, showing the strongest activity, were selected for liposome encapsulation *via* an emulsification method, with particle size reduction by probe sonication. High-performance liquid chromatography (HPLC) was used for chemical analysis, and particle morphology was examined with transmission electron microscopy. Studies on skin penetration, retention, and release were conducted. The optimized liposome (LP4) had a small particle size (< 150 nm), an unilamellar structure, and high entrapment efficiency (99% gallic acid and 92% curcumin). LP4 promoted effective skin retention of curcumin with slow penetration, while the release of gallic acid and curcumin from LP4 followed a Higuchi kinetic model and Zero-order kinetic model, respectively. This delivery system demonstrates potential for targeted antioxidant delivery, offering enhanced protection against oxidative damage in the skin.

Keywords: gallic acid, curcumin, liposome, skin penetration, kinetic releasing

1. Introduction

Oxidative stress is a condition that exists an imbalance of the production of radicals and a neutralized mechanism of these radicals, including reactive oxygen species (ROS) which are hydroxyl radical ($OH^{\bullet}$), superoxide ($O2^{\bullet-}$), and peroxyl radical ($ROO^{\bullet}$), as well as reactive nitrogen species (RNS) (*1*). An excess of free radicals can damage cells and various systems, resulting in protein modification, genetic alterations, and trigger inflammation (*2,3*).

Skin, a primary barrier that functions against the external factors that can elevate free radical levels within the body, including environmental pollutants, ultraviolet (UV) radiation from sunlight. Free radicals in the skin induce inflammation and damage cells in deep skin layers such as fibroblasts, keratinocytes in dermis layer that resulted in skin aging, leading to abnormal pigmentation, and reduced skin barrier functions (*4*). The continuous skin damaged by radicals can lead to chronic skin inflammations like seborrheic dermatitis and eczema and damaging cellular structures, including deoxyribonucleic acid (DNA), proteins, and lipids in dermal cells, ultimately impairing skin function and accelerating aging processes. The substances that function as antioxidants thus play a crucial role in reducing these harmful effects on the body (*5*).

Phenolic substances are found in many kinds of plants which are widely recognized as potential antioxidant properties, have gained substantial attention in pharmaceutical and cosmetic applications. Their chemical structure consists of a benzene ring with at least one hydroxyl group (OH), that grants antioxidant properties by neutralizing free radicals and thereby mitigating oxidative stress and cellular damage (*6,7*). The structural differences among phenolic substances result in varying physicochemical properties and lead to constrain of their applications by poor solubility, instability, and limited skin penetration. Various studies have been reported on the antioxidant and anti-inflammatory properties of phenolic substances, which are used to prevent and reduce skin inflammation. Antioxidants have garnered significant attention in the cosmetic and pharmaceutical industries due to their

potential to alleviate skin damage and promote healthy aging (*8*). Gallic acid (GA), a hydrophilic phenolic compound that possesses strong antioxidative activity with various mechanisms (*9*). Lipophilic phenolic compounds which are curcumin (Cur), a polyphenolic compound major found in turmeric, kaempferol (Kaf) which is a flavonoid that generally found in tea, broccoli, cabbage, kale, beans, and sesamin (Sem) a lignan substance found in sesame seeds have been reported as the potential antioxidants and anti-inflammatory agents (*10–12*). However, the skin permeation through the skin's lipid-rich barrier of those compounds is often limited due to their physicochemical properties such as hydrophilic-lipophilic properties, molecular size, structural complexity, including chemical instability (*13*).

Liposomes have been extensively explored as promising delivery system for hydrophobic and hydrophilic substances. These spherical vesicles, composed of lipid bilayers, facilitate the entrapment and penetration of active compounds into deeper skin layers while allowing controlled release (*14*). The encapsulation of hydrophobic or lipophilic substances in liposomes not only enhances their solubility but also protects them from degradation and improves their overall stability. Encapsulating phenolic compounds in liposomes significantly increases their solubility, enhances skin penetration, and improves their stability (*15*). This delivery method enables more effective targeting of desired sites, thereby augmenting their biological activities, including their antioxidative effects (*7*).

It is therefore interesting to investigate and compare the antioxidative activities of potential substances with different physicochemical properties which are GA, Cur, Kaf, and Sem. Subsequently, the two substances exhibiting the strongest antioxidant activity will be selected to develop substance-encapsulated liposomes as innovative carriers for promising antioxidant delivery through the skin and application in cosmetic formulations.

2. Materials and Methods

2.1. Materials

The reagents and chemicals were of analytical grade. 2,2-Diphenyl-1picrylhydrazyl (DPPH) and GA from Fluka (Werdenberg, Buchs, Switzerland). Ascorbic acid, β-carotene, linoleic acid. tocopheryl acetate from Glentham Life Sciences (Planegg, Munich, Germany). Cur, Kaf, and Sem purchased from Greenway (Nanjing, Jiangsu, China). Phosphate buffer was from HiMedia (Kennett square, Pennsylvania, USA). Sodium nitroprusside (SNP), N-(1-Naphthyl) ethylenediamine dihydrochloride, phosphotungstic acid were from Kemaus (Cherrybrook, New south wales, Australia). Hydrogenated lecithin and cholesterol from Nikko Chemicals (Pulau Seraya, Jurong island, Singapore). Ethylhexyl palmitate, ethylhexyl glycerin dipropylene glycol, polysorbate 80, and sorbitan were from BASF (Ludwigshafen, Rhineland-Palatinate, Germany). Phenoxyethanol from Seppic (La-Garenne Colombes, Paris, France). Phosphotungstic acid from QRëC (Mueang, Chonburi, Thailand). Absolute ethanol, chloroform, methanol from RCI Labscan (Pathumwan, Bangkok, Thailand).

2.2. Determination of antioxidant activity

2.2.1. DPPH assay

This experiment followed a modified method from previous study (*16*). A total of 20 µL of the phenolic substance solution (ranging from 1 to 10,000 µg/mL) that dissolved in absolute ethanol was mixed with 180 µL of DPPH reagent (1.0 M^{-4}) in 96-well plate and incubated in the dark at an ambient temperature for 30 min. Then, the plate was subjected to analyzed using a microplate reader (SPECTROstar Nano, BMG Labtech, Ortenberg, Germany) at the wavelength 520 nm. The antioxidant activity against DPPH radicals was expressed as the percentage of inhibition (% inhibition), calculated using the following equation:

$$\% \text{ Inhibition} = [(Ap - An) - (At - Ad/(Ap - Ar)] \times 100$$

where Ap, An, At, Ar were the absorbances of reagent mixed with diluent, diluent of test sample, tested samples mixed with reagent, and the tested samples mixed with diluent of sample, respectively. Ascorbic acid was used as positive control in comparison.

2.2.2. Nitric oxide (NO) scavenging assay

NO scavenging assay was carid out using Griess test following method of Jagetia with some modification (*17*). A total of 20 µL of the phenolic substance solution (ranging from 1 to 10,000 µg/mL) was added in 96-well plate, followed by adding 60 µL of 10 mM SNP, 20 µL of PBS pH 7.4 and incubated in the dark at an ambient temperature for 150 min. After that, 50 µL of 1% w/v sulfanilamide dissolved in 2% v/v phosphoric acid was added in the tested mixture and continuously incubated in the same condition for 5 min. Then, 50 µL of *N*-(1-naphthyl) ethylenediamine dihydrochloride was added and incubated at 25°C for 10 min. The solution mixtures were measured the nitrite concentration at 540 nm by microplate reader. The activity against NO radicals of the tested samples was expressed as the percentage of scavenging (% scavenging), calculated using the following equation:

$$\% \text{ Scavenging} = [(As - Ab) - (Aw - Ao)/(As - Ab)] \times 100$$

where As, Ab, Aw, Ao were the absorbances of SNP

mixed with diluent; ethanol or DI water and PBS (positive control), diluent (negative control), tested samples mixed with SNP and PBS, sample mixed diluent and PBS, respectively. Ascorbic acid was used as positive control in comparison.

2.2.3. Lipid peroxidation inhibition assay

This study was evaluated β-carotene bleaching inhibitory ability following the method of Elzaawely with some modification (*18*). β-carotene emulsion was prepared by mixing of β-carotene solution in chloroform (2,000 µg/mL) with 200 mg of Tween 20 and 20 mg of linoleic acid. The mixture was then allowed to stand for removal of chloroform using evaporator (MA3S, Eyela, Tokyo, Japan) and a thin film was obtained. Then, adding 50 mL of DI water, the mixture was subjected to shaking, which resulted in the formation of self-emulsion. The emulsion (180 µL) was combined with a sample (20 µL) in 96-well plate. The absorbance was determined at 470 nm at 0, 30, 60, 90, and 120 min. The β-carotene bleaching inhibitory activity of a sample was assessed following equation as shown in 2.2.1.

2.3. High-performance liquid chromatography (HPLC) analysis

The qualitative analysis of GA and Cur was done by using an isocratic HPLC system using an Agilent Eclipse XDB-C18 (4.6 × 150 mm) HPLC column and analyzed on a Shimadzu Prominence HPLC systems (Nakagyo-ku, Kyoto, Japan). The mobile phase consisted of methanol (A) and 1% phosphoric acid in DI water (B) in a ratio of 70%-90% A and 10%-30% B, the flow rate was 0.7 mL/min for 15 min, and the injection volume was 10 µL. The detection wavelength was 280 nm. Mixed GA and Cur solution was used as the sample to investigate the suitable mobile phase ratios for HPLC condition. An intact GA and Cur diluted at a concentration range of 0-500 µg/mL was subjected to the HPLC at the same condition to construct a linear standard curve. All the samples were prepared by dissolved in methanol and filtered through 0.45 µm before analysis.

2.4. Development of liposomal formulations

The preparation was first prepared the primary emulsion. The lipid phase which consists of hydrogenated lecithin, cholesterol, ethylhexyl palmitate and/or ethylhexyl glycerin, dipropylene glycol, tocopheryl acetate, sorbitan oleate, and phenoxyethanol were weighed in the same beaker and mixed with gentle agitation at 60°C for 15 min and the mixer was presented as a clear mixture. An aqueous phase was prepared by dissolving polysorbate 80, sorbitan oleate in DI water with gentle agitation under 60-63°C for 15 min and the mixture showed a clear solution. Subsequently, the lipid and aqueous phases were mixed to obtain liposome primary emulsion, which is then homogenized using a high-shear homogenizer T 25 digital ULTRA-TURRAX® IKA (Breisgau-Hochschwarzwald, Staufen, Germany) at a speed of 7,000 rpm for 15 min to produce a uniform emulsion. Then, particle size was reduced by using probe sonicator (VCX 600, Sonics & Materials, Newtown, Connecticut, USA) at 65% intensity for 15 min with an alternating on-off pattern every 1 second under temperature below 20°C to prevent excessive heat production during the process of size reduction.

2.5. Viscosity study

The viscosity value of each formulation was carried out using a plate and plate rheometer (R/S Brookfiled, Massachusetts, USA). A sample volume of 1-3 g was evaluated with the shear rate ranging from 1-60 s^{-1} for 120 s; at 25 ± 2°C. Brookfield Rheocalc operating software was used to analyze.

2.6. Investigation of particle size and zeta potential

The liposomal particles were investigated the size, size distribution, and zeta potential using a Zetasizer (Malvern, Worcestershire, UK). The sample was diluted 100-fold to 1,000-fold in DI water before analysis, then subjected to the Zetasizer and detected at a fixed angle of 173° at 25°C for size and size distribution. A size distribution was expressed as a polydispersity index (PdI) value. Zeta potential of the particles was also examined using Zetasizer ant 25°C. All measurements were performed in triplicate.

2.7. Entrapment efficiency

For sample preparation, liposomal encapsulated substance formulation was firstly diluted in DI water to 2-fold and then 0.5 mL of diluted sample was centrifuged at 10,000 rpm at 25°C for 30 min using Amicron Ultra (50 kDa) – 0.5 mL centrifugal filters (Merck Millipore Ltd., Carrigtwohill, Cork, Ireland) to separate free substance and liposomal encapsulation. Then, the unentrapped substance (free substance) was quantified using HPLC, and entrapment efficiency (EE) was expressed as percentage (%) and calculated as equation:

$$\% EE = (Co - Cf/Co) \times 100$$

where Co is the total amount of loaded substance and Cf is amount of free substance.

2.8. Liposomal morphology

Transmission electron microscopy (TEM) was used to investigate the morphology of the selected liposome formulation. The formulation was diluted 100-fold with

DI water and analyzed using a TEM JEM-2010 (JEOL, Akishima, Tokyo, Japan) operating at an acceleration voltage of 100 kV. For sample preparation, 10 µL of diluted formulation was carefully dropped onto a 200-mesh copper grid coated with formvar and carbon (FCF-200 mesh Cu, Electron Microscopy Sciences, Hatfield, Pennsylvania, USA) and the sample was allowed to air-dry for 5 min. Excess solution was removed using filter paper and the sample was then stained with a 3% (w/v) phosphotungstic acid solution. After 5 min, the excess staining solution was removed with filter paper. The prepared grid was allowed to dry at an ambient temperature at least 24 h, it was then subsequently subjected into the TEM for analysis.

2.9. Kinetic releasing study

The release of GA and Cur from selected liposome formulation were determined by a dialysis method modified from our previous study (*19*). The release kinetic was analyzed according to Zero-order, First-order, Higuchi model and Korsemeyer-Peppas model. The GA and Cur without loading in liposomes (free form) were used in comparison. PBS pH 7.4 mixed 0.5% w/v Tween 80 was used as releasing medium. 1 mL of LP7 was pipetted into a pre-swollen dialysis bag (regenerated cellulose membrane with MWCO of 12,000). The dialysis bag was tightly closed and immersed into 20 mL of the release medium with stirring at 100 rpm at 37 ± 2°C. Samples (1 mL) of the release medium were drawn peri-odically at time interval of 5, 15, 30, 60, and 120 min. Fresh medium with the same volume was added into the dissolution medium after each sample withdrawal. The amount of GA and Cur was determined by HPLC as described above. The percentage cumulative release of GA and Cur which were the loaded substances at time T (Rt) was calculated using the following equation:

$$Rt = (Rt/Ro) \times 100\%$$

where Rt is the cumulative concentration of loaded substances released in the release medium at time t and Ro is the initial amount loaded substances in liposome. The results obtained were analyzed for drug release kinetics using Microsoft Excel version 2409.

2.10. Skin penetration and skin retention studies

This study was conducted using Franz diffusion cell method modified from the previous study (*20*). The Franz diffusion cell diffusion system (V9-CA, PermeGear Inc., Hellertown, Pennsylvania, USA) composed a diffusion area of 1.77 cm^2, receptor medium capacity of 12 mL which was PBS pH 7.4 and operated under a constant temperature of 37 ± 0.5°C *via* thermostatic bath circulation. The receptor medium was stirred constantly at 350 rpm during the experiments. A porcine membrane was used as a membrane model in this experiment. The 1 mL of tested samples; mixed intact GA-CUR solution and liposomal GA-CUR formulation were placed in donor chamber, and 1 mL of medium from receptor chamber was sampling at 15, 30, 60, 90, 120, 240, 360, and 480 min, then replaced by a fresh medium with an equal volume to maintain the sink condition throughout the investigation. The collected samples were analyzed using HPLC.

The formulation remained on the surface membrane after the end of skin penetration experiment was subsequently removed by washed repeatedly with deionized water. The membrane was then cut into small pieces and extracted with methanol using a sonication bath for 10 min. The quantitative of GA and Cur, the sample extracted from the membrane were analyzed by HPLC. All measurements were performed in triplicate.

2.11. Statistical analysis

All results are presented as mean ± standard deviation (n = 3). Statistical analysis was conducted using SPSS software version 17.0 for Windows. The group differences were investigate using one-way analysis of variance (ANOVA), followed by Tukey's post-hoc test. A P-value ≤ 0.05 was considered to statistical significance.

3. Results

3.1. Antioxidative activities of potential phenolic substances

The antioxidative property of potential phenolic substances that were selected in this study (GA, Cur, Kaf, Sem) were determined in comparison using various mechanisms of testing. Ascorbic acid was used as a positive control of all methods. The results are shown in Table 1.

DPPH assay was performed to assess the potential of the tested sample in scavenging activity against OH^- radical generated from DPPH reagent. The results were expressed as the concentration of the tested sample that could inhibit the generated radicals as 50% (IC_{50}). The IC_{50} values were calculated from the regression equations of each sample. Ascorbic acid possessed the highest activity with IC_{50} of 0.78 ± 0.10 µg/mL. GA exhibited the highest inhibitory activity compared to other tested samples, with the significantly lowest IC_{50} of 2.37 ± 0.32 µg/mL ($P < 0.05$), followed by Cur and Kaf. While Sem did not show the activity at the tested concentration (1,000 µg/mL).

NO scavenging assay was conducted to evaluate the potential of the tested samples in neutralizing RNS or NO radicals which are unstable and typically present under aerobic conditions. The results were expressed as the scavenging concentration required to achieve 50% inhibition of NO radicals (SC_{50}). The SC_{50} of these tested

Table 1. Screening of antioxidant activity with various mechanisms obtained from four phenolic substances

Samples	DPPH assay IC_{50}* (µg/mL)	NO assay SC_{50}* (µg/mL)	Lipid peroxidation inhibition assay % Inhibition* after 2 h (Sample concentration of 10 µg/mL)
GA	2.37 ± 0.32^{b}	943.0 ± 2.91^{c}	94.44 ± 0.00^{a}
Cur	11.77 ± 0.40^{c}	70.0 ± 0.02^{b}	59.26 ± 2.61^{c}
Kaf	10.64 ± 0.26^{c}	$> 1{,}000^{d}$	31.48 ± 6.93^{d}
Sem	$> 1{,}000^{d}$	$> 1{,}000^{d}$	88.89 ± 4.53^{b}
Ascorbic acid	0.78 ± 0.10^{a}	40.0 ± 0.00^{a}	37.04 ± 6.93^{d}

*Lowercase letters indicate significant differences ($P < 0.05$) in each assay.

samples were calculated from the obtained regression equations. It was shown that Cur possessed the highest activity with SC_{50} of 70.0 ± 0.02 µg/mL significantly ($P < 0.05$), followed by GA. Kaf and Sem not presented the activity with the tested concentration (1,000 µg/mL).

β-Carotene bleaching procedure was employed to explore the antioxidant potential through lipid peroxidation mechanism. Antioxidant activity is measured by the stability of the orange color of β-carotene over time against free radicals generated in DI water, a reaction medium, which can degrade β-carotene molecules. The inhibition of β-carotene bleaching is expressed as % Inhibition. The results found that GA possessed the highest inhibition (88%), followed by Sem, Cur, ascorbic acid, and Kam, respectively.

These experiments could conclude that GA and Cur provide a potential antioxidant activity after compared to other samples. Thus, GA and Cur were selected to develop the liposome system.

3.2. HPLC analysis

HPLC conditions were trial with various ratios of mobile phase to obtain GA and Cur peaks under operation using single condition. The suitable ratio of mobile phase contained methanol and 1% PA solution in a ratio of 70:30 which provided a separate HPLC peak of GA and Cur as shown in Figure 1 at the retention time of 2.16 min and 6.53 min, respectively. The GA and Cur quantitative determination along the study were calculated from the linear equations obtained from HPLC analysis following y = 104632 + 653876 of standard GA solution (R^2 = 0.9993) and y = 57880x + 260716 of standard Cur solution (R^2 = 0.9997).

3.3. Liposomal formulations

In the formulations, hydrogenated lecithin was employed as a vesicle membrane (shell), cholesterol could stabilize membrane, ethylhexyl palmitate, ethylhexyl glycerin, and dipropylene glycol were solubilizing agents, tocopheryl acetate used as antioxidants of system, polysorbate 80 and sorbitan oleate were the surfactants, and phenoxyethanol used as a preservative. The liposomal vesicles were self-assembly forming upon mixing of lipid and aqueous phases. The particle size was

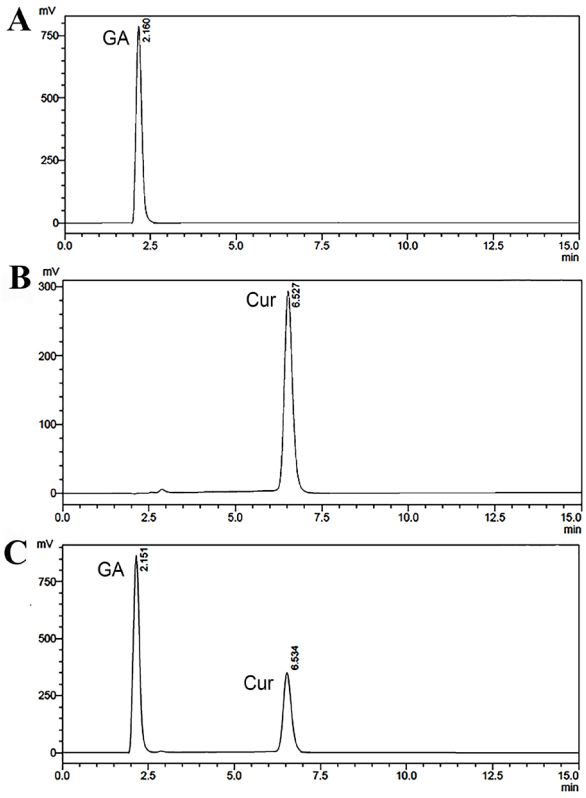

Figure 1. HPLC chromatograms. (A) GA peak at RT of 2.1 min, (B) Cur peak at RT of 6.5 min, and **(C)** HPLC peaks of GA and Cur of mixed solution, analysis at 280 nm.

extensively reduced by ultrasound force.

The formulations were developed by varying the percentages of hydrogenated lecithin, surfactants, cholesterol, and ethylhexyl palmitate as shown in Table 2. The outer appearance of the formulations, as shown in Figure 2, was observed through visual analysis. Blank liposomal formulations (LB) were initially prepared and characterized. It was found that high concentrations of hydrogenated lecithin (LB1 and LB2) affected the turbidity of the formulations. LB1 and LB2 were more translucent than the others. However, phase separation was observed in LB1 after 24 h, whereas LB2 was homogenized and thickened to a cream-like appearance. LB3 was subsequently developed from LB2 by reducing the hydrogenated lecithin content. The appearance of LB3 exhibited increased fluidity with white opacity. Subsequently, LB4 was developed by reducing

Table 2. Composition of blank liposome (LB) and GA-Cur co-loaded in liposome (LP) formulations

Composition	Formulation (% w/w)							
	LB1	LB2	LB3	LB4	LP1	LP2	LP3	LP4
Hydrogenated lecithin	2	2	1	0.5	2	2	1	0.5
Cholesterol	0.4	0.4	0.4	0.2	0.4	0.4	0.4	0.2
Ethylhexyl palmitate	10	10	10	5	10	10	10	5
Ethylhexyl glycerin	6	-	-	-	6	-	-	-
Dipropylene glycol	5	5	5	2.5	5	5	5	2.5
Tocopheryl acetate	1	1	1	1	1	1	1	1
Polysorbate 80	8	16	16	8	8	16	16	8
Sorbitan oleate	10	20	20	10	10	20	20	10
Cur	-	-	-	-	0.5	0.5	0.5	0.5
GA	-	-	-	-	0.5	0.5	0.5	0.5
Phenoxyethanol	0.5	0.5	0.5	0.5	0.5	0.5	0.5	0.5
Water	58.1	44.1	45.1	72.05	58.1	44.1	45.1	72.05

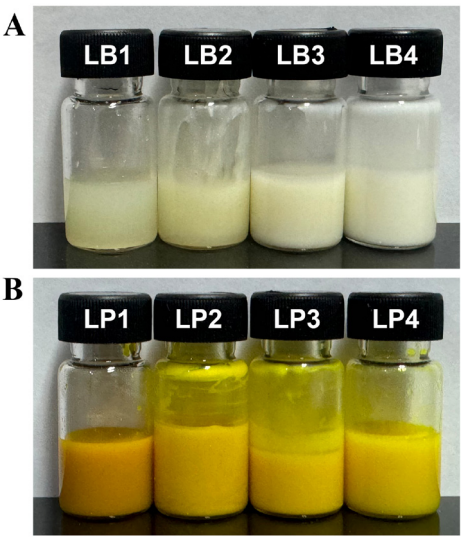

Figure 2. The appearance of liposomal formulations. (A) blank liposome (LB1- LB4) and **(B)** GA-Cur loading in liposome (LP1 – LP4).

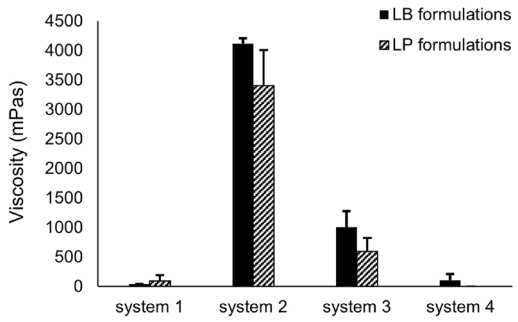

Figure 3. Viscosity of liposomal formulations. Comparison of viscosity between LB and LP formulations for all systems.

the amounts of hydrogenated lecithin, cholesterol, ethylhexyl palmitate, and surfactants used from LB3. This formulation displayed fluidity and white turbidity like milk. Each GA and Cur were incorporated at a concentration of 0.5%. GA was prepared in the aqueous phase, while Cur was prepared in the lipid phase. The appearance of GA-Cur loaded liposomes (LP) was turbid yellow in color, and the fluidity was similar to that of the LB formulations. Insistingly that LP4 exhibited the most stable formulation with a homogeneous appearance.

3.4. Viscosity study

The formulations with and without GA and Cur loading were investigated in comparison. The results were demonstrated in Figure 3. In LB formulations, almost all systems demonstrated higher viscosity compared to their LP in the same system, except for System 1. The LB1 exhibited lower viscosity than the LP1, possibly due to phase separation. System 2 showed the highest viscosity, with values of 4,113.72 ± 97.35 mPas for LB2 and 3,408.96 ± 600.42 mPas for LP2. System 4, which exhibited fluidity, showed low viscosity in LB4 with a value of 104.84 ± 152.19 mPas, whereas the viscosity value could not be determined for LP4.

3.5. Determination of particle size analysis and %EE

The results of particle analysis obtained from Zetasizer that demonstrated in Table 3 were expressed in size, size distribution with polydispersity index (PdI), and zeta potential (ZP) that indicated the trending of stabilized particles. The liposomal particles of LB formulations demonstrate smaller size than the particles of LP which contained GA and Cur in system. The particle size of LB was in a range of 51.53 ± 0.12 to 223.87 ± 16.05 nm whereas the particle size of LP was in a range of 130.07 ± 0.40 to 804.27 ± 74.71 nm. PdI value of formulations varied from 0.24 to 0.90 for LB formulations and in a rage of 0.16 to 0.69 for LP formulations. ZP of LB and LP formulations were a negative charge with a high value (more than – 30 mV) that indicated the stabilized liposomal particles in system. All formulations could entrap GA in system effectively with the entrapment efficiency of almost 100%. The formulation that provided high Cur entrapment in system may in LP2 which was composed of high hydrogenated lecithin and surfactants

Table 3. Characterization liposomal formulations, expressed as particles size, PdI value, ZP, and %EE

Formulations	Size (nm)*	PdI*	ZP (mV)*	% EE*	
				GA	Cur
LB1	157.40 ± 2.03[c]	0.36 ± 0.06[b]	-43.33 ± 0.96[a,b]	-	-
LB2	51.53 ± 0.12[a]	0.24 ± 0.01[a]	-28.33 ± 5.81[c]	-	-
LB3	223.87 ± 16.05[d]	0.90 ± 0.13[d]	-47.80 ± 0.44[a]	-	-
LB4	70.67 ± 5.03[b]	0.42 ± 0.04[c]	-36.17 ± 0.45[b]	-	-
LP1	231.87 ± 2.83[b]	0.30 ± 0.04[b]	-40.60 ± 0.61[b]	99.91 ± 0.03[b,c]	77.13 ± 0.02[d]
LP2	288.07 ± 1.89[b]	0.56 ± 0.08[c]	-49.17 ± 1.00[a]	99.90 ± 0.05[c]	95.43 ± 0.00[a]
LP3	804.27 ± 74.71[c]	0.69 ± 0.02[d]	-30.95 ± 0.15[d]	99.92 ± 0.07[b]	89.99 ± 0.01[c]
LP4	130.07 ± 0.40[a]	0.19 ± 0.01[a]	-36.50 ± 1.04[c]	99.99 ± 0.11[a]	92.93 ± 0.01[b]

*Lowercase letters indicate significant differences in blank liposome group (LB) and liposomal encapsulation group (LP) ($P < 0.05$) in terms of size, PdI, zeta potential and %EE investigation.

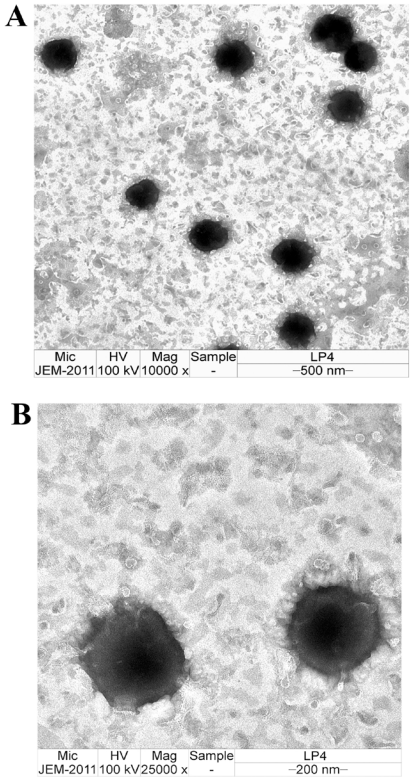

Figure 4. TEM images. The morphology of liposomes LP4 containing GA and Cur curcumin at magnification of **(A)** 10,000× and **(B)** 25,000×.

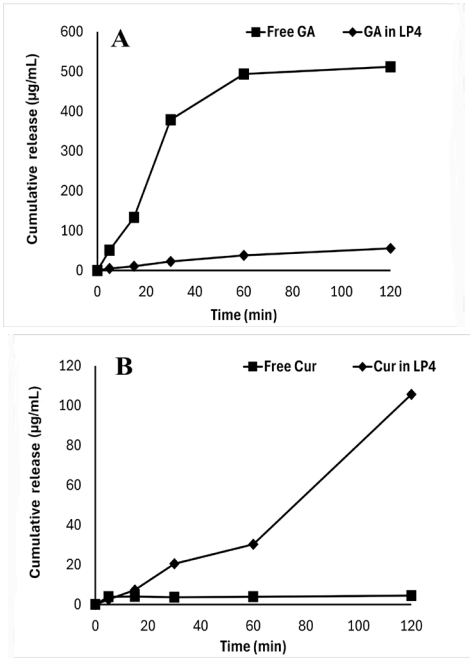

Figure 5. *In vitro* release. (A) Release profile of free GA compared with GA in LP4 and **(B)** free Cur in comparison with Cur in LP4 compared with Cur in LP4.

contents, followed by LP4, LP3, and LP1, respectively.

3.6. Liposomal morphology

From the results of viscosity, appearance characterization, particle size analysis, and %EE, LP4 was considered as the best system to entrapped GA and Cur with a small, stabilized particle size. Thus, LP4 was selected to study in the next step.

The morphology of the liposome LP4 containing GA and Cur investigated under TEM was shown as TEM images. The liposomal particles were a spherical dark shape with a good distribution as shown in Figure 4A. An unilamellar liposomes, a vesicle with a single lipid layer, were observed at a high magnification (25,000×) as shown in Figure 4B. The particle size from TEM images (approximately 200 nm) resembled that conducted from Zetasizer. Some large particles that were observed may be attributed to the dehydration process in sample preparation which resulted in particle aggregation.

3.7. Release study

The release study was performed under the sink conditions. 0.5% Tween 80 in PBS pH 7.4 was used as medium in the *in vitro* release study. The results from this study were shown in Figure 5, demonstrated a slow sustained releasing pattern of GA and Cur from LP4. GA from LP4 gradually released at 15 min with approximately 2% released, followed by a sustained release. Meanwhile, Cur from LP4 demonstrated biphasic release pattern. The release of GA and Cur from

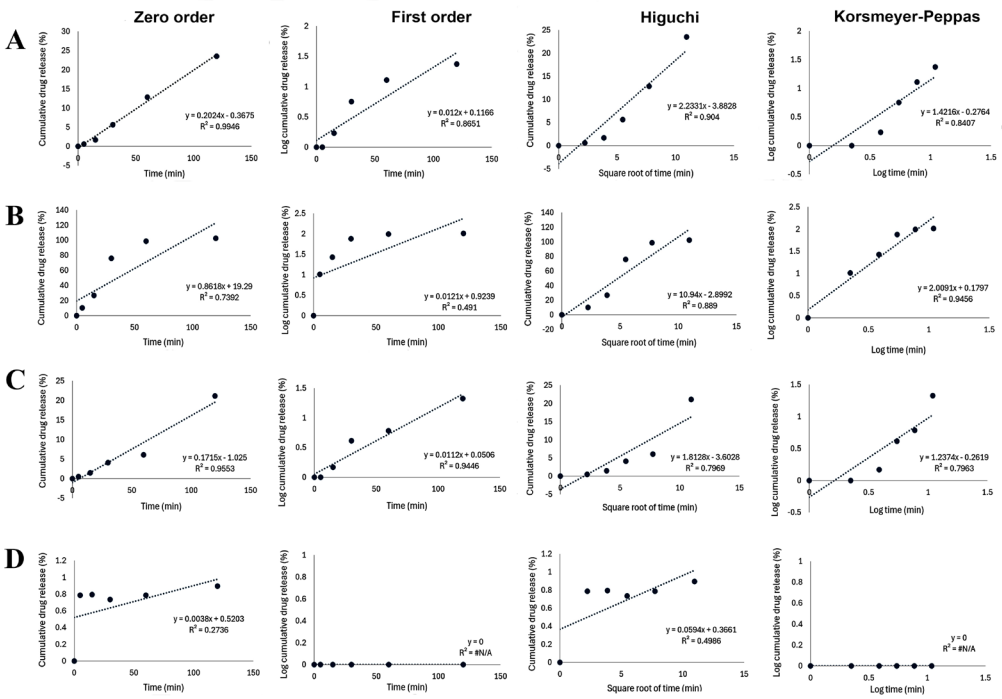

Figure 6. The kinetics of drug release. Release kinetics plot of **(A)** GA in LP4, **(B)** free GA, **(C)** Cur in LP4, and **(D)** free Cur using various kinetic models.

Table 4. Rate of GA and Cur release with various kinetic mechanisms

Samples	Kinetic releasing model							
	Zero-order		First-order		Higuchi		Korsmeyer-Peppas	
	k	R^2	k	R^2	k	R^2	k	R^2
GA in LP4	0.0926	0.9584	0.0097	0.7465	1.0787	0.9706	1.2023	0.7975
Free GA	0.8618	0.7392	0.0121	0.491	10.94	0.889	2.0091	0.9456
Cur in LP4	0.1945	0.9553	0.0123	0.8867	1.9509	0.7969	1.3663	0.7609
Free Cur	0.0038	0.2736	N/A	N/A	0.0594	0.4986	N/A	N/A

N/A: Not Applicable.

liposomes (LP4) at the end of the experiment (120 min) were similarly found to be 11.14 ± 0.10% and 0.90 ± 0.02%, respectively. Whereas, free GA possessed a short initial burst release of 379 ± 0.26 µg/mL (76%) after 30 min and then subsequently sustained released to 100% after 120 min and free Cur was released less than 10 µg/mL along the study time. These results suggest that encapsulation in LP4 effectively modulates the release of both GA and Cur, providing a more controlled and sustained delivery compared to their free forms.

In this study, the release mechanisms of GA and Cur from liposomes, compared to their free forms, were evaluated using four mathematical models: Zero-order, First-order, Higuchi, and Korsmeyer-Peppas. The most suitable model was determined based on the correlation coefficient (R^2) obtained from linear regression analysis for each model, as shown in Figure 6 and Table 4. After 120 min of the release study, the results indicated that the release profile of GA from liposomes followed the Higuchi model, with a release rate constant (k) of 1.0787. In contrast, Cur from liposomes exhibited a release behavior consistent with the Zero-order model, with a slower release rate characterized by a k value of 0.1945. For the free forms, both GA and Cur followed the Higuchi model, suggesting that the release mechanism was governed by Fickian diffusion. Furthermore, free GA was released more rapidly than free Cur, due to its smaller molecular size and higher hydrophilicity.

While the release mechanism analysis based on the R^2 values of various models provides valuable insights, it may not offer a comprehensive understanding of the underlying processes. Moreover, the study duration may be insufficient to capture the complete release profile. Therefore, further investigations are necessary to elucidate the complex interplay of factors governing drug release kinetics from liposomal formulations. Advanced techniques, such as molecular-level simulations, could be employed to provide a more detailed and nuanced understanding of the release phenomena.

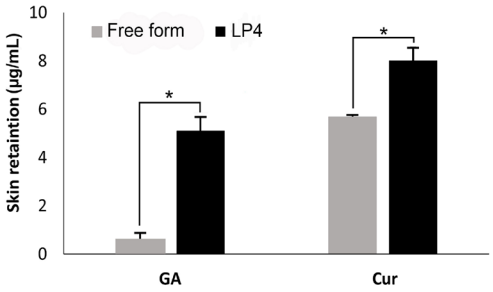

Figure 7. The accumulated compounds in the membrane that were obtained from Franz diffusion cell method. GA and Cur retention in skin membrane results 480 min after the *in vitro* skin permeation study. The quantitative analysis was employed by comparing free form compounds with compounds loading in LP4 (*$P < 0.05$).

3.8. Skin penetration and skin retention studies

The result of skin penetration study obtained from Franz diffusion cell method was found that only free GA and GA in LP4 can penetrate though the membrane to receiver chamber since 5 min of the study with concentration of 2.03 ± 0.27 µg/mL, whereas the initial penetration of GA in LP4 through the receiver chamber was 1.62 ± 0.29 µg/mL. The in-tact GA was rapidly absorbed more GA in LP4 and increased in a time-dependent manner. GA was found in the receiver chamber with concentration of 2.03 ± 0.27, 2.51 ± 0.11, 4.47 ± 0.23, 8.28 ± 1.08, 11.11 ± 0.88, 15.96 ± 0.59, 22.36 ± 1.47, and 29.63 ± 2.18 µg/mL at 5, 15, 30, 60, 120, 240, 360, and 480 min, respectively. Whereas Cur both in LP4 and free form were not found in the medium receiver chamber. However, the results from skin retention study as shown in Figure 7 demonstrated that liposome enhanced GA and Cur penetrated deep skin and retained in the skin significantly ($P < 0.05$). The free GA and free Cur were retained in membrane or skin with a concentration of 0.59 ± 0.07 µg/mL and 5.69 ± 0.29 µg/mL. Whereas GA and Cur in LP4 were found higher in skin than free form with the concentration of 5.08 ± 0.61 µg/mL and 8.00 ± 0.55 µg/mL, respectively.

4. Discussion

Various mechanisms of antioxidant activities have been extensively investigated to characterize how antioxidants against free radicals and oxidative damage. The crucial mechanisms include free radical scavenging, catalysis of ROS or NOS generation by transition metals like iron or copper, and inhibition of lipid peroxidation that affected the chain reaction initiated by free radicals leading to the degradation of polyunsaturated fatty acids in lipid at cell membranes and lipoproteins (*21*). A recent study possessed that GA and Cur were the potential antioxidant with mechanism of scavenging ROS radicals obtained from DPPH assay, inhibit NOS radicals obtained from NO scavenging assay, and inhibition of lipid peroxidation more than other samples, that may be attributed to the strong hydrogen-donating capacity, resulting in effectively binding the free radicals (*22*). The previous study has reported the benefits of GA and Cur combination for use as natural antioxidants with synergistic effects (*23*). However, the application for skin of GA and Cur in binding form were limited caused by their different physiochemical properties, particularly their contrasting of hydrophilicity and lipophilicity.

Drug delivery systems such as liposomal formulations, nanoemulsions, and solid lipid nanoparticles have been widely used to deliver hydrophilic- and lipophilic-compounds through deep skin (*24*). The previous studies have been investigated and developed GA, a hydrophilic compound and Cur, a lipophilic compound co- delivery system such as GA and Cur loaded chitosan microsphere (*25*) and Cur loaded cyclodextrin-conjugated GA (*26*). Liposomes are a promising delivery system due to their ability to encapsulate both hydrophilic and hydrophobic molecules within their lipid bilayer structure, which is formed by phospholipids or hydrogenated lecithin (*27*). This system is thus employed to encapsulate GA and Cur in this study, expected to apply for skin products. The typical composition of liposomes, otherwise phospholipid, are cholesterol, surfactants, and solubilizers to modify liposomal vesicle properties including size, stability, flexibility, and drug loading capacity (*28*). Non-ionic surfactants, such as polysorbate 80, polysorbate 20, and sorbitan oleate, are commonly utilized in liposome formulations for skin applications due to their less toxicity (*29*). These surfactants thus selected employed in the present study. High hydrogenated lecithin and surfactants content lead to high viscosity and rigid structure (*30,31*) which was revealed to this study. LB2, LB3, LP2, and LP3 were composed of high content of hydrogenated lecithin and surfactants in formulation demonstrate high viscosity. Moreover, this study found that the content ratios of hydrogenated lecithin, cholesterol, surfactants, and solubilizers in system significantly influenced size, size distribution, zeta potential (ZP) and compound-entrapments conformed to the reported studies by Pande S and Chen *et al*. (*32,33*). The formulation composed of 0.5% hydrogenated lecithin, 0.2% cholesterol, 5% ethylexyl palmitate, 2.5% di-propylene glycol, 1% tocopheryl acetate, 8% polysorbate 80, 10% sorbitan oleate, and 72.05% DI water was the most suitable ratio that provide homogenous appearance, small particle size with stabilized system with high value of ZP (> -30 mV), high entrapment efficiency both GA and Cur. The zeta potential of liposomal vesicles was negative, attributed to the negative charge obtained from the phosphate group of hydrogenated lecithin (*34,35*).

The release of a formulation is a critical factor influencing efficacy, rate and extent of active ingredient delivery to the target site. This study was done by observing in 120 min according to the further application as topical product same as the release study anti-inflammatory topical formulations (*36*). The results in

the resent study found that LP4 exhibited control release of GA and Cur within the bilayer of liposomes typically exhibits a burst release upon disruption of the liposomal structure, followed by a sustained release phase. Then, GA which is expected to be in the hydrophilic core of vesicle demonstrate a sustained release (*37,38*). GA in LP4, free form of GA and Cur employed the Higuchi kinetic model that possessed the release follows Fick's law of diffusion. This model describes drug diffusion through a homogeneous matrix or solution, driven by a concentration gradient (*39*). The drug release rate depends on the square root of time. Similar release patterns have been observed in matrix-based or solution-based drug delivery systems (*19,40*). Whereas, the release of Cur from LP4 following a Zero-order kinetic model, means that the release rate is constant over time. This appearance might depend on the amount of Cur remaining in the liposome and the limited released into medium, because the cumulative release amount does not increase over the duration of study. These results revealed a previous study that reported abiraterone acetate, hydrophobic drug, loaded liposome found to be sustained release and fit to the Zero-order model (*41*).

The negative charge of particles enhances their skin permeation by promoting electrostatic interactions with the skin negatively charged surface, thereby facilitating penetration, and improving drug localization within the skin layers (*42*). The present study demonstrated that liposomes could enhance Cur skin permeation and skin retention effectively. There was revealed to previous report that curcumin loaded soybean phospholipid-base liposome promoted drug permeation and deposition (*44*). Moreover, the results showed that free GA could penetrate and reach the receiver chamber faster than GA in liposome, and this phenomenon may be due to the molecular properties and the structure of the liposome that provides a controlled release system. GA, a small hydrophilic molecule (Mw ~170 Da), which is within the range favorable for skin absorption *via* transcellular pathway. Whereas liposomes, with their lipophilic bilayer structure, are better suited for permeation through the lipid-rich tight junctions between corneocyte cells, facilitating localized and sustained delivery (*7,44,45*).

In conclusion, liposome-encapsulated gallic acid and curcumin offer significant advantages for topical antioxidant skincare products. Their improved skin penetration facilitates better absorption into deeper layers leading to enhancing effectiveness. Controlled release provides sustained antioxidant protection over time. Encapsulation minimizes direct skin contact, potentially reducing irritation risk. These benefits promising this system for both cosmetic and therapeutic skincare applications.

Acknowledgements

The authors are grateful to the Faculty of Pharmacy, Chiang Mai University for their support.

Funding: This work was supported by a grant from CMU Junior Research Fellowship program (Grant number : JRCMU2566R_098).

Conflict of Interest: The authors have no conflicts of interest to disclose.

References

1. Turkan I. ROS and RNS: Key signaling molecules in plants. J Exp Bot. 2018; 69:3313-3315.
2. Chen J, Liu Y, Zhao Z, Qiu J, Oxidative stress in the skin: Impact and related protection. Int J Cosmet Sci. 2021; 43:495-509.
3. Bickers DR, Athar M. Oxidative stress in the pathogenesis of skin disease. J Invest Dermatol. 2006; 126:256-2575.
4. D'Orazio J, Jarrett S, Amaro-Ortiz A, Scott T. UV radiation and the skin. Int J Mol Sci. 2013; 14:12222-12248.
5. Sivaranjani N, Rao SV, Rajeev G. Role of reactive oxygen species and antioxidants in atopic dermatitis. J Clin Diagn Res. 2013; 7:2683-2685.
6. Tadapaneni RK. Effect of high pressure processing & dairy on the antioxidant activity of strawberry based beverages. J Agric Food Chem. 2012; 60:5795-5802.
7. Phatale V, Vaiphei KK, Jha S, Patil D, Agrawal M, Alexander A. Overcoming skin barriers through advanced transdermal drug delivery approaches. J Control Release. 2022; 351:361-380.
8. Hoang HT, Moon JY, Lee YC. Natural antioxidants from plant extracts in skincare cosmetics: Recent applications, challenges and perspectives. Cosmetics. 2021; 8:8040106.
9. Kahkeshani N, Farzaei F, Fotouhi M, Alavi SS, Bahramsoltani R, Naseri R, Momtaz S, Abbasabadi Z, Rahimi, R, Farzaei MH, Bishayee A. Pharmacological effects of gallic acid in health and diseases: A mechanistic review. Iran J Basic Med Sci. 2019; 22:225-237.
10. Liu S, Liu J, He L, LiuL, Cheng B, Zhou F, Cao D, He Y. A comprehensive review on the benefits and problems of curcumin with respect to human health. Molecules. 2022; 27:2714400.
11. Bangar SP, Chaudhary V, Sharma N, Bansal V, Ozogul F, Lorenzo JM. Kaempferol: A flavonoid with wider biological activities and its applications. Crit Rev Food Sci Nutr. 2023; 63:9580-9604.
12. Dossou SSK, Xu F, Dossa K, Zhou R, Zhao Y, Wang L. Antioxidant lignans sesamin and sesamolin in sesame (*Sesamum indicum* L.): A comprehensive review and future prospects. J Integr Agric. 2023; 22:4-30.
13. Souto EB, Fangueiro JF, Fernandes AR, Cano A, Sanchez-Lopez E, Garcia ML, Severino P, Paganelli MO, Chaud MV, Silva AM. Physicochemical and biopharmaceutical aspects influencing skin permeation and role of SLN and NLC for skin drug delivery. Heliyon. 2022; 8:e08938.
14. Pierre MBR, Dos Santos Miranda Costa I, Liposomal systems as drug delivery vehicles for and transdermal applications. Arch Dermatol Res. 2011; 303:607-621.
15. Figueroa-Robles A, Antunes-Ricardo M, Guajardo-Flores D. Encapsulation of phenolic compounds with liposomal improvement in the cosmetic industry. Int J Pharm. 2021; 593:120125.
16. Phumat P, Chaichit S, Potprommanee S, Preedalikit W,

Sainakham M, Poomanee W, Chaiyana W, Kiattisin K. Influence of *Benincasa hispida* peel extracts on antioxidant and anti-activities, including molecular docking simulation. Foods. 2023; 12:12193555.
17. Jagetia GC, Baliga MS. The evaluation of nitric oxide scavenging activity of certain Indian medicinal plants *in vitro*: A preliminary study. J Med Food. 2004; 7:343-348.
18. Elzaawely AA, Xuan TD, Koyama H, Tawata S. Antioxidant activity and contents of essential oil and phenolic compounds in flowers and seeds of *Alpinia zerumbet* (Pers.) B.L. Burtt. & R.M. Sm. Food Chem. 2007; 104:1648-1653.
19. Okonogi S, Phumat P, Khongkhunthian S, Chaijareenont P, Rades T, Müllertz A. Development of self-nanoemulsifying drug delivery systems containing 4-allylpyrocatechol for treatment of oral infections caused by *Candida albicans.* Pharmaceutics. 2021; 13:167.
20. Nitthikan N, Leelapornpisid P, Naksuriya O, Intasai N, Kiattisin K. Multifunctional biological properties and topical film forming spray base on *Auricularia polytricha* as a natural polysaccharide containing brown *Agaricus bisporus* extract for skin hydration. Cosmetics. 2023; 10:10050145.
21. Jomova K, Raptova R, Alomar SY, Alwasel SH, Nepovimova E, Kuca K, Valko M. Reactive oxygen species, toxicity, oxidative stress, and antioxidants: Chronic diseases and aging. Arch Toxicol. 2023; 97:2499-2574.
22. Lobo V, Patil A, Phatak A, Chandra N. Free radicals, antioxidants and functional foods: Impact on human health. Pharmacogn Rev. 2010; 4:118-126.
23. Naksuriya O, Okonogi S. Comparison and combination effects on antioxidant power of curcumin with gallic acid, ascorbic acid, and xanthone. Drug Discov Ther. 2015; 9:136-141.
24. Stefanov SR, Andonova VY. Lipid nanoparticulate drug delivery systems: Recent advances in the treatment of skin disorders. Pharmaceuticals. 2021; 14:4111083.
25. Ricci A, Stefanuto L, Gasperi T, Bruni F, Tofani D. Lipid nanovesicles for antioxidant delivery in skin: Liposomes, ufasomes, ethosomes, and niosomes. Antioxidants. 2024; 3:1516.
26. Omrani Z, Dadkhah Tehrani A. New cyclodextrin-based supramolecular nanocapsule for codelivery of curcumin and gallic acid. Polym Bull 2020; 77:2003-2019.
27. Akbarzadeh A, Rezaei-Sadabady R, Davaran S, Joo SW, Zarghami N, Hanifehpour Y, Kouhi M, Nejati-Koshki K. Liposome: Classification, preparation, and applications. Nanoscale Res Lett. 2013; 8:102.
28. Jiang Y, Li W, Wang Z, Lu J. Lipid-based nanotechnology: Liposome. Pharmaceutics. 2024; 34:16010034.
29. Lémery E, Briançon S, Chevalier Y, Bordes C, Oddos T, Gohier A, Bolzinger MA. Skin toxicity of surfactants: Structure/toxicity relationships. Colloids Surf A Physicochem Eng Asp. 2015; 469:166-179.
30. Rahman MA, Hussain A. Lecithin-microemulsion based organogels as topical drug delivery system (TDDS). Int J Curr Res Rev. 2011; 3:22-33.
31. Nazdrajic S, Bratovcic A, Alibegic D, Micijevic A, Mehovic M, The effect of mixed surfactants on viscosity, pH and stability of synthesized liquid soaps. Int J Anal Chem. 2024; 14:31-36.
32. Pande S. Factors affecting response variables with emphasis on drug release and loading for optimization of liposomes. Artif Cells Nanomed Biotechnol. 2024; 52:334-344.
33. Shu Q, Wu J, Chen Q. Synthesis, characterization of liposomes modified with biosurfactant MEL-A loading betulinic acid and its anticancer effect in HepG2 Cell. Molecules. 2019; 24:3939.
34. Honary S, Zahir F. Effect of zeta potential on the properties of nano-drug delivery systems –A review (Part 1). Top J Pharm Res. 2013; 12:255-264.
35. de Toledo AMN, Silva NCC, Sato ACK, Picone CSF. A comprehensive study of physical, antimicrobial and emulsifying properties of self-assembled chitosan/lecithin complexes produced in aqueous media. Future Foods. 2021; 4:100083.
36. Burcea-Dragomiroiu GTA, Moroşan E, Popa DE, Niţă S, Rasit I, Panteli M, Golokhvast KS, Ginghină O. *In vivo* testing of the anti-inflammatory action of topical formulations containing cobalt complexes with oxicams. Public Health Toxicol. 2023; 3:1-9.
37. Harwansh RK, Deshmukh R, Shukla VP, Khunt D, Prajapati BG, Rashid S, Ali N, Elossaily GM, Suryawanshi VK, Kumar A. Recent advancements in gallic acid-based drug delivery: Applications, clinical trials, and future directions. Pharmaceutics. 2024; 16:16091202.
38. Fernández-Romero AM, Maestrelli F, Mura PA, Rabasco AM, González-Rodríguez ML. Novel findings about double-loaded curcumin-in-HPβcyclodextrin-in liposomes: Effects on the lipid bilayer and drug release. Pharmaceutics. 2018; 10:10040256.
39. Siepmann J, Peppas NA. Higuchi equation: derivation, applications, use and misuse. Int J Pharm. 2011; 418:6-12.
40. Costa P, Sousa Lobo JM. Modeling and comparison of dissolution profiles. Eur J Pharm Sci. 2001; 13:123-133.
41. Das S, Samanta A, Mondal S, Roy D, Nayak AK. Design and release kinetics of liposomes containing abiraterone acetate for treatment of prostate cancer. Sens Int. 2021; 2:100077.
42. Ogiso T, Yamaguchi T, Iwaki M, Tanino T, Miyake,Y. Effect of positively and negatively charged liposomes on skin permeation of drugs. J Drug Target. 2001; 9:49-59.
43. Chen Y, Wu Q, Zhang Z, Yuan L, Liu X, Zhou L. Preparation of curcumin-loaded liposomes and evaluation of their skin permeation and pharmacodynamics. Molecules. 2012; 17:5972-5987.
44. Zoabi A, Touitou E, Margulis K. Recent advances in nanomaterials for dermal and transdermal applications. Colloids Interfaces. 2021; 5:5010018.
45. Faber I, Pouvreau L, Jan van der Goot A, Keppler J. Modulating commercial pea protein gel properties through the addition of phenolic compounds. Food Hydrocoll. 2024; 154:110123.

Received January 2, 2025; Revised February 1, 2025; Accepted February 21, 2025.

**Address correspondence to:*
Pimpak Phumat, Department of Pharmaceutical Sciences, Faculty of Pharmacy, Chiang Mai University, Chiang Mai 50200, Thailand.
E-mail: pimpak.p@cmu.ac.th

Released online in J-STAGE as advance publication February 26, 2025.

Original Article

DOI: 10.5582/ddt.2025.01002

Decreased serum calcium levels predict severe complications after initial diagnosis in patients with acute type B aortic dissection: A retrospective cohort study

Fangzheng Meng[1,§], Liang Fang[2,§], Jing Zhou[3], Yiyuan Zhou[4], Junfeng Zhao[5,*], Ling Wang[6,7,*]

[1] The Second School of Clinical Medicine, Zhejiang Chinese Medical University, Hangzhou, China;
[2] Department of Ultrasound, Huadong Hospital, Fudan University, Shanghai, China;
[3] Department of Obstetrics and Gynecology, Nanfang Hospital, Southern Medical University, Guangzhou, Guangdong, China;
[4] Department of Obstetrics, the First Affiliated Hospital, Guizhou University of Traditional Chinese Medicine, Guiyang, China;
[5] Department of Emergency, Zhejiang Hospital, Hangzhou, China;
[6] Department of Obstetrics and Reproductive Immunology, Shanghai East Hospital, Tongji University School of Medicine, Shanghai, China;
[7] Guizhou University of Traditional Chinese Medicine (TCM), Guiyang, China.

SUMMARY: This study sought to investigate the temporal variations in serum calcium concentrations among patients with acute type B aortic dissection (ATBAD) following initial diagnosis, document the incidence of severe complications, and evaluate their potential associations. In this retrospective analysis, we examined 42 consecutive patients diagnosed with ATBAD at Zhejiang Hospital between April 2019 and April 2024. Serum-ionized calcium levels were measured at admission and 24 hours post-admission. Based on changes in calcium levels, patients were categorized into either the elevated or decreased groups. Univariate and multivariate logistic regression analyses were performed to compare clinical characteristics and assess the incidence of severe complications following the initial diagnosis. The study further explored the association between 24-hour serum calcium levels, their dynamic changes, and the occurrence of severe complications in patients with ATBAD. The results showed that the decreased group had a significantly higher frequency of severe complications, including mortality, cardiac complications, acute renal failure, and organ hypoperfusion ($P < 0.05$), while no significant differences were observed for neurological or pulmonary complications ($P > 0.05$). Logistic regression revealed that a decline in serum calcium levels within 24 hours was an independent risk factor for severe complications (OR = 16.722, $P = 0.03$). The receiver operating characteristic (ROC) curve showed an area under the curve (AUC) of 0.864. Decreased serum calcium concentration is an independent predictor of severe complications in ATBAD patients, significantly associated with mortality, cardiac complications, acute kidney injury, and inadequate organ perfusion. No significant correlation with neurological and pulmonary complications was observed.

Keywords: Acute stanford type B aortic dissection, serum calcium, severe complications

1. Introduction

Acute aortic dissection (AAD) is a time-critical cardiovascular emergency associated with significant morbidity and mortality if not promptly diagnosed and treated. Without prompt treatment, the majority of patients succumb within hours to days after onset, with a mortality rate of approximately 1%–20% within the first 24 hours and up to 75% within two weeks (*1*). Based on the extent of the dissection, Stanford type B aortic dissection is defined as a dissection that does not involve the ascending aorta, specifically extending distal to the left subclavian artery into the descending thoracic aorta and beyond. When the onset occurs within 14 days, it is termed acute type B aortic dissection (ATBAD) (*2*). ATBAD accounts for 25% to 40% of all AAD cases and is characterized by acute onset, rapid progression, and high mortality. Its elevated mortality rate and complex pathological mechanisms have long been focal points and challenges in cardiovascular research (*3*). Currently, the 5-year survival rate for pharmacological treatment of ATBAD is approximately 60%, while the incidence of severe complications and mortality remains high (*4*). The underlying reasons include interruption of blood supply to specific vascular beds, such as the spinal cord, brain, heart, kidneys, intestines, or limbs. A cardinal pathophysiological hallmark of this condition is the localized inflammatory cascade, characterized

by inflammatory cell infiltration, extracellular matrix degradation, and phenotypic modulation of vascular smooth muscle cells (*5*). In recent years, someone (*6*) has also identified changes in inflammatory markers during the progression of AAD, suggesting a close and significant relationship between inflammation and AAD.

Recent evidence suggests that specific radiological features detected on computed tomography angiography (CTA) may serve as predictors for aortic-related adverse events (*7-9*). Nevertheless, the considerable financial burden and cumulative radiation exposure associated with serial CTA imaging often limit patient compliance with repeated examinations. Consequently, there is an urgent need to identify readily accessible, minimally invasive biomarkers with predictive value. In recent years, increasing studies have shown that changes in serum calcium ion levels are closely related to the occurrence and development of various cardiovascular and cerebrovascular diseases (*10-12*), yet their characteristics and clinical significance remain unclear. Calcium ions, as one of the essential ions for maintaining normal cellular functions and homeostasis, are closely involved in physiological processes such as cell membrane stability, nerve conduction, and myocardial contraction (*13*). Approximately 40% of total calcium in the blood circulation is bound to albumin, and thus influenced by albumin levels, necessitating the calculation of albumin-corrected serum calcium (*14*). Changes in serum calcium concentration and the occurrence and progression of aortic dissection may be related to multiple factors. Firstly, AAD is often accompanied by a severe inflammatory response, with the release of large amounts of inflammatory cytokines potentially leading to dysregulation of intracellular calcium metabolism, thereby causing a decrease in serum calcium levels (*15*). Secondly, AAD can result in impaired tissue perfusion and organ dysfunction, which may also affect the regulation and balance of calcium ions (*16*). Additionally, someone (*17*) has found an association between serum calcium levels and postoperative prognosis in AAD patients; low serum calcium levels may serve as an independent risk factor for poor prognosis, being related to extended hospital stays, increased incidence of complications, and other adverse outcomes. These findings suggest that calcium ions play an important role in maintaining cellular functions and regulating inflammatory responses. Currently, there is a lack of clinical evidence to elucidate the relationship between the decrease in serum calcium levels upon initial presentation and the occurrence of severe complications in ATBAD patients.

This study aims to conduct a retrospective observational analysis of the dynamic monitoring of serum calcium levels in ATBAD patients upon initial presentation, along with an integrative analysis of their clinical data and adverse events. This approach is not only expected to enhance our understanding of the underlying mechanisms of ATBAD development but also provide novel insights for optimizing clinical management strategies for this disease. Furthermore, the study offers crucial leads for exploring novel biomarkers and risk predictors for ATBAD, thereby providing a more accurate and effective foundation for improving patient outcomes and enhancing their quality of life. Collectively, our findings provide novel insights that may facilitate early recognition, risk stratification, and individualized therapeutic strategies for severe complications in patients with ATBAD.

2. Methods

2.1. Ethical statement

This retrospective study was approved by the Ethics Committee of Zhejiang Hospital (approval No. 2024 Preliminary Trial (080K)). The study was conducted by the principles of the 1964 Declaration of Helsinki and its subsequent amendments or comparable ethical standards. Due to the retrospective nature of this study, the requirement for informed consent was waived by the Institutional Review Board.

2.2. Research design

This single-center, retrospective observational study analyzed consecutive patients with confirmed ATBAD who presented to Zhejiang Hospital between April 2019 and April 2024. The inclusion criteria were as follows: (1) a diagnosis of ATBAD confirmed by computed tomography angiography (CTA) and magnetic resonance imaging (MRI), with symptom onset within the past 14 days; and (2) age ≥18 years. The exclusion criteria included: (1) the presence of connective tissue diseases, pregnancy, or traumatic dissection; (2) a history of aortic dissection surgery or concurrent surgical procedures; (3) comorbid conditions such as thyroid disorders, end-stage renal disease, severe infections, hematologic diseases, or malignant tumors; (4) long-term use of medications that could influence blood test results; and (5) incomplete medical records.

All eligible patients initially received standardized medical management. Calcium supplementation was withheld in patients presenting with hypocalcemia. In cases where major complications developed during conservative management, thoracic endovascular aortic repair (TEVAR) or conventional open surgical intervention under general anesthesia was indicated. Patients who refused surgical intervention continued with optimal medical therapy.

2.3. Study size and bias

In this study, we reviewed data from 42 patients with ATBAD. As this was a retrospective study, we had no

control over the choice of study design and sample size. Therefore, we cannot calculate a definite sample size based on pre-set models and assumptions.

We take steps to reduce bias, including standardized data collection, data validation, statistical analysis, and training of researchers. Nevertheless, there is a risk of selection bias, information bias, and statistical analysis bias. We will consider these potential sources of bias when interpreting the results.

Due to the small sample size, we need to interpret the results carefully and take into account potential biases and limitations. The results of this study may not apply to all acute aortic dissection patient populations, and further studies are needed to confirm and extend these findings.

2.4. Data collection

Data collection included baseline patient information and variables of interest following hospital admission. Patient demographics, disease-related details, and laboratory findings were extracted from the electronic medical record system. Demographic data included age, sex, smoking history, and alcohol consumption history, while disease-related information encompassed comorbidities such as hypertension and diabetes. Laboratory parameters collected at admission included hemoglobin, C-reactive protein (CRP), albumin, D-dimer, and serum levels of calcium, potassium, sodium, and chloride. Serum calcium levels were also measured 24 hours post-admission. For this study, blood test indicators were based on measurements obtained at admission and 24 hours thereafter.

Blood samples were analyzed using standard clinical methodologies. Specifically, hemoglobin and high-sensitivity CRP levels were quantified using a fully automated hematology analyzer (Model BC-6800, Mindray Bio-Medical Electronics Co., Ltd., Shenzhen, China). D-dimer levels were measured with a fully automated coagulation analyzer (Model STA-R MAX, Stago, China). Additionally, serum concentrations of albumin, potassium, sodium, chloride, and calcium were measured with a fully automated biochemical and immunoassay analyzer (Model cobas 8000, Roche Diagnostics GmbH, China). For vascular imaging, a 64-slice CT scanner (Model NeuViz Epoch, Neusoft Medical Systems, China) was utilized. To enhance vascular visualization, a non-ionic contrast agent (Iopromide Injection, 100 mL: 76.89 g, Bayer) was administered intravenously. Furthermore, magnetic resonance imaging was conducted on a 3.0 Tesla scanner (Model SIGNA™ Premier Evo 3T, GE HealthCare, USA), where T1-weighted and T2-weighted images were acquired using standard protocols.

The occurrence of serious complications during conservative medical treatment for ATBAD patients was recorded (*18*). These complications included in-hospital all-cause mortality, cardiac-related complications (such as new-onset arrhythmias, heart failure, acute pericardial tamponade, and acute coronary syndrome), neurological complications (including cerebrovascular accidents and ischemic spinal cord injury), pulmonary complications (including pulmonary embolism and respiratory failure), acute kidney injury (AKI), and other organ perfusion disorders (including bowel necrosis, hepatic or splenic infarction, and acute lower limb ischemia/necrosis). Acute kidney injury (AKI) (*19*) was characterized by an increase in serum creatinine (Scr) of at least 0.3 mg/dL within 48 hours or a 1.5-fold rise from baseline within seven days. Hypocalcemia (*20*) was defined as a total serum calcium concentration of less than 2.12 mmol/L, assuming normal plasma protein levels. The albumin-corrected calcium was determined using the equation: total calcium + 0.019 * (49 - albumin).

2.5. Statistical analysis

SPSS 26.0 software was used for data analysis, with $P \leq 0.05$ considered statistically significant. Patients were categorized into "increased" and "decreased" groups based on their serum calcium ion concentrations 24 hours post-admission. The Shapiro-Wilk test was applied to assess the normality of the measurement data. Data following a normal distribution are presented as mean ± standard deviation (SD), and the *t*-test was employed for analyzing continuous variables. The chi-square test was used to evaluate categorical variables. For non-normally distributed data, the Mann-Whitney *U* test was utilized, and results are presented as median (interquartile range, IQR). Categorical data expressed as percentages were analyzed using the chi-square test. To identify risk factors, univariate and multivariate logistic regression analyses were performed to examine the effects of sociodemographic factors, disease-related data, and laboratory results on adverse outcomes while controlling for confounding variables. The correlation between influencing factors and the impact of changes in blood calcium concentration on adverse outcomes was determined by calculating odds ratios (OR) and 95% confidence intervals (CI). Furthermore, the area under the receiver operating characteristic (ROC) curve was used to evaluate the model's discriminative ability, and likelihood ratio tests along with calibration curves were utilized to assess the model's calibration.

2.6. Patient and public involvement

Neither patients nor members of the public were involved in the study design, conduct, reporting, or dissemination plans of this research.

3. Results

3.1. Comparison of baseline characteristics between groups

Among the 75 patients with AAD treated at our hospital, 20 were diagnosed with acute type A aortic dissection (AAAD) and 55 with ATBAD. This observational retrospective study initially included 42 ATBAD patients who met the inclusion criteria. After adjustments, 13 patients were identified with hypocalcemia upon admission, while 31 developed hypocalcemia within 24 hours post-admission. Based on changes in serum calcium levels from admission to 24 hours later, patients were categorized into two groups: the "decreasing" group (n = 29) and the "increasing" group (n = 13). There were no significant differences between the groups regarding sex, age, alcohol consumption, smoking history, history of diabetes, or history of hypertension (P > 0.05). Similarly, there were no statistically significant differences in baseline laboratory parameters, including hemoglobin, CRP, D-dimer, albumin, serum sodium, serum potassium, and serum chloride concentrations (P > 0.05) (Table 1). This indicates that the baseline characteristics of the two groups were comparable.

3.2. Comparison of severe complications after initial diagnosis between groups

No statistically significant differences were observed between the two groups regarding neurological and pulmonary complications (P > 0.05). However, significant differences were observed in the incidence of in-hospital all-cause mortality (27.6% *vs*. 0%), cardiac complications (31.0% *vs*. 0%), acute kidney injury (48.3% *vs*. 7.7%), and other organ perfusion disorders (44.8% *vs*. 7.7%) (P < 0.05). In the increasing group, 5 patients (38.5%) experienced severe complications, whereas 27 patients (93.1%) in the decreasing group developed severe complications. The difference between the two groups was statistically significant (P < 0.05) (Table 2).

3.3. Univariate and multivariate analysis

Relevant risk factors were used as the independent variable, and the occurrence of severe complications after initial diagnosis was considered the dependent variable. Initially, univariate logistic regression analyses were performed for all potential variables. Subsequently, variables demonstrating statistical significance (P < 0.05) in the univariate analysis were entered into a multivariate logistic regression model to identify independent risk factors. The analysis revealed that early changes in serum calcium levels were an independent risk factor for severe complications after initial diagnosis. Compared to the group with increased calcium levels, patients in the decreased calcium group had a significantly higher risk of developing severe complications after initial diagnosis (OR = 16.722, 95% CI = 2.545–109.877, P = 0.03) (Table 3).

3.4. Model discrimination and calibration

The ROC curve was generated based on the prediction model, resulting in an area under the curve (AUC) of 0.864 (95% CI: 0.751–0.977, P = 0.001), the Youden index was 0.644, the sensitivity was 84.4%, the specificity was 80.0%, and the best cutoff value was 0.0250. This indicates that the model has strong discriminative ability. The ROC curve for the prediction model is presented in Figure 1. Furthermore, the likelihood ratio test yielded a χ^2 value of 16.347 (P <

Table 1. Clinical data categorized by changes in serum calcium levels

Clinical features	Total n = 42	Decreased group n = 29	Increased group n = 13	Statistical value	P-value
Age (years)	59.29 ± 16.10	59.10 ± 14.69	59.69 ± 19.54	t = 0.108	0.914[a]
Gender [n(%)]				χ^2 = 0.116	0.733[c]
Male	36 (85.71)	24 (82.75)	12 (92.31)		
Female	6 (14.29)	5 (17.24)	1 (7.69)		
Smoking [n (%)]	17 (40.48)	11 (37.93)	6 (46.15)	χ^2 = 0.252	0.616[b]
Drinking [n (%)]	14 (33.33)	9 (31.03)	5 (38.46)	X^2 = 0.014	0.906[c]
Hypertension [n (%)]	31 (73.81)	23 (79.31)	8 (61.54)	χ^2 = 0.691	0.406[c]
Diabetes mellitus [n (%)]	6 (14.29)	5 (17.24)	1 (7.69)	X^2 = 0.116	0.733[c]
Hb on admission (g/L), mean (SD)	137.55 ± 27.11	138.48 ± 28.00	135.46 ± 26.00	T = -0.330	0.743[a]
CRP on admission (mmol/L), median (IQR)	4.96 (18.97)	3.93 (27.89)	9.51 (13.64)	Z = 2.119	0.145[d]
D-dimer on admission (mmol/L), median (IQR)	3.27 (1.52, 13.07)	4.02 (1.70, 20.00)	2.33 (0.74, 10.08)	Z = 1.079	0.299[d]
Albumin on admission	37.92 (38.17, 46.33)	41.71 ± 5.82	38.29 (33.35, 46.81)	Z = -0.639	0.523[d]
Serum potassium on admission (mmol/L), mean (SD)	3.47 ± 0.35	3.40 ± 0.06	3.63 ± 0.40	T = 2.012	0.051[a]
Serum sodium on admission (mmol/L), mean (IQR)	139.64 (138.39, 141.92)	139.70 (138.57, 142.25)	139.32 (136.77, 140.58)	Z = 1.041	0.308[d]
Serum chloride on admission (mmol/L), mean (IQR)	105.75 (103.78, 107.55)	106.10 (104.25 , 107.65)	104.00 (101.60 , 107.10)	Z = 2.986	0.084[d]

[a]Independent samples t-test, [b]Pearson's chi-squared test, [c]Calibration Pearson's chi-square test, [d]Mann-Whitney U test.

Table 2. Comparison of severe complications based on serum calcium level changes

Prognostic outcome	Total $n = 42$	Decreased group $n = 29$	Increased group $n = 13$	*P*-value
All deaths in the hospital [*n* (%)]	8 (19.05)	8 (27.59)	0 (0.00)	0.043[b]
Cardiac complications [*n* (%)]	9 (21.43)	9 (31.03)	0 (0.00)	0.038[b]
Neurological complications [*n* (%)]	10 (23.81)	9 (31.03)	1 (7.69)	0.211[a]
AKI [*n* (%)]	15 (35.71)	14 (48.28)	1 (7.69)	0.029[a]
Pulmonary complications [*n* (%)]	15 (35.71)	11 (37.93)	4 (30.77)	0.921[a]
Poor perfusion of other organs [*n* (%)]	14 (33.33)	13 (44.83)	1 (7.69)	0.045[a]
Total[*n* (%)]	32 (76.19)	27 (93.10)	5 (38.46)	0.001[a]

[a]Calibration Pearson's chi-square test, [b]Fisher's exact test.

Table 3. Univariate and multivariate analysis of the severe complications group

Variables	Univariate model OR (95%CI)	*P*-value	Multivariate model OR (95%CI)	*P*-value
Gender	0.241 (0.040 - 1.461)	0.122		
Age	0.979 (0.937 - 1.023)	0.342		
Smoking	3.529 (0.646 - 19.280)	0.145		
Drinking	1.222 (0.263 - 5.682)	0.798		
Hypertension	4.333 (0.943 - 19.905)	0.059		
Diabetes mellitus	46210361.473 (46210361.473 - 46210361.473)	0.999		
Laboratory results				
Hb on admission	1.023 (0.995 - 1.051)	0.108		
CRP on admission	1.003 (0.975 - 1.031)	0.850		
D-dimer on admission	1.035 (0.942 - 1.138)	0.470		
Albumin on admission	1.122 (0.996 - 1.265)	0.058		
Serum potassium on admission	0.055 (0.004 - 0.719)	0.027	6.765 (0.446 - 102.511)	0.168
Serum sodium on admission	1.153 (0.899 - 1.478)	0.262		
Serum chloride on admission	1.146 (0.898 - 1.461)	0.273		
Serum calcium on admission	1629.822 (0.624 - 4258494.703)	0.065		
Serum calcium 24 hours of admission	0.000 (0.000 - 1.291)	0.057		
Changes in serum calcium after admission				
Increased group	ref		ref	
Decreased group	21.600 (3.501 - 133.278)	0.001	16.722 (2.545 - 109.877)	0.003

0.001), indicating a good fit of the calibration curve.

4. Discussion

AAD is a life-threatening medical emergency that often presents with hemodynamic alterations and structural changes in the aortic wall (*21,22*). Calcium ions, as an essential electrolyte in the body, play a crucial role in cardiovascular function and the stability of the vascular wall. This retrospective study aimed to evaluate the prognostic value of early serum calcium ion concentration changes within 24 hours of admission for predicting the occurrence of severe complications after initial diagnosis in patients with ATBAD. Using univariate and multivariate logistic regression analyses, we sought to explore the relationship between early serum calcium changes and adverse outcomes, providing insights into the occurrence and progression of severe complications in ATBAD patients and uncovering potential underlying mechanisms.

Our findings revealed that serum calcium levels in ATBAD patients within 24 hours of admission were generally lower than the normal range, suggesting that hypocalcemia may be a significant pathophysiological feature of this disease. This observation aligns with the study by Vianello *et al.* (*15*), which also indicated that hypocalcemia might be associated with the pathogenesis of AAD. Alterations in serum calcium levels may be associated with the inflammatory response in AAD, which is characterized by endothelial-mediated pro-inflammatory mechanisms. These mechanisms involve the release of various inflammatory mediators from injured vascular cells, including pro-inflammatory cytokines (such as interleukin-6 [IL-6]), pro-coagulant factors, and endothelial-derived factors (*15,23-25*). Hypocalcemia may also exacerbate AAD progression by impairing vascular smooth muscle cell (VSMC) function, increasing vascular wall fragility, and promoting dissection (*26,27*). This imbalance may lead to structural and functional abnormalities in the aortic wall, worsening the disease and increasing the risk of complications, ultimately affecting short-term prognosis. Previous research (*28*) has demonstrated that IL-6 can enhance the expression of calcium-sensing receptors (CaSR) in both the parathyroid glands and renal tissue, resulting in decreased serum calcium concentrations.

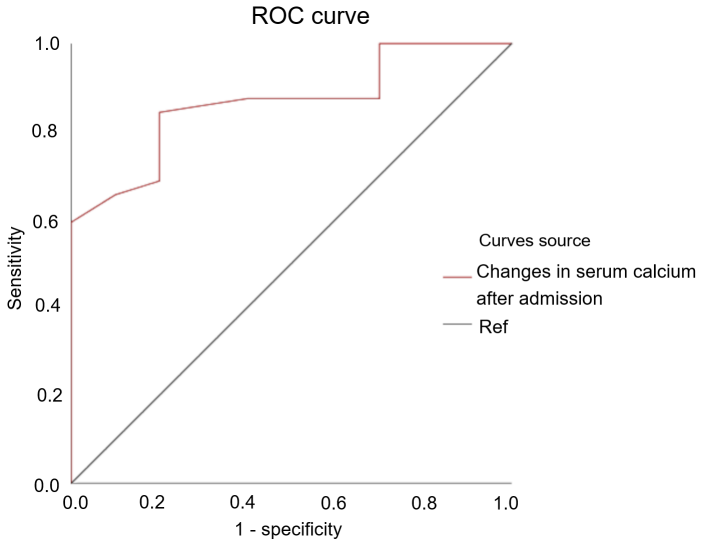

Figure 1. ROC curve of serum calcium level changes and the occurrence of severe complications after initial diagnosis in ATBAD patients. The presented figure illustrates the Receiver Operating Characteristic (ROC) curve for assessing the diagnostic performance of serum calcium changes following patient admission. The x-axis quantifies the false positive rate (1-specificity), while the y-axis represents sensitivity (true positive rate). The purple curve indicates the performance of the test, with values approaching the upper left corner reflecting superior discriminatory ability between positive and negative cases. The diagonal black line serves as a reference for a random classifier, suggesting the baseline performance. The area under the curve (AUC) is a critical metric for evaluating the test's accuracy; an AUC of 1 indicates perfect discrimination, whereas an AUC of 0.5 signifies no diagnostic value. This ROC analysis indicates that changes in serum calcium levels may provide clinically relevant diagnostic information, necessitating further investigation to establish their role in patient management.

Furthermore, inhibiting CaSR has been reported to benefit the cardiovascular system in COVID-19 patients, while calcium supplementation was found to be harmful (*29*). Serum calcium levels may also influence complications in ATBAD through effects on vascular tone and oxidative stress (*30,31*). *In vitro* studies show glutathione (GSH) relies on calcium for vasorelaxation *via* endothelial NO production. Low calcium might impair this, increasing vascular stress. Moreover, oxidative stress in conditions like Marfan syndrome shows disrupted GSH systems, suggesting similar issues in ATBAD, potentially worsened by calcium imbalances. Thus, maintaining calcium homeostasis could be crucial for managing ATBAD severe complications.

Given the dynamic changes in serum calcium levels, we performed a subgroup analysis, which revealed a strong association between these changes and the occurrence of severe complications after initial diagnosis. In this study, we selected mortality, cardiac, renal, pulmonary, neurological complications, and poor organ perfusion as indicators of severe complications in ATBAD patients after initial diagnosis (*18*), as these complications not only reflect the severe impact of dissection on vital organ function but also have significant prognostic value. Our results demonstrated that the incidence of severe complications was significantly higher in the hypocalcemia group compared to the hypercalcemia group ($P = 0.001$), particularly in terms of mortality ($P = 0.043$), cardiac complications ($P = 0.038$), acute kidney injury ($P = 0.029$), and poor organ perfusion ($P = 0.043$). This finding is consistent with previous studies, which have emphasized the regulatory role of calcium ions as a critical second messenger in cellular inflammation, influencing the activation of inflammatory cells, secretion of inflammatory mediators, and the overall inflammatory response. Serum calcium is also involved in regulating myocardial contraction and vascular endothelial function, with fluctuations in calcium levels being crucial for cardiovascular homeostasis. A drop in serum calcium can disrupt endothelial function and alter hemodynamics, contributing to the onset of AAD (*32-34*). Additionally, calcium serves as a crucial regulator in vascular smooth muscle cells (VSMCs) proliferation and apoptosis. Disruption of intracellular calcium homeostasis may lead to dysregulation of calcium-dependent proteins, subsequently promoting vascular calcification, increased arterial stiffness, and enhanced cellular adhesion. These pathological changes may ultimately contribute to the development of aortic dissection (*35*).

Moreover, mortality and AKI, both of which showed significant differences between the hypocalcemia and hypercalcemia groups, are consistent with existing literature. Wang *et al.* (*36*) identified low calcium concentrations as an independent predictor of all-cause mortality and proposed that calcium levels could potentially serve as a prognostic biomarker for assessing the severity of renal impairment in patients with AKI. Correspondingly, Bi *et al.* (*37*) revealed that hypocalcemia during intensive care unit (ICU) admission represents a high-risk factor for developing AKI. In this context, hypocalcemia can trigger the opening of

calcium channels in renal cells, facilitating calcium influx and subsequent cellular overload, thereby further exacerbating kidney damage (*38*). This cascade of events underscores the complex interplay between calcium dysregulation and renal cell injury.

These findings indicate that patients with persistently low or progressively decreasing serum calcium levels tend to have more severe conditions, with a higher incidence of severe complications and mortality. In contrast, patients whose serum calcium levels gradually return to normal tend to have more favorable clinical outcomes. The trend in serum calcium levels may serve as an important indicator of disease severity and prognosis in ATBAD patients. Dynamic monitoring of serum calcium levels could provide valuable insights for risk assessment and clinical decision-making.

The lungs, being the only organ that receives the entire cardiac output, are rich in neutrophils and act as a major filter for venous blood. AAD-induced lung injury has unique characteristics, with inflammation being a widely accepted mechanism of injury (*39,40*). This manifests as vascular endothelial cell (VEC) damage and increased microvascular permeability, leading to decreased compliance, increased intrapulmonary shunting, and refractory hypoxemia. Serum calcium levels may potentially modulate the integrity and permeability of the blood-brain barrier (BBB). Prior studies (*41*) have shown that hypocalcemia can disrupt cellular adhesion within the barrier. Prolonged extracellular calcium depletion increases neuronal apoptosis, exacerbating neurological damage and worsening patient outcomes (*42,43*). Notably, for postoperative complications, the incidence rates of both neurological and pulmonary complications were comparable between the two groups, with no statistically significant differences observed ($P > 0.05$). This discrepancy could be because serum calcium changes may not be the primary factor contributing to acute lung or neurological injuries, or the effects of serum calcium may be masked by other confounding factors.

Through comprehensive univariate and multivariate logistic regression analyses, we further established that a decline in serum calcium levels within the first 24 hours of admission serves as an independent predictor of severe clinical complications. Notably, statistical analysis did not confirm a significant association between two post-admission calcium concentrations and serious complications of aortic dissection ($P > 0.05$). In conclusion, in clinical practice, a single blood calcium level cannot effectively indicate or predict the possibility of serious complications in patients with aortic dissection. The statistically significant elevated odds ratio (OR) substantiates the robust association between early calcium level reduction and adverse clinical outcomes following initial diagnosis. This suggests that dynamic monitoring of serum calcium, especially downward trends, could serve as an early warning sign for the development of severe complications after initial diagnosis. Moreover, the constructed prediction model demonstrated high discriminatory power through ROC curve analysis (AUC = 0.864), confirming the clinical utility of serum calcium changes as a predictive marker. The model's good sensitivity and specificity further support its reliability and effectiveness, offering clinicians a tool to identify high-risk patients early and implement timely interventions.

This study acknowledges several methodological limitations inherent in its design, primarily arising from the constrained sample size and retrospective nature of the investigation, which potentially introduce selection and information biases. Within the current research framework, a comprehensive assessment of additional prognostic biomarkers and clinically relevant variables was not feasible, and the employment of a composite outcome metric for severe complications inevitably limits the granular analysis of individual clinical events. To mitigate these research constraints, future investigations should prioritize large-scale, multicenter prospective studies designed to validate the current findings, meticulously explore the nuanced relationship between serum calcium fluctuations and associated clinical complications, and systematically elucidate the complex pathophysiological mechanisms underlying calcium dysregulation in ATBAD.

5. Conclusion

In conclusion, early declines in serum calcium levels can serve as an independent risk factor for the development of severe short-term complications in ATBAD patients. This dynamic pattern may act as an early warning signal for the occurrence of severe complications after initial diagnosis and may also reflect key pathological mechanisms underlying the disease. These findings provide clinicians with a novel basis for assessing and predicting the progression of severe complications and surgical indications in ATBAD patients, thereby facilitating more precise risk stratification and personalized treatment strategies.

Funding: This work was supported by grants from a project of the National Natural Science Foundation of China (grant No. 82374243 to L Wang).

Conflict of Interest: The authors have no conflicts of interest to disclose.

References

1. Tang X, Lu K, Liu X, Jin D, Jiang W, Wang J, Zhong Y, Wei C, Wang Y, Gao P, Du J. Incidence and survival of aortic dissection in Urban China: Results from the National Insurance Claims for Epidemiological Research (NICER) Study. Lancet Reg Health West Pac. 2021; 17:100280.

2. Zhou M, Fu W. Chinese expert consensus on diagnosis and treatment of stanford type B aortic dissection (2022 edition). Zhongguo Xue Guan Wai Ke Za Zhi. 2022; 14:119-130. (in Chinese)
3. Hughes GC. Management of acute type B aortic dissection; ADSORB trial. J Thorac Cardiovasc Surg. 2015; 149:S158-162.
4. Spec Comm Vasc Surg, Cardiovasc Surg Branch, Chin Med Doctor Assoc. Chinese expert consensus on diagnosis and treatment of aortic dissection. Zhongguo Xue Guan Wai Ke Za Zhi. 2017; 33:641-654. (in Chinese)
5. Zhao KW, Zhang L, Zhou J, Jin ZP. Research progress of macrophage polarization in the treatment of aortic dissection. Zhongguo Xiong Xin Xue Guan Wai Ke Lin Chuang Za Zhi. 2023; 30:1055-1060. (in Chinese)
6. Zhu HQ, Li YM, Zhou J, Jin ZP. Research progress of inflammation involved in the clinical outcome of aortic dissection. Zhongguo Pu Tong Wai Ke Za Zhi. 2020; 29:1509-1514. (in Chinese)
7. Squizzato F, Oderich GS, Bower TC, Mendes BC, Kalra M, Shuja F, Colglazier J, DeMartino RR. Long-term fate of aortic branches in patients with aortic dissection. J Vasc Surg. 2021; 74:537-546.e532.
8. Schwartz SI, Durham C, Clouse WD, Patel VI, Lancaster RT, Cambria RP, Conrad MF. Predictors of late aortic intervention in patients with medically treated type B aortic dissection. J Vasc Surg. 2018; 67:78-84.
9. Krebs JR, Filiberto AC, Fazzone B, Jacobs CR, Anderson EM, Shahid Z, Back M, Upchurch GR, Jr., Cooper M. Outcomes of patients with acute type B aortic dissection and high-risk features. Ann Vasc Surg. 2024; 106:99-107.
10. Zhang K, Han Y, Cai T, *et al*. U-shaped association between serum calcium and in-hospital mortality in patients with congestive heart failure. ESC Heart Fail. 2024; 11:2521-2530.
11. Meng K, Lei X, He D. Association between serum calcium and in-hospital mortality in intensive care unit patients with cerebral infarction: a cohort study. Front Neurol. 2024; 15:1428868.
12. Hou X, Hu J, Liu Z, Wang E, Guo Q, Zhang Z, Song Z. L-shaped association of serum calcium with all-cause and CVD mortality in the US adults: A population-based prospective cohort study. Front Nutr. 2022; 9:1097488.
13. Zhang D, Wang F, Li P, Gao Y. Mitochondrial Ca^{2+} homeostasis: Emerging roles and clinical significance in cardiac remodeling. Int J Mol Sci. 2022; 23:3025.
14. Yang YY, Tao B, Zhao HY, Liu JM, Sun LH. Hypocalcemia clinical feature and emergency treatment of severe hypocalcemia. Zhonghua Yi Xue Za Zhi. 2024; 104:2848-2851. (in Chinese)
15. Vianello E, Dozio E, Barassi A, Sammarco G, Tacchini L, Marrocco-Trischitta MM, Trimarchi S, Corsi Romanelli MM. A pilot observational study on magnesium and calcium imbalance in elderly patients with acute aortic dissection. Immun Ageing. 2017; 14:1.
16. Wang S, Sang X, Li S, Yang W, Wang S, Chen H, Lu C. Author Correction: Increased Ca^{2+} transport across the mitochondria-associated membranes by Mfn2 inhibiting endoplasmic reticulum stress in ischemia/reperfusion kidney injury. Sci Rep. 2024; 14:2478.
17. Lin JL, Li SL, Peng YC, Chen LW, Lin YJ. Analysis of serum calcium change trajectories and prognostic factors in patients with acute type A aortic dissection. BMC Surg. 2023; 23:362.
18. Erbel R, Aboyans V, Boileau C, *et al.* Corrigendum to: 2014 ESC Guidelines on the diagnosis and treatment of aortic diseases. Eur Heart J. 2015; 36:2779.
19. Kidney Disease: Improving Global Outcomes (KDIGO) Glomerular Diseases Work Group. KDIGO 2021 clinical practice guideline for the management of glomerular diseases. Kidney Int. 2021; 100:S1-S276.
20. Yang YY, Zhang D, Ma LY, Hou YF, Bi YF, Xu Y, Xu M, Zhao HY, Sun LH, Tao B, Liu JM. Association of famine exposure and the serum calcium level in healthy Chinese adults. Front Endocrinol (Lausanne). 2022; 13:937380.
21. Wang SQ, Wang LY, Lin ZH, Zhu P, Yang Q, Chen JH. Study on the hemodynamics of personalized stanford type B aortic dissection based on computational fluid dynamics. Zhongguo Xiong Xin Xue Guan Wai Ke Lin Chuang Za Zhi. 2024; 31:594-599. (in Chinese)
22. del Porto F, Proietta M, Tritapepe L, Miraldi F, Koverech A, Cardelli P, Tabacco F, de Santis V, Vecchione A, Mitterhofer AP, Nofroni I, Amodeo R, Trappolini M, Aliberti G. Inflammation and immune response in acute aortic dissection. Ann Med. 2010; 42:622-629.
23. Wen D, Zhou XL, Li JJ, Hui RT. Biomarkers in aortic dissection. Clin Chim Acta. 2011; 412:688-695.
24. Tombetti E, Di Chio MC, Sartorelli S, Bozzolo E, Sabbadini MG, Manfredi AA, Baldissera E. Anti-cytokine treatment for Takayasu arteritis: State of the art. Intractable Rare Dis Res. 2014; 3:29-33.
25. Jiang F, Zhang X, Lu YM, Li YG, Zhou X, Wang YS. Elevated level of miR-17 along with decreased levels of TIMP-1 and IL-6 in plasma associated with the risk of in-stent restenosis. Biosci Trends. 2019; 13:423-429.
26. Moccia F, Tanzi F, Munaron L. Endothelial remodelling and intracellular calcium machinery. Curr Mol Med. 2014; 14:457-480.
27. Ando J, Yamamoto K. Flow detection and calcium signalling in vascular endothelial cells. Cardiovasc Res. 2013; 99:260-268.
28. Hendy GN, Canaff L. Calcium-sensing receptor, proinflammatory cytokines and calcium homeostasis. Semin Cell Dev Biol. 2016; 49:37-43.
29. Singh Y, Ali H, Alharbi KS, Almalki WH, Kazmi I, Al-Abbasi FA, Anand K, Dureja H, Singh SK, Thangavelu L, Chellappan DK, Dua K, Gupta G. Calcium sensing receptor hyperactivation through viral envelop protein E of SARS CoV2: A novel target for cardio-renal damage in COVID-19 infection. Drug Dev Res. 2021; 82:784-788.
30. Zúñiga-Muñoz AM, Pérez-Torres I, Guarner-Lans V, Núñez-Garrido E, Velázquez Espejel R, Huesca-Gómez C, Gamboa-Ávila R, Soto ME. Glutathione system participation in thoracic aneurysms from patients with Marfan syndrome. Vasa. 2017; 46:177-186.
31. Chaothanaphat N, Dhumma-Upakorn P, Jianmongkol S. *In vitro* modulating effects of glutathione on vascular tension and involvement of extracellular calcium. Drug Discov Ther. 2010; 4:19-25.
32. Wang F, Xu B, Sun Z, Wu C, Zhang X. Wall shear stress in intracranial aneurysms and adjacent arteries. Neural Regen Res. 2013; 8:1007-1015.
33. Taguchi E, Nishigami K, Miyamoto S, Sakamoto T, Nakao K. Impact of shear stress and atherosclerosis on entrance-tear formation in patients with acute aortic syndromes. Heart Vessels. 2014; 29:78-82.
34. Jafari M, Di Napoli M, Datta YH, Bershad EM, Divani AA. The role of serum calcium level in intracerebral hemorrhage hematoma expansion: Is there any? Neurocrit

care. 2019; 31:188-195.
35. Tankeu AT, Ndip Agbor V, Noubiap JJ. Calcium supplementation and cardiovascular risk: A rising concern. J Clin Hypertens (Greenwich). 2017; 19:640-646.
36. Wang B, Li D, Gong Y, Ying B, Cheng B. Association of serum total and ionized calcium with all-cause mortality incritically ill patients with acute kidney injury. Clin Chim Acta. 2019; 494:94-99.
37. Bi S, Liu R, Li J, Chen S, Gu J. The prognostic value of calcium in post-cardiovascular surgery patients in the Intensive Care Unit. Front Cardiovasc Med. 2021; 8:733528.
38. Thongprayoon C, Cheungpasitporn W, Chewcharat A, Mao MA, Bathini T, Vallabhajosyula S, Thirunavukkarasu S, Kashani KB. Impact of admission serum ionized calcium levels on risk of acute kidney injury in hospitalized patients. Sci Rep. 2020; 10:12316.
39. Zhang Z, Wu Y, Peng H, Chen S, Wu X. The research progress of acute aortic dissection and acute lung injury. Zhongguo Xiong Xin Xue Guan Wai Ke Lin Chuang Za Zhi. 2021; 37:438-442. (in Chinese)
40. Xiao QB, Wang ZW. Acute aortic dissection and acute lung injury research progress. Adv Cardiovasc Dis. 2020; 41:1260-1263. (in Chinese)
41. Ma X, Liu W. Calcium signaling in brain microvascular endothelial cells and its roles in the function of the blood-brain barrier. Neuroreport. 2019; 30:1271-1277.
42. Wang J, Zhao W, Wang X, Gao H, Liu R, Shou J, Yan J. Enhanced store-operated calcium entry (SOCE) exacerbates motor neurons apoptosis following spinal cord injury. Gen Physiol Biophys. 2021; 40:61-69.
43. Babkina I, Savinkova I, Molchanova T, Sidorova M, Surin A, Gorbacheva L. Neuroprotective Effects of Noncanonical PAR1 Agonists on Cultured Neurons in Excitotoxicity. Int J Mol Sci. 2024; 25:1221.

Received December 15, 2024; Revised February 6, 2025; Accepted February 21, 2025.

[§]These authors contributed equally to this work.

**Address correspondence to:*
Junfeng Zhao, Department of Emergency, Zhejiang Hospital, Hangzhou 310012, China.
E-mail: Zjf7301@163.com

Ling Wang, Department of Obstetrics and Reproductive Immunology, Shanghai East Hospital, Tongji University School of Medicine, No. 1800 Yuntai Road, Shanghai 200100, China.
E-mail: Dr.wangling@vip.163.com

Released online in J-STAGE as advance publication February 26, 2025.

Original Article

DOI: 10.5582/ddt.2025.01003

Isolation and characterization of phosphoglycerate kinase and creatine kinase from bighead carp (*Aristichthys nobilis*): Potential sources for antitumor agents

Yue Gao[1,§], Wanying Liu[2,§], Qing Yan[3], Chunlei Li[1,5,*], Mengke Gu[4], Sixue Bi[1], Weiming Zheng[3], Jianhua Zhu[2], Liyan Song[3,*], Rongmin Yu[1,2,*]

[1] Biotechnological Institute of Chinese Materia Medica, Jinan University, Guangzhou, Guangdong, China;
[2] Department of Natural Product Chemistry, College of Pharmacy, Jinan University, Guangzhou, Guangdong, China;
[3] Department of Pharmacology, College of Pharmacy, Jinan University, Guangzhou, Guangdong, China;
[4] School of Life Sciences, Sun Yat-sen University, Guangzhou, Guangdong, China;
[5] Department of Pharmacy, Qilu Hospital, Cheeloo School of Medicine, Shandong University, Jinan, Shandong, China.

SUMMARY: Bighead carp (*Aristichthys nobilis*) has garnered significant attention due to its potential health benefits, yet its bioactive protein components remain largely unexplored. In this study, two proteins S3 and Z1 were isolated from *Aristichthys nobilis* using ammonium sulfate precipitation and serial column chromatography guided by their *in vitro* antitumor activity. Both proteins were found to be homogeneous in sodium dodecyl sulfate-polyacrylamide gel electrophoresis (SDS-PAGE) with a purity exceeding 95% as confirmed by reverse-phase high performance liquid chromatography (RP-HPLC). Electrospray ionization tandem mass spectrometry (ESI-MS/MS) analysis revealed their precise molecular weights to be 44.335 kDa for S3 and 43.028 kDa for Z1. Their amino acid sequences were elucidated through tandem mass spectroscopy and transcriptome unigene analysis, identifying S3 as phosphoglycerate kinase and Z1 as creatine kinase. Furthermore, secondary structure was measured by circular dichroism and three-dimensional structure was predicted by modeling software. The antitumor potential of S3 was evaluated by an *in vitro* assay, yielding an IC_{50} value of 26.3 ± 2.9 μM against the HT-29 cell line. Z1 demonstrated antiproliferative activity *in vitro* with IC_{50} values of 21.8 ± 1.4, 22.3 ± 2.1, and 22.3 ± 2.5 μM against HT-29, HeLa, and HepG2 cell lines, respectively. Notably, Z1 was found to enhance glucose metabolism and significantly increase the production of lactic acid and CO_2 in tumor cells. These findings suggest that bighead carp (*A. nobilis*) could serve as a promising source for both antitumor agents and functional food ingredients.

Keywords: *Aristichthys nobilis* proteins; purification and characterization; antitumor activities

1. Introduction

With the advancement of science and technology, human beings' living standards have been gradually improved, and our life expectancy has been significantly extended. Due to the incomplete understanding of the pathogenesis of cancer as well as limited treatment drugs and means, malignant tumors have become one of the serious threats to human life and health (*1*). There were close to 20 million new cases of cancer in the year 2022 (including nonmelanoma skin cancers [NMSCs]) alongside 9.7 million deaths from cancer (including NMSC) (*2*). Despite the massive efforts of modern pharmacology and the substantial advances made, such as surgical removal and chemotherapy, tumors are still the main cause of mortality around the world (*3*). With demographics-based predictions indicating that the number of new cases of cancer will reach 35 million by 2050, investments in prevention, including the targeting of key risk factors for cancer (including smoking, overweight and obesity, and infection), could avert millions of future cancer diagnoses and save many lives worldwide, bringing huge economic as well as societal dividends to countries over the forthcoming decades (*2*). Hence, searching for antitumor agents with high efficiency and low toxicity is an ongoing challenge (*4*).

Oceans cover 70% of the earth's surface, and are a rich source of bioactive substances as well as potential therapeutic agents (*5*). Because of their competitive, exigent, and aggressive living environment, many marine organisms produce unique and effective molecules, including bioactive proteins and polypeptides,

polyunsaturated fatty acids (PUFAs), vitamins, polysaccharides, enzymes and antioxidants (*6*).

Marine bioactive proteins have attracted increasing attention and research because of their excellent biological activity, especially antitumor activity. Various marine proteins and their derived peptides possess antitumor activities both *in vitro* and *in vivo* (*7-10*), such as geodiamolide H (*11*), dolastatin 10 (*12*), TZT-1027 (*13*), kahalalide F (*14,15*) and *Eucheuma serra* agglutinin (*16*). Most marine antitumor proteins and peptides that exhibit antiproliferative effect may cause tumor apoptosis by binding target proteins, and inducing apoptotic process *via* both intracellular and extracellular pathways (*17,18*).

Fish flesh, rich in proteins and peptides, is one of the main foods for most people around the world. There are approximately 140 million tons of fish harvested per year all over the world (*19*). Several investigations have researched the relationship between fish intake and tumor incidence. Through meta-analysis, Song concluded that fish intake was negatively correlated with the incidence of lung cancer, with a relative risk of 0.79 and a 95% confidence interval of 0.69-0.92 (*20*). Another meta-analysis showed that fish intake reduced 12% incidence of colorectal cancer, and the relative risk was 0.88 (95% CI = 0.80-0.95) (*21*). In addition, previous studies have identified the polypeptides from tuna dark muscle (*8*), and half-fin anchovy (*7*) possessed good antiproliferative effect.

Bighead carp (*Aristichthys nobilis*), belonging to Cyprinidae family, is an important commercial freshwater fish in China and also a source of bioactive substances. The annual worldwide production of bighead carp was over four million tons. Recently, a novel fucose-binding lectin from the gill of bighead carp has been characterized (*22*). Furthermore, a pyrophosphatase responsible for the hydrolysis of pyrophosphate (PPi) in muscle was purified (*23*). Parvalbumin, an allergen protein, was cloned and expressed, and its allergic activity was detected (*24*). Microcystin-detoxifizyme from bighead carp was also cloned and analyzed (*25*). However, few attempts were made on antitumor activity of substances from bighead carp. The only published study reported a lectin from bighead carp exhibiting antitumor and mitogenic activities (*25*). Little concern was concentrated on proteins and their antiproliferative effect from bighead carp.

In the present study, two proteins, S3 and Z1 were purified from *A. nobilis*, and their physicochemical characterizations were well determined. Otherwise, antitumor activity of two purified proteins was also evaluated using MTT assay, which indicated that *A. nobilis* might be one of the potential sources of antitumor agents and functional foods.

2. Materials and Methods

2.1. Materials

Samples of *A. nobilis* were collected from the Suishi market, college town of Guangzhou, China. Phenyl sepharose CL-4B was purchased from GE Healthcare, Chicago, PO, USA. Tris, sodium dodecyl sulfate (SDS), Coomassie brilliant blue R-250, 3-(4,5-dimethylthiazol-2-yl-)-2,5-diphenyltetrazolium bromide (MTT), dimethyl sulfoxide (DMSO), cisplatin, penicillin, and streptomycin were obtained from Genview Corporation (Beijing, China). RPMI-1640 and fetal bovine serum (FBS) were obtained from GIBCO Invitrogen Corporation (San Diego, CA, USA). Other commercially available chemicals and reagents were of analytical grade.

2.2. Preparation of crude proteins

The raw material from *A. nobilis* was obtained by removing the skin, bone and tail, and then cut into small pieces. After washing it with tap water and distilled water in turn, phosphate buffer (pH 8.0, 30 mM) was used to extract the total proteins at a ratio of 1:4 (w/v) from the raw material. After homogenizing for 2 min with DS-1 high-speed tissue homogenizer (Jingxin Co., Shanghai, China), SB25-12 ultrasonic cleaner (Ningbo Xingzhi Co., Zhejiang, China) with a straight probe and continuous pulse was used to ultrasonicate the sample for 40 min. Then the sample was centrifuged at 10,000× *g* for 30 min. The supernatant was collected and precipitated with 0–70% and 70–100% saturated ammonium sulfate (*26*). The precipitates were collected by centrifugation (10,000× *g* for 30 min), re-dissolved in phosphate buffer, and dialyzed against distilled water at 4°C for 48 h to remove residual ammonium sulfate (*27*). Finally, two fractions, SNP1 and SNP2, were lyophilized and collected. The ability to inhibit cell growth was determined by the MTT assay. All extraction procedures were carried out at 4°C.

2.3. Isolation of proteins

The lyophilized fraction with the higher anti-proliferative activity as well as higher protein content was further separated on phenyl sepharose CL-4B hydrophobic chromatography column (2.5 × 40 cm), which had previously been equilibrated with the 1.0 M $(NH_4)_2SO_4$ prepared in 30 mM phosphate buffer (pH 8.0). SNP2 was dissolved in the above buffer and loaded onto the column, followed by stepwise elution with $(NH_4)_2SO_4$ (1.0, 0.5 and 0 M) prepared in 30 mM phosphate buffer (pH 8.0) at a flow rate of 0.7 mL/min. Each fraction was eluted and monitored at 280 nm. Finally, the three fractions, CL1, CL2 and CL3, were collected, lyophilized, and their ability to inhibit cell growth was measured by MTT assay.

The active fractions, CL2 and CL3, were further purified using high-performance gel permeation chromatography (HP-GPC) coupled with TSK G2000SWXL column (4.6 × 300 mm, Tosoh Co.,

Yamaguchi, Japan), eluted with 0.5 M sodium sulfate buffer over 30 min at a flow rate of 0.5 mL/min. The chromatographic profile was measured at 280 nm. The column temperature was 25°C. One single peak eluting from CL2 fraction was named as S3, while another peak from CL3 fraction was collected as Z1. Cytotoxicity of the purified peaks was measured by MTT assay after lyophilization.

2.4. Characterization of purified proteins

2.4.1. Identification of proteins by tricine-SDS-PAGE

The obtained proteins were analyzed by SDS-PAGE (*28*) using stacking gels (5% concentration of acrylamide) and running gel (16% concentration of acrylamide) (*29*) to check the purity and determine the molecular weight of the purified proteins. Protein bands were detected by the Coomassie blue staining method (*30*). A middle molecular weight calibration kit (Thermo Scientific, Waltham, MA, USA) was used as the standard markers.

2.4.2. Purity determination of proteins by HPLC

The purity of the purified proteins was measured by RP-HPLC on a Shimadzu series LC-20AB HPLC system (Shimadzu Co., Kyoto, Japan) fitted with a ZORBAX® 300SB-C8 column (4.6 × 250 mm, Agilent Co., Palo Alto, CA, USA). The elution solvent system was composed of water–trifluoroacetic acid (solvent A; 100:0.1, v/v) and acetonitrile–trifluoroacetic acid (solvent B; 100:0.1, v/v) (*27*). The polypeptides were eluted with a linear gradient of acetonitrile (15–55%) over 30 min at a flow rate of 1.0 mL/min. The chromatographic profile was measured at 280 nm. The column temperature was 35°C.

2.4.3. Protein and carbohydrate content assay

The protein content of the polypeptides was measured using Bradford method (*31*) where bovine serum albumin (BSA) was used as the standard protein. The protein content was evaluated by monitoring the absorbance of the samples at 595 nm. The saccharide content of the proteins was measured by the phenol–sulfuric acid method (*32-34*) in which glucose was used as standard. The saccharide content of the detected proteins was evaluated through the absorbance of the samples at 490 nm (*35*).

2.4.4. Molecular weight determination

The accurate molecular weight of the purified proteins was measured as reference (*27*). S3, and Z1 were dissolved in ultrapure water and loaded into quadrupole linear ion trap (QTRAP) mass spectrometer (Applied Biosystem, Foster City, CA, USA), respectively. The detection was performed in the positive electrospray ionization (ESI + ve) mode. High-purity nitrogen was used for drying (35 psi) and ESI nebulization (45 psi) process.

2.4.5. Mass spectrometry measurement

The purified proteins were dissolved and loaded on 1D SDS-PAGE with a 5-16% polyacrylamide gradient gel. After SDS-PAGE analysis, the target protein spots on the Coomassie Brilliant Blue-stained gels were manually excised, washed, and mixed with 1 M ammonium bicarbonate for maintaining reaction conditions. Then, 50 mM DTT and 100 mM iodoacetamide were added for reduction reaction. The sample was then desalted and further digested with sequencing-grade trypsin (Promega Co.,, Madison, WI, USA) for 20 h at 37°C. The digested samples were finally dried in a vacuum centrifuge, and then dissolved in 40 µL of 1% (v/v) formic acid.

The resulting samples was loaded onto RP-HPLC column for pre-fractionation and analyzed by nanoESI-orbitrap mass spectrometry for identification. A reverse phase PepMap column (ES802 75 µm × 25 cm, Thermo Co., Waltham, MA, USA) coupled with EASY-nLC 1200 instrument (Thermo Co., Waltham, MA, USA) was used for sample pre-fractionation. Mobile phase A consisted of 0.1% (v/v) formic acid in ultrapure water while mobile phase B consisted of 0.1% (v/v) formic acid in 80% acetonitrile were applied at the flow rate of 300 nL/min to separate hydrolyzed peptides. Afterwards, the eluted peptides were directly introduced into a nanoESI Q-Exactive mass spectrometer (Thermo Co., Waltham, MA, USA). The data were acquired and processed using the MASCOT program (*http://www.matrixscience.com*). The transcriptome sequencing of *A. nobilis* has been previously completed (NCBI Short Read Archive accession number: SRX1950353). MS/MS data were examined and matched both in the assembled transcriptome database of *A. nobilis* and National Center for Biotechnology Information (NCBI) basic local alignment search tool (BLAST) database.

2.4.6. Structure elucidation

The secondary structures of the two proteins were analyzed using circular dichroism (CD) spectroscopy based on the reported method (*36*). The purified proteins at the concentration of 0.05 mg/mL in distilled water were filtered through 0.22 µm membrane before CD analysis. Afterwards, the samples were loaded onto Jasco J-810 spectropolarimeter (Japan Spectroscopic Co., Ltd., Tokyo, Japan) with the parameters as a scan range of 250–190 nm, scan speed of 50 nm/min, the data interval of 1 nm, the bandwidth of 2 nm. Each spectrum was detected triplicated and recorded as the average of 3 scans. Three-dimensional structures of two purified proteins were elucidated using multiple template

modeling by MODELER 4.0 software and visualized in Pymol 2.7 software.

2.5. *In vitro* cell growth inhibition assay

Three tumor cell lines were used in this study including Hela (cervical carcinoma cell line), HepG2 (human liver carcinoma cell line), and HT-29 (human colon carcinoma cell line). Cell lines were purchased from the Zhongshan School of Medicine, Sun Yat-sen University, and maintained in RPMI 1640 medium supplemented with heat-inactivated 10% FBS, 1.0 mg/mL $NaHCO_3$, 0.2 mg/L L-glutamine, 100 units/mL streptomycin, and 100 units/mL penicillin in a humidified incubator at 37°C and 5% CO_2.

The cytotoxicity of the two purified proteins was measured by MTT assay. The S3 samples were dissolved and diluted to 0.1, 0.4, 1.4, 5.8, and 23.0 μM with RPMI-1640 medium.The Z1 samples were dissolved and diluted to 0.3, 1.3, 5.3, 21.3, and 42.6 μM with RPMI-1640 medium. Cisplatin was used as the positive control. *In vitro* cytotoxic activity was evaluated using MTT assay according to the published procedure (*37*) with some modifications.

Cells in the logarithmic phase were detached with 0.25% trypsin to make a single cell suspension using RPMI-1640 complete culture solution. After counting the cells, they were inoculated into a 96-well culture plate and incubated at 37°C in a humidified incubator with 5% CO_2. After 24 h, the different concentrations of samples were added into the wells and the plate was incubated for a set time. Then, 20 μL of MTT solution was added to each well and the plate was incubated for another 4 h at 37°C. The supernatant was removed and the MTT-formazan crystals were dissolved in 200 μL of DMSO and the absorbance was read at 570 nm. The percentage inhibition of cell growth was calculated according to the following equation:

$$\text{Inhibitory rate\%} = (A_{570,\text{control}} - A_{570,\text{sample}}) \div (A_{570,\text{control}} - A_{570,\text{blank}}) \times 100\% \quad (1)$$

2.6. Effect of purified proteins on the metabolic rate of tumor cells

Before adding MTT, samples of the cell supernatant in each well at the end of the cell proliferation inhibition experiment were taken, and the detection was carried out according to the operating instructions of the GLU kit (Nanjing Jiancheng Bioengineering Institute, China). The 3 μL of sample and calibrator was mixed with 300 μL of the reaction solution R respectively. Distilled water was used as the blank control. The reaction was carried out at 37°C for 10 min and the absorbance was read at 500 nm. The initial glucose concentration in the culture medium, which is 16.65 mmol/L. The glucose consumption was calculated according to the following equation:

$$\text{GLU (mmol/L)} = A_{500,\text{sample}}/A_{500,\text{calibrator}} \times \text{Calibrator (mmol/L)}$$

$$\Delta\text{GLU (mmol/L)} = \text{GLU (mmol/L, initial)} - \text{GLU (mmol/L, end)}$$

Similarly, samples of the cell supernatant in each well at the end of the cell proliferation inhibition experiment were taken, and the detection was carried out according to the operating instructions of the Lactic Acid LD kit (Guangzhou Kofa Biotechnology Corporation, China). A total of 20 μL of the standard (3 mmol/L), 20 μL of the sample, 1,000 μL of the enzyme reaction solution, and 200 μL of the chromogenic solution were added successively and mixed. Distilled water was used as the blank control. The reaction was carried out at 37°C for 10 min and 2,000 μL of the stop solution was added. The absorbance was read at 530 nm and the content of lactic acid was calculated according to the following equation:

$$\text{Lactic acid (mmol/L)} = A_{530,\text{sample}}/A_{530,\text{standard}} \times \text{Standard (mmol/L)}$$

2.7. Statistical analysis

All of the assays were conducted in triplicate and the experimental data were expressed as the mean ± standard deviation. GraphPad Prism 5.0 was used for statistical analysis. Two-sample comparisons were performed using Student's *t*-test; $P < 0.05$ was considered statistically significant.

3. Results

3.1. Purification of proteins

The total proteins were firstly released from the flesh of *A. nobilis*, and afterwards fractionated by salting-out at increasing levels of saturation of ammonium sulfate at 4°C. Two fractions, named as SPN1 and SPN2, were obtained at an ammonium sulfate saturation of 0–70% and 70–100%, respectively. Since it possessed higher protein concentration and better antiproliferative activity, SPN2 was loaded onto a phenyl sepharose CL-4B hydrophobic chromatography column and eluted with decreasing concentrations of $(NH_4)_2SO_4$ for further purification. Three resulting peaks, namely as CL1, CL2 and CL3, were obtained (Figure 1A). Due to the protein and saccharide content determination, CL1 contained the highest protein concentration (Table S1, *https://www.ddtjournal.com/action/getSupplementalData.php?ID=243*), then followed with CL3. CL2 contained only 31.6% protein content and 8.3% saccharide content. With the guidance of bioassay, CL2 and CL3 were

further purified using high-performance gel permeation chromatography (HP-GPC). Finally, a protein, designated as S3, was purified from CL2. And another protein Z1 was obtained from CL3 (Figures 1B and 1C).

3.2. Characterization of purified proteins

3.2.1. Purity determination

SDS-PAGE is a pervasive method to characterize the purity of proteins according to the protein molecular weights (*36,37*). The electrophoresis technique also provides a foundation for further evaluation of proteins. In the present investigation, the two purified proteins were determined by SDS-PAGE (Figures 2A and 2B). SDS-PAGE analysis revealed that S3 and Z1 were composed of a diffuse single band respectively, which indicated both of them are monomeric, homogeneous proteins after purification. In addition, S3 and Z1 similarly shared an approximate molecular weight about 43 kDa.

RP-HPLC was another common technique to determine the purity of the purified proteins. As shown in Figures 2C and 2D, the RP-HPLC elution profiles

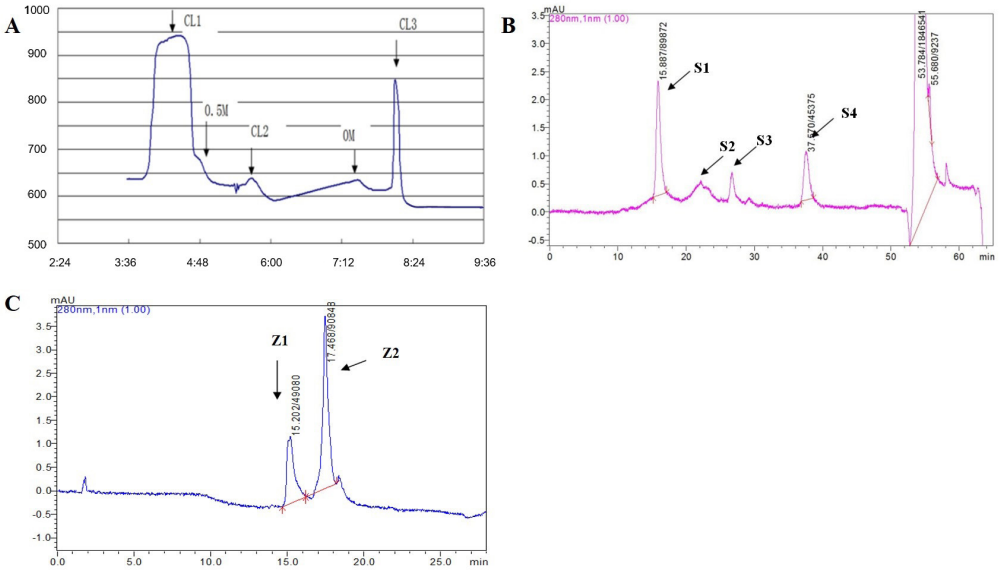

Figure 1. Purification of proteins from *A. nobilis*. (A) Elution profile of SPN2 by phenyl sepharose CL-4B hydrophobic chromatography; **(B)** Elution profile of CL2 by HP-GPC; **(C)** Elution profile of CL3 by HP-GPC.

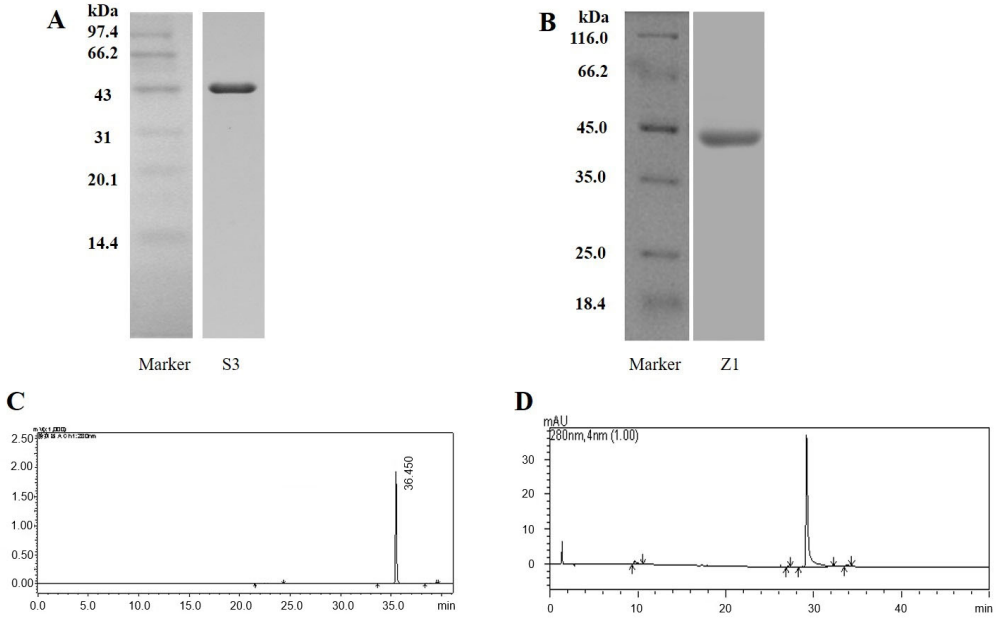

Figure 2. The purity determination of proteins from *A. nobilis*. (A) SDS-PAGE of S3 from CL2 fraction. **(B)** Z1 from CL3 fraction. **(C)** RP-HPLC profile of S3; **(D)** RP-HPLC profile of Z1.

of S3 and Z1 with elution time at 35.450 and 29.190 min showed a symmetric single peak with the purity of 97.6% and 95.6%, respectively (Table S2, *https://www.ddtjournal.com/action/getSupplementalData.php?ID=243*).

3.2.2. Molecular weight

A number of researches have shown that marine antitumor proteins are macromolecular proteins (*38-40*). For example, two proteins with 27.1 kDa and 20.5 kDa purified from *Arca inflata* showed high anti-proliferation effect against human tumor cells *in vitro (41,42)*. At the present investigation, the accurate molecular weights of S3 and Z1 were determined by ESI-MS/MS as 44.335 and 43.028 kDa, respectively.

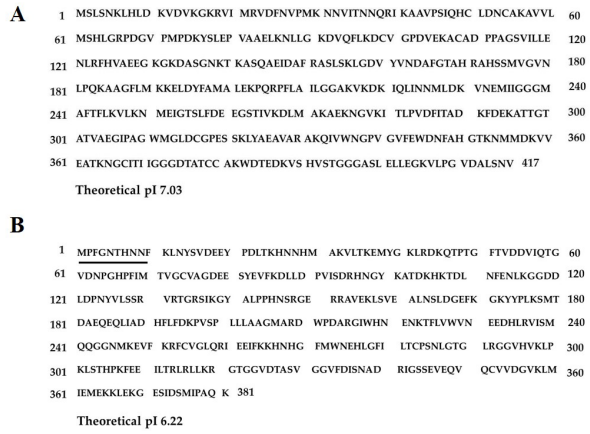

Figure 3. Amino acid sequences of S3 (A) and Z1 (B). N-terminal sequence of Z1 determined by Edman degradation was underlined, nevertheless, the N-terminal sequence of S3 was blocked.

3.2.3 Amino acid sequence analysis

High resolution tandem mass spectrometry, state of the art technique for the characterization and sequencing of proteins, was used in this study. Trypsin hydrolysis was applied to produce amounts of peptides at lysine and arginine cleavage sites. Those peptides were pre-separated by EASY-nLC 1200 and further determined by nano ESI-MS/MS instrument. The tested peptide fragments were identified and aligned with transcriptome of *A. nobilis* (Tables S3 and S4, *https://www.ddtjournal.com/action/getSupplementalData.php?ID=243*). According to the tandem mass spectrometry, the complete amino acid sequences of the two purified proteins were obtained (Figure 3). Aligning with NCBI BLAST database, S3 and Z1 were identified as phosphoglycerate kinase and creatine kinase, respectively (Figure 4).

3.2.4. Structure elucidation

CD spectroscopy provides an exquisitely sensitive and rapid method for the analysis of protein secondary structures. It is widely used in protein folding and protein conformation studies. In the circular dichroic ultraviolet wavelength zone (190-240 nm), the main chromophore is a peptide chain, and the CD spectrum of this wavelength range contains information on the conformation of the main chain of a protein. The CD spectrum of the α-helical conformation has a negative peak at 222 nm and 208 nm and a positive peak at around 190 nm. The CD spectrum

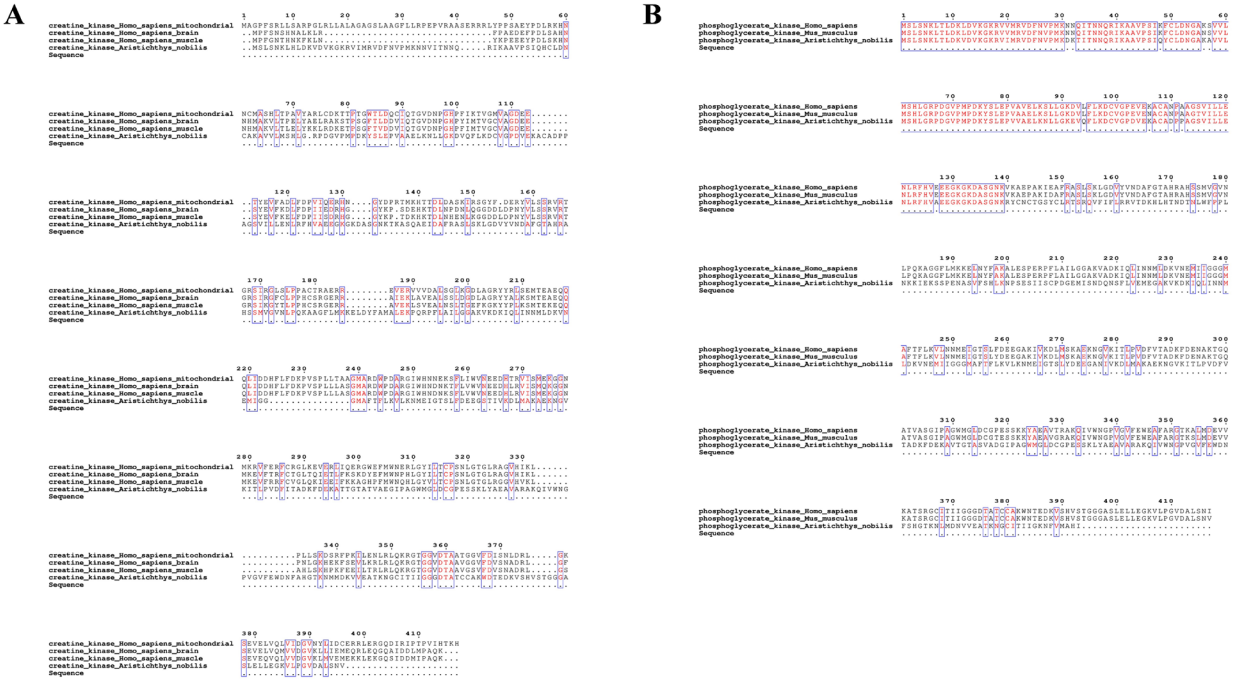

Figure 4. Sequence alignment among Z1 (A) and S3 (B), respectively.

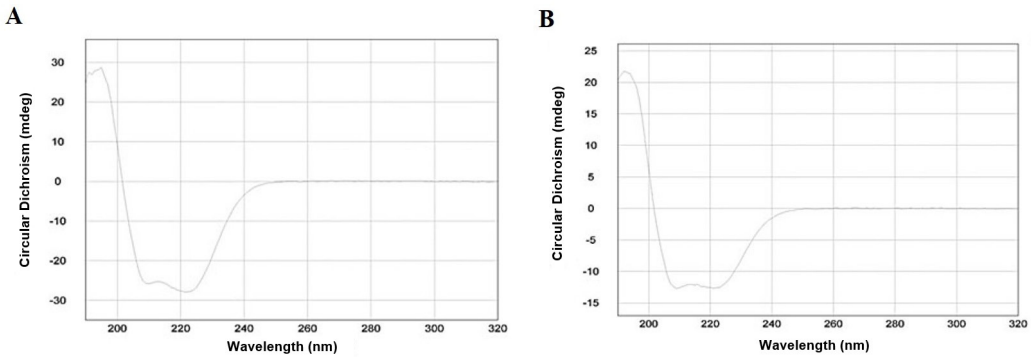

Figure 5. Secondary structure determination of S3 (A) and Z1 (B) by circular dichroism spectroscopy.

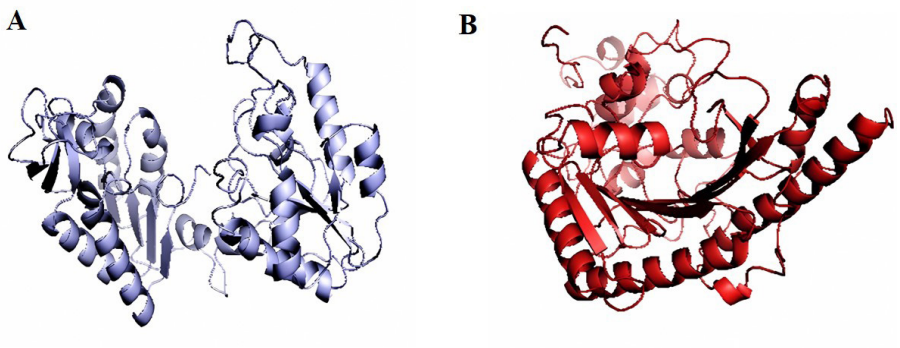

Figure 6. Three-dimensional predicted structures of S3 (A) and Z1 (B) using multiple templates modeling. Three templates (2xe6, 2y3i, and 5m1r) were used for modeling S3 structure and three other templates (1i0e, 1vrp, and 2crk) were used for modeling Z1 structure.

of the β-sheet conformation has a negative peak at 217-218 nm and a strong positive peak at 195-198 nm. The CD spectrum of the random coil conformation has a negative peak around 198 nm and a small and broad positive peak around 220 nm (*43,44*). As shown in Figure 5, the CD spectrum of two proteins exhibited one strong positive peak at 195 nm, as well as two negative ellipticity signals at 210 and 222 nm, respectively, which were typical features of α-helical and β-sheet conformations of folded proteins. Proposed secondary structure conformations were acquired using the tested CD data and Jasco secondary structure estimation program software. S3 displayed 46.0% α-helix, 34.4% β-sheet, and 19.6% random coil of secondary structure. In addition, Z1 showed 56.2% α-helix, 23.6% β-sheet, and 20.2% random coil of secondary structure. Tertiary structures predicted by homology modeling of S3 and Z1 were shown in Figure 6.

3.3. Cytotoxicity of purified proteins

The cytotoxicity of two purified proteins against three human tumor cell lines including HepG2, HeLa and HT-29 were examined using MTT assay (Table 1). Cisplatin was used as a positive control and performed anti-proliferative activity against HepG2, HeLa and HT-29 cells with IC_{50} values of 4.3, 5.0 and 4.7 μM, respectively. Z1 possessed the highest cytotoxicity and displayed anti-proliferative effect against HepG2, HeLa and HT-29 cell lines with IC_{50} values of 22.3, 22.3 and 21.8 μM, respectively.

Table 1. Anti-proliferative activities of two purified proteins against three tumor cell lines

Polypeptides	IC_{50} (μM) (mean ± SD, n = 3)		
	HeLa	HepG2	HT-29
Z1	22.3 ± 2.1	22.3 ± 2.5	21.8 ± 1.4
S3	> 30	> 30	26.3 ± 2.9
Cisplatin	5.0 ± 1.0	4.3 ± 1.0	4.7 ± 0.3

In addition, the effect of Z1 on the metabolic rate of tumor cells was determined. When Z1 was applied to HepG2, HeLa and HT-29 tumor cells at 22 μM for 72 h, the cell growth was about half of the blank group, but the actual consumption of glucose of Z1 group was about the same as the blank group. As shown in Figure 7, the glucose consumption of those tumor cells was 1.49, 2.21 and 2.68 mmol/L, respectively. Combining the lower growth of Z1 group, the rates of glucose consumption of Z1 group were 1.48, 2.43 and 2.36 times that of the non-administered group in HepG2, HeLa and HT-29 cells. Similarly, the amounts of lactic acid were 0.62, 0.74, and 0.86 mmol/L, which was 2.21, 2.33, and 2.48 times of the control group, respectively. The production of CO_2 was 4.32, 6.25 and 8.53 mmol/L, which was 2.18, 2.87 and 2.91 times compared with that of the non-administered group respectively based

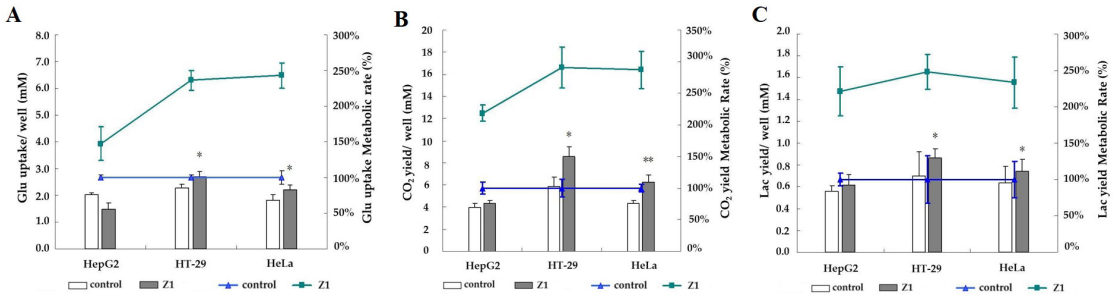

Figure 7. Effect of Z1 on glucose (A), lactic acid (B) and CO_2 (C) consumption of three tumor cells (HepG2, HeLa and HT-29) at IC_{50} concentration (n = 3, *$P < 0.05$, **$P < 0.01$)

on the growth rate.

4. Discussion

There are a number of fish species identified with potential pharmaceutical values. Bioactive proteins and their derivatives from muscles of various fish species have shown diverse biological functions including antihypertensive, antioxidant, anti-inflammatory, anticoagulant, and antibacterial activities. And they may be a potential material for biomedical and food industries. The proteins derived from sardine and hair tail meat exhibited inhibitory activities against angiotensin I-converting enzyme (ACE) (*45*). Furthermore, another ACE inhibitory protein was derived from bigeye tuna dark muscle (*46*). Hence, fish muscles are valuable natural resources and show the potential use in nutraceutical and pharmaceutical industries. It is necessary to investigate the bighead carp flesh and reveal the hidden functional components.

S3 exhibited 73% homology with predicted phosphoglycerate kinase 1 derived from sheepshead minnow (*Cyprinodon variegatus*) (Figure 4B). This demonstrated that S3 was a newly discovered phosphoglycerate kinase 1 from bighead carp (*A. nobilis*), which had not previously been extensively characterized.

In addition, Z1 showed 100% homology with muscle-type creatine kinase. Z1 from *A. nobilis* displayed high homology with *Cyprinus carpio* and *Carassius auratus*, which indicated the highly similar genetic background among these three species (Figure 4A). The N-terminal amino acid sequences of Z1 determined by protein sequencer (Figure 3B) were well matched with the amino acids detected by tandem mass spectrometry, which implied the accuracy of the results produced by tandem mass spectrometry. Nevertheless, the N-terminal amino acid sequence of S3 was blocked and failed to detect, which indicated that S3 might have posttranslational modification at N-terminal sites.

Diverse bio-active peptides attributes to highly ordered and stable conformations, such as possessing high ratio of β-sheet and α-helix conformation in secondary structures. S3 and Z1 both exhibited highly ratio of α-helix and β-sheet conformation and performed tightly folded conformation. This result is similar to the antitumor protein α-sarcin produced by the mold *Aspergillus giganteus*, which had highly α-helix and β-sheet content and ordered a tightly conformation (*47*). Three-dimensional structures of two proteins were simulated by multiple template modeling (Figure 6). The simulation results possessed highly ordered structures, which were well matched with CD spectrum of two proteins.

Z1 was identified as muscle-type creatine kinase from bighead carp. Creatine kinase is a key enzyme in the process of cellular energy metabolism, and exists in humans in the form of four isoenzymes, CK-BB (brain type), CK-MB (hybrid type), CK-MM (muscle type) and CK-Mt (mitochondrial type). Creatine kinase and creatine kinase isoenzymes are widely used in the diagnosis of clinical myocardial infarction, muscle atrophy and other diseases (*48*). CK-Mt is located in the intracellular mitochondrial membrane and mitochondrial outer membrane space, which promotes ATP production and catalyzes the reversible transfer of phosphate bond between creatine and ATP. CK-Mt plays a very important role in the stability of intracellular ATP pool and the regulation of the energy metabolism (*49*). However, an increasing number of studies have shown that the high expression of CK-Mt levels may be closely related to the strong energy demand of tumor growth. According to the recent investigations, high expression of CK-Mt was involved in cancer energy metabolism and facilitated cancer cell division and inhibited apoptosis. Our experiments show that CK-MM can multiply the metabolism of glucose, and the production of lactic acid and CO_2 also increases exponentially in tumor cells (Figure 7).

Z1, muscle-type creatine kinase from *A. nobilis*, exhibited anti-proliferative activity against multiple tumor cell lines. As illustrated in Figure 4A, Z1 showed high homology with human muscle-type (CK-BB) and brain-type creatine kinase (CK-MM) but low homology with mitochondrial-type creatine kinase (CK-Mt), which indicated that Z1 might exhibit anti-proliferation effect through competitive binding the target of human CK-Mt. Moreover, compared with cytotoxicity against other

tumor cells, S3 showed better anti-proliferation effect on colon tumor cell line HT-29 with an IC_{50} value of 26.3 μM (Table 1), which showed better activity than cecropin B peptide from silkworm pupae (*50*).

5. Conclusion

In summary, two proteins, S3 and Z1 were purified from bighead carp (*A. nobilis*). S3 and Z1 were identified as phosphoglycerate kinase and creatine kinase, respectively. Physicochemical properties of two purified proteins were further determined. Moreover, Z1 and S3 showed anti-proliferative activity against HT-29, HeLa and HepG2 cell lines. The structural and functional characterization of proteins S3 and Z1 is poised to facilitate advancements in therapeutic and nutritional applications. This investigation has significantly broadened the knowledge base regarding the proteome of the bighead carp, thereby necessitating further in-depth studies aimed at the exploration and development of biomacromolecules within this species. Concurrently, the elucidation of the antitumor mechanisms of Z1 and S3 is currently under rigorous investigation.

Funding: This work was supported by National Natural Science Foundation of China (No. 81503303 and 82174019), Major Science and Technology Projects / Significant New Drugs Creation of Guangdong Province (No. 2013A022100032), and Ocean and Fisheries Science and Technology Development Projects of Guangdong Province (No. A201501C04).

Conflict of Interest: The authors have no conflicts of interest to disclose.

References

1. Stephenson J. Cancer No. 1 killer by 2010. JAMA. 2009; 301:263.
2. Bray F, Laversanne M, Sung H, Ferlay J, Siegel RL, Soerjomataram I, Jemal A. Global cancer statistics 2022: GLOBOCAN estimates of incidence and mortality worldwide for 36 cancers in 185 countries. CA Cancer J Clin. 2024; 74:229-263.
3. Cheong S, Kim E, Hwang J, Kim Y, Lee J, Moon, S, Jeon B, Park P. Purification of a novel peptide derived from a shellfish, *Crassostrea gigas* and evaluation of its anticancer property. J Agr Food Chem. 2013; 61:11442-11446.
4. Cragg G, Grothaus P, Newman D. Impact of natural products on developing new anti-cancer agents. Chem Rev. 2009; 109:3012-3043.
5. Jo C, Khan F, Khan M, Iqbal J. Marine bioactive peptides: Types, structures, and physiological functions. Food Rev Int. 2017; 33:44-61.
6. Kim S, Ravichandran Y, Khan S, Kim Y. Prospective of the cosmeceuticals derived from marine organisms. Biotechnol Bioprocess Eng. 2008; 13:511-523.
7. Lee Y, Lee K, Ji Y, Kim K, Lee H. Induction of apoptosis in a human lymphoma cell line by hydrophobic peptide fraction separated from anchovy sauce. Biofactors. 2004; 21:63-67.
8. Hsu K, Li-Chan E, Jao C. Antiproliferative activity of peptides prepared from enzymatic hydrolysates of tuna dark muscle on human breast cancer cell line MCF-7. Food Chem. 2011; 126:617-622.
9. Kim E, Kim Y, Hwang J, Lee J, Moon S, Jeon B, Park P. Purification and characterization of a novel anticancer peptide derived from *Ruditapes philippinarum*. Process Biochem. 2013; 48:1086-1090.
10. Harnedy P, FitzGerald R. Bioactive peptides from marine processing waste and shellfish: A review. J Funct Foods 2012; 4:6-24.
11. Freitas V, Rangel M, Bisson L, Jaeger R, Machadosantelli G. The geodiamolide H, derived from Brazilian sponge *Geodia corticostylifera*, regulates actin cytoskeleton, migration and invasion of breast cancer cells cultured in three-dimensional environment. J Cell Physiol. 2008; 216:583-594.
12. Yamamoto N, Andoh M, Kawahara M, Fukuoka M, Niitani H. Phase I study of TZT-1027, a novel synthetic dolastatin 10 derivative and inhibitor of tubulin polymerization, given weekly to advanced solid tumor patients for 3 weeks. Cancer Sci. 2009; 100:316-321.
13. Tamura K, Nakagawa K, Kurata T, Satoh T, Nogami T, Takeda K, Mitsuoka S, Yoshimura N, Kudoh S, Negoro S, Fukuoka M. Phase I study of TZT-1027, a novel synthetic dolastatin 10 derivative and inhibitor of tubulin polymerization, which was administered to patients with advanced solid tumors on days 1 and 8 in 3-week courses. Cancer Chemother Pharmacol. 2007; 60:285-293.
14. Rademaker-Lakha J, Horenblas S, Meinhardt W, Stokvis E, de Reijke T, Jimeno J, Lopez-Lazaro L, Martin J, Beijnen J, Schellens J. Phase I and pharmacokinetic study of Kahalalideij F in patients with advanced androgen refractory prostate cancer. Clin Cancer Res. 2005; 11:1854-1862.
15. Martın-Algarra S, Espinosa E, Rubió J, López J, Manzano J, Carrión L, Plazaola A, Tanovic A, Paz-Ares L. Phase II study of weekly kahalalide F in patients with advanced malignant melanoma. Eur J Cancer. 2009; 45:732-735.
16. Sugahara T, Ohama Y, Fukuda A, Hayashi M, Kawakubo A, Kato K. The cytotoxic effect of *Eucheuma serra* agglutinin (ESA) on cancer cells and its application to molecular probe for drug delivery system using lipid vesicles. Cytotechnology. 2001; 36:93-99.
17. Lee K, Bode A, Dong Z. Molecular targets of phytochemicals for cancer prevention. Nat Rev Cancer. 2011; 11:211-218.
18. Lin X, Liu M, Hu C, Liagents ao D. Targeting cellular proapoptotic molecules for developing anticancer from marine sources. Curr Drug Targets 2010; 11:708-715.
19. Benhabiles M, Abdi N, Drouiche N, Lounici H, Pauss A, Goosen M, Mameri N. Fish protein hydrolysate production from sardine solid waste by crude pepsin enzymatic hydrolysis in a bioreactor coupled to an ultrafiltration unit. Mater Sci Eng C. 2012; 32:922-928.
20. Song J, Su H, Wang B, Zhou Y, Guo L. Fish consumption and lung cancer risk: systematic review and meta-analysis. Nutr Cancer. 2014; 66:539-549.
21. Wu S, Feng B, Li K, Zhu X, Liang S, Liu X, Han S, Wang B, Wu K, Miao D, Liang, J, Fan D. Fish consumption and colorectal cancerrisk in humans: A systematic review and meta-analysis. Am J Med. 2012; 125:551-559.

22. Pan S, Tang J, Gu X. Isolation and characterization of a novel fucose-binding lectin from the gill of bighead carp (*Aristichthys nobilis*). Vet Immunol Immunopathol. 2010; 133:154-164.
23. Gao R, Xue C, Yuan L, Zhang J, Li Z, Xue Y, Feng H. Purification and characterization of pyrophosphatase from bighead carp (*Aristichthys nobilis*). LWT Food Sci Technol. 2008; 41:254-261.
24. Wang H, Li L, Liu Z, Wu Y, Chen J. Cloning, expression and purification of allergen parvalbumin from *Aristichthys nobilis* and its allergic activity. Wei Sheng Yan Jiu. 2011; 40: 555-558. (in Chinese)
25. Yao D, Pan S, Zhou M. Structural characterization and antitumor and mitogenic activity of a lectin from the gill of bighead carp (*Aristichthys nobilis*). Physiol Biochem. 2012; 38:1815-1824.
26. Murphy E, Edmondson R, Russel D, Colles S, Schroeder F. Isolation and characterization of two distinct forms of liver fatty acid binding protein from the rat. Biochim Biophys Acta. 1999; 1436:413-425.
27. Zhu J, Xu J, Wang Y, Li C, Chen Z, Song L, Gao J, Yu R. Purification and structural characterization of a novel anti-tumor protein from *Arca inflate*. Int J Biol Macromol. 2017; 105:103-110.
28. Laemml U. Cleavage of structural proteins during the assembly of the head of bacteriophage T4. Nature. 1970; 227:680-685.
29. Chen L, Song L, Li T, Zhu J, Xu J, Zheng Q, Yu R. A new antiproliferative and antioxidant peptide isolated from *Arca subcrenat*a. Mar Drugs. 2013; 11:1800-1814.
30. Stephano J, Gould M, Rojas-Galicia L. Advantages of picrate fixation for staining polypeptides in polyacrylamide gels. Anal Biochem. 1986; 152:308-313.
31. Bradford M. A rapid method for the quantitation of microgram quantities of protein utilizing the principle of protein-dye binding. Anal Biochem. 1976; 72:248-254.
32. Saha A, Brewer C. Determination of the concentrations of oligosaccharides, complex type carbohydrates, and glycoproteins using the phenol-sulfuric acid method. Carbohydr Res. 1994; 254:157-167.
33. Dong Q, Zheng L, Fang J. Modified phenol-sulfuric acid method for determination of the content of oligo- and polysaccharides. Zhongguo Yao Xue Za Zhi. 1996; 31:550-553. (in Chinese)
34. Bao X, Fang J. Studies on difference between sporoderm-broken and nonbroken spores of *Ganoderma lucidum* (Leyss. ex Fr.) Karst. by polysaccharide analysis. Zhongguo Zhong Yao Za Zhi. 2001; 26:326-328. (in Chinese)
35. Masuko T, Minami A, Iwasaki N, Majima T, Nishimura S, Lee Y. Carbohydrate analysis by a phenol-sulfuric acid method in microplate format. Anal Biochem. 2005; 339:69-72.
36. Zhu J, Xu J, Wang Y, Li C, Chen Z, Song L, Gao J, Yu R. Purification and structural characterization of a novel anti-tumor protein from *Arca inflate*. Int J Biol Macromol. 2017; 105:103-110.
37. Wang W, Guo Q, You Q, Zhang K, Yang Y, Yu J, Liu W, Zhao L, Gu H, Hu Y, Tan Z, Wang X. The anticancer activities of wogonin in murine sarcoma S180 both *in vitro* and *in vivo*. Biol Pharm Bull. 2006; 29:1132-1137.
38. Wang M, Nie Y, Peng Y, He F, Yang J, Wu C, Li X. Purification, characterization and antitumor activities of a new protein from *Syngnathus acus*, an official marine fish. Mar Drugs. 2012; 10:35-50.
39. Wang M, Qin S, He F, Li X. Bioassay-guided isolation of a novel protein with antitumor activity from *Trachyrhamphus serratus* (Syngnathidae). Arch Pharm Res. 2001; 34:893-899.
40. Song L, Ren S, Yu R, Yan C, Li T, Zhao Y. Purification, characterization and *in vitro* anti-tumor activity of proteins from *Arca subcrenata Lischke*. Mar Drugs. 2008; 6:418-430.
41. Xu J, Chen Z, Song L, Chen L, Zhu J, Lv S, Yu R. A new *in vitro* anti-tumor polypeptide isolated from *Arca inflate*. Mar Drugs. 2013; 11:4773-4787.
42. Zhu J, Xu J, Wang Y, Li C, Chen Z, Song L, Gao J, Yu R. Purification and structural characterization of a novel anti-tumor protein from *Arca inflate*. Int J Biol Macromol. 2017; 105:103-110.
43. Morrisett J, David J, Pownall H, Gotto A. Interaction of an apolipoprotein (apoLP-alanine) with phosphatidylcholine. Biochemistry. 1973; 12:1290-1299.
44. Pelton J, McLean L. Spectroscopic methods for analysis of protein secondary structure. Anal Biochem. 2000; 277:167-176.
45. Suetsuna K, Osajima K. The inhibitory activities against angiotensin I-converting enzyme of basic peptides originating from sardine and hair tail meat. Bull Jpn Soc Sci Fish. 1986; 52:1981-1984.
46. Qian Z, Je J, Kim S. Antihypertensive effect of angiotensin I converting enzyme-inhibitory peptide from hydrolysates of bigeye tuna dark muscle thunnus obesus. J Agric Food Chem. 2007; 55:8398-8403.
47. Pozo A, Gasset M, Oñaderra M, Gavilanes J. Conformational study of the antitumor protein α-sarcin. Biochim Biophys Acta. 1988; 953:280-288.
48. Adams J, Schechtman K, Landt Y, Ladenson J, Jaffe A. Comparable detection of acute myocardial infarction by creatine kinase MB isoenzyme and cardiac troponin I. Clin Chem. 1994; 40:1291-1295.
49. Yan Y. Creatine kinase in cell cycle regulation and cancer. Amino Acids. 2016; 48:1775-1784.
50. Wu J, Jan P, Yu H, Haung H, Fang H, Chang Y, Cheng J, Chen H. Structure and function of a custom anticancer peptide, CB1a. Peptides. 2009; 30:839-848.

Received January 9, 2025; Revised February 21, 2025; Accepted February 22, 2025.

[§]These authors contributed equally to this work.

*Address correspondence to:
Chunlei Li, Biotechnological Institute of Chinese Materia Medica, Jinan University, Guangzhou 510632, China. Department of Pharmacy, Qilu Hospital, Cheeloo School of Medicine, Shandong University, Jinan 250021, China.
E-mail: lcl992@126.com

Rongmin Yu, Biotechnological Institute of Chinese Materia Medica, Jinan University, Guangzhou 510632, China.
E-mail: tyrm@jnu.edu.cn

Liyan Song, Department of Pharmacology, College of Pharmacy, Jinan University, Guangzhou 510632, China.
E-mail: tsly@jnu.edu.cn

Released online in J-STAGE as advance publication February 26, 2025.

Original Article

DOI: 10.5582/ddt.2025.01006

Imaging and serum antigen levels that influence the treatment and prognosis of cryptococcosis in immunocompetent and immunocompromised patients: A 10-year retrospective study

Yi Su[1], Meixia Wang[2], Qingqing Wang[1], Bijie Hu[1], Jue Pan[1,*]

[1] Department of Infectious Diseases, Zhongshan Hospital, Fudan University, Shanghai, China;
[2] Department of Hospital Infection Management, Zhongshan Hospital (Xiamen), Fudan University, Xiamen, Fujian, China.

SUMMARY: This article was to summarize the treatment course and prognosis of immunocompetent and immunocompromised patients with pulmonary cryptococcal infections and to analyse the relevant factors. The chi-squared test was used to test for differences in categorical variables, and the independent samples t test was used to compare continuous variables. Multivariable analyses using the Cox proportional hazards model were used to estimate the effect of prognostic factors on treatment time and improvement time. A total of 243 patients were included in the analysis. Immunocompetent patients with diffuse imaging infiltrates had an extension of the treatment course within six months ($P = 0.048$) and an extension of the improvement days within four weeks ($P = 0.008$). In immunocompromised patients, an antigen assay ≥ 40 ($P = 0.013$) is an unfavourable factor leading to an extension of treatment by nine months. The serum antigen assay in 26/98 (26.53%) immunocompetent patients who did not turn negative when the treatment had finished was significantly lower than that in 14/29 (48.28%) immunocompromised patients ($P = 0.027$). All patients who underwent surgical resection had a good prognosis. Diffuse imaging infiltrates suggest longer treatment days and a longer improvement time in immunocompetent patients. Higher serum antigen levels in immunocompromised patients indicate longer treatment. Serum antigen assays in immunocompromised patients are difficult to negative.

Keywords: pulmonary cryptococcosis, immunocompetent, immunocompromised, treatment, prognosis, serum antigen assay

1. Introduction

Cryptococcosis is an invasive fungal infection caused by *Cryptococcus neoformans* or *Cryptococcus gattii* and has become increasingly common in both immunocompetent and immunocompromised patients. In addition to causing localized respiratory disease, combined lung and central nervous system (CNS) infection is common (*1*). Other sites of infection include the musculoskeletal system, skin and soft tissues, prostate, abdominal organs and the eye, either in combination with lung and/or CNS infection or in isolation (*2,3*).

During prolonged treatment adhering to clinical guidelines (*4*), physicians may encounter several inquiries, such as whether to continue treatment when the capsule antigen assay is still positive, risk of disease recurrence, and should it be replaced immediately or continued if inefficacy of fluconazole occurs in a short period. While some literature has reported on the clinical manifestations of cryptococcosis in both immunocompetent and immunocompromised patients (*5,6*), there are scarce articles available on the treatment course and prognosis due to the extended treatment time and follow-up period needed. This article presents a summary of the treatment course and prognosis of patients who had pulmonary cryptococcal infections in our hospital over the previous decade. It also investigates the factors that influence their treatment course and prognosis, with the aim of lending insights for the management of cryptococcal infections among both immunocompetent and immunocompromised patients.

2. Methods

2.1. Case series

Patients were eligible if the patients were admitted to the Infectious Diseases Department at Zhongshan Hospital, Fudan University, between January 1, 2012, and December 31, 2021. Data regarding patient demographics,

clinical features, laboratory results, pathogenic findings, treatments, and outcomes were obtained from the Zhongshan Hospital Information System. This project received approval from the Ethics Committee of Zhongshan Hospital and informed consent was obtained from all subjects or their legal guardians. All research was performed in accordance with relevant guidelines and the Declaration of Helsinki. All data were reviewed by two physicians (QQW and YS), while any discrepancies in interpretation between the primary reviewers were resolved by a third researcher (JP). The data that support the findings of this study are available from the corresponding author.

2.2. Case definition

Cryptococcosis patients are comprised of confirmed and clinical patients. Confirmed cryptococcosis was identified as a positive result of *Cryptococcus* culture from any site. Clinical cryptococcosis was identified by positive histopathology or cryptococcal antigen results, together with clinical or radiographic evidence of disease (*7*). Immunocompromised individuals were identified as having at least one underlying condition, which included AIDS, liver cirrhosis, haematologic malignancy, malignant solid tumour, chronic steroid use, and rheumatologic diseases such as rheumatoid arthritis, lupus, psoriatic arthritis, ankylosing spondylitis and inflammatory myopathy (*8*). The treatment duration refers to the period between starting the medication and discontinuing it. Improvement days denote the period between the initiation of medication and the improvements seen on chest imaging. The CT scan's morphological features have been categorized as either solitary nodule/mass, multiple nodules/masses, consolidation, or diffuse infiltrates (nodules/mass with consolidation) (*9*).

2.3. Statistical analysis of the data

Depending on the data distribution, sex, clinical symptoms at onset, and treatment prescription, categorical variables were presented as percentages, while continuous variables comprising age, leukocyte count, neutrophil count, lymphocyte count, CD4 count, erythrocyte sedimentation rate, high-sensitivity C-reactive protein, interleukin-2, interleukin-6 and interferon-gamma were presented in terms of the mean and standard deviation. Median and quartile values were used to present the serum antigen assay and treatment duration. Categorical variables were screened for differences using the chi-square test, while the independent samples *t* test was employed to compare continuous variables between immunocompetent and immunocompromised patients. Prognostic factors' effects on treatment time and improvement time were estimated using multivariable analyses with the Cox proportional hazards model. Statistical analyses were executed using IBM's SPSS 23.0 software (Armonk, NY, USA), and the graphs were produced utilizing GraphPad Prism 8.0.

3. Result

3.1. Case selection and classification

A total of 243 patients were analysed. Among them, 238 patients with pulmonary *Cryptococcus* infection or other site infection in combination with pulmonary infection were further analysed (Figure 1).

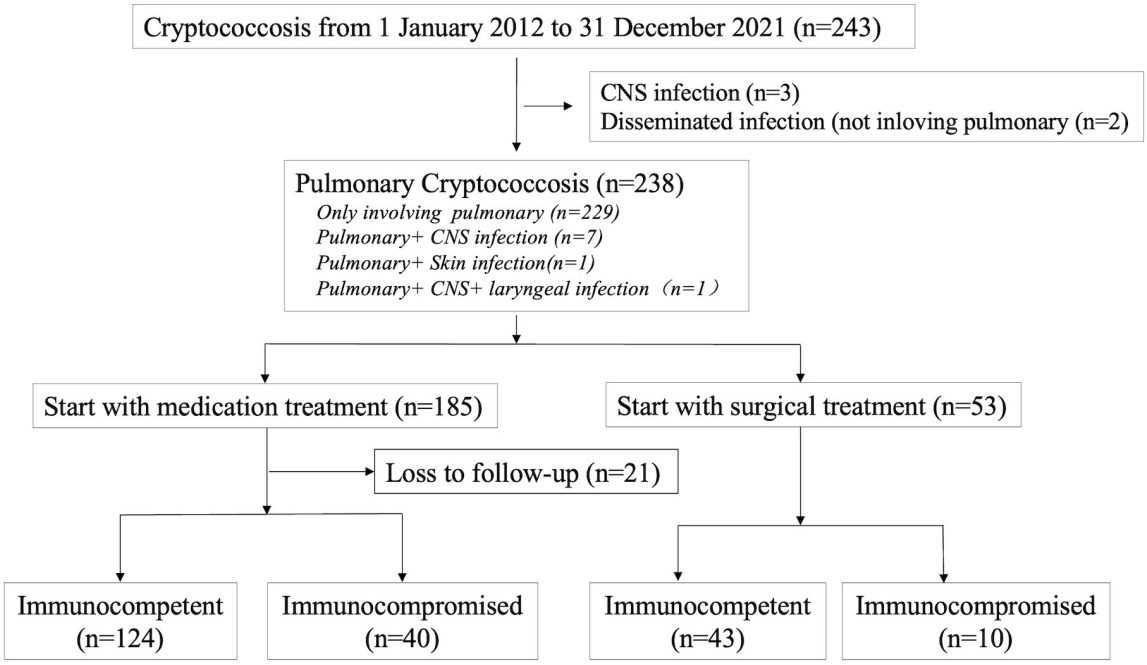

Figure 1. Flow chart of cases selection and classification. CNS: central nervous system.

Table 1. Clinical manifestations and laboratory results

Items	Immunocompetent (n = 163)	Immunocompromised (n = 46)	P
Medical treatment	n = 124 (%)	n = 40 (%)	
Male/Female	74/50	21/19	0.424
Age, years	47.69 ± 13.06	59.00 ± 13.66	< 0.001*
Involving other parts	4 (3.23)	4 (10.00)	0.191
Clinical symptoms at onset	56 (45.16)	21 (52.50)	0.419
Fever	21(16.94)	7 (17.50)	0.934
Cough	48 (38.71)	10 (25.00)	0.115
Expectoration	38 (30.65)	8 (20.00)	0.193
Chest pain	10 (8.06)	2 (5.00)	0.766
Shortness of breath	1 (0.81)	4 (10.00)	0.016*
Serum antigen assay	20 (10,160)	80 (25,640)	0.028*
Leukocyte × 10^9/L	6.77 ± 2.55	7.52 ± 3.22	0.209
Neutrocyte × 10^9/L	4.38 ± 2.27	5.79 ± 3.18	0.018*
Lymphocytes × 10^9/L	1.71 ± 0.56	1.06 ± 0.65	< 0.001*
CD4 (cells/μL)	535.98 ± 348.67	412.49 ± 338.47	0.158
ESR (mm/H)	17.78 ± 19.85	30.50 ± 23.17	0.004*
CRP (mg/L)	6.54 ± 17.51	23.27 ± 39.02	0.022*
IL-2 (U/mL)	388.75 ± 220.20	739.05 ± 725.38	0.052
IL-6 (pg/mL)	2.77 ± 2.20	7.32 ± 6.48	0.009*
INF-γ (pg/mL)	8.57 ± 8.16	28.58 ± 79.28	0.287
Surgical treatment	n = 43	n = 10	
Male/Female	31/12	3/7	0.033*
Age, years	53.60 ± 9.26	53.00 ± 17.89	0.919
Leukocyte *10^9/L	6.71 ± 2.39	6.19 ± 1.92	0.523
Neutrocyte *10^9/L	4.44 ± 2.45	4.27 ± 1.77	0.840
Lymphocytes *10^9/L	1.27 ± 0.47	0.87 ± 0.38	0.193
CRP (mg/L)	6.26 ± 9.86	4.38 ± 6.67	0.664

The values in brackets are the percentage except for the values in brackets of the serum antigen assay, which are the quartiles. Bold and * indicate significant differences. ESR: erythrocyte sedimentation rate, CRP: high-sensitivity C-reactive protein, IL-2: interleukin-2, IL-6: interleukin-6, INF-γ: interferon-gamma. Involving other parts: Four patients of pulmonary and CNS infections were included in immunocompetent patients, while immunocompromised patients had two cases of pulmonary and CNS infections, one case of pulmonary and skin infections, and one case of pulmonary, CNS, and laryngeal infections. One immunocompromised patient was lost to follow-up and therefore was not included in the study.

3.2. Clinical manifestations and laboratory results

Table 1 shows clinical manifestations and laboratory results of immunocompetent and immunocompromised patients. This study comprised 53 patients who had undergone surgical resection. Before surgery, 19 patients underwent serum antigen assay testing, of which only 2 had positive results. Following surgery, 21 patients were treated with antifungal therapy for a median duration of 81 days. The remaining patients were not administered any medication.

3.3. Antifungal treatment and treatment course

Anticryptococcal treatment and treatment course in patients with different immune states were shown in Table 2. The median duration of treatment for immunocompetent patients was 207 (137.5, 319) days, whereas for immunocompromised patients, it was 253.5 (156.25, 344.25) days. After ineffective treatment with fluconazole at 400 mg qd initially, five immunocompetent patients were prescribed fluconazole and flucytosine. Four out of seven immunocompromised patients received both fluconazole and flucytosine as initial treatment, while the remaining three received fluconazole alone, which proved ineffective and was subsequently switched to the combination therapy. Three immunocompromised patients were administered amphotericin B/amphotericin B liposomes after one month of ineffective fluconazole treatment. The duration of their treatment course was significantly shorter than others.

3.4. Related factors of treatment course and prognosis

The study analysed the relevant factors affecting the treatment duration of immunocompetent patients within 180 days and immunocompromised patients within 270 days based on the data provided in Table 2. The results showed that immunocompetent patients with diffuse imaging infiltrates had a significantly longer treatment course (P = 0.048) (Figure 2). Meanwhile, in immunocompromised patients, an antigen assay level of ≥ 40 (P = 0.013) was associated with an unfavourable outcome leading to prolonged treatment (Figure 2).

Among 124 immunocompetent patients, 2 out of 120 (1.67%) with pulmonary infection only and 1 out of 4 (25.00%) with pulmonary and CNS infection progressed. Among 40 immunocompromised patients, 1 out of 36 patients (2.78%) with only pulmonary infection progressed because of the underlying disease, and 1 out of 4 patients (25.00%) with pulmonary and skin infection progressed.

Table 2. Anticryptococcal treatment and treatment course in patients with different immune states

Medicine	Treatment			Treatment days		
	Immunocompetent (n = 124)	Immunocompromised (n = 40)	P	Immunocompetent	Immunocompromised	P
Triazoles ± Fluorocytosine						
Fluconazole	87 (70.16)	24 (60.00)	0.232	200 (137.5,300)	274 (183.25,356.25)	0.128
Voriconazole	7 (5.65)	5 (12.50)	0.272	173 (154.75,347.25)	179 (158,222)	0.373
Itraconazole	1 (0.81)	/	/	264	/	/
Fluconazole + Fluorocytosine	5 (4.03)	7 (17.50)	0.013*	335 (315,596)	311 (253.5,374.5)	0.512
Voriconazole after Fluconazole	1 (0.81)	/	/	573	/	/
Amphotericin B/Amphotericin B Liposome ± Fluorocytosine						
Amphotericin B/Amphotericin B Liposome after Fluconazole	17 (13.71)	3 (7.50)	0.444	170 (131,285)	111 (105,132.5)	0.022*
Amphotericin B/Amphotericin B Liposome	5 (4.03)	/	/	199 (91,366)	/	/
Amphotericin B/Amphotericin B Liposome + Fluorocytosine	1 (0.81)	1 (2.50)	0.429	654	1642	/

The values in brackets of treatment are thepercentages. The values in brackets of treatment days are the quartiles. Bold and * indicate significant differences. Voriconazole after fluconazole: Fluconazole was ineffective in treating the condition, and thus, the treatment was switched to voriconazole. Amphotericin B/Amphotericin B Liposome after fluconazole: Fluconazole was ineffective in treating the condition, and thus, the treatment was switched to Amphotericin B/Amphotericin B Liposome.

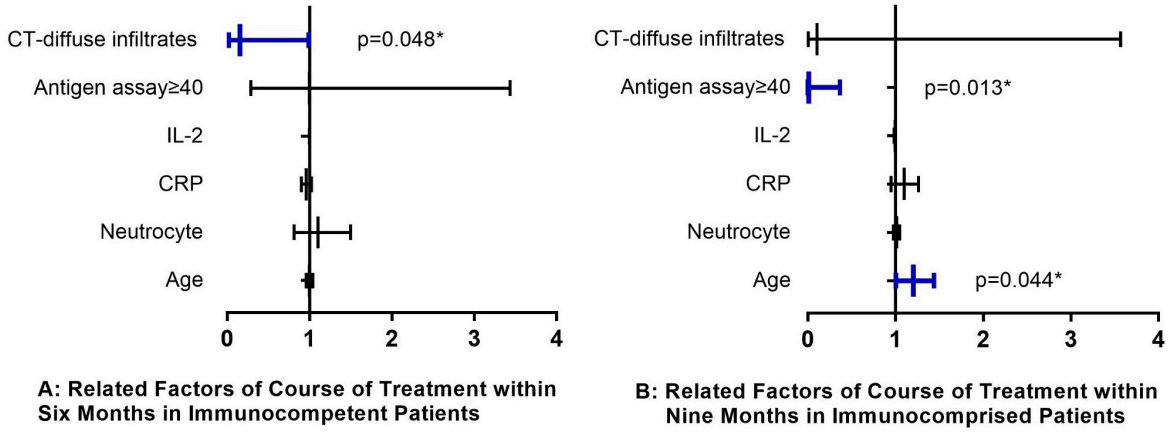

Figure 2. Related factors of treatment course.

Of the eight patients with *Cryptococcus* infection affecting both the lungs and other sites, the disease of one patient advanced due to aplastic anaemia, and the others were treated for more than one year. Due to the limited sample size, the results cannot be subjected to statistical analysis.

Ninety-eight immunocompetent patients were monitored by serum antigen assay, and 26 (26.53%) of them remained positive. Twenty-nine immunocompromised patients were monitored by serum antigen assay, and 14 (48.28%) remained positive (P = 0.027).

3.5. Related factors of improvement days

The median time for pulmonary infection improvement was 32.5 days in immunocompetent patients and 34.5 days in immunocompromised patients. Diffuse pulmonary infiltrates (P = 0.008) and CRP (P = 0.024) were significant factors for improvement days exceeding 4 weeks in immunocompetent patients, whereas age (P = 0.033) and neutrocyte count (P = 0.038) were significant factors for improvement days exceeding 4 weeks in immunocompromised patients (Figure 3).

Five immunocompetent patients (5/124) demonstrated spontaneous improvement in their pulmonary imaging prior to receiving medication. Chest imaging of these patients showed infections affecting one or two lobes. In the immunocompromised patients, no spontaneous improvement was observed.

4. Discussion

In the past, many patients with pulmonary cryptococcosis presented as a solitary nodule, leading to misdiagnosis as a tumour and subsequent surgical resection. In recent years, the use of serum antigen assays and percutaneous lung puncture technology (*10,11*) has become widespread,

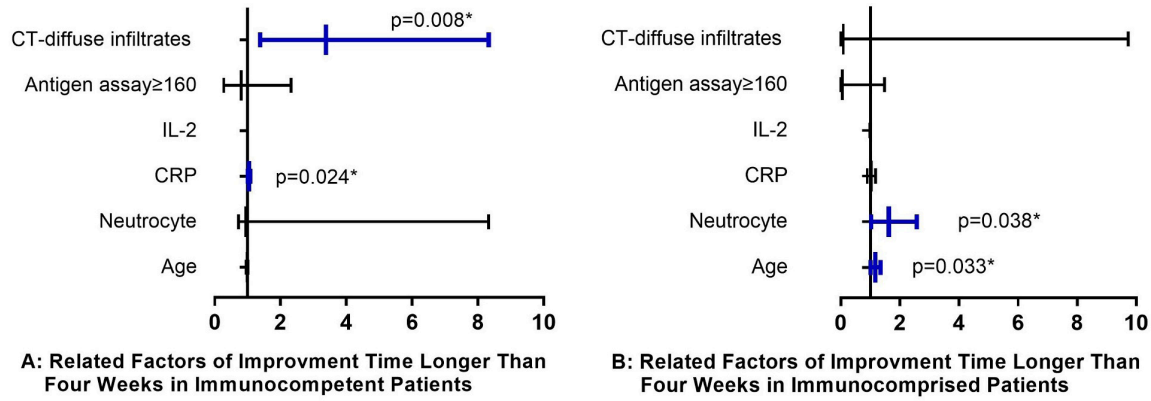

Figure 3. Related factors of improvement days.

resulting in increased presurgical diagnoses of cryptococcosis presenting as solitary nodules. However, our study demonstrated that 89.5% of patients who underwent thoracic surgery presented negative serum antigen assays. This is because serum antigen assays from patients with pulmonary cryptococcosis are seldom positive when disseminated disease is absent (*12*). As such, a diagnosis of cryptococcosis cannot be excluded with a negative serum antigen assay if a patient visits the thoracic surgery department with a single nodule. Therefore, a lung biopsy is needed for a clear diagnosis.

There is insufficient evidence in evidence-based medicine to support the use of fluconazole and flucytosine for cryptococcal infections affecting multiple sites. The World Health Organization now recommends a high dose of fluconazole (1,200 mg) and flucytosine as induction therapy for cryptococcal meningitis in HIV-infected patients to be administered over 14 days (*13*). Fluconazole and flucytosine were investigated as viable therapies for cryptococcal meningitis for non-HIV and non-transplant-associated cryptococcal meningitis (*14*). According to those studies, the combination of fluconazole and flucytosine can be used for multiple sites of cryptococcal infection. In our case study, a kidney transplant recipient with infections in the lungs, central nervous system, and larynx was treated with fluconazole and flucytosine, exhibiting a positive outcome. However, two out of three patients who had cryptococcal infections in more than one site used fluconazole only as initial treatment and had a poor prognosis in our study, and the conclusions drawn from the literature were consistent with ours (*15*).

Nodular lesions were the predominant CT (computed tomography) type in immunocompetent patients. Consolidation and multiple lesions indicated infection spread, reflecting the challenge in managing fungal infections, which were more prevalent in immunocompromised patients (*16*). Immunocompromised patients exhibited a higher prevalence of multiple lesions, air bronchial signs, and cavitation (*17*). In our study of immunocompetent patients, those with diffuse imaging infiltrates who had an increased burden of fungal infection needed a treatment course sixty to ninety days longer than patients with solitary or multiple nodules. The imaging features of patients with varying immune statuses have been examined (*18,19*), and the possibility of forecasting prognosis through different imaging presentations merits additional investigation.

The serum and CSF lateral flow cryptococcal antigen assay is now the preferred test because of its speed, accuracy and cost (*20,21*). The antigen assay has been reported to predict meningitis and death in cryptococcal meningitis, and based on our research, an increased antigen assay in immunocompromised patients with pulmonary cryptococcal infection signifies a prolonged treatment time. Therefore, it is important to use the antigen assay in the future to personalize therapy for prevention, treatment and prognosis (*22*). Additionally, our research has revealed that almost 50% of immunocompromised patients do not achieve negative results in serum antigen assays at the end of treatment. Therefore, negative conversion of serum antigen assays should not be relied upon as the sole basis for discontinuing medication. Instead, a comprehensive evaluation of clinical symptoms, improvements in imaging, and inflammatory indicators should be conducted.

In conclusion, diffuse infiltrates in imaging in immunocompetent patients indicated longer treatment days and longer improvement time. A higher serum antigen assay of immunocompromised patients indicates a longer treatment time. Solitary nodules from surgical resection have a good prognosis.

Acknowledgements

We would like to thank all the study participants whose data were used in this study. We are most grateful for the assistance and support of clinicians, laboratory technicians and radiologists at Zhongshan Hospital Fudan University.

Funding: This work was supported by grants from the National Key Research and Development Program of

China (2021YFC 2300400) and the Fund of Zhongshan Hospital Fudan University (2021ZSFZ15).

Conflict of Interest: The authors have no conflicts of interest to disclose.

References

1. Beardsley J, Sorrell TC, Chen SC. Central Nervous System Cryptococcal Infections in Non-HIV Infected Patients. J Fungi (Basel). 2019; 5:71.
2. Papadakis SA, Gourtzelidis G, Pallis D, Ampadiotaki M, Tatakis F, Tsivelekas K, Georgousi K, Kokkinis C, Diamantopoulou K, Lelekis M. *Cryptococcus neoformans* osteomyelitis of the tibia: a case report and review of the literature. J Med Case Rep. 2023; 17:188.
3. Huang H, Pan J, Yang W, Lin J, Han Y, Lan K, Zeng L, Liang G. First case report of Cryptococcus laurentii knee infection in a previously healthy patient. BMC Infect Dis. 2020; 20:681.
4. Perfect JR, Dismukes WE, Dromer F, Goldman DL, Graybill JR, Hamill RJ, Harrison TS, Larsen RA, Lortholary O, Nguyen MH, Pappas PG, Powderly WG, Singh N, Sobel JD, Sorrell TC. Clinical practice guidelines for the management of cryptococcal disease: 2010 update by the infectious diseases society of America. Clin Infect Dis. 2010; 50:291-322.
5. Kohno S, Kakeya H, Izumikawa K, Miyazaki T, Yamamoto Y, Yanagihara K, Mitsutake K, Miyazaki Y, Maesaki S, Yasuoka A, Tashiro T, Mine M, Uetani M, Ashizawa K. Clinical features of pulmonary cryptococcosis in non-HIV patients in Japan. J Infect Chemother. 2015; 21:23-30.
6. Xiong CL, Lu JG, Chen T, Xu R. Comparison of the clinical manifestations and chest CT findings of pulmonary cryptococcosis in immunocompetent and immunocompromised patients: a systematic review and meta-analysis. BMC Pulm Med. 2022; 22:415.
7. Baddley JW, Perfect JR, Oster RA, Larsen RA, Pankey GA, Henderson H, Haas DW, Kauffman CA, Patel R, Zaas AK, Pappas PG. Pulmonary cryptococcosis in patients without HIV infection: factors associated with disseminated disease. Eur J Clin Microbiol Infect Dis. 2008; 27:937-943.
8. Brizendine KD, Baddley JW, Pappas PG. Predictors of mortality and differences in clinical features among patients with cryptococcosis according to immune status. PloS One. 2013; 8:e60413.
9. Kohno S, Kakeya H, Izumikawa K, Miyazaki T, Yamamoto Y, Yanagihara K. Clinical features of pulmonary cryptococcosis in non-HIV patients in Japan. Infect Chemother. 2015; 21:23-30.
10. Brioulet J, David A, Sagan C, Cellerin L, Frampas E, Morla O. Percutaneous CT-guided lung biopsy for the diagnosis of persistent pulmonary consolidation. Diagn Interv Imaging. 2020; 101:727-732.
11. Hu Q, Li X, Zhou X, Zhao C, Zheng C, Xu L. Clinical utility of cryptococcal antigen detection in transthoracic needle aspirate by lateral flow assay for diagnosing non-HIV pulmonary cryptococcosis: A multicenter retrospective study. Medicine (Baltimore). 2022; 101:e30572.
12. Setianingrum F, Rautemaa-Richardson R, Denning DW. Pulmonary cryptococcosis: A review of pathobiology and clinical aspects. Med Mycol. 2019; 57:133-150.
13. Guidelines for The Diagnosis, Prevention and Management of Cryptococcal Disease in HIV-Infected Adults, Adolescents and Children: Supplement to the 2016 Consolidated Guidelines on the Use of Antiretroviral Drugs for Treating and Preventing HIV Infection. Geneva: World Health Organization; 2018 Mar.
14. Li Z, Liu Y, Chong Y, Li X, Jie Y, Zheng X, Yan Y. Fluconazole plus flucytosine is a good alternative therapy for non-HIV and non-transplant-associated cryptococcal meningitis: A retrospective cohort study. Mycoses. 2019; 62:686-691.
15. Nussbaum JC, Jackson A, Namarika D, Phulusa J, Kenala J, Kanyemba C, Jarvis JN, Jaffar S, Hosseinipour MC, Kamwendo D, van der Horst CM, Harrison TS. Combination flucytosine and high-dose fluconazole compared with fluconazole monotherapy for the treatment of cryptococcal meningitis: a randomized trial in Malawi. Clin Infect Dis. 2010; 50:338-344.
16. Wang DX, Zhang Q, Wen QT, Ding GX, Wang YG, Du FX, Zhang TY, Zheng XY, Cong HY, Du YL, Sang JZ, Wang MD, Zhang SX. Comparison of CT findings and histopathological characteristics of pulmonary cryptococcosis in immunocompetent and immunocompromised patients. Sci Rep. 2022; 12:5712.
17. Hu Y, Ren SY, Xiao P, Yu FL, Liu WL. The clinical and radiological characteristics of pulmonary cryptococcosis in immunocompetent and immunocompromised patients. BMC Pulm Med. 2021; 21:262.
18. Xiong C, Lu J, Chen T, Xu R. Comparison of the clinical manifestations and chest CT findings of pulmonary cryptococcosis in immunocompetent and immunocompromised patients: a systematic review and meta-analysis. BMC Pulm Med. 2022; 22:415.
19. Yao KL, Qiu XF, Hu HJ, Han YX, Zhang WM, Xia RM, Wang L, Fang JM. Pulmonary cryptococcosis coexisting with central type lung cancer in an immuocompetent patient: a case report and literature review. BMC Pulm Med. 2020; 20:161.
20. Schub T, Forster J, Suerbaum S, Wagener J, Dichtl K. Comparison of a Lateral Flow Assay and a Latex Agglutination Test for the Diagnosis of *Cryptococcus Neoformans* Infection. Curr Microbiol. 2021; 78:3989-3995.
21. Temfack E, Rim JJB, Spijker R, Loyse A, Chiller T, Pappas PG, Perfect J, Sorell TC, Harrison TS, Cohen JF, Lortholary O. Cryptococcal Antigen in Serum and Cerebrospinal Fluid for Detecting Cryptococcal Meningitis in Adults Living With Human Immunodeficiency Virus: Systematic Review and Meta-Analysis of Diagnostic Test Accuracy Studies. Clin Infect Dis. 2021; 72:1268-1278.
22. Rajasingham R, Wake RM, Beyene T, Katende A, Letang E, Boulware DR. Cryptococcal Meningitis Diagnostics and Screening in the Era of Point-of-Care Laboratory Testing. J Clin Microbiol. 2019; 57:e01238-18.

Received September 9, 2024; Revised February 6, 2025; Accepted February 23, 2025.

**Address correspondence to:*
Jue Pan, Department of Infectious Diseases, Zhongshan Hospital of Fudan University, 180 Fenglin Road, Shanghai 200032, China.
E-mail: pjzjzy@163.com

Released online in J-STAGE as advance publication February 26, 2025.

Brief Report

DOI: 10.5582/ddt.2025.01001

Human gut associated *Bacteroides* and *Akkermansia* bacteria exhibit immunostimulatory activity in the silkworm muscle contraction assay

Fumiaki Tabuchi[1], Chie Kano[2], Tatsuhiko Hirota[2], Tomomasa Kanda[2], Kazuhisa Sekimizu[3], Atsushi Miyashita[1]

[1] Institute of Medical Mycology, Teikyo University, Tokyo, Japan;
[2] Asahi Quality and Innovations, Ltd., Tokyo, Japan;
[3] School of Pharma-Science, Teikyo University, Tokyo, Japan.

SUMMARY: The immunoregulatory activity of human gut bacteria has attracted attention in recent years. To assess the innate immune-stimulatory activity of various samples *in vivo* efficiently, we previously introduced a silkworm-based assay as a novel alternative method. The method has been used for over a decade to screen for substances with potential physiological activity. In this study, we prepared heat-killed cells of four strains of human gut bacteria (*Bacteroides ovatus*, *B. thetaiotaomicron*, *B. uniformis*, and *Akkermansia muciniphila*) and assessed their innate immune-stimulatory activity within the silkworm model. Our findings indicate that the sample from either *B. ovatus* or *B. thetaiotaomicron* has immunostimulatory activity in the silkworm, in contrast to *B. uniformis* and *A. muciniphila*. Moreover, a pathogenicity assessment using the silkworm infection model was conducted to determine the safety of these bacterial strains for human consumption when considered as food ingredients. None of the four gut bacterial strains exhibited pathogenic effects in silkworms, with *Pseudomonas aeruginosa* serving as a positive control of the pathogenicity test. These results suggest that the silkworm-based assay can distinguish between the immunostimulatory effects of different human gut microbes and may enhance the safety evaluation of microbial ingredients.

Keywords: gut bacteria, silkworm model, muscle contraction assay, innate immune system

1. Introduction

Throughout history, humanity has achieved significant advancements in medicine and health sciences by discovering and developing numerous beneficial foods and pharmaceuticals. Such progress has been made under the rigorous evaluation of physiological functionality and safety at the developmental phases of foods and pharmaceuticals. It is believed that the enhancement of evaluation systems at various stages, from basic research to applied research, will lead to the accumulation of further knowledge and the efficient derivation of products contributing to health promotion. In this study, we primarily focus on the immune system and explore the potential of using silkworms as a model organism for physiological function assessment.

The challenge of applying silkworms to health science is one that we have been proposing for approximately 20 years (*1-12*). Our research group has demonstrated that human pathogenic bacteria such as *Staphylococcus aureus* and *Pseudomonas aeruginosa* can cause fatal infections in silkworms, and we have also shown that the therapeutic effects of antibiotics against bacterial infections can be evaluated using this model. Furthermore, we have been exploring compounds with therapeutic effects against *S. aureus* infections from a soil bacterial library. As a result, we have developed a novel antibiotic lysocin E, which has shown excellent therapeutic efficacy in mammals and is currently put in clinical development pipeline (*9,13*). Conventionally, mammalian animals such as mice have been commonly used for *in vivo* assays. However, such evaluations incur significantly higher costs compared to *in vitro* assays and alternative methods using invertebrate species.

We propose that this issue can be overcome by using silkworms, which offers the advantage of easy administration of quantitative samples and allow for the evaluation of pharmacological effects of compounds at the organismal level (*11-13*). Furthermore, silkworms have the advantage of requiring less housing space compared to mice and other mammals. Moreover, in the average-sized research laboratory at universities and

national research institutions, compound screening using silkworms allows for the evaluation of approximately 100 compounds per day (with one dose, using 300 silkworms with n = 3/compound) (*14*). Hence, assessments using silkworms offer significant economic advantages. To elucidate the effects of various compounds and food materials on the immune system, we have also been working on understanding the innate immune system using silkworms. Our studies have indicated that the contraction of silkworm muscles is synchronized with the triggering of their innate immunity (*15-17*). A peptide known as the paralytic peptide (PP) found in silkworms causes paralysis and prompts muscle contraction, while stimulating the silkworm's hemocytes (*18,19*). The activation of this peptide can be gauged by observing the resultant muscle contractions in the silkworms, using these as a physiological marker of the peptide's activity. Utilizing this information, we have developed a method using silkworms to identify substances in food that activate the innate immune response. Our findings include the identification of certain polysaccharides, like β-glucans, which exhibit a high activity (*17,20*). These polysaccharides are believed to not only improve the health of silkworms but also hold potential as indicators for evaluating similar health benefits in humans.

Bacteroides ovatus and *Bacteroides thetaiotaomicron*, gut bacteria in humans, have been reported to maintain skin condition (*21*) and improve sleep quality (*22*) by ingesting prebiotics that increase the abundance of these bacteria (*23*) . Additionally, other effects on human health, such as immune system, have also been anticipated, although details have remained unclear. In this study, we used four bacterial species of the genera *Bacteroides* and *Akkermansia* present in the human gut and evaluated their immunostimulatory capacity. Furthermore, in order to assess the potential safety risk of these gut bacteria for humans, we conducted pathogenicity tests for these bacteria using silkworms.

2. Materials and Methods

2.1. The bacterial strains used in the experiment and their cultivation conditions

In this study, we obtained *Bacteroides ovatus* JCM5824, *B. thetaiotaomicron* JCM5827, *B. uniformis* JCM5828, and *Akkermansia muciniphila* JCM33894 from the Japan Collection of Microorganisms (JCM; Ibaraki, Japan) and used them in the experiments. The above-mentioned three strains of *Bacteroides* were inoculated into Gifu anaerobic medium (GAM) (Nissui Pharmaceutical Co., Ltd.; Tokyo, Japan) and cultured anaerobically at 37°C for 48 hours. Additionally, *A. muciniphila* was inoculated into GAM medium supplemented with 0.4% mucin (Fujifilm; Osaka, Japan) and cultured anaerobically at 37°C for 48 hours. *Pseudomonas aeruginosa* strain PAO1 was inoculated into Luria-Bertani (LB) 10 medium and cultured aerobically at 37°C overnight.

2.2. The rearing of silkworms

The silkworm eggs used in the experiment were obtained from the Ehime Sanshu (Ehime, Japan). Silkworm rearing followed the previously reported method (*6*). The hatched silkworms were reared at 27°C. Silkworms were fed Silkmate 2S (Nihon Nosan Kogyo; Kanagawa, Japan). Approximately 1 gram of feed per individual was provided to the silkworms on the first day of the fifth instar, and the silkworms on the second day of fifth instar were used in the experiment.

2.3. The muscle contraction assay using silkworms

The silkworm muscle contraction assay followed the experimental method reported previously (*17,24*). In brief, decapitated individual silkworm specimens were suspended with thread, and the contraction of silkworm muscles was measured when 50 μL of the sample was injected into the haemocoel using a 1 mL syringe with a 27-gauge needle (Terumo; Tokyo, Japan). The muscle contraction was calculated as the C-value, which is the percentage decrease in muscle length from its maximum length after injection of the sample. Additionally, following the report by Fujiyuki *et al*., the activity of inducing 15% contraction in silkworm muscles was defined as 1 Unit (*17*).

2.4. The pathogenicity tests of each bacterial strain on silkworms

Fifty μL of ten-fold concentrated anaerobic culture of the four gut bacterial strains and a serial-diluted solution of the *P. aeruginosa* culture were injected into the body fluids of silkworms on the second day of fifth instar using a 1 mL syringe with a 27-gauge needle and the survival of silkworms was observed. Each group of silkworms used in this experiment consisted of 5 individuals per dose. The 50% lethal dose (LD_{50}) of each bacterial strain on silkworms was estimated from the survival rate of silkworms in each group 24 hours after injection and the number of viable bacteria for each strain.

3. Results and Discussion

3.1. Quantification of the innate immunostimulatory capacity of human gut bacteria

The insect cytokine PP (paralytic peptide) is known to induce the muscle contraction and activation of the innate immune system in silkworms. Therefore, measuring muscle contractions in silkworms injected with the test substance can provide insight into the response of the innate immune system. Utilizing this assay system, the ability of microorganisms from the

human gut to induce the silkworm paralytic peptides (insect cytokines) was measured in this study (Figure 1). As a result, among *B. ovatus*, *B. thetaiotaomicron*, *B. uniformis,* and *A. muciniphila*, two bacteria, *B. ovatus* and *B. thetaiotaomicron*, exhibited muscle contraction-inducing activity in silkworms (Table 1). On the other hand, *B. uniformis* and *A. muciniphila* did not show the activity (Table 1). These results suggest that substances present in *B. ovatus* and *B. thetaiotaomicron,* among the genus *Bacteroides*, may have innate immune-stimulatory effect with potential to human application.

3.2. Pathogenicity test

Either of the four human gut bacteria was injected into the hemolymph of silkworms, which were subsequently raised at 37°C. As a result, all silkworms survived after 24 hours, and the LD_{50} values were: > 1.3×10^9 (*B. ovatus*), > 2.5×10^8 (*B. thetaiotaomicron*), > 4.6×10^8 (*B. uniformis*), and > 1.7×10^8 (*A. muciniphila*) colony forming units (CFU) /larva. In contrast, silkworms injected with the *P. aeruginosa* died within 24 hours, with an LD_{50} value of 1.1 CFU/larva (Table 2). These results suggest that the aforementioned gut bacteria do not possess pathogenicity against silkworms and are of minimal risk for human consumption.

In this study, we found that among the four strains of human gut-derived bacteria (*B. ovatus*, *B. thetaiotaomicron*, *B. uniformis*, and *A. muciniphila*), *B. ovatus* and *B. thetaiotaomicron* induced muscle contractions in silkworms. Previous research has shown that silkworm muscle contractions are induced by the activation of paralytic peptide (PP) in the hemolymph (*18,19*). Furthermore, since the activation of PP has been shown to contribute to host resistance against pathogenic microorganisms (*15,19*), *B. ovatus* and *B. thetaiotaomicron* were suggested to activate the innate immune system of silkworms. Additionally, none of the four strains of gut-derived bacteria used in this study were lethal to silkworms even when administered, suggesting that these strains do not possess pathogenicity against silkworms.

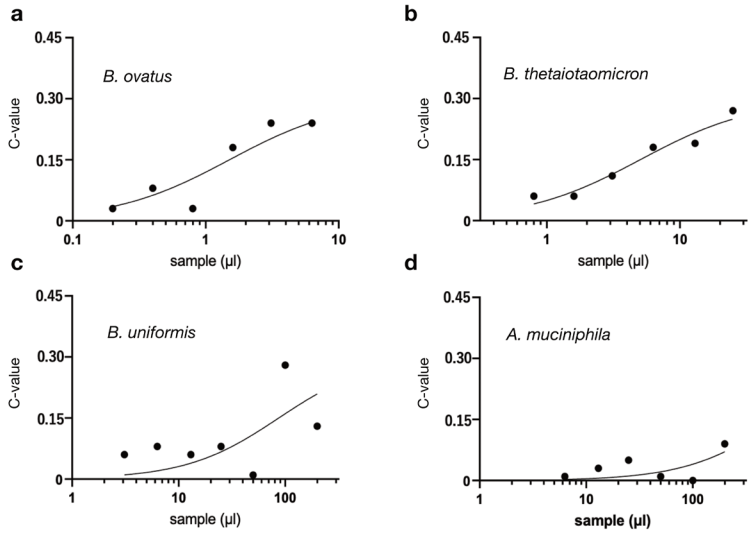

Figure 1. Activation of insect cytokines (paralytic peptides) by human gut-derived bacteria. A dilution series of heat-killed cells of each strain was prepared, and muscle contraction was measured when injected into silkworm muscle specimens. Samples injected into silkworms were (**a**) *B. ovatus*, (**b**) *B. thetaiotaomicron*, (**c**) *B. uniformis*, and (**d**) A. *muciniphila*. The C-value indicates the percentage of the muscle specimen that contracted and shortened from its original state after the sample was injected.

Table 1. Muscle contraction activity of the *Bacteroides* and *Akkermansia* strains

	Sample Conc. [mg/mL]	Activity per volume [U/mL]	Specific Activity [U/mg]	Reference
B. ovatus JCM5824	8.9	660	74	This study
B. thetaiotaomicron JCM5827	11	200	17	
B. uniformis JCM5828	0.88	< 5.0	< 5.7	
A. muciniphila JCM33894	3.5	< 5.0	< 1.4	
Curdlan	-	-	100	Fujiyuki *et al*. (2012)
Yeast β-glucan (Sigma)	-	-	33	
Lichenan	-	-	6	
Laminaran	-	-	< 1	

The muscle contraction activity of each gut-bacterial sample was measured when injected into silkworm muscle. One unit (U) is defined as the activity of a sample that causes a silkworm muscle specimen to contract by 15%. The specific activity was determined from the concentration of each sample and the muscle contraction activity per volume.

Table 2. Lack of virulence in the *Bacteroides* and *Akkermansia* strains (intra-hemocoel infection)

	LD_{50} [CFU/larva]	Fold
B. ovatus JCM5824	$> 1.3 \times 10^9$	$> 1.2 \times 10^9$
B. thetaiotaomicron JCM5827	$> 2.5 \times 10^8$	$> 2.3 \times 10^8$
B. uniformis JCM5828	$> 4.6 \times 10^8$	$> 4.2 \times 10^8$
A. muciniphila JCM33894	$> 1.7 \times 10^8$	$> 1.5 \times 10^8$
P. aeruginosa PAO1	1.1	1

Samples obtained from cultures of bacteria of the genera *Bacteroides* and *Akkermansia* and *P. aeruginosa* PAO1 were injected into silkworms, and the 50% lethal dose (LD_{50}) of each bacterium to the silkworm was determined from the survival rate of the silkworm after 24 hours. Fold indicates the magnification of each strain when the LD_{50} of *P. aeruginosa* is set as 1.

In previous studies using silkworms, various polysaccharides have been evaluated for their muscle contraction activity. Fujiyuki *et al*. compared the activities of structurally different β-glucans and reported the activity ranging from 0-100 units/mg using the same assay system as in the present study (*17*). The activity values of the samples examined in the present study that exhibited activity also fell within this range, consistent with previous results. Additionally, we have recently reported that neutral polysaccharides derived from broccoli exhibit higher activity (*20*). However, it is important to note that the broccoli-derived neutral polysaccharides used were semi-purified fractions obtained through ethanol precipitation or organic solvent extraction, making direct comparisons of activity levels difficult.

The human gut bacteria, which exhibited innate immune-stimulatory activity in silkworms in this study, have been reported to possess various functions such as anti-rotavirus (*25*) and anti-inflammatory effects (*26,27*). The prebiotics which selectively propagate *B. ovatus* and *B. thetaiotaomicron*, in particular, are known (*23*). These bacterial species are expected to be potent candidates of novel probiotics, and as their beneficial effects on humans become clearer, it is likely that their utilization in functional foods and supplements will be further explored.

In the development of functional foods, safety assessment is indispensable. Currently, *in vitro* assays using cultured cells are predominantly employed alternative methods for studying the safety and functionality of food materials. For example, the *in vitro* 3T3 neutral red uptake (NRU) phototoxicity test evaluates the toxicity of substances excited by light based on the uptake of neutral red by Balb/c 3T3 cells, and it is widely used for testing food additives and similar substances (*28*). Additionally, analyzing the genomic sequences of organisms used as food materials leads to infer factors that may be harmful to the human body or understand the functions of functional components (*29*). However, safety assessments at the cellular level may not fully capture the effects of metabolism that food components undergo in the body, leading to insufficient verification of their toxicity. Moreover, the information obtained from genome sequences is limited to known factors, thus proving inadequate when exploring unknown functionalities and toxicities. From the perspective of complementing these data, there is a need for new experimental models capable of alternative organisms with multiple organs as evaluation systems. Therefore, we propose the use of silkworms, an insect species, as an experimental model for investigating the functionality and safety of food components (*6,12,20,24,29*).

The human gut bacteria discovered in this study hold promise for use in food development research as probiotics and for research and development aimed at isolating active substances to obtain useful compounds. The differences in the innate immune-stimulatory ability in the silkworm among the bacterial strains discovered in this study (based on muscle contraction assay) are presumed to stem from differences in cell wall composition among the strains. For example, bacterial cell walls contain a polysaccharide-based structure called peptidoglycan. Peptidoglycan has a structure in which glycan chains consisting of repeating units of *N*-acetylglucosamine and *N*-acetylmuramic acid are cross-linked by short peptide chains (*30*). It is known that the structure of peptidoglycan varies among bacterial species (*30,31*). Furthermore, it has been reported that peptidoglycan, through peptidoglycan recognition proteins (PGRPs), is recognized by insects, triggering their innate immune response (*32*). Although the differences in peptidoglycan structure among the gut bacteria used in this study may potentially influence the differences in muscle contraction activity, the investigations into such structure-activity relationships are future tasks. Especially, for such bacterial-derived polysaccharides, it is considered useful to conduct biochemical purification of active substances based on physiological activity, as well as verification using chemically synthesized compounds of the respective substances (verification based on partial structures).

Additionally, an important research question remaining is whether the innate immune-stimulatory effect of gut bacteria administration demonstrated in this study can induce immune priming response of silkworms, as we have previously reported, and thereby confer resistance to human pathogenic microbial infections (*6,33*). Through such investigations, it is anticipated that the full extent and mechanism of action of the innate immune-stimulatory function of the samples identified in this study will be elucidated at the molecular level, leading to the creation of functional food ingredients that can be extrapolated to humans.

Funding: This work was financially supported by Asahi Quality and Innovations Inc., JSPS KAKENHI Grant Number 20K16253 to A.M., and a research grant from

The Uehara Memorial Foundation to A.M. Genome Pharmaceuticals Institute Co., Ltd. provided technical supports for the muscle contraction assay..

Conflict of Interest: The authors have no conflicts of interest to disclose.

References

1. Kaito C, Akimitsu N, Watanabe H, Sekimizu K. Silkworm larvae as an animal model of bacterial infection pathogenic to humans. Microb Pathog. 2002; 32:183-190.
2. Hamamoto H, Kurokawa K, Kaito C, Kamura K, Manitra Razanajatovo I, Kusuhara H, Santa T, Sekimizu K. Quantitative evaluation of the therapeutic effects of antibiotics using silkworms infected with human pathogenic microorganisms. Antimicrob Agents Chemother. 2004; 48:774-779.
3. Fujiyuki T, Imamura K, Hamamoto H, Sekimizu K. Evaluation of therapeutic effects and pharmacokinetics of antibacterial chromogenic agents in a silkworm model of Staphylococcus aureus infection. Drug Discov Ther. 2010; 4:349-354.
4. Miyashita A, Iyoda S, Ishii K, Hamamoto H, Sekimizu K, Kaito C. Lipopolysaccharide O-antigen of enterohemorrhagic *Escherichia coli* O157:H7 is required for killing both insects and mammals. FEMS Microbiol Lett. 2012; 333:59-68.
5. Miyashita A, Kizaki H, Kawasaki K, Sekimizu K, Kaito C. Primed immune responses to gram-negative peptidoglycans confer infection resistance in silkworms. J Biol Chem. 2014; 289:14412-14421.
6. Miyashita A, Takahashi S, Ishii K, Sekimizu K, Kaito C. Primed Immune Responses Triggered by Ingested Bacteria Lead to Systemic Infection Tolerance in Silkworms. PLoS One. 2015; 10:e0130486.
7. Tabuchi F, Matsumoto Y, Ishii M, Tatsuno K, Okazaki M, Sato T, Moriya K, Sekimizu K. Synergistic effects of vancomycin and β-lactams against vancomycin highly resistant *Staphylococcus aureus*. J Antibiot (Tokyo). 2017; 70:771-774.
8. Tabuchi F, Matsumoto Y, Ishii M, Tatsuno K, Okazaki M, Sato T, Moriya K, Sekimizu K. D-cycloserine increases the effectiveness of vancomycin against vancomycin-highly resistant *Staphylococcus aureus*. J Antibiot (Tokyo). 2017; 70:907-910.
9. Hamamoto H, Panthee S, Paudel A, Ishii K, Yasukawa J, Su J, Miyashita A, Itoh H, Tokumoto K, Inoue M, Sekimizu K. Serum apolipoprotein A-I potentiates the therapeutic efficacy of lysocin E against *Staphylococcus aureus.* Nat Commun. 2021; 12:6364.
10. Mikami K, Sonobe K, Ishino K, Noda T, Kato M, Hanao M, Hamamoto H, Sekimizu K, Okazaki M. Evaluation of pathogenicity and therapeutic effectiveness of antibiotics using silkworm *Nocardia* infection model. Drug Discov Ther. 2021; 15:73-77.
11. Miyashita A, Hamamoto H, Sekimizu K. Applying the silkworm model for the search of immunosuppressants. Drug Discov Ther. 2021; 15:139-142.
12. Miyashita A, Sekimizu K. Using silkworms to search for lactic acid bacteria that contribute to infection prevention and improvement of hyperglycemia. Drug Discov Ther. 2021; 15:51-54.
13. Hamamoto H, Urai M, Ishii K, *et al.* Lysocin E is a new antibiotic that targets menaquinone in the bacterial membrane. Nat Chem Biol. 2015; 11:127-133.
14. Miyashita A, Mitsutomi S, Mizushima T, Sekimizu K. Repurposing the PDMA-approved drugs in Japan using an insect model of staphylococcal infection. FEMS Microbes. 2022; 3:xtac014.
15. Ishii K, Hamamoto H, Kamimura M, Nakamura Y, Noda H, Imamura K, Mita K, Sekimizu K. Insect cytokine paralytic peptide (PP) induces cellular and humoral immune responses in the silkworm *Bombyx mori*. J Biol Chem. 2010; 285:28635-28642.
16. Dhital S, Hamamoto H, Urai M, Ishii K, Sekimizu K. Purification of innate immunostimulant from green tea using a silkworm muscle contraction assay. Drug Discov Ther. 2011; 5:18-25.
17. Fujiyuki T, Hamamoto H, Ishii K, Urai M, Kataoka K, Takeda T, Shibata S, Sekimizu K. Evaluation of innate immune stimulating activity of polysaccharides using a silkworm (*Bombyx mori*) muscle contraction assay. Drug Discov Ther. 2012; 6:88-93.
18. Ha SD, Nagata S, Suzuki A, Kataoka H. Isolation and structure determination of a paralytic peptide from the hemolymph of the silkworm, *Bombyx mori*. Peptides. 1999; 20:561-568.
19. Ishii K, Hamamoto H, Kamimura M, Sekimizu K. Activation of the silkworm cytokine by bacterial and fungal cell wall components *via* a reactive oxygen species-triggered mechanism. J Biol Chem. 2008; 283:2185-2191.
20. Miyashita A, Kataoka K, Tsuchida T, Ogasawara AA, Nakajima H, Takahashi M, Sekimizu K. High molecular weight glucose homopolymer of broccoli (*Brassica oleracea* var. *italica*) stimulates both invertebrate and mammalian immune systems. Front Food Sci Technol. 2023; 3. https://doi.org/10.3389/frfst.2023.1012121
21. Tanihiro R, Sakano K, Oba S, Nakamura C, Ohki K, Hirota T, Sugiyama H, Ebihara S, Nakamura Y. Effects of Yeast Mannan Which Promotes Beneficial Bacteroides on the Intestinal Environment and Skin Condition: A Randomized, Double-Blind, Placebo-Controlled Study. Nutrients. 2020; 12:3673.
22. Tanihiro R, Yuki M, Sasai M, Haseda A, Kagami-Katsuyama H, Hirota T, Honma N, Nishihira J. Effects of Prebiotic Yeast Mannan on Gut Health and Sleep Quality in Healthy Adults: A Randomized, Double-Blind, Placebo-Controlled Study. Nutrients. 2023; 16:141.
23. Oba S, Sunagawa T, Tanihiro R, Awashima K, Sugiyama H, Odani T, Nakamura Y, Kondo A, Sasaki D, Sasaki K. Prebiotic effects of yeast mannan, which selectively promotes *Bacteroides thetaiotaomicron* and *Bacteroides ovatus* in a human colonic microbiota model. Sci Rep. 2020; 10:17351.
24. Li W, Miyashita A, Sekimizu K. Peanut triacylglycerols activate innate immunity both in insects and mammals. Sci Rep. 2022; 12:7464.
25. Varyukhina S, Freitas M, Bardin S, Robillard E, Tavan E, Sapin C, Grill JP, Trugnan G. Glycan-modifying bacteria-derived soluble factors from *Bacteroides thetaiotaomicron* and *Lactobacillus casei* inhibit rotavirus infection in human intestinal cells. Microbes Infect. 2012; 14:273-278.
26. Delday M, Mulder I, Logan ET, Grant G. *Bacteroides thetaiotaomicron* ameliorates colon inflammation in preclinical models of Crohn's disease. Inflamm Bowel Dis. 2019; 25:85-96.

27. Ihekweazu FD, Fofanova TY, Queliza K, Nagy-Szakal D, Stewart CJ, Engevik MA, Hulten KG, Tatevian N, Graham DY, Versalovic J. *Bacteroides ovatus* ATCC 8483 monotherapy is superior to traditional fecal transplant and multi-strain bacteriotherapy in a murine colitis model. Gut microbes. 2019; 10:504-520.
28. Lynch AM, Wilcox P. Review of the performance of the 3T3 NRU *in vitro* phototoxicity assay in the pharmaceutical industry. Exp Toxicol Pathol. 2011; 63:209-214.
29. Matsumoto Y, Ishii M, Hasegawa S, Sekimizu K. *Enterococcus faecalis* YM0831 suppresses sucrose-induced hyperglycemia in a silkworm model and in humans. Commun Biol. 2019; 2:157.
30. Vollmer W, Blanot D, De Pedro MA. Peptidoglycan structure and architecture. FEMS Microbiol Rev. 2008; 32:149-167.
31. Vollmer W. Structural variation in the glycan strands of bacterial peptidoglycan. FEMS Microbiol Rev. 2008; 32:287-306.
32. Kordaczuk J, Sułek M, Wojda I. General overview on the role of Peptidoglycan Recognition Proteins in insect immunity. Acta Biochim Pol. 2020; 67:319-326.
33. Miyashita A, Kizaki H, Kawasaki K, Sekimizu K, Kaito C. Primed immune responses to gram-negative peptidoglycans confer infection resistance in silkworms. J Biol Chem. 2014; 289:14412-14421.

Received January 6, 2025; Revised January 29, 2025; Accepted February 19, 2025.

**Address correspondence to:*
Atsushi Miyashita, Institute of Medical Mycology, Teikyo University, 359 Otsuka, Hachioji, Tokyo 192-0352, Japan.
E-mail: atmiyashita@main.teikyo-u.ac.jp

Released online in J-STAGE as advance publication February 27, 2025.

Correspondence

DOI: 10.5582/ddt.2025.01010

Suzetrigine: The first Nav1.8 inhibitor approved for the treatment of moderate to severe acute pain

Shasha Hu[1], Dong Lyu[2], Jianjun Gao[3,*]

[1] Department of Pathology, The Affiliated Hospital of Qingdao University, Qingdao, Shandong, China;
[2] Department of Burn and Plastic Surgery, Weihai Central Hospital Affiliated to Qingdao University, Weihai, Shandong, China;
[3] Department of Pharmacology, School of Pharmacy, Qingdao University, Qingdao, Shandong, China.

SUMMARY: Opioids are commonly prescribed for the management of moderate to severe pain, but their use is associated with dependency and other adverse effects. For decades, the development of safe and effective non-addictive alternatives for treating moderate to severe pain has seen limited progress. On January 30, 2025, the U.S. Food and Drug Administration approved suzetrigine, the first Nav1.8 inhibitor, for the treatment of moderate to severe acute pain. Nav1.8 is a voltage-gated sodium channel that is selectively expressed in peripheral nociceptive neurons, which are responsible for transmitting pain signals. By highly selectively inhibiting the Nav1.8 channel, suzetrigine can effectively alleviate pain. Unlike opioids, this drug does not induce euphoria or excitement in the brain, thereby eliminating concerns about addiction. Suzetrigine offers a novel therapeutic option and a potential combination for multimodal analgesia, with the promise of transforming acute pain management and establishing new treatment standards.

Keywords: Opioids, Nav1.8, pain, postoperative, painful diabetic peripheral neuropathy (DPN), painful lumbosacral radiculopathy (LSR)

Acute pain refers to sharp, transient, and localized pain that occurs due to various physical, chemical, traumatic, or infectious factors. Research indicates that about 75% of patients experience moderate to severe pain postoperatively (*1*). Opioids, such as morphine, fentanyl, and pethidine, are widely used to manage moderate to severe acute pain. However, their use carries the risk of dependence and other adverse effects. It is reported that over 80 million Americans are prescribed medications for moderate to severe acute pain each year, with approximately 40 million of them being prescribed opioids (*2*). Among patients initially treated with opioids for acute pain, nearly 10% will continue using opioids long-term, and around 85,000 patients develop opioid use disorder annually (*2*). Poor management of acute pain can lead to reduced quality of life for patients, the development of chronic pain, and an increased burden on the healthcare system and society. Currently, there is a pressing clinical need for safe, effective, non-addictive alternatives to opioids for treating moderate to severe pain.

Suzetrigine (brand name: Journavx) is an oral, selective Nav1.8 sodium channel blocker developed by Vertex Pharmaceuticals (*2*). It was approved by the U.S. Food and Drug Administration on January 30, 2025, for the treatment of moderate to severe acute pain (*3*). Nav1.8 is a voltage-gated sodium channel that plays a key role in the transmission of pain signals in the peripheral nervous system (*4*). It is selectively expressed in dorsal root ganglia (DRG) and trigeminal ganglion (TG) neurons. When neurons are stimulated, the Nav1.8 channel opens, allowing a large influx of sodium ions, which causes depolarization of the cell membrane, generating an action potential and triggering the sensation of pain (*5*). Suzetrigine selectively acts on the Nav1.8 channels of peripheral nociceptive neurons, inhibiting the rapid influx of sodium ions and the generation of action potentials, thus blocking pain signal transmission (*5*). Since Nav1.8 channels are not expressed in the human central nervous system, suzetrigine does not produce excitatory effects or euphoria, and therefore does not have addictive properties (*5*).

Multiple clinical trials have demonstrated that suzetrigine is effective in relieving moderate to severe acute pain. Phase 2 and phase 3 randomized controlled trials tested suzetrigine's analgesic effects following abdominoplasty and bunionectomy (*5-7*). The results showed that, compared to a placebo, suzetrigine at a 100 mg loading dose followed by a 50 mg dose every 12 hours within 48 hours post-surgery resulted

Table 1. The Nav1.8 inhibitors that are currently undergoing clinical trials

Drug candidates	Indication	Clinical trial	Company
Suzetrigine (VX-548)	Painful diabetic peripheral neuropathy;	Phase 3;	Vertex Pharmaceuticals Incorporated
	Painful lumbosacral radiculopathy	Phase 2	
VX-993	Acute pain after a bunionectomy;	Phase 2;	Vertex Pharmaceuticals Incorporated
	Painful diabetic peripheral neuropathy	Phase 2	
LTG-001	Acute pain after third molar removal surgery in adults	Phase 2	Latigo Biotherapeutics
JMKX000623	Diabetic peripheral neuropathic pain	Phase 2	Jemincare
HRS-2129	Postoperative analgesia in orthopaedics	Phase 1	Shandong Suncadia Medicine
VX-973	—	Phase 1	Vertex Pharmaceuticals Incorporated
LTG-305	—	Phase 1	Latigo Biotherapeutics
HBW-004285	—	Phase 1	Hyperway Pharmaceutical
FZ008-145	—	Phase 1	Guangzhou Fermion Technology
STC-004	—	Phase 1	SiteOne Therapeutics

in statistically significant and clinically meaningful reductions in moderate to severe pain. In a subsequent phase 3 single-arm clinical trial, suzetrigine was administered for up to 14 days to patients with moderate to severe acute pain resulting from surgical and non-surgical causes, further confirming its analgesic efficacy (*5*). Regarding safety, the results from three phase 3 clinical trials, which included a total of 2,447 participants, indicated that suzetrigine does not carry a potential for addiction (*5*). The most common adverse reactions were itching, muscle spasms, elevated blood creatine phosphokinase levels, and rash (*2,7*).

The approval of suzetrigine highlights that targeting Nav1.8 could be an important strategy for treating moderate to severe acute pain. Currently, the number of Nav1.8 inhibitors that have entered clinical research is still limited (Table 1). The approval of suzetrigine is expected to encourage pharmaceutical companies to develop more Nav1.8 inhibitors for pain treatment. In addition to postoperative pain, candidate drugs in clinical research are expanding into new indications. Suzetrigine has already entered a phase 3 clinical trial for the treatment of painful diabetic peripheral neuropathy (DPN) (*8*), and a phase 2 trial for treating painful lumbosacral radiculopathy (LSR) have been completed, with the potential to move into phase 3 trials (*9*). If clinical studies targeting these new indications are successful, the pain-relieving applications of Nav1.8 inhibitors will become more diverse, benefiting a broader range of patients.

Suzetrigine offers a novel non-opioid treatment option for patients with acute pain. However, whether suzetrigine can serve as a replacement for opioids and help reduce the public health issues caused by opioid abuse requires further clinical research. Regardless, suzetrigine provides a novel drug option and combination for multimodal analgesia, with the potential to transform the paradigm of acute pain management and establish new treatment standards. It is anticipated that analgesic drugs with novel mechanisms will bring advancements in the clinical treatment of both acute and chronic pain.

Funding: None.

Conflict of Interest: The authors have no conflicts of interest to disclose.

References

1. Gan TJ, Habib AS, Miller TE, White W, Apfelbaum JL. Incidence, patient satisfaction, and perceptions of post-surgical pain: results from a US national survey. Curr Med Res Opin. 2014; 30:149-160.
2. Vertex Announces FDA Approval of JOURNAVX™ (suzetrigine), a First-in-Class Treatment for Adults With Moderate-to-Severe Acute Pain. *https://investors.vrtx.com/news-releases/news-release-details/vertex-announces-fda-approval-journavxtm-suzetrigine-first-class* (accessed February 10, 2025).
3. FDA Approves Novel Non-Opioid Treatment for Moderate to Severe Acute Pain. *https://www.fda.gov/news-events/press-announcements/fda-approves-novel-non-opioid-treatment-moderate-severe-acute-pain* (accessed February 8, 2025).
4. Goodwin G, McMahon SB. The physiological function of different voltage-gated sodium channels in pain. Nat Rev Neurosci. 2021; 22:263-274.
5. Osteen JD, Immani S, Tapley TL, Indersmitten T, Hurst NW, Healey T, Aertgeerts K, Negulescu PA, Lechner SM. Pharmacology and Mechanism of Action of Suzetrigine, a Potent and Selective Na(V)1.8 Pain Signal Inhibitor for the Treatment of Moderate to Severe Pain. Pain Ther. 2025.
6. Jones J, Correll DJ, Lechner SM, et al. Selective Inhibition of Na(V)1.8 with VX-548 for Acute Pain. N Engl J Med. 2023; 389:393-405.
7. JOURNAVX (suzetrigine) tablets, for oral use. *https://www.accessdata.fda.gov/drugsatfda_docs/label/2025/219209Orig1s000lbl.pdf* (accessed February 12, 2025).
8. Evaluation of Efficacy and Safety of Suzetrigine for Pain Associated With Diabetic Peripheral Neuropathy. *https://clinicaltrials.gov/study/NCT06628908?intr=vx-548&page=2&rank=19* (accessed February 10, 2025). .

9. Suzetrigine (VX-548) Phase 2 results in painful lumbosacral radiculopathy. *https://investors.vrtx.com/news-releases/news-release-details/vertex-announces-results-phase-2-study-suzetrigine-treatment* (accessed February 10, 2025).

Received February 13, 2025; Accepted February 23, 2025.

**Address correspondence to:*
Jianjun Gao, Department of Pharmacology, School of Pharmacy, Qingdao University, Qingdao, Shandong, China.
E-mail: gaojj@qdu.edu.cn

Released online in J-STAGE as advance publication February 27, 2025.

DD&T
Drug Discoveries & Therapeutics

Guide for Authors

1. Scope of Articles

Drug Discoveries & Therapeutics (Print ISSN 1881-7831, Online ISSN 1881-784X) welcomes contributions in all fields of pharmaceutical and therapeutic research such as medicinal chemistry, pharmacology, pharmaceutical analysis, pharmaceutics, pharmaceutical administration, and experimental and clinical studies of effects, mechanisms, or uses of various treatments. Studies in drug-related fields such as biology, biochemistry, physiology, microbiology, and immunology are also within the scope of this journal.

2. Submission Types

Original Articles should be well-documented, novel, and significant to the field as a whole. An Original Article should be arranged into the following sections: Title page, Abstract, Introduction, Materials and Methods, Results, Discussion, Acknowledgments, and References. Original articles should not exceed 5,000 words in length (excluding references) and should be limited to a maximum of 50 references. Articles may contain a maximum of 10 figures and/or tables. Supplementary Data are permitted but should be limited to information that is not essential to the general understanding of the research presented in the main text, such as unaltered blots and source data as well as other file types.

Brief Reports definitively documenting either experimental results or informative clinical observations will be considered for publication in this category. Brief Reports are not intended for publication of incomplete or preliminary findings. Brief Reports should not exceed 3,000 words in length (excluding references) and should be limited to a maximum of 4 figures and/or tables and 30 references. A Brief Report contains the same sections as an Original Article, but the Results and Discussion sections should be combined.

Reviews should present a full and up-to-date account of recent developments within an area of research. Normally, reviews should not exceed 8,000 words in length (excluding references) and should be limited to a maximum of 10 figures and/or tables and 100 references. Mini reviews are also accepted, which should not exceed 4,000 words in length (excluding references) and should be limited to a maximum of 5 figures and/or tables and 50 references.

Policy Forum articles discuss research and policy issues in areas related to life science such as public health, the medical care system, and social science and may address governmental issues at district, national, and international levels of discourse. Policy Forum articles should not exceed 3,000 words in length (excluding references) and should be limited to a maximum of 5 figures and/or tables and 30 references.

Case Reports should be detailed reports of the symptoms, signs, diagnosis, treatment, and follow-up of an individual patient. Case reports may contain a demographic profile of the patient but usually describe an unusual or novel occurrence. Unreported or unusual side effects or adverse interactions involving medications will also be considered. Case Reports should not exceed 3,000 words in length (excluding references).

Communications are short, timely pieces that spotlight new research findings or policy issues of interest to the field of global health and medical practice that are of immediate importance. Depending on their content, Communications will be published as "Comments" or "Correspondence". Communications should not exceed 1,500 words in length (excluding references) and should be limited to a maximum of 2 figures and/or tables and 20 references.

Editorials are short, invited opinion pieces that discuss an issue of immediate importance to the fields of global health, medical practice, and basic science oriented for clinical application. Editorials should not exceed 1,000 words in length (excluding references) and should be limited to a maximum of 10 references. Editorials may contain one figure or table.

News articles should report the latest events in health sciences and medical research from around the world. News should not exceed 500 words in length.

Letters should present considered opinions in response to articles published in *Drug Discoveries & Therapeutics* in the last 6 months or issues of general interest. Letters should not exceed 800 words in length and may contain a maximum of 10 references. Letters may contain one figure or table.

3. Editorial Policies

For publishing and ethical standards, *Drug Discoveries & Therapeutics* follows the Recommendations for the Conduct, Reporting, Editing, and Publication of Scholarly Work in Medical Journals issued by the International Committee of Medical Journal Editors (ICMJE, *https://icmje.org/recommendations*), and the Principles of Transparency and Best Practice in Scholarly Publishing jointly issued by the Committee on Publication Ethics (COPE, *https://publicationethics.org/resources/guidelines-new/principles-transparency-and-best-practice-scholarly-publishing*), the Directory of Open Access Journals (DOAJ, *https://doaj.org/apply/transparency*), the Open Access Scholarly Publishers Association (OASPA, *https://oaspa.org/principles-of-transparency-and-best-practice-in-scholarly-publishing-4*), and the World Association of Medical Editors (WAME, *https://wame.org/principles-of-transparency-and-best-practice-in-scholarly-publishing*).

Drug Discoveries & Therapeutics will perform an especially prompt review to encourage innovative work. All original research will be subjected to a rigorous standard of peer review and will be edited by experienced copy editors to the highest standards.

Ethical Approval of Studies and Informed Consent: For all manuscripts reporting data from studies involving human participants or animals, formal review and approval, or formal review and waiver, by an appropriate institutional review board or ethics committee is required and should be described in the Methods section. When your manuscript contains any case details, personal information and/or images of patients or other individuals, authors must obtain appropriate written consent, permission and release in order to comply with all applicable laws and regulations concerning privacy and/or security of personal information. The consent form needs to comply with the relevant legal requirements of your particular jurisdiction, and please do not send signed consent form to *Drug Discoveries & Therapeutics* to respect your patient's and any other individual's privacy. Please instead describe the information clearly in the Methods (patient consent) section of your manuscript while retaining copies of the signed forms in the event they should be needed. Authors should also state that the study conformed to the provisions of the Declaration of Helsinki (as revised in 2013, *https://wma.net/what-we-do/medical-ethics/declaration-of-helsinki*). When reporting experiments on animals, authors should indicate whether the institutional and national guide for the care and use of laboratory animals was followed.

Reporting Clinical Trials: The ICMJE (*https:// icmje.org/recommendations/browse/publishing-and-editorial-issues/clinical-trial-registration.html*) defines a clinical trial as any research project that prospectively assigns people or a group of people to an intervention, with or without concurrent comparison or control groups, to study the relationship between a health-related intervention and a health outcome. Registration of clinical trials in a public trial registry

at or before the time of first patient enrollment is a condition of consideration for publication in *Drug Discoveries & Therapeutics*, and the trial registration number will be published at the end of the Abstract. The registry must be independent of for-profit interest and publicly accessible. Reports of trials must conform to CONSORT 2010 guidelines (*https://consort-statement.org/consort-2010*). Articles reporting the results of randomized trials must include the CONSORT flow diagram showing the progress of patients throughout the trial.

Conflict of Interest: All authors are required to disclose any actual or potential conflict of interest including financial interests or relationships with other people or organizations that might raise questions of bias in the work reported. If no conflict of interest exists for each author, please state "There is no conflict of interest to disclose".

Submission Declaration: When a manuscript is considered for submission to *Drug Discoveries & Therapeutics*, the authors should confirm that 1) no part of this manuscript is currently under consideration for publication elsewhere; 2) this manuscript does not contain the same information in whole or in part as manuscripts that have been published, accepted, or are under review elsewhere, except in the form of an abstract, a letter to the editor, or part of a published lecture or academic thesis; 3) authorization for publication has been obtained from the authors' employer or institution; and 4) all contributing authors have agreed to submit this manuscript.

Initial Editorial Check: Immediately after submission, the journal's managing editor will perform an initial check of the manuscript. A suitable academic editor will be notified of the submission and invited to check the manuscript and recommend reviewers. Academic editors will check for plagiarism and duplicate publication at this stage. The journal has a formal recusal process in place to help manage potential conflicts of interest of editors. In the event that an editor has a conflict of interest with a submitted manuscript or with the authors, the manuscript, review, and editorial decisions are managed by another designated editor without a conflict of interest related to the manuscript.

Peer Review: *Drug Discoveries & Therapeutics* operates a single-anonymized review process, which means that reviewers know the names of the authors, but the authors do not know who reviewed their manuscript. All articles are evaluated objectively based on academic content. External peer review of research articles is performed by at least two reviewers, and sometimes the opinions of more reviewers are sought. Peer reviewers are selected based on their expertise and ability to provide quality, constructive, and fair reviews. For research manuscripts, the editors may, in addition, seek the opinion of a statistical reviewer. Every reviewer is expected to evaluate the manuscript in a timely, transparent, and ethical manner, following the COPE guidelines (*https://publicationethics.org/files/cope-ethical-guidelines-peer-reviewers-v2_0.pdf*). We ask authors for sufficient revisions (with a second round of peer review, when necessary) before a final decision is made. Consideration for publication is based on the article's originality, novelty, and scientific soundness, and the appropriateness of its analysis.

Suggested Reviewers: A list of up to 3 reviewers who are qualified to assess the scientific merit of the study is welcomed. Reviewer information including names, affiliations, addresses, and e-mail should be provided at the same time the manuscript is submitted online. Please do not suggest reviewers with known conflicts of interest, including participants or anyone with a stake in the proposed research; anyone from the same institution; former students, advisors, or research collaborators (within the last three years); or close personal contacts. Please note that the Editor-in-Chief may accept one or more of the proposed reviewers or may request a review by other qualified persons.

Language Editing: Manuscripts prepared by authors whose native language is not English should have their work proofread by a native English speaker before submission. If not, this might delay the publication of your manuscript in *Drug Discoveries & Therapeutics*.

The Editing Support Organization can provide English proofreading, Japanese-English translation, and Chinese-English translation services to authors who want to publish in *Drug Discoveries & Therapeutics* and need assistance before submitting a manuscript. Authors can visit this organization directly at *https://www.iacmhr.com/iac-eso/support.php?lang=en. IAC-ESO* was established to facilitate manuscript preparation by researchers whose native language is not English and to help edit works intended for international academic journals.

Copyright and Reuse: Before a manuscript is accepted for publication in *Drug Discoveries & Therapeutics*, authors will be asked to sign a transfer of copyright agreement, which recognizes the common interest that both the journal and author(s) have in the protection of copyright. We accept that some authors (*e.g.*, government employees in some countries) are unable to transfer copyright. A JOURNAL PUBLISHING AGREEMENT (JPA) form will be e-mailed to the authors by the Editorial Office and must be returned by the authors by mail, fax, or as a scan. Only forms with a hand-written signature from the corresponding author are accepted. This copyright will ensure the widest possible dissemination of information. Please note that the manuscript will not proceed to the next step in publication until the JPA Form is received. In addition, if excerpts from other copyrighted works are included, the author(s) must obtain written permission from the copyright owners and credit the source(s) in the article.

4. Cover Letter

The manuscript must be accompanied by a cover letter prepared by the corresponding author on behalf of all authors. The letter should indicate the basic findings of the work and their significance. The letter should also include a statement affirming that all authors concur with the submission and that the material submitted for publication has not been published previously or is not under consideration for publication elsewhere. The cover letter should be submitted in PDF format. For an example of Cover Letter, please visit: Download Centre (*https://www.ddtjournal.com/downcentre)*.

5. Submission Checklist

The Submission Checklist should be submitted when submitting a manuscript through the Online Submission System. Please visit Download Centre (*https://www.ddtjournal.com/downcentre)* and download the Submission Checklist file. We recommend that authors use this checklist when preparing your manuscript to check that all the necessary information is included in your article (if applicable), especially with regard to Ethics Statements.

6. Manuscript Preparation

Manuscripts are suggested to be prepared in accordance with the "Recommendations for the Conduct, Reporting, Editing, and Publication of Scholarly Work in Medical Journals", as presented at *http://www.ICMJE.org*.

Manuscripts should be written in clear, grammatically correct English and submitted as a Microsoft Word file in a single-column format. Manuscripts must be paginated and typed in 12-point Times New Roman font with 24-point line spacing. Please do not embed figures in the text. Abbreviations should be used as little as possible and should be explained at first mention unless the term is a well-known abbreviation (*e.g.* DNA). Single words should not be abbreviated.

Title page: The title page must include 1) the title of the paper (Please note the title should be short, informative, and contain the major key words); 2) full name(s) and affiliation(s) of the author(s), 3) abbreviated names of the author(s), 4) full name, mailing address, telephone/fax numbers, and e-mail address of the corresponding author; 5) author contribution statements to specify the individual contributions of all authors to this manuscript, and 6) conflicts of interest (if you have an actual or potential conflict of interest to disclose, it must be included as a footnote on the title page of the manuscript; if no conflict of interest

exists for each author, please state "There is no conflict of interest to disclose").

Abstract: The abstract should briefly state the purpose of the study, methods, main findings, and conclusions. For article types including Original Article, Brief Report, Review, Policy Forum, and Case Report, a one-paragraph abstract consisting of no more than 250 words must be included in the manuscript. For Communications, Editorials, News, or Letters, a brief summary of main content in 150 words or fewer should be included in the manuscript. For articles reporting clinical trials, the trial registration number should be stated at the end of the Abstract. Abbreviations must be kept to a minimum and non-standard abbreviations explained in brackets at first mention. References should be avoided in the abstract. Three to six key words or phrases that do not occur in the title should be included in the Abstract page.

Introduction: The introduction should provide sufficient background information to make the article intelligible to readers in other disciplines and sufficient context clarifying the significance of the experimental findings.

Materials/Patients and Methods: The description should be brief but with sufficient detail to enable others to reproduce the experiments. Procedures that have been published previously should not be described in detail but appropriate references should simply be cited. Only new and significant modifications of previously published procedures require complete description. Names of products and manufacturers with their locations (city and state/country) should be given and sources of animals and cell lines should always be indicated. All clinical investigations must have been conducted in accordance with the Declaration of Helsinki (as revised in 2013, *https://wma.net/what-we-do/medical-ethics/declaration-of-helsinki*). All human and animal studies must have been approved by the appropriate institutional review board(s) and a specific declaration of approval must be made within this section.

Results: The description of the experimental results should be succinct but in sufficient detail to allow the experiments to be analyzed and interpreted by an independent reader. If necessary, subheadings may be used for an orderly presentation. All Figures and Tables should be referred to in the text in order, including those in the Supplementary Data.

Discussion: The data should be interpreted concisely without repeating material already presented in the Results section. Speculation is permissible, but it must be well-founded, and discussion of the wider implications of the findings is encouraged. Conclusions derived from the study should be included in this section.

Acknowledgments: All funding sources (including grant identification) should be credited in the Acknowledgments section. Authors should also describe the role of the study sponsor(s), if any, in study design; in the collection, analysis, and interpretation of data; in the writing of the report; and in the decision to submit the paper for publication. If the funding source had no such involvement, the authors should so state.

In addition, people who contributed to the work but who do not meet the criteria for authors should be listed along with their contributions.

References: References should be numbered in the order in which they appear in the text. Citing of unpublished results, personal communications, conference abstracts, and theses in the reference list is not recommended but these sources may be mentioned in the text. In the reference list, cite the names of all authors when there are fifteen or fewer authors; if there are sixteen or more authors, list the first three followed by *et al*. Names of journals should be abbreviated in the style used in PubMed. Authors are responsible for the accuracy of the references. The EndNote Style of *Drug Discoveries & Therapeutics* could be downloaded at **EndNote** (*https://www.ddtjournal.com/examples/Drug_Discoveries_Therapeutics.ens*).

Examples are given below:

Example 1 (Sample journal reference):

Nakata M, Tang W. Japan-China Joint Medical Workshop on Drug Discoveries and Therapeutics 2008: The need of Asian pharmaceutical researchers' cooperation. Drug Discov Ther. 2008; 2:262-263.

Example 2 (Sample journal reference with more than 15 authors):

Darby S, Hill D, Auvinen A, *et al*. Radon in homes and risk of lung cancer: Collaborative analysis of individual data from 13 European case-control studies. BMJ. 2005; 330:223.

Example 3 (Sample book reference):

Shalev AY. Post-traumatic stress disorder: Diagnosis, history and life course. In: Post-traumatic Stress Disorder, Diagnosis, Management and Treatment (Nutt DJ, Davidson JR, Zohar J, eds.). Martin Dunitz, London, UK, 2000; pp. 1-15.

Example 4 (Sample web page reference):

World Health Organization. The World Health Report 2008 – primary health care: Now more than ever. *https://apps.who.int/iris/handle/10665/43949* (accessed September 23, 2022).

Tables: All tables should be prepared in Microsoft Word or Excel and should be arranged at the end of the manuscript after the References section. Please note that tables should not in image format. All tables should have a concise title and should be numbered consecutively with Arabic numerals. If necessary, additional information should be given below the table.

Figure Legend: The figure legend should be typed on a separate page of the main manuscript and should include a short title and explanation. The legend should be concise but comprehensive and should be understood without referring to the text. Symbols used in figures must be explained. Any individually labeled figure parts or panels (A, B, *etc*.) should be specifically described by part name within the legend.

Figure Preparation: All figures should be clear and cited in numerical order in the text. Figures must fit a one- or two-column format on the journal page: 8.3 cm (3.3 in.) wide for a single column, 17.3 cm (6.8 in.) wide for a double column; maximum height: 24.0 cm (9.5 in.). Please make sure that artwork files are in an acceptable format (TIFF or JPEG) at minimum resolution (600 dpi for illustrations, graphs, and annotated artwork, and 300 dpi for micrographs and photographs). Please provide all figures as separate files. Please note that low-resolution images are one of the leading causes of article resubmission and schedule delays.

Units and Symbols: Units and symbols conforming to the International System of Units (SI) should be used for physicochemical quantities. Solidus notation (*e.g*. mg/kg, mg/mL, mol/mm^2/min) should be used. Please refer to the SI Guide *www.bipm.org/en/si/* for standard units.

Supplemental data: Supplemental data might be useful for supporting and enhancing your scientific research and *Drug Discoveries & Therapeutics* accepts the submission of these materials which will be only published online alongside the electronic version of your article. Supplemental files (figures, tables, and other text materials) should be prepared according to the above guidelines, numbered in Arabic numerals (*e.g*., Figure S1, Figure S2, and Table S1, Table S2) and referred to in the text. All figures and tables should have titles and legends. All figure legends, tables and supplemental text materials should be placed at the end of the paper. Please note all of these supplemental data should be provided at the time of initial submission and note that the editors reserve the right to limit the size

and length of Supplemental Data.

7. Online Submission

Manuscripts should be submitted to *Drug Discoveries & Therapeutics* online at *https://www.ddtjournal.com/login*. Receipt of your manuscripts submitted online will be acknowledged by an e-mail from Editorial Office containing a reference number, which should be used in all future communications. If for any reason you are unable to submit a file online, please contact the Editorial Office by e-mail at *office@ddtjournal.com*

8. Accepted Manuscripts

Page Charge: Page charges will be levied on all manuscripts accepted for publication in *Drug Discoveries & Therapeutics* (Original Articles / Brief Reports / Reviews / Policy Forum / Communications: $140 per page for black white pages, $340 per page for color pages; News / Letters: a total cost of $600). Under exceptional circumstances, the author(s) may apply to the editorial office for a waiver of the publication charges by stating the reason in the Cover Letter when the manuscript online.

Misconduct: *Drug Discoveries & Therapeutics* takes seriously all allegations of potential misconduct and adhere to the ICMJE Guideline (*https://icmje.org/recommendations*) and COPE Guideline (*https://publicationethics.org/files/Code_of_conduct_for_journal_editors.pdf*). In cases of suspected research or publication misconduct, it may be necessary for the Editor or Publisher to contact and share submission details with third parties including authors' institutions and ethics committees. The corrections, retractions, or editorial expressions of concern will be performed in line with above guidelines.

(As of December 2022)

Drug Discoveries & Therapeutics
Editorial and Head Office
Pearl City Koishikawa 603,
2-4-5 Kasuga, Bunkyo-ku,
Tokyo 112-0003, Japan.
E-mail: office@ddtjournal.com